Electronic structure of the high-temperature oxide superconductors

Warren E. Pickett

Complex Systems Theory Branch, Condensed Matter and Radiation Sciences Division, Naval Research Laboratory, Washington, D.C. 20375-5000

Since the discovery of superconductivity above 30 K by Bednorz and Müller in the La copper oxide system, the critical temperature has been raised to 90 K in $YBa_2Cu_3O_7$ and to 110 and 125 K in Bi-based and Tl-based copper oxides, respectively. In the two years since this Nobel-prize-winning discovery, a large number of electronic structure calculations have been carried out as a first step in understanding the electronic properties of these materials. In this paper these calculations (mostly of the density-functional type) are gathered and reviewed, and their results are compared with the relevant experimental data. The picture that emerges is one in which the important electronic states are dominated by the copper *d* and oxygen *p* orbitals, with strong hybridization between them. Photon, electron, and positron spectroscopies provide important information about the electronic states, and comparison with electronic structure calculations indicates that, while many features can be interpreted in terms of existing calculations, self-energy corrections ("correlations") are important for a more detailed understanding. The antiferromagnetism that occurs in some regions of the phase diagram poses a particularly challenging problem for any detailed theory. The study of structural stability, lattice dynamics, and electron-phonon coupling in the copper oxides is also discussed. Finally, a brief review is given of the attempts so far to identify interaction constants appropriate for a model Hamiltonian treatment of many-body interactions in these materials.

CONTENTS

I. INTRODUCTION AND OVERVIEW

A. Brief history

Since the discovery of superconductivity by Kammerlingh Onnes in 1911 in Hg at 4 K, one of the primary objectives of superconductivity research has been to raise the transition temperature T_c. By almost any criterion, progress was slow. The discovery of T_c above 10 K in NbC and NbN was one breakthrough; the discovery of the $A15$ compounds, with T_c finally breaking through the 20-K barrier in the late 1960s and early 1970s, represented the culmination of two decades of intense search for higher transition temperatures. This research involved extensive investigations into materials properties and gave rise to "Matthias's Rules" (Hulm and Blaugher, 1972) for promoting higher values of T_c.

(1) Cubic transition metals are best.

(2) Niobium is the best transition metal.

(3) Certain values of electron/atom (e/a) ratio are special.

(4) High T_c's lie in the regime of lattice instabilities.

Certain aspects of these rules have been understood on a basic level; for example, in the cubic transition metals, the transition-metal carbonitrides, and the $A15$ compounds, the special e/a ratios (roughly 4.7 and 6.5) correspond to regions of high density of states $N(E_F)$ at the Fermi level E_F. Niobium not only tends to lead to e/a ratios near 4.7, but also lies near the center of the transition-metal series where the electron-phonon interaction is strongest. These trends have been reviewed by Klein and Pickett (1983). In addition, it became clear that both high-T_c and lattice instabilities arise from strong electron-phonon interactions so they tend to occur together; there is no definite causal relationship between lattice instability and high T_c. Contrary to early speculations, the best estimates now seem to indicate that low phonon frequencies contribute little to high values of T_c.

The breakthrough in higher T_c's resulted from Bednorz and Müller's discovery (1986) in the copper oxide system. They were convinced that it was necessary to move beyond the standard high-T_c classes to obtain a real breakthrough. They chose to work on transition-metal oxides, both because they were different and because they often displayed polaronic effects typical of extremely strong electron-phonon interactions. In 1986 they found evidence of a superconducting transition occurring near 30 K in the La-Ba-Cu-O system, a result that was rapidly confirmed and refined by a number of laboratories in the U.S., Japan, and Europe. It was established that T_c in the range 20–40 K occurs for $La_{2-x}M_xCuO_{4-y}$, with M=Ba,Sr,Ca, and that application of pressure leads to a large pressure coefficient of T_c and drives T_c above 50 K in the M=Sr system. The crystal structure was identified (see below), and it has since become clear that high-temperature superconductivity is only the most astounding of a number of unusual properties of this system. (To shorten notation somewhat, we shall refer to this class of materials generically as La214, and to the individual members by the widely used acronyms LSCO, LBCO, and LCCO.)

Since pressure was so effective in increasing T_c, Wu *et al.* (1987) simulated "chemical pressure" by replacing atoms in the La214 system by smaller isovalent ones. The replacement of La by Y in LBCO produced in early 1987 a 90-K superconductor, later identified as $YBa_2Cu_3O_{7-y}$ (to be denoted Y123 or YBCO). Like the initial system, this material was prepared by ceramic processing techniques. High-temperature annealing in an oxygen-containing atmosphere was necessary to produce the oxygen content and the crystalline phase necessary to give high T_c. Although other growth techniques have now been found that result in the high-T_c phase, already it was clear from preparations considerations that the new copper oxides were completely different from the previous high-temperature superconductors.

Although there were numerous reports of resistive and magnetic anomalies at much higher temperatures, the next breakthrough came in early 1988 with the discovery by Maeda *et al.* (1988) and Chu *et al.* (1988) of $Bi_2Sr_2CaCu_2O_{8-\delta}$ (denoted here Bi2212 or BSCCO). This Bi-based compound not only showed onsets around 110 K, but also contained no rare-earth element. It was also distinguished by its highly micaceous nature, indicating more pronounced layering than its predecessors. This breakthrough was followed rapidly by the discovery by Sheng *et al.* (1988) of onsets at 115 K in the Tl-Sr-Ca-Cu-O system. The superconducting phase was identified as $Tl_2Ba_2CaCu_2O_{8-y}$ (denoted Tl2212 or TBCCO), and this was soon improved to above 120 K by several groups. The crystal structures of these systems were identified and found to share certain features in common with the La-M-Cu-O and Y-Ba-Cu-O materials, particularly the existence of square Cu-O layers separated by more-or-less ionic regions.

This period of rapid discovery may well continue for some time. While it is certainly early to review any aspect of these novel materials, intense effort has been turned toward the understanding of their electronic structures and properties, and it is useful to collect the results and contemplate their implications. Developing a clear understanding of the electronic structure of these high-T_c materials is central not only to identifying the pairing mechanism, but also to describing the host of other essential, and often unusual, properties displayed by these materials. Although a complete understanding of the important electronic properties would include the electronic response to perturbations of various kinds, this

is an area in which little detailed work has been done.

In this review I shall attempt to provide a composite, if not coherent, picture of the calculational theory of the electronic structures of these copper oxides, with emphasis on the parameter-free density-functional viewpoint. The picture that emerges is one of materials with both metallic and strongly ionic character and with very large anisotropy in the electronic properties. This is a combination that may lie somewhat beyond the regime where both calculational approaches and physical intuition have been developed over the past three decades. Perhaps this collection of the early work in this field can help to identify the important questions to address next.

B. Phase diagram

Before addressing specific topics, it may be useful to provide some perspective by giving a brief review of the wide range of phenomena that have been identified in these systems. Besides the normal-superconducting phase transition, the new copper-oxide materials show an unusually complex generalized phase diagram. The high-temperature phase of the La214 materials is tetragonal. Studies of the temperature dependence of the crystal structure of the La214 compounds revealed a tetragonal-to-orthorhombic transition (Jorgensen, Schüttler, *et al.*, 1987), reviving speculations about the connections between lattice instability and superconductivity. These crystal structures are discussed in Sec. II.

Magnetic susceptibility studies indicated a magnetic transition, probably (and later confirmed to be) antiferromagnetism, in some samples. The transition was found to be highly sensitive to the oxygen vacancy concentration, which is easily varied in ceramic (polycrystalline) samples by heat treatment. Initial studies suggested that antiferromagnetism did not occur in stoichiometric ($y=0.00$) samples, but occurred with $y=0.03$ and disappeared for slightly larger y. However, absolute oxygen concentrations are very difficult to establish on this scale, and, in addition, La substoichiometry is common in samples. These studies did serve to establish the extreme sensitivity of magnetic ordering to materials parameters in the La214 system.

Later, polarized neutron-diffraction studies established that antiferromagnetism does occur, and the dependence of the Néel temperature T_N on the oxygen concentration y and the divalent metal concentration x has subsequently been mapped out. It has become "common wisdom" that stoichiometric La214 with $x=0$, $y=0$ is an antiferromagnet at low temperatures, although it is still questionable whether this "fact" has indeed been established by systematic studies of susceptibility on samples whose stoichiometry and crystalline perfection are also established, say, by Rietveld refinement of neutron-diffraction data.

Due to the large crystalline, and therefore electronic, anisotropy in these layered materials, the question of metallic-nonmetallic character could be settled only with single-crystal samples. Ceramic samples of undoped ($x=0.0$) La214 showed extremely large resistivities, which increased as the temperature was lowered, in nonmetallic fashion. However, individual measurements differed greatly, due to sample differences such as texturing, due to difficulties in establishing ohmic contacts, and due no doubt to varying sample stoichiometries. Subsequent work on single crystals and oriented films did clarify that clear nonmetallic resistivities occurred for small x, which decreased rapidly with increasing x and become metallic below room temperature for x greater than about 0.06. This behavior introduces yet another phase transition, a metal-insulator transition, into the x-T phase diagram.

Thus in the La214 system there is a normal-superconducting transition, a tetragonal-to-orthorhombic structural transition, a paramagnetic-antiferromagnetic transition, and a metal-insulator transition, all in the range $T<500$ K, $x<0.2$. A schematic representation of the phase diagram, such as has been presented by Aharony *et al.* (1988) and others, is shown in Fig. 1. The spin-glass behavior noted by several workers has also been included in this figure. Clearly there is an unusual assortment of competing chemical, magnetic, and thermal interactions in this system which provide a rich field for research.

The Y123 compounds also display a wide range of behavior, including the metallic superconductor-to-magnetic insulator change due to variation of the oxygen content. These features, as well as the incommensurate charge-density wave feature of the Bi2212 system, will be discussed in the following section, which provides a description of the crystal and magnetic structures. Clearly there is a great deal of unusual behavior in these Cu-O based systems, and there is a tendency to expect connec-

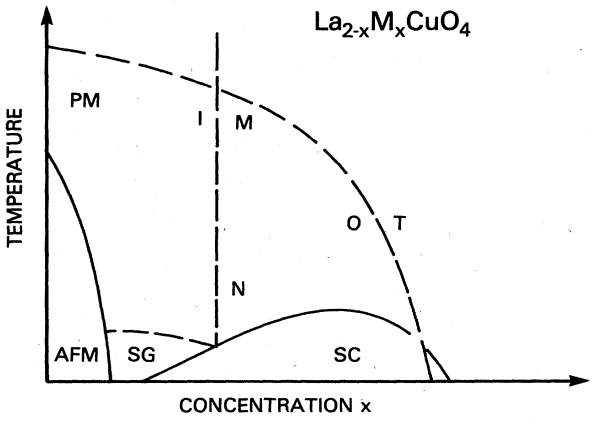

FIG. 1. Schematic phase diagram for $La_{2-x}M_xCuO_4$, M = Sr or Ba, in the temperature-concentration (x) plane. AFM = antiferromagnetic, PM = paramagnetic, I = insulating, M = metallic, SG = spin-glass, N = normal, SC = superconducting, T = tetragonal, O = orthorhombic. A closely related phase diagram is applicable to the $YBa_2Cu_3O_{6+x}$ system.

tions between any type of unexpected property and the unusually high T_c. A large part of the task of researchers is to discover the interrelationships between the various anomalies and finally to provide not only an understanding of the superconductivity but a general predictive theory of these materials that display both metallic and ionic characteristics.

C. Purpose of this article

In the two years since the discovery of high-temperature superconductivity in copper oxides by Bednorz and Müller, thousands of papers on the subject have been published. In a field so new and so rapidly developing, it is impossible to provide any review of the standard type. In this article I will confine the objective to reviewing the large number of papers that bear on the electronic structure of the cuprates, and more particularly will focus on the extent to which the normal-state properties appear to be accounted for by self-consistent electronic structure calculations. There are in addition a large number of papers that use a model Hamiltonian ansatz to try to account for properties, particularly the superconducting properties, of the cuprates; these studies are beyond the scope of this paper. The superconducting state and the pairing will be discussed very little in this article. Indeed, the point of view here is that, until the normal-state electronic structure and excitations are better understood, there is meager hope of establishing the true pairing mechanism(s).

Any discussion of the copper oxides necessitates a knowledge of the crystal structures, and this is particularly true of the calculations reviewed here, as their details often are sensitive to specifics of the atomic geometries. A discussion of the crystal structures is given in Sec. II. Some general aspects of the crystal chemistry of the copper oxides are discussed in Sec. III. In Sec. IV the methods of solid-state electronic structure calculations are briefly described and many of the band-structure features are pointed out. The current picture arising from spectroscopic studies is reviewed in Sec. V, with a view toward indicating which data may be described within a band-structure picture and which properties cannot.

The remaining sections deal with some of the wide variety of properties that electronic structure calculations can address. Section VI is devoted to reviewing the investigations of the effects of chemical disorder: oxygen vacancies, which are pervasive, and alloying on the cation sites. Section VII reviews what has been done in calculating transport properties and comparing with the data. The question of whether current electronic structure methods are able to account for the ordered magnetic states of the cuprates is discussed in Sec. VIII within the context of other transition-metal oxides. Structural stability, lattice dynamics, and the electron-phonon interaction are addressed in Secs. IX and X. The final section is given to a consideration of how correlations more complex than those treated in standard band theory can be addressed in the future. Results in this area are even fewer and more tentative than in the rest of this article.

II. CRYSTAL STRUCTURE

The single most important experiment to be performed on a new superconducting material is to determine its crystal structure. Virtually no serious conjecture as to the properties of a compound can be made without this knowledge. In fact, almost the contrapositive holds; just as soon as the structure of a novel material is established, a number of models for their properties will appear.

This observation is especially true for determinations of the electronic structure. It is widely recognized of course that results of electronic structure calculations are sensitive to the positions of atoms (and to details of the calculations). Just as important to recognize is that the crystal structure itself gives important and sometimes detailed clues into the electronic structure; this is not to say that the information is always unambiguous, and it may be easy to misinterpret its importance. Since it is paramount that the structure be understood clearly, we shall present here the structural information on the La214 and Y123 systems in detail and provide a brief description of a few of the large number of superconducting structures that are being identified in the Bi- and Tl-based oxides.

A. The La214 system

1. Tetragonal phase

At high temperature the $La_{2-x}M_xCuO_{4-y}$ materials are in the body-centered-tetragonal (bct) $I4/mmm$ K_2NiF_4 structure (Jorgensen, Beno, *et al.*, 1987) shown in Fig. 2. This can be pictured as a layered perovskite structure, in which a slab of La_2CuO_4 is much like a similar slab of the cubic perovskite structure $LaCuO_3$. Instead of sharing O atoms at the top and bottom of the CuO_6 octahedra and La atoms at the perovskite cube corner, however, the next slab is distinct and is displaced by $(a/2)(1,1,0)$ with respect to the one below. This not only leads to one more apical O and one more La per formula unit, but also lowers the symmetry so that the O and La atoms do not lie at the same height. The structure can also be pictured as alternating planes of the perovskite slab and a (buckled) rocksalt LaO slab of two layers, rotated by 45° in the basal plane.

The Cu atoms lie at a site (0,0,0) of tetragonal $4/mmm$ symmetry. They are strongly bonded at a distance of 1.89 Å in a square planar arrangement with the four O atoms in the plane (O_{xy}) at $(0,\frac{1}{2},0)$ and $(\frac{1}{2},0,0)$ with mmm site symmetry, while the apical O atoms (O_z) lie at a distance of 2.43 Å. The O_z and La atom sites $(0,0,z)$ have $4mm$ symmetry, each with a positional parameter z

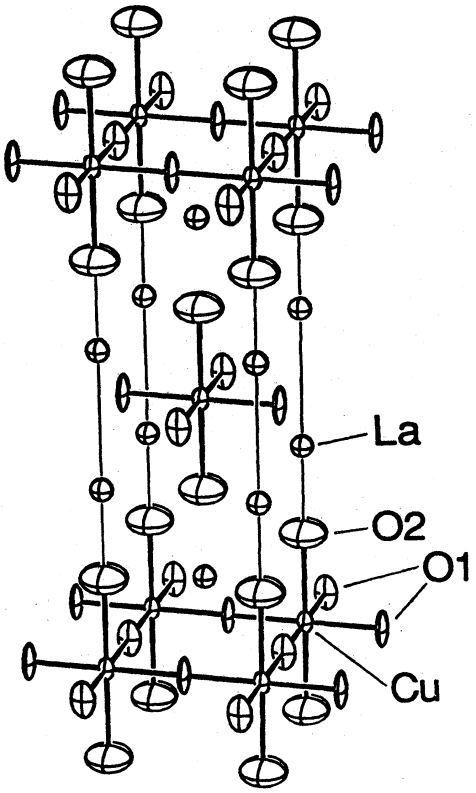

FIG. 2. The crystal structure of La_2CuO_4, with (O1, O2) denoting the sites denoted (O_{xy}, O_z) in the text. The ellipsoids reflect the probability density resulting from neutron scattering refinements of the structure. The probability density can reflect both dynamic and quasistatic, uncorrelated displacements from the ideal sites.

that is not fixed by symmetry. Both Longo and Raccah (1973) and Grande, Müller-Buschbaum, and Schweizer (1977) give $z(\mathrm{La})=0.362c$, while the former give $z(O_z)=0.182c$ and the latter give $z(O_z)=0.187c$. This latter value is in disagreement with most recent data. Since the La site at (0,0,0.362c) is equivalent to the site at (0.5a,0.5a,0.138c), the La-O_z "planes" in this structure can be seen to be strongly corrugated, with the O_z and La heights differing by $(0.187-0.138)c=0.6$ Å.

2. Orthorhombic phase

When the temperature is lowered below about 500 K, La_2CuO_4 transforms to a single-face-centered orthorhombic D_{2h}^{18} structure, which can be described crystallographically as *Abma*, *Bmba*, or *Cmca*. Since the descriptions of the symmetry of this phase in the literature are somewhat confusing, and particularly since the distortion involved in this phase may be relevant for understanding both the antiferromagnetism and the superconductivity, we shall try to give a clear description of this structure, which is pictured in Fig. 3.

The tetragonal-to-orthorhombic (T-O) distortion can

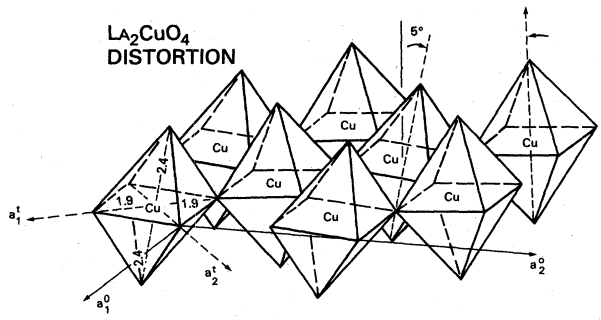

FIG. 3. Pictorial representation of one layer of orthorhombic La_2CuO_4, corresponding to a freezing in of the tilt mode. Superscripts t,o indicate the tetragonal and orthorhombic axes, respectively. The structure is characterized by an alternating rotation by 5° of successive CuO_6 octahedra along a ⟨110⟩ direction. Oxygens (not marked) lie at each of the vertices of the octahedra.

be viewed at the simplest level as an approximate $\sqrt{2}\times\sqrt{2}$ superlattice formation, in which $a'\approx b'\approx\sqrt{2}a$, and $c'\approx c$. However, since in this space group a' and b' are symmetry-unrelated axes, they will in general have distinct lengths. Herein lies the confusion in the literature. The "standard" crystallographic designation is $Cmca=C\,2/m\,2/c\,2_1/a$; however, this standard description defines $|b|>|a|>|c|$ and thus puts the orthorhombic b axis along the tetragonal c axis perpendicular to the planes. Since it seems less confusing for most purposes to keep c' parallel to c, the *Abma* crystallographic description will be used here and below. For the *Abma* designation the face-centering lattice translation lies in the b'-c' plane. With this description $A=a'$ is the special crystallographic axis, that is, the face-centering translation lies in the A plane, but $c'=c$ remains the direction perpendicular to the Cu-O planes. Delgado *et al.* (1988) have discussed these choices of description of the face-centered orthorhombic structure; they chose, however, to use the equivalent, but distinct, *Bmab* designation. These authors have also provided an extensive comparison of their single-crystal neutron-diffraction study of $La_2Cu_{0.95}Li_{0.05}O_4$ (with La and O occupancies determined to be within 0.4 at. % of the stoichiometric values) with previous structural studies of the La214 system.

Accompanying the orthorhombic distortion is an internal displacement of atoms, originally identified by Grande, Müller-Buschbaum, and Schweizer (1977). This distortion consists primarily of a rigid rotation by 5° of the CuO_6 octahedra (Fig. 3) around the ⟨1,−1,0⟩ tetragonal axis (say), but with neighboring octahedra alternating in the direction of rotation. This distortion results in a corrugation of the Cu-O layers in the tetrahedral ⟨1,1,0⟩ direction, which in the *Abma* setting is the orthorhombic a' axis. In addition, the lowering of symmetry allows a change of position of the La along the a' direction. The shift is in the direction *toward* the O_z

atom at an octahedron apex which has rotated toward it.

Two more items are useful for understanding the orthorhombic structure. One of them, the cell size, is not symmetry related, and is given by $(a',b',c')=(5.406, 5.370, 13.15)$ Å by Grande *et al.* (1977) and (5.3990,5.3562,13.1669) Å by Jorgensen, Schüttler, *et al.* (1987), both essentially at room temperature. Differences are likely due to sample stoichiometry. The other item, which defines the stacking of the distorted perovskite sheets, is the direction of the face-centering symmetry operation. Since in this crystal structure the perovskite-like layers not only do not share edges but do not even share apices, the stacking is not determined by connectivity of the sheets in the c direction. The observed stacking is such that the face-centering lattice vector lies in the b'-c' plane, consistent with the wave vector describing the instability lying entirely in the ab plane. It is natural to ask whether this choice of stacking is an obvious one, considering the tilt of the octahedra in each plane.

At first glance the transition appears similar to those occurring commonly in the perovskite class of materials, which appear to be driven by purely ionic considerations: ionic charges, ionic radii, and steric effects. Certainly the rigid rotation of the octrahedra is commonly observed in perovskites, and the displacements of the La ions, which can be viewed as a dimerization (pairing) of the O_z^{2-} and La^{3+} ions, also appears to be consistent with an attraction of oppositely charged ions. Yet another observation is consistent with the dominance of ionic forces, this one involving O ion repulsion. The stacking of layers has the effect that when the apical O ion at (0,0,0.187) is displaced along $\langle 110 \rangle$, the nearest apical O ion in the layer above [i.e., at (0.5,0.5,0.313)] also moves along $\langle 110 \rangle$. If the face-centering vector were to lie in the a'-c' plane, i.e., if the tilting alternated from layer to layer (which in any case is inconsistent with the observed symmetry), the second ion would be displaced toward the first, increasing the ionic interaction energy. All of these considerations are consistent with a purely ionic picture of the structural instability.

An unusual feature of this specific *Abma* structure is that a' is greater than b'. If one considers the rotation of *rigid* octahedra of the sort that occurs here, one notes that the buckling of the Cu-O squares is in the a' direction, making it shorter, while there is no buckling along the b' direction. The observed value of $|a'|/|b'|=1.008$ then reflects that the O_{xy}-Cu-O_{xy} angle that straddles the a' direction has decreased, from 90° to 89.6°. The distortion is thus described more correctly as a rotation of nonrigid octahedra, although the nonrigidiity certainly is small. It is not clear yet whether such nonrigid behavior follows simply from an ionic picture or not. This point will be discussed in Sec. IX.

When La is alloyed with a divalent M atom (M=Ba,Sr), the structural transition temperature decreases (Cava, Santoro, *et al.*, 1987; Jorgensen, Beno, *et al.*, 1987; Moss *et al.*, 1987; Paul *et al.*, 1987). Fleming *et al.* (1987) mapped out the transition in $La_{2-x}Sr_xCuO_4$ in the (x,T) plane. For $x>0.20$, neither any superconductivity nor a T-O transition was observed. The best superconductors, in terms of transition temperature and volume fraction, occurred in the composition range near $x=0.15$, where the T-O transition temperature approaches T_c. Even here, however, sample dependence seems to be an issue. Francois, Yvon, *et al.* (1987) report from neutron-powder-diffraction data that $La_{1.85}Sr_{0.15}CuO_4$ with $T_c=35$ K displayed a 3° rotation and $|a'|/|b'|=1.005$, which is more than half the $x=0.0$ distortion amplitude.

The stabilization of the tetragonal lattice by M-atom alloying has not been widely studied by theorists. The data are consistent either with a picture in which the introduction of 2+ ions of different sizes for the tripositive La ion causes a randomization of the ionic forces and therefore a loss of long-range orthorhombic order, or with a picture in which the carriers screen the ionic forces sufficiently to inhibit the transition.

3. Lower symmetry

There are several indications that the structural phase diagram involves a lower-symmetry structure at low temperature. From the temperature dependence of high-resolution x-ray diffraction data on $La_{1.8}Ba_{0.2}CuO_4$, Moss *et al.* (1987) find line broadening at $T=10$ K that is not consistent with orthorhombic symmetry. They conclude that this broadening is only consistent with symmetry that is monoclinic or lower. Paul *et al.* (1987), using high-resolution powder-neutron-diffraction data, found a highly unusual temperature dependence of the orthorhombic strain $(a'-b')/[(a'+b')/2]$ in $La_{1.85}Ba_{0.15}CuO_4$. The strain increases normally below the T-O transition at 180 K, but at 70 K it drops rapidly by a factor of 2 and then stays constant (at least to 20 K). Similar behavior apparently has been observed by Day *et al.* (1987) in the LSCO at the same concentration, except that the drop occurs only near 20–25 K and the studies were not extended to lower temperature, and by Skelton *et al.* (1987), who correlated x-ray diffraction data with a resistive anomaly at 36 K. Lang *et al.* (1987) have found that $La_{2-x}Sr_xCuO_4$, $x=0.0$ and 0.15, undergoes an anomaly in the thermal expansion that (at least for the $x=0.0$ compound) is indicative of a structural phase transition.

Jorgensen (1987) suggests that these data can be understood in terms of another structural phase at low temperature. The symmetry would be monoclinic or lower, and no explicit structures seem to have been suggested. The difficulty in determining the structure derives from the apparently small atomic displacements involved and the formation of multiple domains (Geiser *et al.*, 1987), so that even the high-resolution studies referred to above could see only anomalous broadening and a variation of "orthorhombic" strain.

There is also clear evidence of another form of lower symmetry in the La214 system, even at high temperature. From Rietveld refinements of powder-neutron-diffraction data, a number of groups have found unusually large thermal ellipsoids, particularly for the O_z atoms. These displacements, shown in Fig. 2, appear as "pancakes" parallel to the Cu-O layers, and the La sites also show similar behavior. Since these thermal ellipsoids are nearly T independent, they correspond to static or quasistatic displacements of the atoms from their ideal sites.

Egami *et al.* (1987) have found additional evidence for (quasi)static displacements of the atoms from their ideal sites. Using pulsed neutron scattering data, they extracted the pair distribution function for La214, for LSCO, and for LBCO ($x=0.15$ superconducting samples) by Fourier transformation of the structure factor. The data were analyzed by comparing with structural models corresponding to the orthorhombic and tetragonal structures described above, with pair distribution peaks broadened to describe the Cu-O nearest-neighbor peak at 1.9 Å correctly. For La_2CuO_4 at 10 K, which is in the orthorhombic phase, the orthorhombic model gave a fair representation of the pair distribution function, but there were clear indications of random or incommensurate displacements of atoms from their ideal crystallographic sites.

For LBCO and LSCO with $x=0.15$, the samples are (crystallographically) tetragonal, or very nearly so because the orthorhombic distortion is so small. Thus ideally the pair distribution function should compare well with the tetragonal model. The tetragonal pair distribution function differs from the orthorhombic by having much sharper peaks at 2.6 and 3.8 Å, a sharpness that is not seen in these superconducting materials. The clear implication is that a local tilting of CuO_6 octahedra occurs in the tetragonal as well as in the orthorhombic phase, and therefore that the O-T transition as temperature is raised is not caused by the loss of the tilt but rather by the loss of correlations between the fluctuating tilting of octahedra. This identifies the transition to be of the order-disorder type rather than a vanishing of the tilting, and this interpretation is consistent with the observed thermal ellipsoids.

In addition, Egami *et al.* (1987) found evidence for another local distortion due to the addition of the divalent species (Ba or Sr). In both materials they observed peaks in the pair distribution function at 2.16 Å, which they identified as Cu-O_z separations near a divalent atom. This separation is 2.4 Å in La_2CuO_4, so the implication is that doping changes drastically the local environment of the Cu ion, more or less consistent with the expected chemistry of a Cu^{3+} ion, which would prefer six oxygen atoms at 1.9 Å rather than the coordination preferred by the Cu^{2+} ion. Egami (1987) has taken this point of view to construct a model of strong electron-phonon coupling due to doping in these materials.

Recently Axe *et al.* (1989) have clarified the low-temperature structure of *doped* La214 materials. They found that, for a Ba content of $x=0.1$, the crystal structure changes at 52 K to another tetragonal phase, with space group $P4_2/ncm$. This structure can be pictured as arising from a coherent superposition of the two domain modifications of the *Abma* orthorhombic structure. This structural modification, however, does not extend to the stoichiometric $x=0.0$ compound.

B. The Y123 system

1. Orthorhombic structure

Following the discovery by Wu *et al.* (1987) of T_c above 90 K in the YBCO system, a large number of papers reported on the crystal structure of this class of mater- ials. The high-temperature superconducting phase of $YBa_2Cu_3O_7$ forms in an orthorhombic *Pmmm* structure with a single formula unit per primitive cell. The structure is about as simple as conceivable for a quaternary compound with ratios 1:2:3:7. It can be viewed as a defect perovskite lattice $(Y\text{-}Ba)_3Cu_3O_{9-\delta}$, based on three Cu-centered perovskite cubes with both O vacancy ordering and Y-Ba ordering along the c axis. Of the two O vacancies ($\delta=2$), one occurs in every third Cu-O plane, along the a axis (say) at the site $(\frac{1}{2},0,0)$, resulting in the orthorhombic (rather than tetragonal) symmetry. The Y and two Ba ions order along the c axis, and the other O vacancy occurs in the Y plane. The structure is illustrated in Fig. 4. The space group is *Pmmm* (D^1_{2h}, No. 47 in the International Tables).

The resulting structure is usually described in terms of Cu-O planes or layers and Cu-O chains. The chains consist (using common but by no means universal notation for the sites) of Cu1 and O1 atoms along the b axis, at

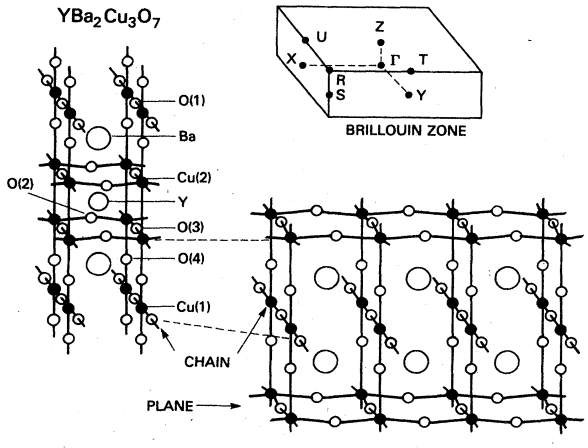

FIG. 4. Crystal structure of $YBa_2Cu_3O_7$, illustrating the CuO chains and the CuO_2 planes. Also shown is the corresponding simple orthorhombic Brillouin zone, with symmetry points marked.

(0,0,0) and $(0,\frac{1}{2},0)$, respectively. These chains are more properly regarded as ribbons, however, since the O4 atom lies above and below the Cu1 atom at the $(0,0,z_{O4})$ position, and the Cu1-O4 separation is the smallest Cu-O distance in the structure. Thus the Cu1 atom is fourfold coordinated with O ions, and each O1 ion is shared by two Cu1 atoms.

The layers consists of Cu2 sites at $(0,0,z_{Cu2})$ neighbored by O2 and O3 sites at $(\frac{1}{2},0,z_{O2})$ and $(0,\frac{1}{2},x_{O3})$. The heights are, in units of c, given by $z_{Cu2}=0.3574$, $z_{O2}=0.3767$, and $z_{O3}=0.3804$, according to Jorgensen, Beno, *et al.* (1987), who also report $z_{O4}=0.1542$, $a=3.8591$ Å, $b=3.9195$ Å, $c=11.8431$ Å. (These values, like all the structural parameters, depend somewhat on the stoichiometry and history of the sample. See, for example, Capponi *et al.*, 1987; Francois, Walker, *et al.*, 1987; LePage *et al.*, 1987; McIntyre *et al.*, 1987; Siegrist *et al.*, 1987; Yan *et al.*, 1987; Williams *et al.*, 1988.) The Cu-O layers are therefore somewhat dimpled, with two oxygens O2 and O3 being nearly coplanar, but with the Cu2 site lying out of this plane by $\sim 0.022c=0.25$ Å. The Cu2 displacement out of the O2-O3 plane is *toward* the O4 site; however, the Cu2-O4 distance is still large (2.38 Å) compared to the Cu1-O4 distance of 1.78 Å.

With Cu1 chosen at the origin, as was done here, the Y site is at $(\frac{1}{2},\frac{1}{2},\frac{1}{2})$ and the Ba site is at $(\frac{1}{2},\frac{1}{2},z_{Ba})$, with $z_{Ba}=0.1895$. Thus the Ba and O4 sites form a warped rocksaltlike layer between the layers and the chains. Oxygen atoms are entirely missing from the Y layers, which separate the Cu-O layers in the unit cell. For later reference we list the site symmetries: Cu1, O1, and Y: *mmm*; Cu2, O2, O3, O4, and Ba: *mm*.

The crystal chemistry of this structure, which is discussed to some degree in Sec. III, is not well understood. A particularly interesting question is why are the O sites in the Y layer vacant rather than (some of) the O sites in the Ba layers? Since the Y ion is expected to be 3+, and is verified to be so by calculations, it would appear that the electrostatic energy could be lowered by placing the negative oxygen ions nearer to the Y ion, that is, in the Y layer. Yet it does not occur and, presumably because the O sites are unoccupied, the Cu-O layers reduce their separation. No resolution of such questions about the crystal structure appears to exist at present.

2. Tetragonal structure

For lower oxygen concentrations, which can be obtained by appropriate heat treatment, the structure assumes tetragonal symmetry. Moreover, at elevated temperature the material with high oxygen concentrations assumes the same tetragonal symmetry. The ideal symmetry of these phases can be described in terms of the composition $YBa_2Cu_3O_6$, whose structure differs from the orthorhombic *Pmmm* structure described above by the removal of the O ion from the chain O1 site. With the O1 site empty, it becomes equivalent to the O5 orthorhombic site, which corresponds in $YBa_2Cu_3O_7$ to the vacancy at $(\frac{1}{2},0,0)$. The resulting structure is pictured in Fig. 5. The high-oxygen-concentration material assumes the same symmetry at high temperature as the result of an order-disorder transformation, in which the ions on the O1 sites randomly occupy both the O1 and O5 sites, resulting in average tetragonal symmetry.

The resulting space group is $P4/mmm$ (D_{4h}^1, No. 123 in the International Tables), with $a=3.863$ Å, $c=11.830$ Å reported by Swinnea and Steinfink (1987) for material near the stoichiometric composition (i.e., O_6). These authors also report $z_{Ba}=0.1934$, $z_{Cu2}=0.3604$, $z_{O4}=0.1533$, and $z_{O2}=0.3793$ (O2 and O3 become equivalent). Thus the internal structural parameters appear to change very little as a result of the loss of the O1 ion. The site symmetries are Cu1, Cu2, and Y: $4/mmm$; O1: *mmm*; O2: *mm*; O4 and Ba: $4mm$.

Several studies have been made of the effect of intermediate oxygen concentrations between $n=6$ and $n=7$ upon the crystal structure. The structure changes from orthorhombic to tetragonal in the range $n=6.35-6.65$, depending on the preparation of the material. If samples are cooled slowly, the oxygen vacancies strongly tend to order, while rapid cooling inhibits the ordering. If the

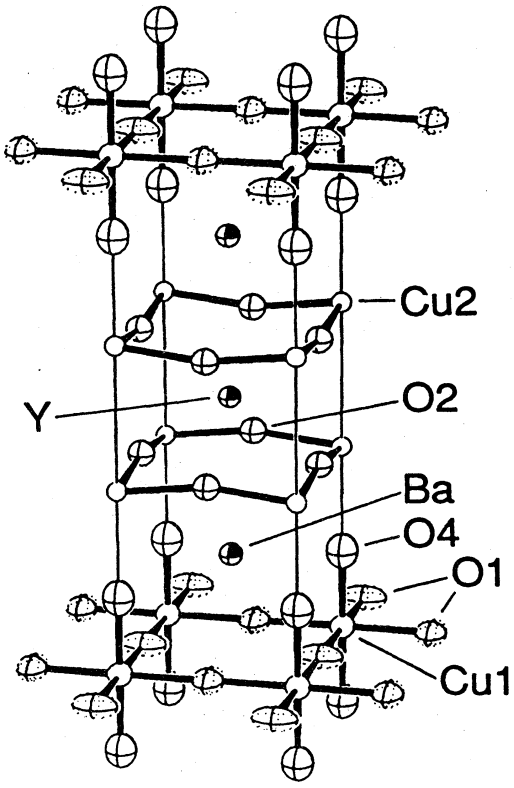

FIG. 5. Tetragonal structure of $YBa_2Cu_3O_{6+x}$. For $x=0$, the oxygen atoms on sites denoted by the dashed ellipsoids are missing, leaving $Cu(O4)_2$ dumbells oriented along the c axis.

vacancies order, the orthorhombic symmetry can be retained to lower vacancy concentration than if the vacancies are disordered. A number of detailed studies of this behavior have been published, and a $T_c = 60$ K plateau in this region of vacancy concentration has been observed by several groups. However, since the details of these phases are complex, they will be addressed in the section on oxygen vacancy calculations only to the extent necessary to evaluate the relevance of the calculations.

3. Lower symmetry?

As in the La214 system, unusually large and nearly temperature-independent thermal ellipsoids have been observed in YBCO. Moreover, due apparently to the increased interest arising from the very high T_c, there have been an extensive number of YBCO studies. It is well known that, in a Rietveld refinement of a structure from neutron-powder-diffraction data, the parameters describing the thermal ellipsoids are the least well determined of the fitting parameters. However, with a substantial number of studies having been reported, it is possible to draw meaningful conclusions if there is broad agreement between the different studies. Moreover, several reports have noted that correlations between the thermal parameters and the other structural parameters are weak, further suggesting that at least semiquantitative conclusions can be drawn from the Rietveld refinements.

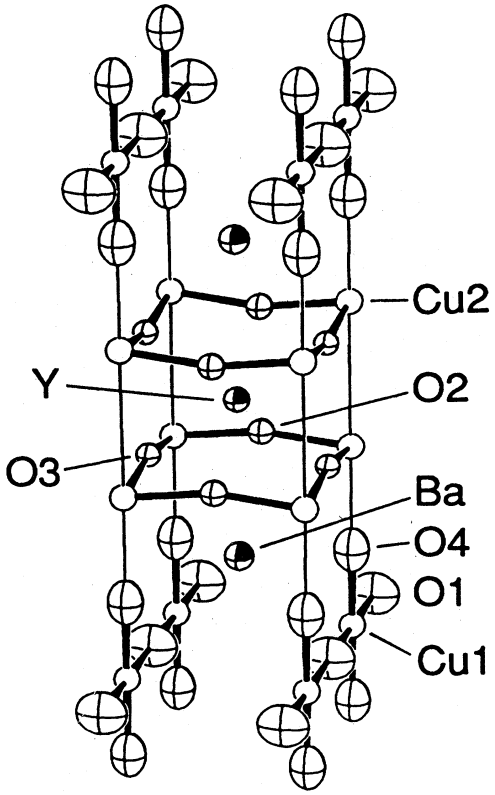

FIG. 6. Structure of orthorhombic $YBa_2Cu_3O_7$, with the ellipsoids denoting schematically the probability density resulting from neutron scattering refinements of the structure. Finer details are mentioned in the text.

Several studies have reported large thermal ellipsoids for the oxygen sites, particularly the O1 site, as shown schematically in Fig. 6. Beno *et al.* (1987) found an isotropic value of the displacement $u_{rms} = 0.13$ Å, which when refined in an anisotropic model became an elongated cigar shape with the direction of large displacement lying in the x-y plane but perpendicular to the Cu1-O1 bond, rather than the pancake shape displayed in Fig. 6. Williams *et al.* (1988) have used joint x-ray and neutron-diffraction data to extract reliable structural data. They found a cigar-shaped ellipsoid qualitatively consistent with the model of Beno *et al.* but much less elongated. More interesting among their results was the indication of large z-direction displacement of the Ba, Cu2, and O2 atoms of about 0.14 Å each, which they interpreted as a correlated motion involving these atoms.

Capponi *et al.* (1987) have reported structural refinements of neutron-powder-diffraction data at a series of temperatures between 5 and 300 K. They find thermal ellipsoids that are generally weakly dependent on temperature. For the O1 site, which in their refinement has large displacements along both the x and z directions perpendicular to the Cu1-O1 bond, the rms displacement decreases by 30–50 % from 300 to 75 K, but stays relatively constant below 75 K.

C. Bi- and Tl-based compounds

Bi-based copper oxide materials with T_c onsets over 100 K were discovered by Maeda *et al.* (1988) and Chu *et al.* (1988) in the Bi-Sr-Ca-Cu-O system and have been verified by several others (Subramanian, Torandi, Calabrese *et al.*, 1988; Sunshine *et al.*, 1988; Tarascon *et al.*, 1988). The introduction of Bi into La214 materials by Michel, Provost, *et al.* (1987) earlier had found a slight enhancement of T_c (to 42 K), and Michel, Hervieu, *et al.* (1987) had also investigated the Bi-Sr-Cu-O system and found onsets near 30 K. Values of T_c above 100 K in this system were novel not only because of the record high temperature (at that time) but also because this material contained none of the rare-earth elements that were present in the previous high-T_c compounds.

The subsequent discovery of high-temperature superconductivity in Tl-based materials by Sheng *et al.* (1988) was related to that of the Bi-based materials both because of the high-T_c values and because of the structure, which was determined quickly thereafter to be similar to that of the Aurivillius (1950a, 1950b, 1950c) phases. We discuss first the structure of $Tl_2Ba_2CaCu_2O_8$ (Tl2212) shown in Fig. 7, which Subramanian, Torardi, Gopalakrishnan, *et al.* (1988) identified as (slightly distorted from a) body-centered-tetragonal $I4/mmm$, which is the same space

group as the high-temperature phase of the La214 system. The unit cell contains two CuO_2 layers separated by Ca ions, and two TlO layers separated from each of the CuO_2 layers by a BaO layer. The structural data suggest that the true structure involves a subtle rearrangement of atoms in the TlO planes (FitzGerald *et al.*, 1988).

Dmowksi *et al.* (1988) have used pair distribution functions obtained from pulsed-neutron scattering to conclude that the structure in the Tl-O planes is locally of much lower symmetry than given by the average structure. Both Tl and O atoms are displaced from their ideal sites, allowing shorter Tl-O bonds than are available if these atoms are confined to their ideal sites.

The Bi2212 material ($Bi_2Sr_2CaCu_2O_8$) has a structure that is closely related to that of Tl2212. Note that in the Bi material Sr cations are needed to stabilize the phase, in place of the Ba cations in the Tl material. The "parent" structure of Bi2212 is the same as the Tl2212 structure, but there are rather stronger internal displacements and superlattice structure in Bi2212. Tarascon *et al.* (1988), from whose paper Fig. 7 was originally taken, described the parent structure as having $a=3.817$ Å, $c=30.5$ Å. Several reports suggested an approximate $\sqrt{2}\times 5\sqrt{2}$ superlattice formation in the a-b plane, making the actual structure orthorhombic, with the modulation occurring mainly in the Bi-O layers. Gao *et al.* (1988) have carried out structural refinements on single crystals that were slightly deficient in Bi and Sr. (Whether similar deficiencies occur in other samples is often not determined.) They conclude that there are sinusoidal displacements of up to 0.4 Å for both the Bi and Sr ions in both the a and c directions, with as much as 0.3-Å displacements of the Cu atoms in the c direction only. While there is no simple explanation for the superstructure formation, a mismatch of Bi-O ionic radii to the Cu-O layer cell has been suggested as the cause.

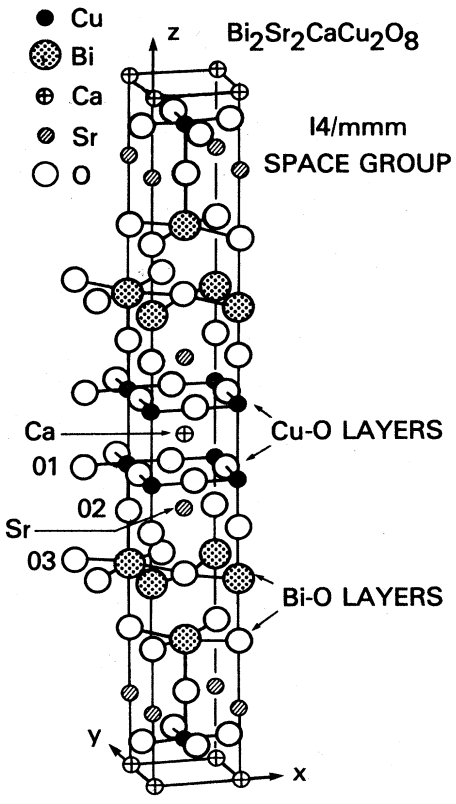

FIG. 7. Idealized crystal structure of $Bi_2Sr_2CaCu_2O_8$, which is also the structure of $Tl_2Ba_2CaCu_2O_8$. There are two Cu-O1 layers and two Bi-O3 layers per cell, with the Cu-O1 layers separated by Ca ions and the Cu-O1 layers separated from the Bi-O3 layers by a Sr-O2 layer.

Kirk *et al.* (1988) have used scanning tunneling microscopic studies on cleaved Bi2212 single crystals to discern the origin of the superlattice structure. They find that every ninth or tenth row of Bi atoms in both $\langle 110 \rangle$ directions is missing, apparently as a result of minimizing strain energy resulting from the mismatch in Bi-O bond distance with respect to the Cu-O lattice constant. If the missing Bi rows are characteristic of the bulk, substoichiometry of Bi of the order of 10% is to be expected.

Subsequent to the initial discoveries, a series of structures of the forms $Bi_2Sr_2Ca_{n-1}Cu_nO_{4+2n}$ and $Tl_2Ba_2Ca_{n-1}Cu_nO_{4+2n}$ have been reported, with T_c increasing with the structure index n. These structures are analogous to the $n=2$ structures described above, except that there are n CuO_2 layers separated by Ca^{2+} ions (Haldar *et al.*, 1988; Parkin *et al.*, 1988; Subramanian, Torardi, Gopalakrishnan, *et al.*, 1988; Torardi, Subramanian, Calabrese, *et al.*, 1988; Torrance *et al.*, 1988). The $n=1$, 2, and 3 structures are shown side by side in Fig. 8. Beginning in early 1988 other superconducting copper oxides too numerous to review here were discovered, many of which have values of T_c over 50 K (see, for example, Ihara *et al.*, 1988 and Marsh *et al.*, 1988). Although a critical comparison of these novel materials might shed important light on the origin of their superconductivity, such a task is not the purpose of this article.

There is, however, one final structure that should be mentioned. Siegrist *et al.* (1988) have reported the "parent structure of the copper oxide superconductors," the $n\rightarrow\infty$ limit of the series mentioned above. It is composed of only a single CuO_2 layer per unit cell, with the layers separated by a divalent cation. The combination $Ca_{1-x}Sr_xCuO_2$, $x=0.14$, was grown as single crystals and identified as space group $P4/mmm$ (simple tetragonal), with no free internal parameters. The lattice parameters were $a=3.8611$ Å, $c=3.1995$ Å. Formal valence counting leads to a Cu^{2+} assignment, and indeed the material is reported by Vaknin *et al.* (1989) to be an antiferromagnetic insulator with $T_N=540$ K and to have planar Cu moment ordering similar to the previously known copper-oxide antiferromagnets (see Sec. VIII).

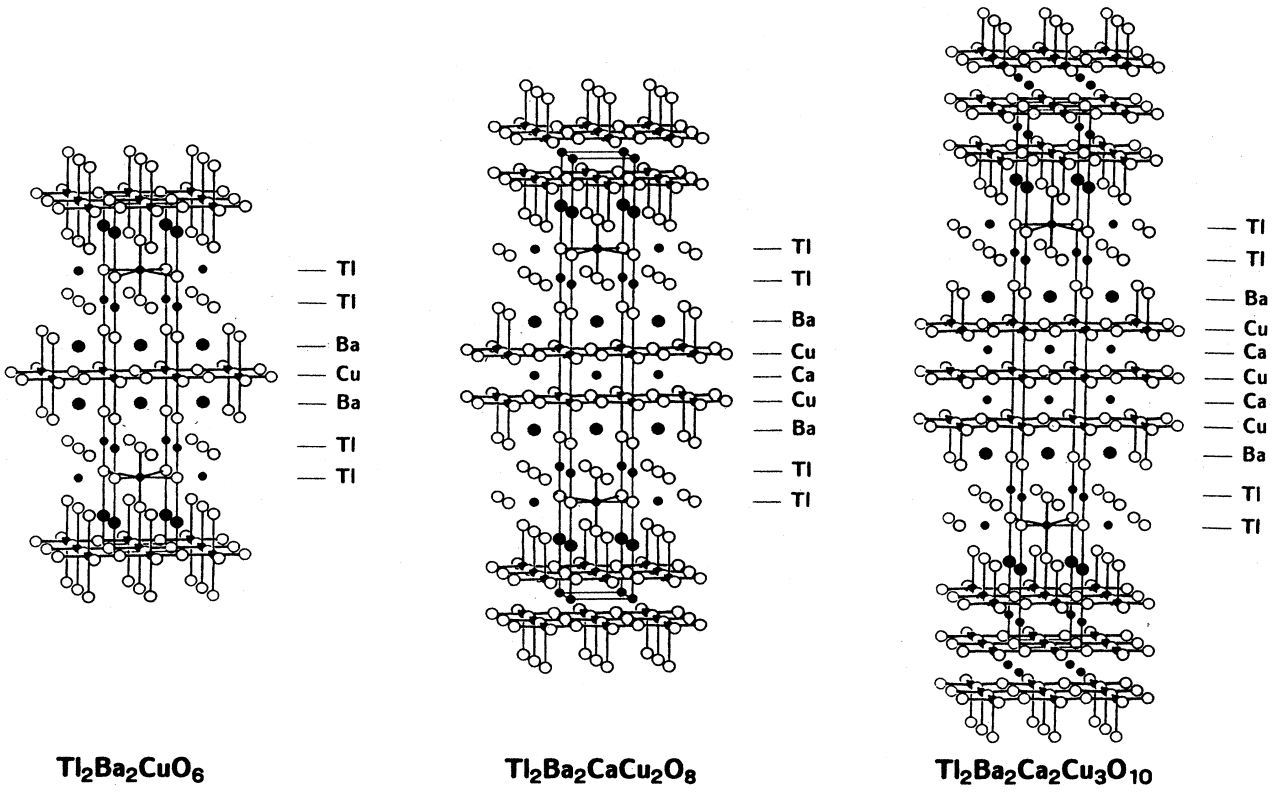

FIG. 8. Crystal structures of the series of compounds $Tl_2Ba_2Ca_{n-1}Cu_nO_{4+2n}$, for $n=1$, 2, and 3. They differ by additional CuO_2 layers separated by Ca ions. Courtesy of C. C. Torardi.

III. GENERAL CHEMICAL CONCEPTS

A. Ionic charges and radii

The structure and stability of the cuprates appear to be dominated by ionic forces and sizes, as indeed is the structurally related perovskite class of materials. Most of the perovskites are ionic insulators. In such materials the concept of the "formal valence" is very useful, and often this valence closely approximates the actual ionic charge it is meant to represent. Formal valences are integral, and their sum over the unit cell must vanish. For many atoms they are conventionally agreed upon; even for atoms with different possible values they are often fixed for a given class of materials. However, valences are not in any real sense measurable quantities. In ionic crystals the valences have been extremely useful for classification, and they also have gained wide use in chemical and physical models. In materials with largely covalent or metallic characters, however, the formal valence concept rapidly loses its relevance, in large part because the assignment of charge to particular atoms becomes so arbitrary.

The formal valence of many of the atoms occurring in the high-temperature superconductors is clear (whether they are actually fully ionic, or indeed integral valued, in a particular material is a separate question). Alkaline earth metals are dipositive; rare-earth metals and lanthanides are tripositive (complications, such as in Ce, may arise); oxygen is doubly negative. A central question, then, is the formal valence of Cu in the La214 and Y123 materials, and of the Bi and Tl ions in the crystals based on those atoms.

In La_2CuO_4 the assignment of formal valence is easy: $(La^{3+})_2Cu^{2+}(O^{2-})_4$. The Cu^{2+} ion is one electron away from a closed shell and thus would tend to have a moment, which fits nicely with the antiferromagnetism in this compound. Substitution of La by a dipositive ion (Ba, Sr, Ca), which leads to T_c values up to 40 K, has led workers to consider Cu^{3+}, O^{1-}, and mixed valences including Cu^{1+}. There is now considerable evidence, from a number of experiments as well as electronic structure studies, that there is strong hybridization between the Cu d states and the O p states, a feature that carries over to the Y123 system and to the Bi- and Tl-based materials, which also have similar CuO_2 layers. This hybridization and its implications are discussed extensively in later sections.

An illustration of the conundrum presented by the copper oxides in discussing the formal valence is given by

$LaCuO_3$, which assumes a slightly distorted perovskite structure. In this compound, valence counting leads to a tripositive Cu ion; however, as noted below, the 3+ charge state is an exotic one for the Cu ion. The lack of a Jahn-Teller distortion also implies that the Cu ion is not divalent. The most consistent picture for this material is that the bonding is covalent/metallic rather than ionic, and formal valences then become irrelevant. For the copper oxides that are nonmetallic, however, the formal valences often provide important insights into the occurrence of fabricated compounds and the structures they assume.

The formal valence of $YBa_2Cu_3O_7$ is commonly stated as $Y^{3+}(Ba^{2+})_2(Cu^{2+})_2Cu^{3+}(O^{2-})_7$, with the tripositive Cu ion lying on the chain site. This compound is, however, metallic, so the valence concept itself is problematic. Its O-poor companion $YBa_2Cu_3O_6$ is insulating and antiferromagnetic and might seem a better candidate for assigning a formal valence. The obvious choice leads to a Cu^{1+} ion on the chain site. Interestingly, if one wants to consider only Cu^{2+} ions, valences sum to zero only for an O concentration of 6.5. In this region the properties of the material are extremely sensitive to the ordering among the vacancies, but near this region there is a metal/insulator transition, superconductivity vanishes for small O concentrations, and antiferromagnetic ordering vanishes for larger O concentrations. Again the formal valency concept seems to have little to contribute, even in classifying behavior.

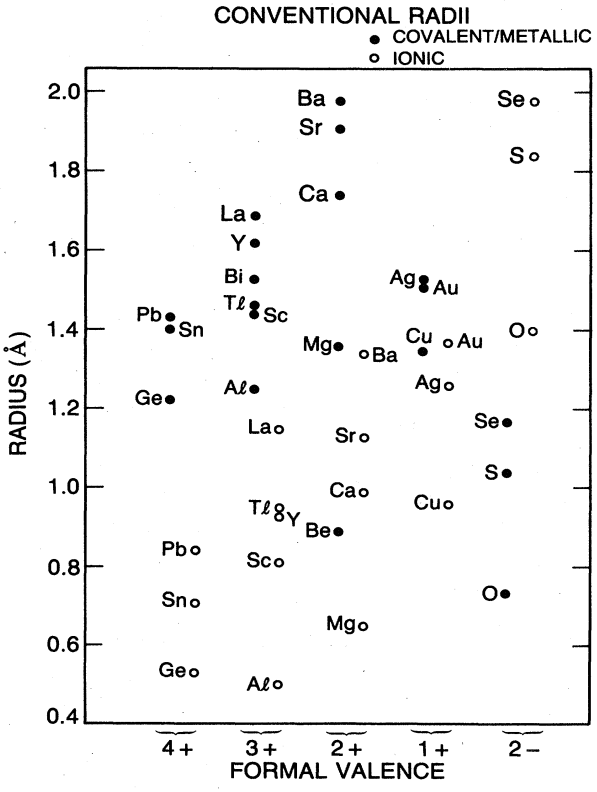

FIG. 9. Radii of most of the ions occurring in the copper oxides: ●, metallic radii; ○, ionic radii. Note particularly the difference in sizes of the Cu and O radii in the two pictures.

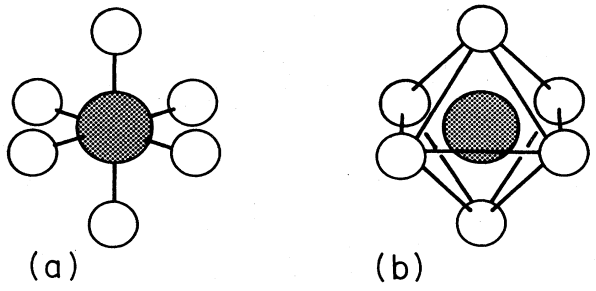

FIG. 10. Diagrams of the CuO_6 octahedron consistent with a picture in which (a) Cu-O interactions are dominant, and (b) O-O interactions are of prime importance. As discussed throughout this article, the copper oxides probably present an intermediate regime where both types of interaction are important.

With the proliferation of structures in the Bi- and Tl-based materials, it is beyond the scope of this brief section to evaluate the validity of a formal valence picture. It is interesting to note that, in the series of compounds $Tl_2Ba_2Ca_{n-1}Cu_nO_{4+2n}$, formal valences make sense if, in addition to the most common assignment of +2 to Cu, one makes Tl tripositive. Apparently the analogous Bi compounds all occur as well, although the structure is not as simple; Bi then would also be tripositive. The fact that these materials are metallic and mostly high-temperature superconductors again calls into question the applicability of formal valence counting. These compounds, which have been identified for $n=1$, 2, 3, and possibly 4, differ in the number of CuO_2 layers separated by Ca ions that occur in the unit cell. The integrity of the CuO_2 layers suggests that covalency is important here, as in the La214 and Y123 systems, while the similarity of the Tl-O (or Bi-O) layers in these compounds and the layering may be mostly due to ionic forces.

A "Wigner-Seitz local environment" study of the structures of the La214 and Y123 systems has been presented by Melamud, Bennett, and Watson (1988). In their approach the atomic radii (either ionic or metallic) are used to construct generalized space-filling Wigner-Seitz cells, and it is reasoned that the area of the face shared by a pair of atoms is a crude, semiquantitative measure of the strength of the bonding between those two atoms. When metallic radii are used, the Wigner-Seitz cells display shapes and coordinations consistent with the application of this analysis to other compounds, in particular, the perovskite structure itself. When ionic radii are used, however, some Wigner-Seitz cells assume highly unusual shapes which suggest that this picture is unrealistic. Melamud *et al.* conclude that the covalent/metallic picture is the chemically more reasonable picture for the bonding.

The root of these differences is the large value of the

ionic radius of the O^{2-} ion, which is twice as large as its metallic radius. For illustration, the ionic and metallic radii for most of the atoms occurring in the copper oxides are shown in Fig. 9. Implications of the distinction between ionic and metallic radii are illustrated in Figs. 10 and 11. Figure 10(a) shows a CuO_6 octahedron in a picture in which the Cu-O interactions are dominant, while Fig. 10(b) provides the corresponding picture emphasizing the O-O interactions. This difference is nontrivial, as illustrated in Fig. 11, which pictures the Cu-O plane as overlapping ions, in both the metallic picture and the ionic picture. With metallic radii, only the Cu-O bonding (in tight-binding language, Cu-O overlap) appears to be important. In fact, the early models of the cuprates relied only on Cu d, O p interactions to represent the band structure. Figure 11(a), which uses realistic ionic radii, immediately suggests the importance of O-O overlap, and this feature has recently become recognized as crucial in any realistic description of the electronic structure of the copper oxides. Since one of the central problems in the copper oxides appears to be to identify, characterize, and describe the metallic and ionic characters and their interaction, it is useful to have such a picture in mind as a point of reference.

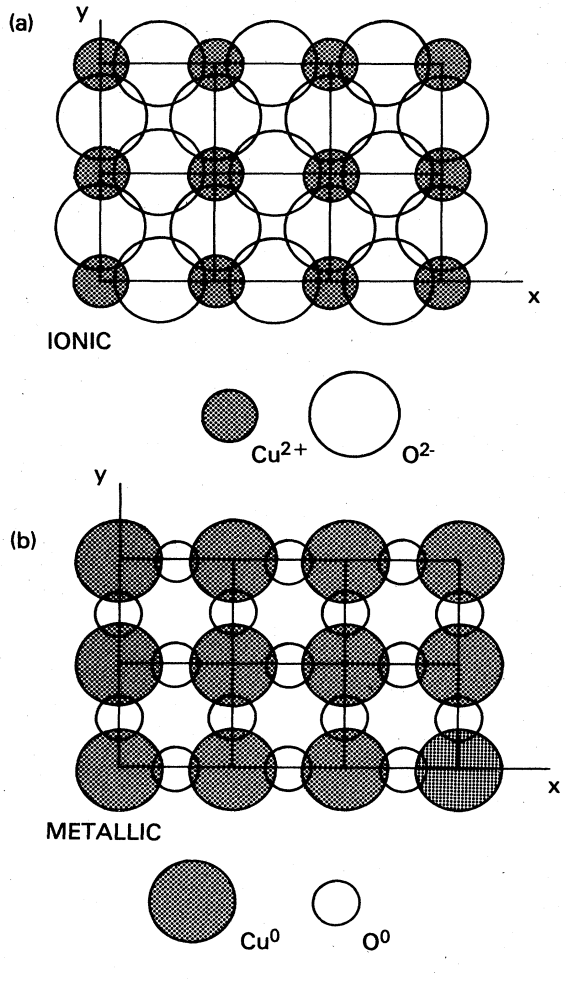

FIG. 11. Diagram of the CuO_2 plane illustrating the different pictures obtained when assuming that (a) ionic bonding is paramount, and (b) bonding is primarily metallic. Ionic radii from the literature are used in the figure. The ionic picture (a) immediately suggests the importance of O-O p-p overlap for the electronic structure.

B. Jahn-Teller effect

The so-called Jahn-Teller distortion in the La214 system has received widespread attention, particularly in attempts to account for the strong distortion of the CuO_6 octahedra, which have four in-plane bonds 1.9 Å long and two axial bonds of 2.4 Å. The Jahn-Teller effect (Jahn and Teller, 1937) arises because orbitally degenerate ground states of highly symmetric coordination polyhedra are unstable with respect to distortions. The Cu^{2+} ion is a well-known Jahn-Teller ion (Kanamori, 1960), which almost exclusively assumes fourfold, fivefold, or sixfold coordination (Reinen, 1983). Assuming a Cu^{2+} d^9 configuration and a cubic environment, we find that the d hole energy will be orbitally degenerate, either threefold if the e_g manifold is lowest, so the t_{2g} states are partially filled, or twofold in the reverse case.

The latter situation holds for octahedral coordination that occurs in La_2CuO_4. The t_{2g} states, though strongly hybridized with O p states, are fully occupied. The (also hybridized) $d(z^2)$ partner in the e_g manifold is also occupied, since the elongation of the octahedron makes the $d(x^2\text{-}y^2)$ orbital the more antibonding and therefore the last to be occupied. One of these orbitals is unoccupied, or, in a (paramagnetic) band picture, the corresponding (hybridized) band is half unfilled, leaving one $d(x^2\text{-}y^2)$ "hole" and thus accounting, at least qualitatively, for the strong distortion of the octahedron.

The Jahn-Teller distortion and its incorporation into the electronic structure of the copper oxides is illustrated somewhat schematically for a CuO_6 octahedron in Fig. 12. Beginning with isolated atomic levels for separated Cu and O ions, interactions within the octahedron split the Cu level into states appropriate to its site symmetry (cubic), and similarly for O (with very low site symmetry in this example). The orbitally degenerate e_g level being partially occupied, a Jahn-Teller distortion occurs, separating it into orbitally nondegenerate $d(z^2)$ and $d(x^2\text{-}y^2)$ levels, the latter lying higher. Then all Cu states hybridize with the O states, but the $pd\sigma$ interaction, being largest, leads to widely separated bonding and antibonding Cu-O σ bands at the extremes, with a complex of other bands between.

It should be recognized at the outset that there is no true Jahn-Teller distortion in La_2CuO_4 or in most of the other cuprates, and there is not yet any direct calculational evidence whether the related pseudo-Jahn-Teller effect, in which the structure takes additional advantage of the nonspherical ion (Reinen, 1983), is appreciable.

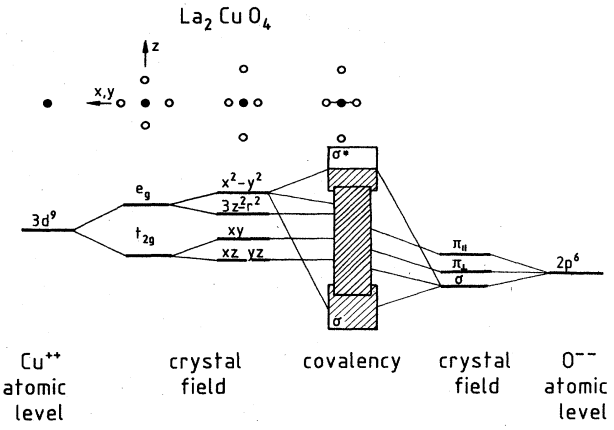

FIG. 12. Schematic picture of the origin of the hybridized Cu-O bands arising in many of the copper oxides, with atomic positions shown schematically at the top. Representative atomic 3*d* and 2*p* levels are shown at the left and right edges, respectively. These are split by the crystal field as shown; the effect of the "Jahn-Teller" distortion of the octahedron on the cubic Cu e_g and t_{2g} states is illustrated schematically. In the center the bonding complex of bands, and specifically the separation of bonding and antibonding σ bands, is illustrated. From Fink *et al.* (1989).

First, the Cu site symmetry in either the La214 or the Y123 system is nowhere near to cubic; both are strongly layered structures. The crystal field in La214 would not approach cubic symmetry very closely even if the CuO_6 octahedron were regular. Moreover, there is no geometry remotely close to the observed one that gives cubic symmetry for the Cu site and that could serve as a reference for a true Jahn-Teller effect. Second, purely ionic calculations (Cohen, Boyer, *et al.*, 1988; Cohen, Pickett, Boyer, *et al.*, 1988; Cohen, Pickett, Krakauer, and Boyer, 1988), which are discussed further in Sec. IX, indicate that at least half of the octrahedral distortion results if one assumes *spherical* ions, the distortion occurring simply because of the strongly layered crystal structure and the large ionic interactions. No doubt the missing $d(x^2\text{-}y^2)$ electron contributes to the distortion (referred to above as the pseudo-Jahn-Teller effect). Terakura *et al.* (1987) have discussed the distortion of the CuO_6 octahedron in terms of a simple tight-binding picture. There may be no better way to obtain evidence on how large this effect might be than to compare with related materials composed of non-Jahn-Teller ions.

Weber (1988b) has taken the point of view that the Jahn-Teller instability of the Cu^{2+} ion is so strong that it inhibits any near-cubic structure, leading to structures that can incorporate this energy in the atomic arrangements. Clearly this energy is not the determining factor in the La_2CuO_4 structure, because the identical structure is found for La_2NiO_4, and Ni is not a Jahn-Teller ion. However, the difference in axial ratios (Cu-O_z bond length relative to the Cu-O_{xy} bond length) is substantial: 1.28 to 1.1. This can be regarded as reflecting the pseudo-Jahn-Teller effect mentioned above; the crystal structure takes advantage of the specific nonspherical symmetry of the Cu ion to relax. It will be seen in Secs. IX and X that this effect is accounted for extremely well by local-density total-energy studies.

Another phenomenon related to the Jahn-Teller distortion (either true or pseudo) is possible ordering of unoccupied orbitals on adjacent Cu ions (Kanamori, 1960). A periodic Jahn-Teller distortion of each octahedron leads to a ferroelastic distortion of the crystal. An alternative is to form an antiferrodistortive phase resulting from orbital ordering. This situation, which avoids macroscopic lattice strains, is realized in K_2CuF_4 (Khomskii and Kugel, 1973), which otherwise is isostructural with La_2CuO_4.

C. Charge states

A much discussed question in early models of cuprates is the charge state of the Cu ion, and more particularly how and to what extent it might change upon alloying on the cation site(s) or when the oxygen vacancy concentration is varied. In the system $La_{2-x}M_xCuO_{4-y}$ for divalent *M*, many times it has been suggested that the Cu^{2+} ion may be altered, to Cu^{1+} or Cu^{3+}. While the cuprous and cupric ions are common to chemists, the tripositive ion is a very exotic charge state for Cu. The reason is straightforward: the third ionization potential of Cu, 36.8 eV (Moore, 1952), is very large and thus effectively prohibits such a high level of oxidation. Contrary to several early suggestions, there now seems to be no clear evidence for Cu^{3+} ions in the cuprates.

Introduction of divalent *M* ions on the La sites reduces the number of electrons, or equivalently, introduces holes into the crystal. From the formal valence viewpoint, if the Cu ion cannot absorb the charge difference, the oxygen must, leading to O^{1-}. Experimentally, there is strong evidence that the holes do have strong oxygen character. The experimental data on this subject will be discussed in Sec. V. Wilson (1987, 1988) has discussed at some length both the question of charge states and Jahn-Teller distortions in copper-oxide superconductors. Sleight (1988) has also reviewed the crystal chemistry of the copper-oxide and barium-lead–oxide superconductors.

D. Cluster calculations

One approach toward discerning the local bonding characteristics of a crystal is through cluster calculations. Several workers have applied different variations in attempts to elucidate the electronic structure of the cuprates. When one approximates a crystal by a finite, and in practice very small, cluster several undesirable effects may arise. The loss of periodicity implies that (1) a surface of some sort is present, and (2) long-range Coulomb terms are ignored, or at best accounted for in an *ad hoc* manner. Surface effects are widely recognized, and as a

result cluster studies are most useful for comparison of *differences,* such as the effects of an oxygen vacancy. On the positive side, cluster calculations may be very useful for studying local correlations, which are exceedingly difficult to treat in a periodic solid.

While in high-density metals, where such interactions are screened out, the neglect of long-range Coulomb interactions may not be severe, one must be cautious in crystals such as these cuprates which have a strong ionic component. The ordering of oxygen vacancies in the c direction suggests that long-range Coulomb interactions are especially important along the c axis. A Madelung contribution to the potential of the cluster can be used to simulate the effect of the rest of the crystal, and in highly ionic insulators this procedure works rather well. In the cuprates, however, the charges one would assign, especially to the Cu and O sublattices, are uncertain, and most cluster studies have not retained any Madelung field.

For oxides the neglect of the Madelung field may be especially severe. There is wide agreement that the O ions are reasonably close to doubly negative. The O^{2-} ion, however, does not exist in free space, but is only stabilized by the crystalline Madelung field, and its character at or near a surface may be substantially different from that in the bulk. It is well to keep these possible limitations in mind when assessing the implications of cluster studies.

A number of cluster studies, from a variety of viewpoints, have appeared. They have been applied to such diverse areas as estimating electron correlation parameters, studying effects of oxygen vacancies, and examining exchange interactions and the character of uppermost occupied orbitals. These results will be discussed in the appropriate places in the following sections.

IV. LOCAL-DENSITY BAND STRUCTURES

A. Density-functional theory

The formal justification of current electronic stucture studies ("band-structure calculations") lies in the density-functional theorems of Hohenberg and Kohn (1964). Since the formalism, the approximations, and the results of a large number of applications have been reviewed widely elsewhere (see, for example, the book edited by Devreese and Van Camp, 1984), only an outline will be presented here. In the context of solids, one considers the N-electron problem in the field of ionic potentials

$$V_{\rm ion}(\mathbf{r})=\sum_m v_{\rm ion}(\mathbf{r}-\mathbf{R}_m) \tag{4.1}$$

at (static) positions $\{\mathbf{R}_m\}$,

$$H=\sum_i p_i^2/2m+\int n(\mathbf{r})V_{\rm ion}(\mathbf{r})d\mathbf{r} +\tfrac{1}{2}\int\int n(\mathbf{r})v(\mathbf{r}-\mathbf{r}')n(\mathbf{r}')d\mathbf{r}\,d\mathbf{r}' . \tag{4.2}$$

Here $n(\mathbf{r})$ is the electron density operator and $v(\mathbf{r}-\mathbf{r}')$ is the Coulomb interaction. Hohenberg and Kohn established that there is a one-to-one correspondence between the ionic potential $V_{\rm ion}$ (neglecting an irrelevant arbitrary constant) and the ground-state density n. Thus the many-body problem can be considered as a functional of the density rather than the given functional (4.2) of the potential.

Interest has centered on the ground-state energy functional $E[n]$. Hohenberg and Kohn also established that for variations of the density δn which conserve the particle number N, $E[n]$ is minimized by the ground-state density and corrections are quadratic in δn. The resulting variational principle is crucial for obtaining accurate numerical results as well as for establishing formal properties of the theory.

The energy functional was written by Kohn and Sham (1965) in the form

$$E[n]=T_0[n]+\int V_{\rm ion}(\mathbf{r})n(\mathbf{r})d\mathbf{r} +\tfrac{1}{2}\int\int n(\mathbf{r})v(\mathbf{r}-\mathbf{r}')n(\mathbf{r}')d\mathbf{r}\,d\mathbf{r}'+E_{\rm xc}[n] , \tag{4.3}$$

where $T_0[n]$ is the kinetic energy of a system of *noninteracting* electrons with the same density $n(\mathbf{r})$, and the exchange-correlation energy $E_{\rm xc}[n]$ is defined by this expression. If one has acceptable approximations for $T_0[n]$ and $E_{\rm xc}[n]$, the energy can be obtained directly from Eq. (4.3) by minimizing the energy with respect to $n(\mathbf{r})$. One application of such an approach will be discussed in Sec. IX.

The more usual way of obtaining the energy is by the use of the Kohn-Sham (1965) formalism, which builds in the fact that $T_0[n]$ can be obtained exactly from the kinetic energies of one-particle wave functions. They derived the set of equations

$$[p^2/2m+V_{\rm eff}(\mathbf{r};n)]\psi_i(\mathbf{r})=E_i\psi_i , \tag{4.4a}$$

$$V_{\rm eff}(\mathbf{r};n)=V_{\rm ion}(\mathbf{r})+\int v(\mathbf{r}-\mathbf{r}')n(\mathbf{r}')d\mathbf{r}'+v_{\rm xc}(\mathbf{r};n) , \tag{4.4b}$$

$$n(\mathbf{r})=\sum_i^{\rm occ}|\psi_i(\mathbf{r})|^2 , \tag{4.4c}$$

where

$$v_{\rm xc}(\mathbf{r};n)=\delta E_{\rm xc}[n]/\delta n(\mathbf{r}) . \tag{4.5}$$

The self-consistent density resulting from these equations minimizes the energy functional. The calculational procedure for beginning and iterating to self-consistency is illustrated in Fig. 13.

Within density-functional theory the one-electron eigenvalues and eigenfunctions have no physical meaning. Specifically, they are the true excitation energies and single-electron wave functions of the system of noninteracting electrons that arises from the "external" potential $V_{\rm eff}$, which has the same density as the interacting

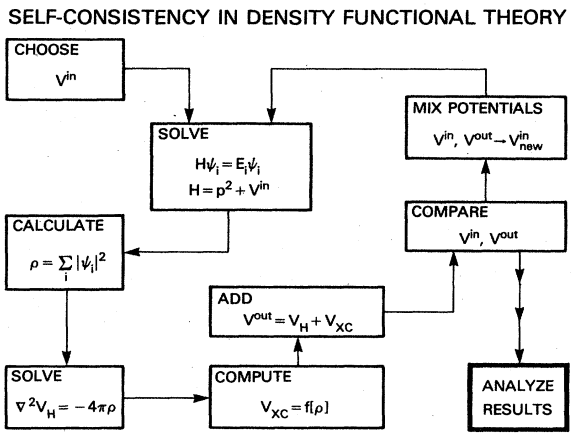

FIG. 13. Flow diagram of the calculational procedure arising in the solution of the Kohn-Sham equations. The key ingredient is the self-consistency loop, within which the electron density is required to become consistent with the Coulomb (V_H) plus exchange and correlation (V_{xc}) potential, which itself arises from the density.

material of interest. This system is of course not physically realizable. Nevertheless, there is intense interest in the eigenvalues and eigenfunctions that result, because of the following indirect connection to excitations.

When well-defined quasiparticles exist (i.e., their width is much less than their energy), they are described by the non-Hermitian problem

$$(p^2/2m)\psi_i(\mathbf{r},E_i)+\int M(\mathbf{r},\mathbf{r}',E_i)\psi_i(\mathbf{r}',E_i)=E_i\psi_i(\mathbf{r}) , \tag{4.6}$$

which bears a formal resemblance to the Kohn-Sham eigenvalue equation (4.4a). The local Hermitian effective potential $V_{\rm eff}$ is replaced by a nonlocal, complex, energy-dependent "mass operator," or self-energy, M. In a wide variety of solids it has been established, particularly using angle-resolved photoemission studies, that the bands from Eq. (4.4a) bear a close resemblance to the single-particle excitations in the valence–conduction-band region. In such cases the self-energy is well represented by a local, real, energy-independent effective potential $V_{\rm eff}$. Conversely, when the excitations do not correspond directly to the calculated bands, one can conclude that the nonlocality or energy dependence of the self-energy is necessary for an understanding of the excitations. The lack of correspondence between the calculated bands and observed excitations does *not* in itself invalidate the formalism for obtaining ground-state properties.

The exchange-correlation functional $E_{xc}[n]$ remains unknown. The large majority of calculations invokes the highly successful local-density approximation,

$$E_{xc}[n]=\int \varepsilon_{xc}(n(\mathbf{r}))n(\mathbf{r})d\mathbf{r} , \tag{4.7}$$

where $\varepsilon_{xc}(n)$ is the exchange-correlation energy density of the homogeneous interacting electron gas with density n, which is known. Reviews containing discussions of applications of density-functional theory and of the generalization to spin-polarized systems are given, for example, in the book edited by Devreese and Van Camp (1984).

B. Methods of calculation

Because there have been a number of calculations carried out that show differences, always in detail and sometimes in important aspects, it is necessary to be familiar with the methods and the approximations intrinsic to them. Here a brief description will be given of the various methods that have been used for a substantial number of calculations. Discrepancies between calculational results will be noted and discussed throughout the paper.

1. Linear augmented plane-wave (LAPW) method

In the LAPW method (Wimmer *et al.*, 1981) the cell is partitioned into spheres centered on the atoms (and possibly elsewhere) and the remaining interstitial region. The basis set consists of LAPW's, which are plane waves in the interstitial region and are augmented within the spheres by an angular momentum representation, which consists of solutions of the spherical radial equation for $s,p,d,f,\ldots$ ($l=0,1,2,3,\ldots$) multiplied by the corresponding spherical harmonics. This expansion is routinely carried out to $l=8$, 10, or 12, as deemed necessary. In the augmented plane-wave method, out of which the LAPW method grew, the radial functions are energy dependent. The energy dependence of the radial functions is linearized around an energy E_l for each l, and the first two terms of the expansion are retained. A linear combination of these functions is joined continuously and differentiably to the plane waves at the sphere boundary.

The LAPW basis set is particularly well suited to periodic solids: it represents the all-electron wave functions naturally both in the interstitial region, where they are relatively smooth, and near the atoms, where there may be stronger variations as well as core orthogonalization wiggles. They can be used readily for semicore and core states as well as the valence and conduction bands.

The density and potential are represented in a similar dual representation, as a plane-wave expansion in the interstitial region and in a symmetry-adapted lattice harmonic representation inside each sphere. Much of the construction of the potential can be done directly; however, at least the exchange-correlation potential requires least-squares fitting to several calculated values to be put into the dual representation. The particular methods of carrying this out differ among the various groups; however, the various implementations show very good agreement when the levels of convergence are similar.

2. Linearized muffin-tin-orbital (LMTO) method

The LMTO method (Andersen, 1975; Skriver, 1984) introduces several approximations in the self-consistent solutions of the one-electron equations which allow much faster calculations. In the formulation, space is divided up into spheres, as in the LAPW method, and these spheres are usually centered at atoms. A muffin-tin orbital is a local function (such as a spherical Neumann function) outside each sphere, which is augmented by energy-linearized radial solutions inside each sphere, again similarly to the LAPW method.

While formulated for nonoverlapping spheres, the first approximation that is made is to increase the sphere radii until overlapping, "space-filling" spheres are obtained (i.e., the sums of volumes of the spheres is equal to the cell volume). This is referred to as the "atomic sphere approximation." Strictly speaking, the basis function is overspecified (specified twice) within regions of overlapping spheres, and underspecified (and never used) in interstitial regions that lie inside no sphere. Therefore it is important to fill as much of the unit cell with as little overlap as possible, within the constraints of the structure. In most implementations of the LMTO, only the spherical part of the charge density within each sphere is calculated. This charge density gives rise to a complex form of potential, but only the spherical part is retained.

Thus the approximations of the LMTO method are several. The gain, however, is a computationally efficient local orbital basis. Most atoms require only nine basis orbitals (s, p, and d), but f symmetry states may also be necessary for well-converged results (16 basis orbitals). This number can be compared with 80–120 basis functions per atom for the LAPW method (or more for precise total-energy studies). Thus the matrix diagonalization is speeded up by a factor of $(5-10)^3 \sim 100-1000$, and other parts of the computations are speeded up by 1–2 orders of magnitude as well. In practice the LMTO method is probably not this much faster than the LAPW method, however.

In close-packed solids the approximations made in the LMTO method are very good, and in addition it is possible to implement a correction to the energy bands ("combined correction terms") that compensates for the region of overlapping spheres. Several studies have shown that when the corrections are included, the LMTO band structures and even Fermi surfaces are realistic, and the method has been especially useful for total-energy studies of solids.

In materials that are not close packed, the method is less accurate. The high-T_c copper-oxide materials fall into this class; even the Cu-O layers themselves are not close packed, but have holes in which the density is quite low (Sec. III). Several of the perovskite-based structures have planes of cations (Y in the Y123 structure, Ca in the $Bi_2Sr_2CaCu_2O_8$, etc.) in which all the oxygen sites are empty. These systems should be treated well with empty spheres on these empty sites, however.

3. Pseudofunction method

The pseudofunction method, developed by Kasowski and co-workers (1986), has been used for a number of studies of high-T_c copper-oxide materials, so a brief description of the method will be given here. The pseudofunction method grew out of the LMTO method and shares a number of features with it. The basis set consists of augmented "pseudofunctions," which are atom-centered localized functions. As in the LAPW method, space is partitioned into atom-centered muffin-tin spheres and the remaining interstitial region. Outside the sphere the pseudofunction is a smooth, decaying function, typically chosen to be similar to the muffin-tin orbitals discussed above. A restriction central to the method is that these "tail functions" can be expanded accurately in a Fourier representation. Within a sphere, the pseudofunction is augmented with radial functions that are solutions of the radial equation at energy E_l and their energy derivatives, again similarly to the LAPW and LMTO methods.

A key simplification in the pseudofunction method is that the pseudofunctions can be expanded in plane waves, since the core orthogonalization wiggles that occur in the eigenfunctions are not in the pseudofunctions. The charge density arises from the pseudofunctions and from the augmenting functions, which are well localized at an atom. The approximation is made that the nonspherical part of the charge from the augmentation functions can be neglected; then the potential is simply the sum of a simple plane-wave representation and that arising from nonoverlapping spherical objects. A further approximation is made that the nonspherical terms in the sphere are evaluated using the pseudofunctions rather than the full (augmented) basis functions. This results in further speed-up of the computation and results in only small additional loss of accuracy.

The pseudofunction method, then, consists of a local orbital basis-set approach, which both (i) utilizes only a small number of orbitals per atom, and (ii) includes the full variation of the potential in the interstitial region, as well as much of the nonspherical variation inside the spheres. As such, the method achieves much of the computational speed-up of the LMTO method while retaining more of the variations of the density and potential that are included so laboriously in the LAPW approach. Thus in philosophy, construction, speed, and accuracy the pseudofunction method should be intermediate between the LAPW and LMTO methods, when each method is well converged.

The actual accuracy attained in a given calculation will depend on the local orbital basis as well as the approximations discussed above. A comparison of the pseudofunction method with the self-consistent norm-conserving pseudopotential method, the LAPW method, and the extended LMTO method for silicon has been given by Tsai, Dow, and Kasowski (1988). Most valence-band eigenvalues were very similar to the other

three methods, except for the valence bandwidth, which was 4–5 % larger. Conduction bands were also realistic, although some differences of up to 1 eV occurred in the bands within 5 eV of the gap. These discrepancies are presumably due to truncation of the basis set, which was not specified. The equilibrium lattice constant, bulk modulus, and its pressure derivative were in very good agreement with the experimental values.

In calculations on the copper oxides, the practice has been to use an sp^3 basis set for the oxygen atoms and an sp^3d^5 basis set for the Cu, rare-earth, and alkaline-earth atoms. This is in some sense a minimal basis set for reproducing the bands of interest. Comparison with LAPW and LMTO results will be noted for a few cases in the discussion below.

C. Self-consistent calculations: La214 system

1. La_2CuO_4: tetragonal phase

The local-density band structure of the La214 compound has been calculated by several groups using the methods discussed above. In Fig. 14 the Brillouin zone, with labeling of the high-symmetry points and lines, is pictured. The *paramagnetic* band structure of La_2CuO_4 calculated by the LAPW method (Pickett, Krakauer, Papaconstantopoulos, and Boyer, 1987), is shown in Fig. 15 along several high-symmetry lines in the Brillouin zone. An important feature to note is that this compound contains an odd number of electrons in the unit cell, so a paramagnetic band structure must be metallic. The five Cu d states and the three O p states for each of the four oxygen atoms form a complex of 17 hybridized p-d valence bands. The total bandwidth is 9 eV.

In spite of the complex nature of the valence-band complex, the band structure near E_F is rather simple. A

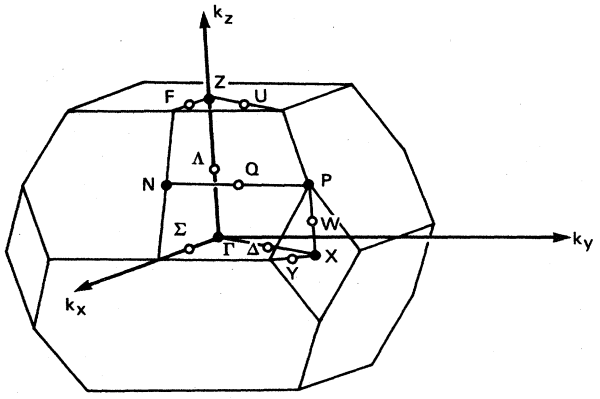

FIG. 14. Brillouin zone for the body-centered-tetragonal structure of La_2CuO_4, with symmetry points labeled. The top (F-Z-U) face of neighboring zones is co-planar with the central (Σ-Γ-Δ) plane of this zone.

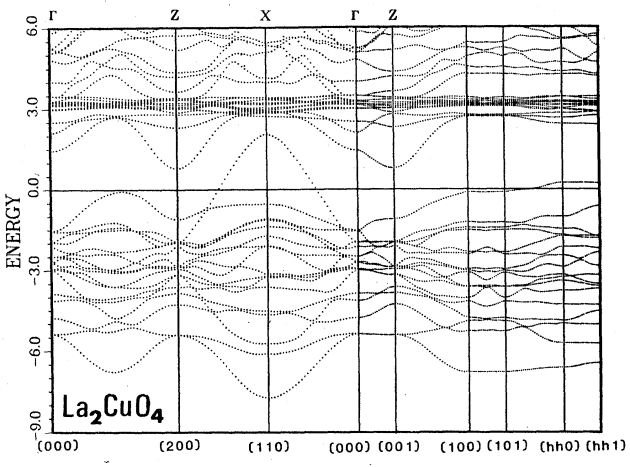

FIG. 15. Energy-band structure of La_2CuO_4 (h denotes $\frac{1}{2}$). The Fermi energy is taken as the energy zero. The dispersion along Γ-Z at the center of the figure indicates that dispersion along the c axis is not negligible. Bands clustered at 3 eV are La f bands. Bands at and below the Fermi energy are Cu-O bands. From Krakauer, Pickett, Papaconstantopoulos, and Boyer (1987).

single band of antibonding $pd\sigma$ character crosses E_F, which is obtained by all methods of calculation. Beyond this similarity, however, many of the calculations show differences in detail, and occasionally differences in important aspects. One item that is straightforward to compare is the position of the highest occupied band at Γ. The well-converged (in basis set) LAPW calculations of Xu *et al.* (1987) and Krakauer *et al.* (1987) put this band at -1.5 eV (relative to E_F), as does the LCAO calculation of Leung *et al.* (1988) (for Sc_2CuO_4). The LAPW calculation of Mattheiss (1987), which was carried out at somewhat lower convergence, put the band at about -1.2 eV.

Mattheiss has noted that valence-band extrema, which occur at the zone corner X point, are directly related to the bonding and antibonding combinations of Cu $d(x^2\text{-}y^2)$ and O_{xy} $p(x,y)$ orbitals. A simple tight-binding model derived from these states, with on-site energies $E_d = E_p = -3.2$ eV (relative to E_F) and $(pd\sigma) = -1.85$ eV, reproduced the dispersion near these extrema. A detailed tight-binding analysis of the band structure will be presented in Sec. IV.G. The total and atom-projected densities of states (DOS) in Fig. 16 confirm that the centroids of the Cu d and O p states are more or less coincident. This result is quite different from the rocksalt-structure transition-metal oxides MO, M=Mn, Fe, Co, and Ni, which have been studied by Mattheiss (1972), by Andersen *et al.* (1979), and by Terakura, Williams, *et al.* (1984). In these rocksalt oxides the O p bands are completely filled and lie below the d bands, although the mixing is certainly not negligible and becomes larger for the heavier members of the series.

A first guess might be that the coincidence of Cu and

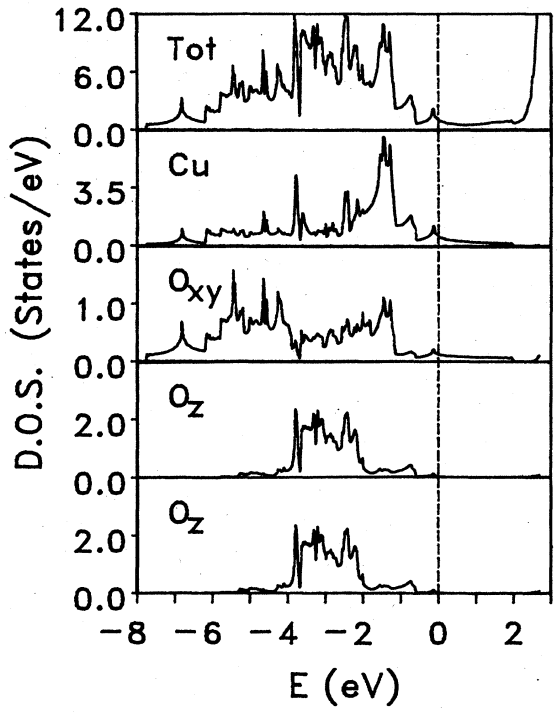

FIG. 16. Total and partial density of states for La_2CuO_4. Note the van Hove singularity lying just below the Fermi level (at −0.1 eV). The O_{xy} partial density of states is nearly twice as broad as for O_z. From Pickett, Krakauer, Papaconstatopoulos, and Boyer (1987).

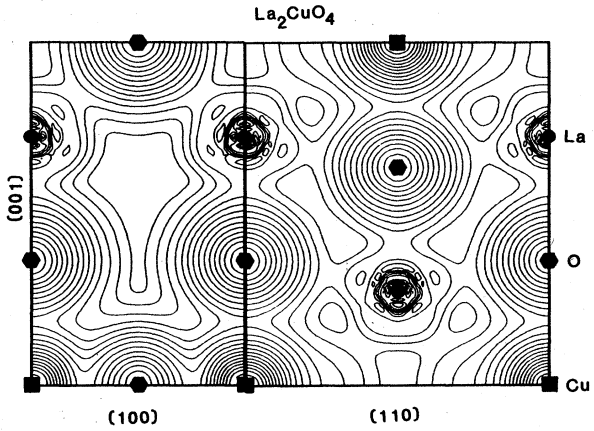

FIG. 17. Contours of constant values of the logarithm of the valence density of La_2CuO_4, in two high-symmetry planes as labeled. The La ion is nearly (but not completely) ionized to La^{3+}, the O_z ion is fully ionic (O^{2-}), while the Cu and O_{xy} atoms (bottom and top of the figure) are covalently bonded to some degree.

O on-site energies in La_2CuO_4 might be the result of ionic contributions to the crystal field, which could serve to lower the Cu site energy with respect to the O site energy. For (fictitious) rocksalt-structure CuO, however, Papaconstantopoulos (1988) has shown that again the Cu d and O p states lie at about the same energy and are completely hybridized (see Sec. VII). Thus ionic contributions to the crystal field do not appear to be responsible for the strong Cu-O hybridization; rather, it is primarily the natural falling of the Cu d states across the transition-metal series that leads to the intimate mixing in copper oxides. CuO actually forms in an unusual distorted structure with four formula units per cell, and apparently the electronic structure of this reference material has never been published. [Ghijsen *et al.* (1988) have presented a broadened density of states from otherwise unpublished calculations of M. Y. Czyzyk and R. A. de Groot. A cluster model study has been presented by Eskes, Tjeng, and Sawatzky (1989).]

There are several aspects of the band structure that provide insight into the unusual properties in this system. The charge density itself, shown in high-symmetry planes in Fig. 17, reflects the strong ionic nature of this compound. While the charge along the Cu-O_{xy} nearest-neighbor directions looks metallic, there are regions of very small density between the La and O_z ions, as well as at the center of the Cu-O_{xy} squares within the planes. It is tempting to try to obtain the "ionic charges" on the various atoms, but such attempts typically are rather sensitive to how the charge between atoms is assigned to particular atoms, and the results are unconvincing.

There is an unambiguous way in which some aspects of the ionic nature of the charge density can be identified. This is to compare the crystal density with some reference density that is "understood" or well characterized. For example, if one takes as the reference density overlapping ionic densities corresponding to La^{3+}, Cu^{2+}, and O^{2-}, and subtract that from the self-consistent crystal density, the difference obtained is as shown in Fig. 18. The difference around the La and O_z sites is very small, showing that these ionic representations are very good. The method of preparing the density of the O^{2-} ion, which is only stabilized by the crystal field of ionic crystals, is discussed in a later section.

In the region of the Cu and O_{xy} atoms, the density difference is rather large. Most noticeable is that the difference is strongly nonspherical; the overlapping ion model puts more charge along the Cu-O bond than should be there, except exactly in the middle, where there is a small increase over the overlapping ion density. For definiteness we consider the region containing a Cu atom at the origin and the O atom along the x direction at $(\frac{1}{2},0,0)a$. The primary result is that charge leaves this region, where it is represented in the crystal by Cu $d(x^2\text{-}y^2)$ and O $p(x)$ states, and moves to the regions described by $d(z^2)$ and $p(z)$ states. This is an indication that the $d(x^2\text{-}y^2)$ and $p(x)$ states are unfilled. For the O atom along the y direction, it would be the $p(y)$ state that is unfilled. This conclusion is consistent with the observation from the band structure and DOS (above) that the single half-filled band is of $pd\sigma$ character, since this character involves precisely the same atomic states.

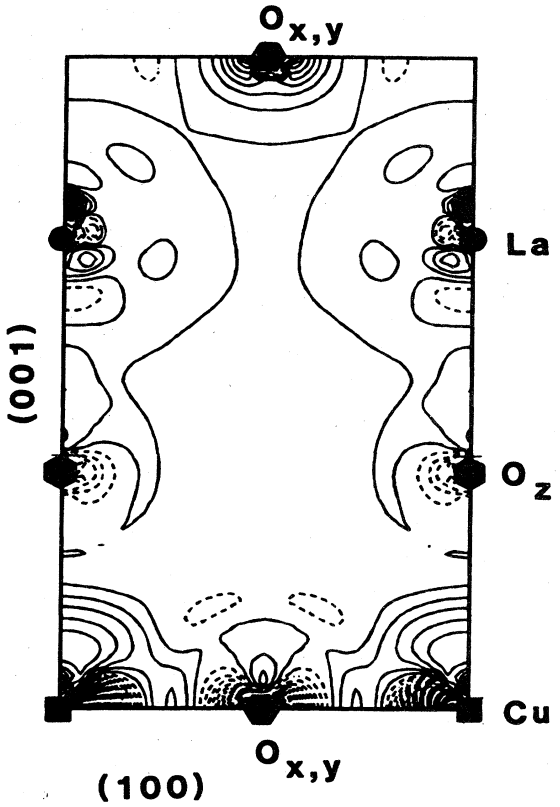

FIG. 18. Contour plot of the difference between the crystal density of La_2CuO_4 (Fig. 17) and a model density constructed from spherical La^{3+}, Cu^{2+}, and O^{2-} ions. The La and O_z ions are well represented by spherical closed-shell ions, while considerable charge rearrangement occurs in the Cu-O_{xy} layers. From Cohen, Pickett, Boyer, and Krakauer (1988a) and Cohen, Pickett, Krakauer, and Boyer (1988).

Although it is not possible to assign ionic charges exactly in systems such as this, where there is strong metallic or covalent bonding betwen some of the atoms, rough guidelines can be given. Clearly the La and O_z ions are essentially fully ionic. Charge neutrality then requires that, if the Cu ionic charge is designated as $+(2-2\delta)$, the O_{xy} charge is $-(2-\delta)$. The fraction of empty states on the Cu and O_{xy} atoms could be obtained by integration of the respective atom-projected DOS, leading to an estimate, but these numbers have not been published. A different method, which uses the rms difference between overlapping ionic densities and the crystal density, has been used to estimate ionic charges in $YBa_2Cu_3O_7$ (Sec. IV.D).

Now we return to the band structure itself. The dispersion perpendicular to the Cu-O layers is small but not vanishingly so. This dispersion can be seen directly in the band-structure plots along the short Γ-Z direction. It is also reflected in the near symmetry of the bands along the line $\Gamma-\Delta-U-Z=(k_x,0,0)$ (the first panel in Fig. 15); two-dimensional (2D) bands would have reflection symmetry about the midpoint of this line, a fact that follows from the bct symmetry. This approximate symmetry is also reflected in the Fermi-surface cross sections shown below; a truly 2D Fermi surface will be the same when viewed from Γ and from Z.

The coupling of states from one plane to another must proceed via the La or O_z atoms, or both, along routes such as (Cu,O_{xy})-A-B-(Cu,O_{xy}), where either atom in parentheses may apply, and the pairs (A,B) can be (La,La), (O_z,O_z), or (La,O_z). The states via which the interaction can occur, that is, those states nearest in energy, are, for La, the unoccupied d and possibly the f states, and for O_z the occupied p states. The La d states extend down to within 1–2 eV of E_F, while O_z p states, while filled, extend right up to E_F. Thus it may be expected that for states at and below E_F, the most important interplanar interactions are mediated by the O_z p states. We shall return to this point below in discussing and analyzing tight-binding fits to the band structure.

The states at the Fermi energy are not spread evenly over the unit cell, but rather are confined strongly to the Cu-O networks in the layer. The charge density of the state at E_F midway between Γ and X has been calculated and plotted by Yu, Freeman, and Xu (1987). A large fraction of the density of this state lies within a slab of thickness no more than 20% of the interplanar separation ($c/2=6.2$ Å), i.e., a slab of about 1 Å thickness. Moreover, the charge is not spread evenly over the slab, but stays close to the Cu and O atoms, leaving a square array of large holes in the center of the squares. These observations are consistent with expectations arising from the analysis of the charge density given above and may have implications that are not yet completely understood.

The Fermi surface, which is relatively simple and roughly two dimensional, is shown in Fig. 19. The Fermi-surface shape has a number of implications for the observed properties of the 214 system. In the crudest approximation, in which the bands are described by the simple $pd\sigma$ bands discussed above, the Fermi surface for the half-filled band is an array of square cylinders touching at the corners, which can be regarded as containing electrons around Γ or containing holes around X. Such a Fermi surface has perfect nesting for the wave vector $\mathbf{q}=X=(1,1,0)\pi/a$. Strong nesting can lead to either a charge-density wave, which for this commensurate wave vector could show up as an X-point soft-mode transition, or a spin-density wave, or possibly both. In fact, candidates for both of these instabilities occur, leading to a considerable amount of analysis and speculation about Fermi-surface-driven instabilities in the La214 system.

The tendency toward Fermi-surface-driven instabilities is given a general measure in terms of the generalized susceptibility $\chi(\mathbf{Q})$, by

$$\chi(\mathbf{Q})=\sum_{\underline{k}}(f_{\underline{k}}-f_{\underline{k}+Q})/(E_{\underline{k}+Q}-E_{\underline{k}})\ ,$$

where $E_{\underline{k}}$ is the band energy and $f_{\underline{k}}=f(E_{\underline{k}})$ is the Fermi function. The susceptibility toward charge-density or

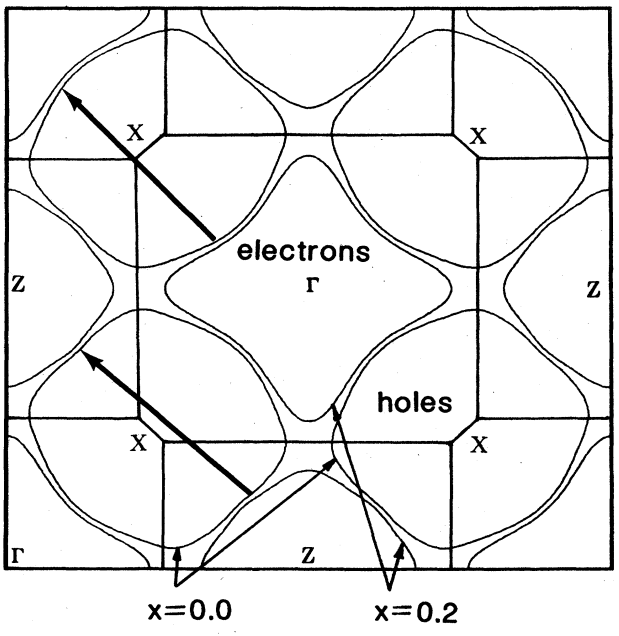

FIG. 19. Fermi surface of paramagnetic $La_{2-x}M_xCuO_4$ in the $k_z=0$ plane, for $x=0.0$ and 0.20, showing the change in topology from enclosed holes for E_F above the van Hove singularity to enclosed electrons for E_F below the van Hove singularity. The area between the enclosed regions represents electrons for $x=0.0$ and holes for $x=0.2$. The bold arrows represent approximate nesting wave vectors; both of those drawn are somewhat longer than the Γ-X distance. From Pickett, Krakauer, and Cohen (unpublished).

spin-density wave instabilities in a crystal involves a matrix generalization of χ with appropriate matrix elements. However, the **Q** dependence is usually provided by this generalized scalar form. Structure depends mostly on near-parallel sheets of Fermi surface, with the stronger nesting leading to sharper structure.

The susceptibility has been calculated along the Γ-X direction by Leung, Wang, and Harmon (1988) and by Xu *et al.* (1987). Leung *et al.* obtained the results shown in Fig. 20, with χ increasing away from Γ, reaching a plateau halfway to the X point, and increasing to a rather broad maximum at X which is twice its value at Γ. Only the band crossing E_F is included in the calculation, since other bands can give contributions that are only weakly dependent on **Q**. The peak at X is significant in that it coincides with the ordering wave vector in the antiferromagnetic state, just as would be expected for a Fermi-surface-driven spin-density wave.

The results of Xu *et al.* are shown in Fig. 21. For the stoichiometric compound their results are consistent with those of Leung *et al.* They also calculated χ for (rigid-band) doping concentrations of $x=0.17$ (corresponding to their van Hove peak) and $x=0.20$, also shown in Fig. 21. The susceptibility peak now occurs away from the X point, about 10% toward Γ, and is only about 30% higher than at the zone center. The movement of the peak away from the X point is particularly relevant to the recent discovery (Birgeneau, Endoh, *et al.*, 1989) that, in doped La214 materials, the ordering wave vector (magnetic scattering peak) moves inward from the X point in a

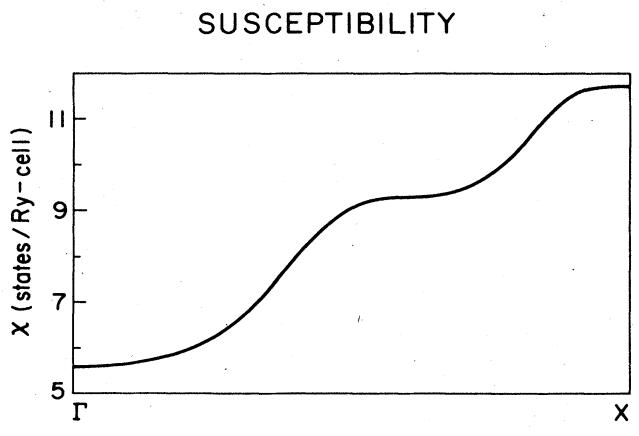

FIG. 20. Generalized susceptibility of La_2CuO_4 along Γ-X calculated by Leung, Wang, and Harmon (1988). The peak occurring at the X point suggests the possibility of Fermi-surface-driven instabilities at this wave vector.

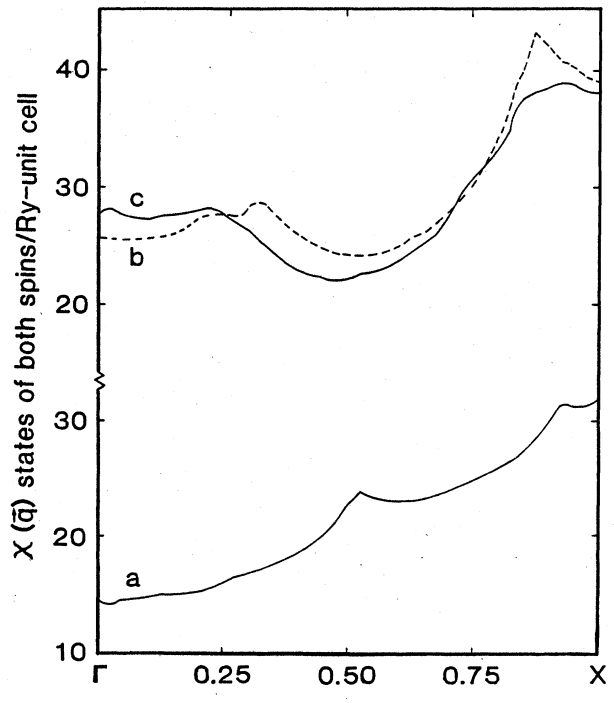

FIG. 21. Generalized susceptibility of $La_{2-x}M_xCuO_4$: *a*, $x=0.0$; *b*, $x=0.17$; *c*, $x=0.20$; calculated by Xu, Watson-Yang, Yu, and Freeman (1987). Note the different scale for curves *b* and *c*. Although the peak near X strengthens somewhat with doping level (increasing x), the **q** dependence weakens dramatically due to the strong increase at $\mathbf{q}=0$ [reflecting the increase in $N(E_F)$].

very similar fashion. Xu *et al.* argued that the movement of the peak in χ away from the X point with doping could account for the loss of the tetragonal-to-orthorhombic instability with doping. As discussed in Secs. IX and X, however, this instability does not appear to be driven by Fermi-surface nesting.

2. La_2CuO_4: T-O structural instability, orthorhombic phase

The first implication of either the charge-density or the spin-density wave state is that the Fermi surface or at least a substantial portion of it, is destroyed and a gap opens up at E_F. Such a symmetry-breaking instability could result in a nonmetal and, therefore, a nonsuperconductor. The band energy gain arising from the gap is usually thought to drive such a transition by overwhelming the loss in Coulomb and strain energy which favors the symmetric state. A crucial relationship to explore, then, is which X-point instabilities, either structural or magnetic, open a gap at E_F.

Mattheiss (1987) observed that there are two obvious candidates for a structural distortion in the 214 system, if the $pd\sigma$ bands at E_F are the important ones. One distortion has quadrupolar symmetry around the Cu atom, with one pair of O_{xy} atoms moving in toward the Cu and the other pair moving outward. The other one Mattheiss considered was the planar breathing mode, in which all four O_{xy} atoms move toward the Cu [and away from Cu neighbors at $(1,1,0)a$]. Both of these distortions lead to first-order changes in the $pd\sigma$ interaction. Using a tight-binding picture, he found that only the breathing distortion opened a gap, and therefore it should be most strongly coupled to the electronic system. (Note that neither of these distortions is a normal mode of the actual crystal structure, although they may be reasonable approximations due to large mass differences between the various atoms.)

Mattheiss performed LAPW calculations for a doubled cell of La_2CuO_4 in which a breathing distortion of the O_{xy} atoms was frozen in. He used a nearest-neighbor Cu-O displacement of 0.064 Å in analogy with the magnitude of the R-point breathing displacement in $BaBiO_3$. The gap that opened at E_F varied between 0.2–0.5 eV, corresponding to large deformation potentials of 1.6–3.9 eV/Å. This calculation confirmed a substantial coupling of the planar breathing mode to the lattice. Although this breathing distortion has orthorhombic symmetry, it is different from the *Abma* space group of the observed orthorhombic phase.

Since this straightforward picture suggests that the breathing-mode distortion should be most unstable, it was somewhat surprising that the observed structural transformation, described in Sec. II, did not involve the breathing mode at all, but rather a mode that was not considered by Mattheiss. It was pointed out by Whangbo *et al.* (1987a) and Kasowski, Hsu, and Herman (1987a) that the actual distortion, shown in Fig. 3, will not create a gap. The reason is illuminated in Fig. 22, which shows how the body-centered-tetragonal Brillouin zone is folded down into the face-centered-orthorhombic Brillouin zone due to the unit-cell doubling. The symmetry of the low-temperature *Abma* (*Cmca*) space group implies twofold degeneracies (besides the spin degeneracy) along several zone boundary lines in the low-temperature *Abma* structure. Since the number of valence electrons in $(La_2CuO_4)_2$, which is 66, is not divisible by four, at least one of these degenerate bands must cross E_F, so no gap can occur in the paramagnetic

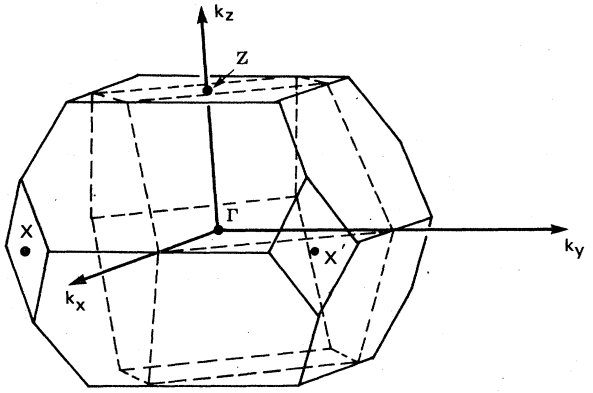

FIG. 22. Illustration of the folding of the Brillouin zone at the structural transition from body-centered-tetragonal (solid lines) to face-centered-orthorhombic (dashed lines). The X point is folded back to Γ, while the X' point is folded back to Z. Bands on the hexagonal face of the orthorhombic zone are doubly degenerate by symmetry.

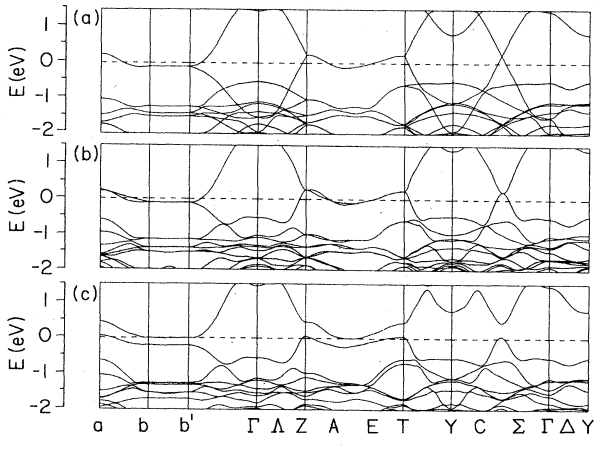

FIG. 23. La_2CuO_4 band structure in the orthorhombic zone for (a) undistorted, (b) frozen-in tilt mode (orthorhombic La_2CuO_4 at the experimental amplitude), and (c) frozen-in planar Cu-O breathing mode. The breathing mode creates a splitting throughout the zone near the Fermi level (dashed line), while the tilt mode does not do so. The points a, b, and b' are (100), (110), and (111) in units of π/a, π/b, π/c. From Cohen, Pickett, and Krakauer (1989).

band structure. This argument is somewhat analogous to the fact that a paramagnetic system with an odd number of electrons in the primitive cell cannot be insulating (in the band picture). As will be shown in Sec. VIII, antiferromagnetism breaks an essential symmetry which makes the two Cu sites equivalent and allows a gap to occur.

Cohen, Pickett, and Krakauer (1989) have calculated the effect of both the breathing mode and the tilt mode on the paramagnetic band structure of La_2CuO_4. The reference band structure in the orthorhombic zone is shown in Fig. 23, together with the bands with frozen-in tilt and breathing modes. The opening of the gap described by Mattheiss can be seen; due to the strong coupling of this mode the gap opens rapidly, but due to its curvature (i.e., imperfect nesting) the Fermi surface disappears smoothly. This figure also illustrates that no gap is opened by the tilt mode, although bands at E_F are split and the Fermi surface is altered. As shown in Fig. 24, this (paramagnetic) Fermi surface is altered rather more severely by the orthorhombic tilt distortion than is apparent from the bands in Fig. 23(b).

The preliminary conclusion of the studies of the effect on the band structure of the various distortions is that the T-O transformation is not driven by Fermi-surface nesting. Upon further consideration, this conclusion is not so surprising. Polarized neutron scattering experiments and transport studies have established that La_2CuO_4 is an antiferromagnetic insulator below the Néel temperature $T_N = 250$ K, which is below the T-O transformation temperature $T_s = 500$ K. Moreover, these experiments have also established that even above T_N and T_s, spin correlations persist (Sec. VIII) and the material remains nonmetallic. This suggests that locally the material can still be considered as an antiferromagnetic insulator, with the accompanying energy gap at E_F. These phenomena can then be understood if the spin-density wave instability is stronger than the charge-density wave instability, effectively destroying the Fermi surface at all temperatures. Whether this interpretation can be defended by antiferromagnetic band-structure calculations is discussed at some length in Sec. VIII.

D. Self-consistent calculations: Y123 system

Since the Y123 system has two CuO_2 layers, which should be rather weakly coupled (electronically) to the CuO chain, a pair of layer-derived CuO_2 $pd\sigma$ bands is expected to cross E_F, each similar to the corresponding bands in the La214 system. In addition, since the Cu1, O1, and two O4 atoms form in a first approximation a one-dimensional system, bands with roughly one-dimensional (1D) dispersion are expected as well. Both of these expectations are borne out by the band calculations. The complete bands calculated by Krakauer, Pickett, and Cohen (1988) using the LAPW method, are shown in Fig. 25. The corresponding orthorhombic Brillouin zone and symmetry point and line labeling are included in Fig. 4.

Several LAPW calculations for this compound have been reported (Krakauer and Pickett, 1987; Massidda *et al.*, 1987; Krakauer, Pickett, and Cohen, 1988; Mattheiss

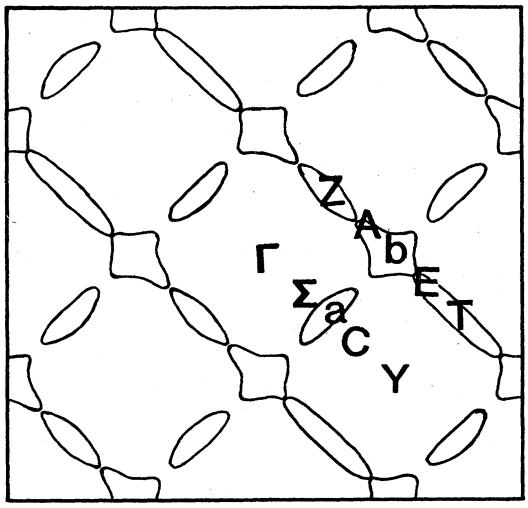

FIG. 24. Effect of the orthorhombic *Abma* distortion on the calculated Fermi surface of La_2CuO_4, with labels denoting symmetry points. The distortion not only strongly suppresses Fermi-surface nesting, but the Fermi surface becomes noticeably nontetragonal, in spite of the small amplitude of the distortion. This Fermi surface can be compared directly to that of tetragonal La_2CuO_4 shown in Fig. 19, which is drawn in the same plane. From Cohen, Krakauer, and Pickett (1988).

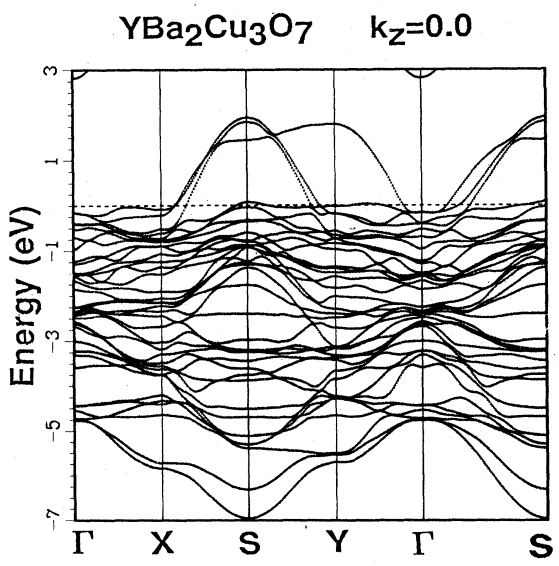

FIG. 25. Full band structure of $YBa_2Cu_3O_7$, from Krakauer, Pickett, and Cohen (1988). The total Cu-O bandwidth is calculated to be more than 9 eV. The band dispersing downward from above E_F along Y-Γ is the chain O-Cu $pd\sigma$ antibonding band. The Cu-O layer bands disperse downward from above E_F along both S-X and S-Y.

and Hamann, 1988c; Park *et al.*, 1988). The calculations of Mattheiss and Hamann were initiated at an early stage, before the structure was known in detail, and they guessed (incorrectly) that the Cu-O chains lay along the a direction (i.e., the short lattice constant direction). In addition, the number of LAPW basis functions was only about 70% of the number used by Krakauer and Pickett to give high convergence. Nevertheless, the antibonding layer and chain bands crossing the Fermi level were similar to the other LAPW bands; some aspects of the resulting Fermi surface were of course different. An interesting and unexpected feature is another band crossing E_F, which in fact remains near E_F all along the Σ-Y-Γ symmetry lines. In Mattheiss and Hamann's calculation this band is considerably different from what it is in the other LAPW studies, and even in these other calculations there are noticeable differences in detail. Unfortunately most of the publications have been rather brief and have not been specific about the details of the computations, so it is often not possible to establish the origin of the differences.

Using the wave functions, it is possible to discern which bands in the Cu-O valence-band complex arise from the chains and which arise from the layers. This has been done in Fig. 26 where it can be seen that, due to band crossings and hybridization, different parts of a "band" can arise from the different subsystems. The first thing to notice from this figure is that the chain and layer $pd\sigma$ antibonding bands are well in evidence; the layer bands [Fig. 26(b)] look much like those of La_2CuO_4, while the chain bands [Fig. 26(a)] are different. One chain band disperses strongly along the chain direction and arises from O1-Cu1 $pd\sigma$ interactions, as expected from simple considerations. The other chain band, discussed at greater length below, has much less dispersion near E_F, and its occurrence is not obvious from simple models. Another feature to note from Fig. 26 is that a large majority of bands within 0.6 eV below E_F is associated with the chain. This will also show up in the discussion of the DOS given below.

Let us return to the discussion of the unexpected band at E_F. Krakauer and Pickett and Yu *et al.* find very similar dispersion: it is positive (i.e., above E_F) at the zone corner S, disperses to negative values along S-Y, lies almost at E_F at Y, and becomes positive halfway along Y-Γ. Park *et al.*, however, find it above E_F only at S, leading to only a small hole pocket surface from this band while the other two calculations will give rise to a more complicated Fermi surface and DOS peaks near E_F, as described below. Yu *et al.* describe this as a π-bonding band formed from Cu1 $d(xy)$–O1 $p(x)$–O4 $p(y)$ orbitals. Krakauer and Pickett have plotted the charge density at the midpoint between Γ and S (the center of the irreducible zone). As shown in Fig. 27(a), the character in the yz plane is just as described by Yu *et al.*, with some Cu2 $d(x^2\text{-}y^2)$ character as well. In the xz plane, shown in Fig. 27(b), the state is seen also to have Cu1 $d(xz)$ and O4 $p(x)$ character. The most remarkable aspect to note from Fig. 27 is that a very large fraction of the weight lies on the O1 and O4 atoms (many of the high-density contours are not shown), with rather little on the Cu atoms. Thus this is a state that lies primarily on the chain, that has the Cu1 atom as its backbone, but that avoids the Cu1 atom.

The possible significance of such character is only recently becoming clear. Electrons in this state propagate along the chain by hopping from O1 to O4 to O1 atoms without spending appreciable time on the Cu1 site. This type of propagation is allowed by large O1-O4 $pp\sigma$ hopping. McMahan, Martin, and Satpathy (1988) have

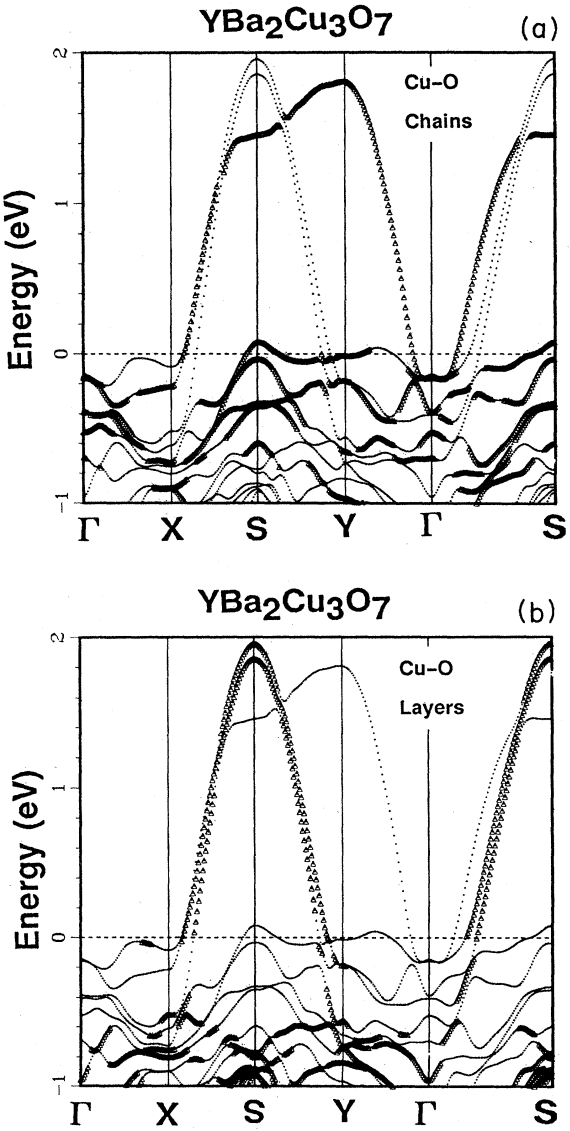

FIG. 26. Band structure of $YBa_2Cu_3O_7$ near the Fermi level. In (a), the chain-related bands are accentuated with large symbols, while in (b) the layer-related bands are accentuated. Note that most of the bands within 0.6 eV below E_F (denoted by the dashed horizontal line) are chain-derived states. From Krakauer, Pickett, and Cohen (1988).

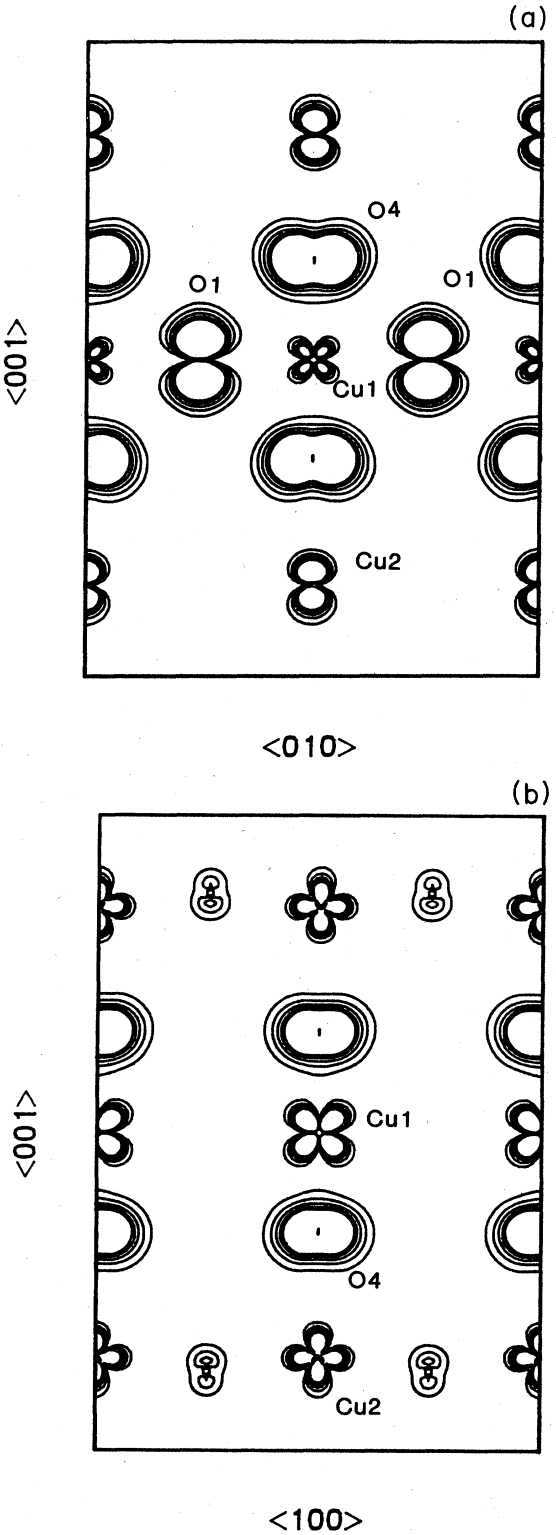

FIG. 27. Contour plot of the charge density of the state just below E_F in $YBa_2Cu_3O_7$, discussed in the text. Two symmetry planes, one containing the Cu1-O1 chain and one perpendicular to it, are shown. The state is more than 90% on the O1 and O4 atoms, and strongly avoids the Cu1 atom. From Krakauer, Pickett, and Cohen (1988).

demonstrated that such O-O hopping in La_2CuO_4 leads to a 6-eV bandwidth even before consideration of O-Cu hopping. Many of the model Hamiltonian approaches to the cuprates which initially included only O-Cu $pd\sigma$ hopping parameters have now been generalized to include this essential feature. In many of the model Hamiltonian pictures, electrons/holes are discouraged from hopping to the Cu site because of a large Coulomb repulsion of existing Cu electrons/holes, and therefore tend to hop from oxygen to oxygen within the ligand coordination shell. It is therefore highly significant that states of similar character, though certainly not of identical origin, also occur at E_F in the band calculations. The proximity of these states to the Fermi level suggests such character may be involved in some of the unusual behavior shown in this system, particularly considering that oxygen-deficient material has oxygen vacancies in these chains. Such states are also crucially involved in the interpretation of electronic spectroscopies and are discussed in Sec. V.

Band structures of $YBa_2Cu_3O_m$, $m=6$, 7, and 8, have been calculated with a variety of methods. The $m=6$ compound is antiferromagnetic, and studies of the nature of the magnetism are discussed in Sec. VIII. Here we discuss only the paramagnetic calculations. Pseudofunction calculations of the bands near E_F have been reported by Herman, Kasowski, and Hsu (1987a, 1987b, 1988), for $m=6$, 7, and 8. For the superconducting $m=7$ compound, the $pd\sigma$-derived bands are similar to the LAPW bands described above, but the layer-derived bands are more strongly split. The $pd\pi$ band differs in some details. LMTO band structures have been presented by several groups, with representative bands reported by Temmerman, Szotek, *et al.* (1987). [The LMTO results of Szpunar and Smith (1988c) are in severe disagreement with all other calculations and must reflect some calculational error.] The bands generally are very similar to the LAPW bands, except that details, such as the precise positions and dispersion of the $pd\pi$ band, do differ, as expected from the simplifications inherent in this method. Results of Xu, Ching, and Wong (1988), using a self-consistent linear combination of atomic orbitals method, also differ in the details of the $pd\pi$ bands but are very similar otherwise. These comparisons point out the importance of a sufficiently complete basis set and a full representation of the density and potential for representing details of the bands.

The total and partial densities of states for $YBa_2Cu_3O_7$ are shown in Fig. 28, with an enlargement near E_F in Fig. 29. The Fermi level falls just above the high-DOS region, and lies 0.1 eV above a very sharp peak of chain-derived O1-O4 states described above. The value of $N(E_F)$ has been reported as 5.54 (Krakauer, Pickett, and Cohen, 1988) and 6.8 (Massidda *et al.*, 1987), in states/eV-cell, both spins. (The values reported by Massidda *et al.*, although stated only as "per cell," must also be per spin to give their DOS curve the correct normalization.) The difference in these two numbers, which this

author believes to be the most accurate, reflects the sensitivity of $N(E_F)$ to the calculational details. The value of Massidda *et al.* is higher because the peak below E_F is only 0.05 eV below, whereas Krakauer, Pickett, and Cohen find a peak that is sharper and 0.1 eV below. The DOS and Fermi level were obtained by Krakauer, Pickett, and Cohen using an improved Fourier spline interpolation method (Pickett, Krakauer, and Allen, 1988), and convergence parameters of the LAPW method were more strict. Generally both the total and partial DOS of these two calculations are in excellent agreement.

Several features can be noted from the partial DOS in Fig. 29. The O2 and O3 densities of states are virtually identical, indicating that the orthorhombicity arising from the chain has very little effect on the electronic structure of the Cu-O layer; otherwise the O2 and O3 partial densities of states would differ. There is a strong difference between the partial DOS of Cu1 and that of Cu2 near E_F: the chain Cu1 atom has considerable weight within 1 eV of E_F, whereas the corresponding weight of Cu2 appears to be shifted downward by 1 eV. Their spectral distribution at lower energies is very similar, however, so this difference cannot be ascribed simply

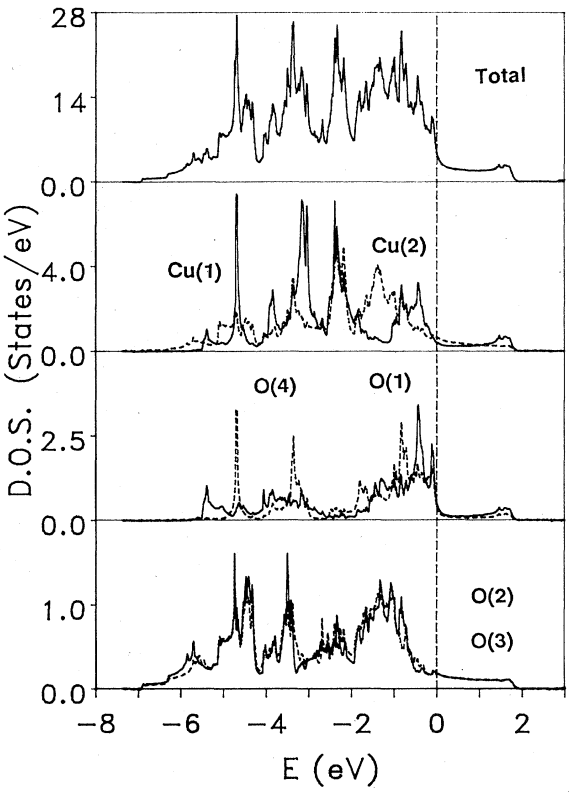

FIG. 28. Total and partial densities of states (DOS) of $YBa_2Cu_3O_7$, from Krakauer, Pickett, and Cohen (1988). Top panel, total DOS; second panel, Cu1 (solid) and Cu2 (dashed) DOS; third panel, O1 (solid) and O4 (dashed) DOS; bottom panel, O2 and O3 DOS, which are nearly identical.

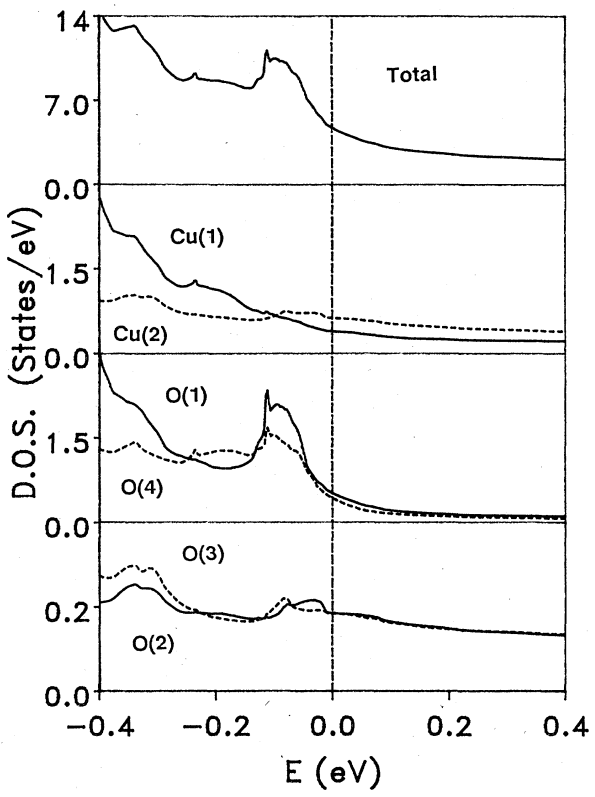

FIG. 29. Enlargement of the densities of states of Fig. 28 near the Fermi level. From Krakauer, Pickett, and Cohen (1988). Note that the striking peak just below E_F involves *only* chain oxygen (O1 and O4) states.

to a difference in site energies of 1 eV. Another difference is that, although the layer and chain bands extend to very similar positions at the top of the bands (above E_F), the partial DOS curves show that the chain-derived bands (i.e., Cu1, O1, O4) extend down only to (roughly) -5.5 eV, while the layer bands extend to -7 eV. The total layer valence bandwidth therefore is 9 eV, whereas the chain bandwidth is 7.5 eV. Many other details are discussed in the original papers. Figure 29 reveals that the sharp peak just below E_F is totally chain derived, as would be expected from Fig. 26.

The Fermi surface calculated by Krakauer, Pickett, and Cohen (1988) is shown in Fig. 30, in planes parallel to the *ab* planes and for $k_z=0.0$ and at the zone boundary. The difference between right and left panels directly reflects the amount of dispersion in the *c* direction. There are two nearly degenerate Fermi surfaces arising from the two Cu-O layer bands, and these are rather similar in all calculations. It should be noted that these surfaces must be regarded not as one arising from each Cu-O layer, but rather as due to bonding and antibonding combinations of states on the Cu-O layers. Their similarity indicates the small interaction between them. They can be described roughly as squares with rounded corners. The large flat pieces lie perpendicular to the

(1,0,0) and (0,1,0) directions and provide large nesting at wave vectors in these directions with magnitudes of roughly $\frac{2}{3}\pi/a$ (between neighboring surfaces) and $\frac{4}{3}\pi/a$ (within the same surface). These nesting vectors have no clear relation to any known instability of the system.

A striking feature of these layer-derived surfaces is that they are oriented differently (rotated by $\pi/4$) with respect to the (also layer-derived) Fermi surface in paramagnetic La_2CuO_4. There have been many conjectures that in the La214 system the strong Fermi-surface nesting, which occurs very near the X point, may be related not only to the structural instability but also to the antiferromagnetically ordered state. (As discussed elsewhere in this article, the evidence for Fermi-surface-driven instabilities is *not* strong.) Park, Terakura, *et al.* (1988) have emphasized that the orientation of the calculated Fermi surface in $YBa_2Cu_3O_6$, which is quite similar to those in Fig. 30, is compltely wrong to have any relation to the antiferromagnetism, which has the same *ab*-plane wave vector as in La_2CuO_4. The reason for the difference in orientation of the Fermi surfaces in the La214 and Y123 systems does not seem to be understood. Park, Oguchi, *et al.* (1988) ascribe the difference to the axial oxygen coordination, but do not give any analysis.

The chains give rise to quite different types of Fermi surface, which are subject to some uncertainty because of the sensitivity of these bands to the convergence of the calculation. The surfaces shown in Fig. 30 consist of a zone corner S-centered tube along the c axis enclosing holes, and a one-dimensional-like slab with edges perpendicular to the k_y direction (the chain direction). This latter sheet should give rise to strong nesting for **Q** along the chain direction with magnitude $(0.2-0.25)\pi/b$, which could encourage instabilities in the Cu-O chain subsystem.

The valence charge density is shown in Fig. 31 in three

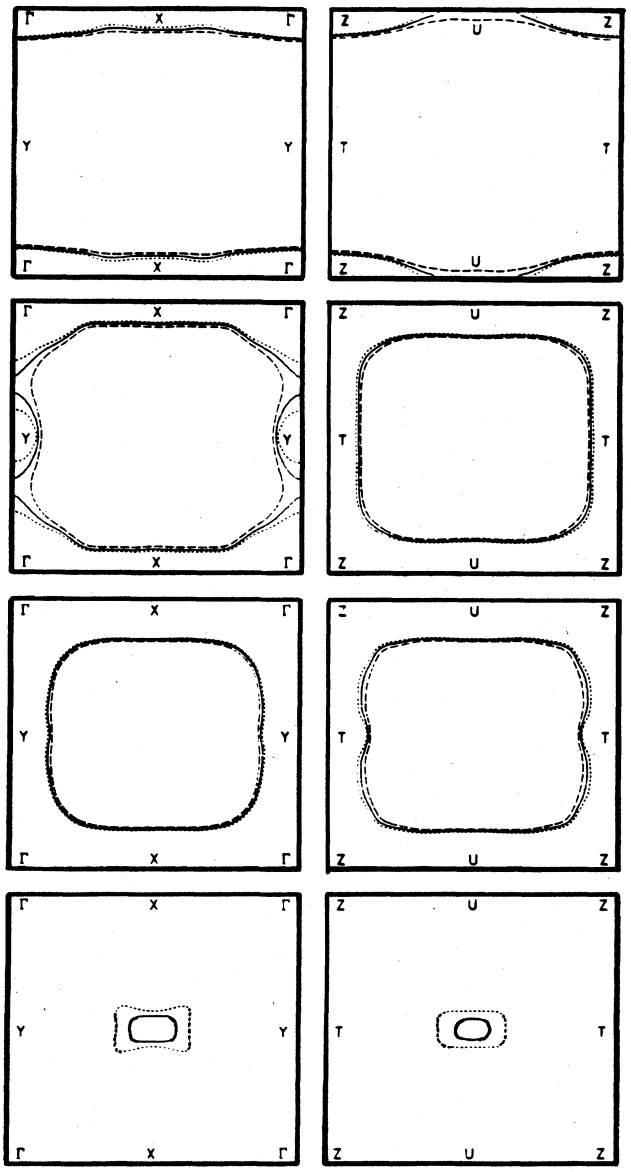

FIG. 30. Calculated Fermi surfaces of $YBa_2Cu_3O_7$ using the LAPW method, from Krakauer, Pickett, and Cohen (1988). The two middle panels show sheets arising primarily from the Cu-O layers, while the top and bottom panels show sheets arising from the Cu-O chains. The solid lines mark the calculated Fermi surface, while the short- (long-) dashed curve corresponds to a surface containing 0.2 fewer (more) electrons. The separation of the curves reflects the band mass.

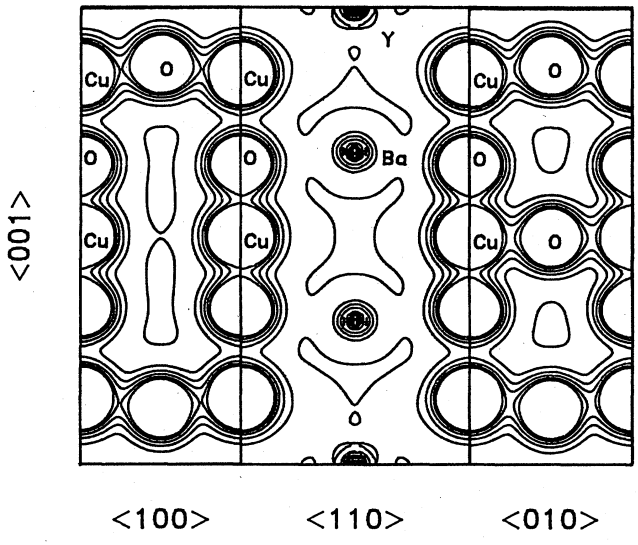

FIG. 31. Contours of constant valence charge density in $YBa_2Cu_3O_7$, in three high-symmetry planes, from Krakauer, Pickett, and Cohen (1988). Near the Ba and Y sites there is very little valence density, illustrating the nearly fully ionic character of the Ba and Y cations, and also accounting for the observed magnetic isolation of the Y site. Large contours at the Cu and O sites are not shown. The strong interaction between Cu1 and O4 atoms, and the relatively weak interaction between Cu2 and O4 atoms, can be seen from the contours.

high-symmetry planes containing atoms. It reveals that the Y and Ba ions are nearly completely ionized to Y^{3+} and Ba^{2+}. The valence charge density decreases to very small values in the interstitial regions, similar to what occurs in ionic materials. The Cu and O atoms are *not* representative of the corresponding ions in an ionic material, however. As a direct result of the short Cu-O distances, the densities of Cu and O ions are not distinct, but overlap strongly. This is especially apparent in the Cu-O2-O3 layers and in the Cu-O1-O4 chains. The overlap between the Cu2 and O4 (bridging) ions is much less than other intralayer or intrachain overlaps, as expected from the large Cu2-O4 separation. The lack of significant valence density at the Y site accounts for the "magnetic isolation" of this site seen experimentally, in which magnetic rare-earth ions placed at this site do not interfere at all with high-temperature superconductivity. Overall, the density reflects a material with components that are both strongly ionic and covalent or metallic in character.

Krakauer, Pickett, and Cohen (1988) have provided an analysis of the crystal density in terms of overlapping spherical ions. The assignment of ionic charges to atoms in crystals, even rather ionic ones, is a notoriously ill-defined task. However, a well-defined procedure may be meaningful even if it is nonunique. These authors compared the crystal density with a model density constructed from spherical densities, defining the goodness of the representation by the rms difference of the densities over the unit cell. The difference density is shown in Fig. 32. They found that the crystal density was best represented, within this picture, by Cu and O ions of net charges $+1.62$ and -1.69, respectively. Although there are still substantial differences, primarily due to additional nonsphericities of the crystalline density, these charges gave substantially smaller rms differences than did either $(+2.33, -2.00)$ or $(+2.00, -1.86)$ for the (Cu, O) charges. They did not try (nor see the need) to generalize the representation to different ionic charges on the crystallographically distinct sites, as is allowed by symmetry.

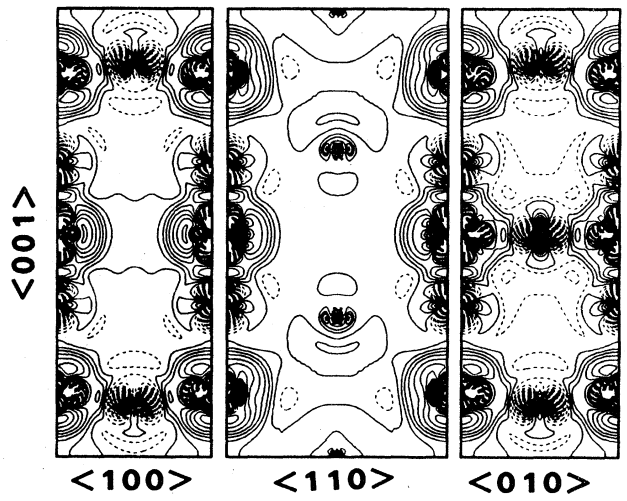

FIG. 32. Contour plot of the difference between the $YBa_2Cu_3O_7$ crystal density and a model density constructed from overlapping Y^{3+}, Ba^{2+}, $Cu^{1.62+}$, and $O^{1.69-}$ spherical ions. The differences are primarily due to nonspherical charge distortions on the Cu atoms and neighboring oxygen atoms. The differences are small on the Y and Ba ions. Atoms are placed as in Fig. 31. From Krakauer, Pickett, and Cohen (1988).

The calculations also provide other information that is important for the interpretation of experiments, such as the positions of core and semicore levels. Whereas deep-core-level energies are not given accurately by local-density approximation calculations (and no excitation energies are guaranteed by density-functional theory; Sec. IV.A), often the positions of the semicore levels are close to experimental core-level binding energies. More importantly for these copper oxides, the calculations give the differences in core-level positions for the inequivalent sites, which should be quite accurate (the systematic "errors" cancel). Massida *et al.* (1987) have reported positions of semicore levels. Krakauer, Pickett, and Cohen (1988) have also given the core-level differences for the Cu and O sites. For Cu, the core levels differ by 0.2–0.45 eV, depending on the particular core state, with the Cu1 energies being more tightly bound. For the O sites, the 1*s* core levels fall in the order of decreasing binding energy as O2 (0.00, taken as reference), O3 (-0.09), O1 (-0.29), O4 (-0.69), with relative binding energies in eV given in parentheses. These numbers give some measure of the difference in site energies and indicate that there will be an intrinsic spread of 0.7 eV in O 1s core-level spectroscopy because of the different crystallographic sites.

E. Self-consistent calculations: Bi, Tl systems

1. Bismuth compounds

The discovery of high-temperature superconductivity in $Bi_2Sr_2CaCu_2O_8$ (Bi2212) was significant not only because of the higher T_c, but also because it was the first high-T_c oxide that contained no rare-earth element. Although Bi commonly occurs in the 3+ (and 5+) valence state in salts, its chemistry differs significantly from that of the tripositive rare earths. This compound showed a T_c onset above 110 K and, unlike the Y123 and La214 systems, it does not require prolonged processing in an oxygen-containing atmosphere at high temperature. A number of calculations of the electronic structure and properties of Bi2212 have appeared. As noted in Sec. II, the structure of Bi2212 is complicated considerably for band studies by the existence of a superlattice formation, like that from a charge-density wave, with wavelength $4.76\sqrt{2}a$, where 3.812 Å is the lattice constant of a parent structure that is comparatively simple. All band-structure studies have been carried out for some variant of this parent crystal structure, which is body-centered

tetragonal $I4/mmm$ with $c=8a=30.52$ Å. LAPW calculations for Bi2212 have been reported by Krakauer and Pickett (1988), Massidda, Yu, and Freeman (1988a), and Mattheiss and Hamann (1988a). LMTO calculations have been presented by Hybertsen and Mattheiss (1988) and by Sterne and Wang (1988b), while Herman, Kasowski, and Hsu (1988) have completed pseudofunction studies. Thus the basic electronic structure of this system is already very well analyzed from the local-density viewpoint. We use the designation of O1, O2, and O3 sites presented in Sec. II.

Formal valence arguments would assign a 3+ state to the Bi ion. However, since the compound is metallic rather than insulating, it is clear from the start that the formal valences are of limited usefulness. The band structure, Fig. 33, and total and partial DOS, Fig. 34, immediately clarify this picture. As expected from the La214 and Y123 compounds, each of the Cu-O1 layers contributes a dispersive $pd\sigma$ band crossing E_F. In addition, the Bi-O3 layers each contribute to bands of Bi p and O p character, which lie mostly 2–3 eV above E_F, but dip below E_F along the Γ-Z direction. Around E_F these bands hybridize strongly with the Cu-O bands that lie immediately below E_F. Due to the occupied Bi p states in this part of the Brillouin zone, Bi will not be a fully tripositive ion, and due to the unoccupied partial DOS of O1, O2, and O3, these ions are not fully negative. The metallic states therefore extend over the complete O1-Cu-O2-Bi-O3 complex.

All the studies have noted the above features and the fact that the c-axis dispersion is smaller than in the La214 and Y123 systems, making them more two dimensional. Krakauer and Pickett (1988) noted that the valence density, shown in Fig. 35, is very small between adjacent Bi-O layers. Although the same observation holds for the two Cu-O layers, between the Cu-O layers there are Ca^{2+} ions, which can be regarded as providing one electron to the metallic $CuSrBiO_4$ slab on either side and therefore providing an ionic bonding to the slabs. Since there are no ions between the Bi-O layers, there is only very weak bonding from Bi-O layer to Bi-O layer, resulting in a natural exfoliation plane. The structure therefore consists of distinct neutral layers of one formula unit each, loosely stacked in the c direction. This feature of the bonding accounts for the highly lamellar, micaceous character of the material.

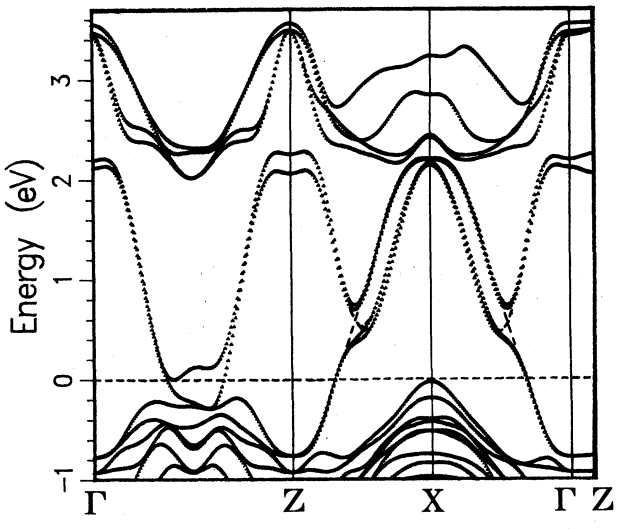

FIG. 33. Band structure of $Bi_2Sr_2CaCu_2O_8$, from Krakauer and Pickett (1988). In addition to the expected Cu-O bands derived from layers, two Bi-O bands drop below E_F along the Γ-Z direction. Dashed lines along Z-X-Γ indicate actual band crossings that were not well represented by the Fourier expansion used to plot the bands.

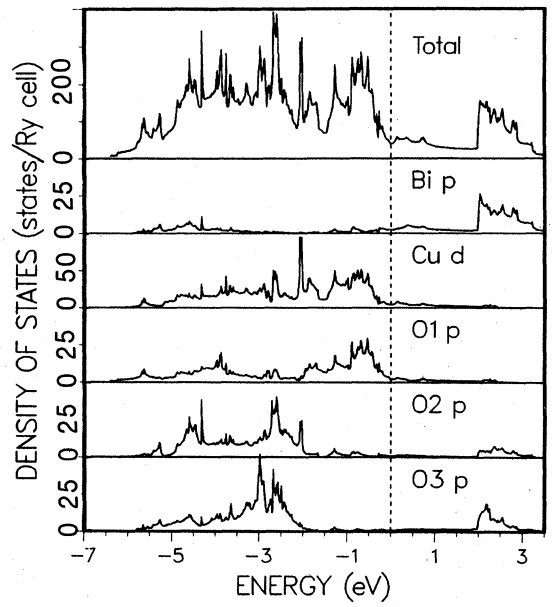

FIG. 34. Total and partial densities of states of $Bi_2Sr_2CaCu_2O_8$, from Krakauer and Pickett (1988). For Cu and O1, the distribution is similar to that of other cuprates. The Bi spectral density lies mostly 2–3 eV above E_F, but two Bi derived bands drop to or below E_F.

Hybertsen and Mattheiss (1988) provided a simple tight-binding analysis of the band structure. From the partial DOS of Fig. 34 they found Bi character well below E_F. The tight-binding analysis revealed a Cu-O1 $pd\sigma$ band as expected and in addition a Bi-O3 bonding complex of bands that extends to -5 eV. To provide a reasonable model of the Bi-O bands, Hybertsen and Mattheiss required Bi-Bi $pp\sigma$ and $pp\pi$ parameters of 0.5 and -0.25 eV, respectively, in addition to the Bi-O $pp\sigma=2.0$ eV parameter. The corresponding orbital energies were 0.7 eV for Bi p and -2.0 eV for O1 p states. Hybertsen and Mattheiss suggested that the Bi-O3 bands may act as a metallic reservoir, which, first, is not expected to suffer from possible correlation effects as the Cu-O states may and, second, seems to provide an electron pocket that allows an increase in the number of holes in

the Cu-O bands. Thus the Bi-O bands may provide an appropriate "electronic environment," similar to cation doping in the La214 system and the chains in the Y123 system, to promote superconducting Cu-O layers.

This picture was reaffirmed by the calculations of Sterne and Wang (1988b). They studied not only the Bi2212 material but also the corresponding Bi2201 material, which has only one Cu-O layer. This latter compound, which has T_c in the range 6–22 K, has much less Bi-O character at the Fermi level, and with small doping could even become insulating. Sterne and Wang suggest that the metallic Bi-O layer is important not only in possibly doping the Cu-O layers properly, but also in providing additional coupling of superconducting pairs along the c axis to allow higher values of T_c.

Mattheiss and Hamann (1988a) amplified on the tight-binding analysis of Hybertsen and Mattheiss and provided a very instructive decomposition of the bands into those which are primarily O1-Cu $pd\sigma$ bands, planar Bi-O3 bands, and the remainder. This decomposition illustrates very clearly the structure suggested by the tight-binding analysis described above. These authors also noted that, although the bonding between adjacent Bi-O3 layers is relatively weak, as discussed above, there is noticeable bonding between these layers. The bonding occurs between the Bi ion in one layer and the O3 ion in the adjacent layer; this can be seen in Fig. 35. The crescent moon of charge reflects this bonding, which appears to be more a polarization of the loosely bound Bi p charge than an actual covalent bond.

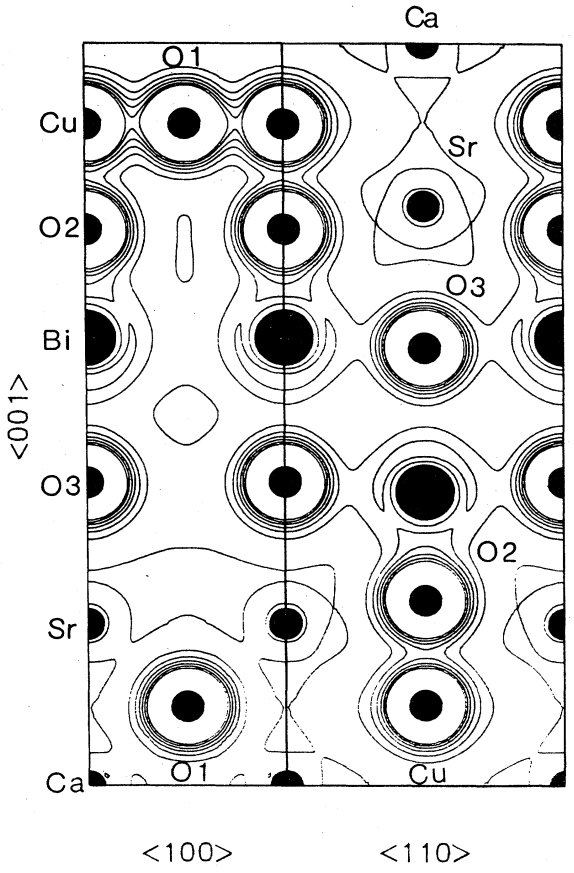

FIG. 35. Contours of constant charge density for $Bi_2Sr_2CaCu_2O_8$, showing the bonding within the Bi-O2-Cu-O1-Cu-O2-Bi-O3 complex. Note that there is very little bonding between the two BiO3 layers, providing a natural exfoliation plane. From Krakauer and Pickett (1988).

Herman, Kasowski, and Hsu (1988) investigated the effects of structural rearrangements of the Bi-O layers. Their work was prompted by the structural complexities (superlattice formations) that make the actual structure of the Bi-O layers uncertain. They found that the position and dispersion of the Bi-O bands are sensitive to assumed geometry of these layers. Therefore one must be careful not to attach too much significance to details of the bands calculated for the idealized crystal structures that have been assumed.

Massida, Yu, and Freeman (1988a) have provided a characterization of some of the important states in Bi2212. Their density plots of specific states are in agreement with the analysis given above; a plot of a Bi-O3 state explicitly shows Bi-Bi bonding as well as Bi-O3 bonding. They also point out that, for the structural model they used, there is a 1.5-eV spread in the O 1s core-level energies that needs to be taken into account in interpreting core-level spectroscopic data. This spread is larger than the corresponding 0.7-eV spread in the Y123 system discussed in the previous subsection. Both these authors and Krakauer and Pickett have presented the resulting Fermi surfaces. However, since the structural model is a simplification and the Bi-O3 bands are known to be sensitive to the Bi-O3 geometry, the details of these surfaces should be interpreted with caution.

2. Thallium compounds

Several Tl-based structural variations of the form $Tl_2Ba_2Ca_{n-1}Cu_nO_{4+2n}$ [denoted Tl22($n-1$)n], having n Cu-O layers, have already been studied with local-density approximation methods. These materials have T_c values in the range of 80, 100, and 120 K for $n=1$, 2, and 3, respectively. LAPW calculations have been reported by Hamann and Mattheiss (1988) for Tl2201 and by Yu, Massidda, and Freeman (1988) for Tl2212 and Tl2223. Kasowski, Hsu, and Herman (1988) have reported pseudofunction calculations for the $n=1$, 2, 3, and 4 members of this series. Generally, the electronic structures bear considerable resemblance to the Bi-based materials, with the exception of the Tl- and Bi-derived states. The discussion here will focus only on the differences due to this replacement.

The main feature of the electronic structure, in addition to the expected Cu-O layer-derived bands crossing E_F, is the presence of Tl s, O p antibonding bands, which lie mainly above the Fermi level but which dip below at Γ. The band structure for the Tl2201 structure calculat-

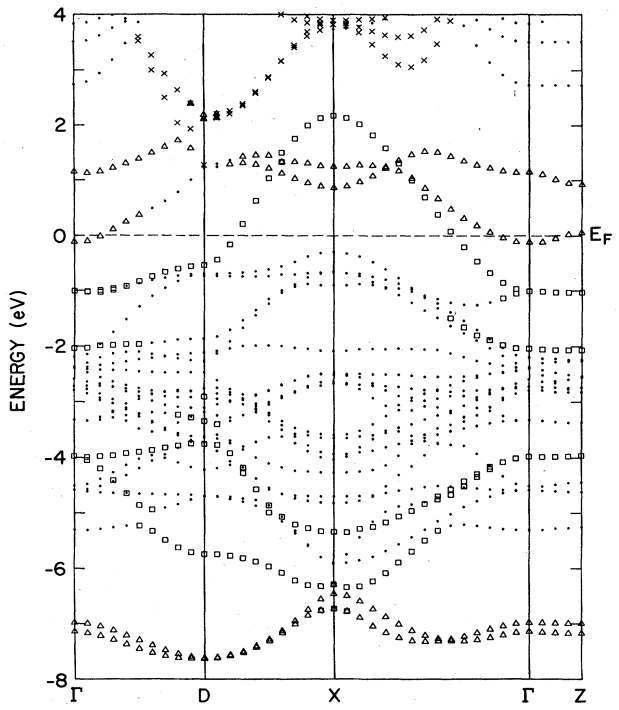

FIG. 36. Energy bands of $Tl_2Ba_2CuO_6$ along symmetry lines of the body-centered-tetragonal zone, showing the character of the bands. Triangles denote bands of predominantly Tl s and O2, O3 p character; squares denote bands with strong Cu-O $pd\sigma$ character; crosses denote the high-lying Tl $p(x)$, $p(y)$ bands. Note that one Tl-O band crosses E_F, forming an electron pocket at Γ. From Hamann and Mattheiss (1988).

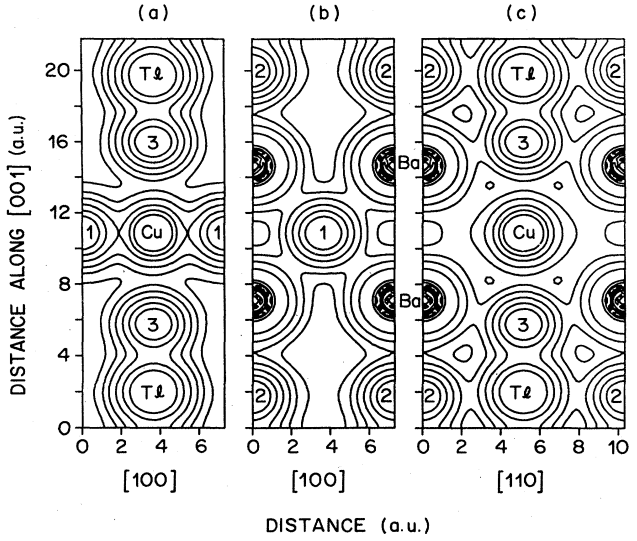

FIG. 37. Contours of constant logarithm of the charge density in high-symmetry planes for $Tl_2Ba_2CuO_6$. O1, O2, and O3 atoms are denoted 1, 2, 3, respectively. The strongest bonding occurs for the planar Cu-O1 interaction. From Hamann and Mattheiss (1988).

ed by Hamann and Mattheiss is shown in Fig. 36. These bands, which are nearly decoupled from the Cu-O bands, have a different type of dispersion from the Bi-O bands in the Bi compounds (minimum at the zone center rather than inside the zone, for example) but can be considered to serve much the same purpose in providing a metallic layer between the Cu-O layers and in slightly doping the Cu-O layers away from what would occur for insulating Tl-O layers. Actually, each of the two Tl-O layers contributes a band near but above E_F, and their interaction results in the bonding combination's dropping below E_F while the antibonding member stays well above. The bands in Fig. 36 have been coded according to their orbital character. Kasowski, Hsu, and Herman (1988) obtain relatively flat Cu-O bands at, or even above, E_F along some symmetry lines, while in the calculations of Hamann and Mattheiss and of Yu, Massidda, and Freeman the flat Cu-O bands remain well below the Fermi level.

Yu, Massidda, and Freeman present the Fermi surfaces for the $n=2$ member. It consists of a circular Tl-O tube, containing electrons centered at Γ, and a pair of large Cu-O surfaces centered at X, one of which is a square with rounded corners and the other one approaching a circle. As in the Bi-based compounds, the disper-

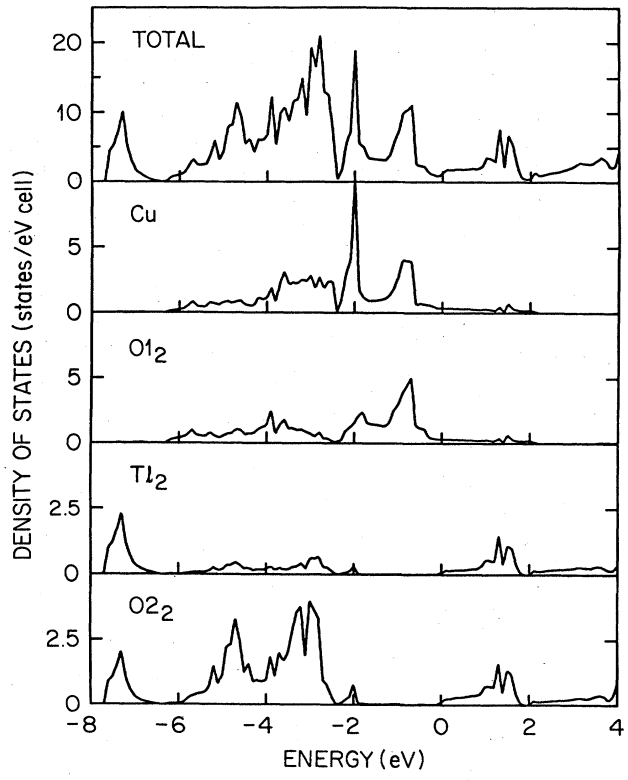

FIG. 38. Total (top) and partial densities of states for $Tl_2Ba_2CuO_6$, from Hamann and Mattheiss (1988). The Cu-O1 spectral density is similar to what is found for other cuprates. The Tl and O2 spectral density extends just to E_F from above.

sion in the c direction is very small.

The charge density calculated by Hamann and Mattheiss is shown in Fig. 37 for three high-symmetry planes. Strong covalent-type bonding occurs in the Cu-O layer, as it does in other layered copper oxides. In addition, the Tl ion is strongly bonded to its O neighbors, denoted as O2 and O3 in the figure, although the bond along the c axis to the O3 ion is stronger. The interaction between the Ba valence density, which can be seen in the figure, and the nearby O ions may be greater in this material than in the $YBa_2Cu_3O_7$ compound.

The total and partial densities of states of Tl2201 are pictured in Fig. 38. While the Cu and O1 (i.e., layer) spectral densities are similar to those of other cuprates, the wide range of Tl spectral density, from -8 to $+2$ eV, is a new feature. The band decomposition of Fig. 36 shows this character to be mostly Tl 6s states. The value of $N(E_F)$ is low, 1.24 states/eV cell. Hamann and Mattheiss note that the position, and hence the filling, of the Tl 6s band at E_F is very sensitive to the Tl-O2 and Tl-O3 separations. Larger bond lengths would increase the filling of this subband, making it more metallic, while decreasing the Tl-O separations would render the Tl-O layer insulating.

F. Self-consistent calculations: related oxides

Several oxides not containing copper are superconducting above 10 K. Although no attempt will be made here to describe in detail the calculations on these materials, they may be very important in pointing to the properties that are significant for superconductivity. Here these oxides, as well as other related copper oxides, will be noted and described briefly.

1. $BaPb_{1-x}Bi_xO_3$

The electronic structure of this system, which has T_c up to 13 K near $x=0.25$ (Sleight *et al.*, 1975), has been studied in detail by Mattheiss and Hamann (1982, 1983). They have investigated both of the end members and the alloys in a virtual-crystal approximation and have studied both the cubic (perovskite) and monoclinic phases. The electronic structure is dominated by a ten-band complex around E_F arising from O 2p and Pb-Bi 6s states. The valence-band region contains two 16-eV-wide σ-bonding 2p-6s subbands, which have their centers near a number of nonbonding O 2p bands. The band structures lead to metallic behavior for all x in the cubic phase.

These materials show transitions from the high-temperature cubic structure to tetragonal ($x=0.3$) and monoclinic ($x=1.0$) structures at room temperature and display a metal-to-insulator transition near $x=0.3$. Many of these features can be accounted for, qualitatively and in some cases quantitatively, by the band-structure calculations. For example, a strong Fermi-surface-driven instability is predicted for the $x=1$ member, which accounts for the stability of the monoclinic structure as well as its semiconducting behavior.

The studies of the changes of electronic structure due to distortions allowed Mattheiss and Hamann (1982) to draw conclusions about the strength and character of the electron-phonon interaction in this system. They concluded that values up to T_c of 13 K could be accounted for by strong electron-phonon coupling arising from the strong $sp\sigma$ interaction between nearest-neighbor Pb-Bi 6s and O 2p orbitals at the Fermi level.

2. $Ba_{1-x}K_xBiO_3$

The potassium-doped member of the $BaBiO_3$ compound recently has been found to be superconducting above 30 K by Mattheiss, Gyorgy, and Johnson (1988) and investigated more fully by Cava *et al.* (1988). Band-structure studies by Mattheiss and Hamann (1988b) reveal that K substitution on the Ba site does not disrupt the dominant antibonding Bi 6s–O 2p $sp\sigma$ bands at E_F. They find that the K extends the metallic range within this system closer to half filling, where the electron-phonon coupling is stronger, particularly for the O-related breathing modes, which strongly modulate the ($sp\sigma$) overlap. Like the $Ba(Pb,Bi)O_3$ system, this system also has a relatively low density of states for a metallic material.

3. $LiTi_2O_4$

This cubic spinel-structure oxide, which is superconducting at 12 K, has been investigated by Satpathy and Martin (1987) and by Massidda, Yu, and Freeman (1988b). It contains two formula units per cell (14 atoms). They find the Fermi energy to lie in a region of Ti d bands, with only one-half an electron/Ti occupying this band. The O 2p bands are filled, indicative of a highly ionic material, and they lie about 2.5 eV below E_F, in agreement with photoemission data for this compound.

Satpathy and Martin point out that the electronic structure of this material, with a small pocket of d electrons lying above filled O 2p bands, is not a common occurrence in transition-metal spinel compounds. Since there are twice as many Ti sites as there are 3d electrons to occupy this lower d band, the possibility of site ordering (as in Fe_3O_4) exists. The lattice structure of the Ti atoms, however, does not favor an ordering of different charge states. If the enhancement of the specific-heat density of states over the band value is assumed to be due to electron-phonon coupling, the resulting coupling constant $\lambda=1.8$ can easily account for the 12-K transition temperature.

Massidda, Yu, and Freeman (1988b) calculated the electronic structure for both ideal (cubic) and true (distorted) crystal structures. The structural distortion leads to important shifts in bands near the Fermi energy and changes the Fermi surface. The distortion also appears to decrease somewhat the strength of the electron-

phonon interaction, but, consistent with Satpathy and Martin, Massidda *et al.* conclude that this compound is most probably an electron-phonon coupled superconductor.

4. La_2NiO_4

While this compound is not superconducting, it is an important material for comparison, since it is both isostructural with La_2CuO_4 and an antiferromagnetic semiconductor. Guo and Temmerman (1988) have carried out calculations on this material in paramagnetic, ferromagnetic, and antiferromagnetic states. The band structure in the paramagnetic case is very similar to that of paramagnetic La_2CuO_4, except that the Fermi level lies lower in the bands and $N(E_F)$ is larger. No ferromagnetic solution was obtained. The ground state was found to be an antiferromagnetic with a spin moment of $0.8\mu_B$ per Ni atom (a large, very good k-point sampling was necessary to obtain this magnetic solution). Guo and Temmerman quote experimental values for the moment near $0.6\mu_B$/Ni, with some uncertainty in this value. The ground-state energy was 5 mRy/formula unit lower for the antiferromagnetic state than for the paramagnetic state. Typical exchange splittings for d states were 0.5 eV. The resulting band structure is metallic rather than insulating, although they indicate that a simple lowering of symmetry by a structural distortion could lead to a gap at E_F.

5. CuO, Cu_2O

At first sight, these two compounds could be expected to provide a reference point for discussing the superconducting cuprates, but rather little has been done toward calculating their local-density electronic structures. In fact, neither may be related very closely to the layered cuprates. Cu_2O has a symmetric structure, with the oxygen ions forming a bcc lattice and the Cu ions tetrahedrally coordinated with the O ions. The resulting lattice has two formula units per cell and exhibits linear O-Cu-O coordination, which is quite rare for copper oxides. Cu_2O is expected to provide a closed Cu d shell and a closed O p shell, which according to Ghijsen *et al.* (1988) should then be described well by local-density band theory.

CuO is distinct from the layered cuprates in that it forms a three-dimensional crystal structure. The crystal structure is monoclinic $C2/c$ (Yang, Tranquada, and Shirane, 1988) with four formula units per cell, and it is antiferromagnetic below 225 K. Yang, Tranquada, and Shirane (1988) report a commensurate antiferromagnetic state, while Forsyth, Brown, and Wanklyn (1988) report a slightly incommensurate state. Ghijsen *et al.* (1988) quote unpublished calculations of Czyzyk and de Groot, which indicate that local spin-density calculations (discussed at some length in Sec. VIII) do not obtain an antiferromagnetic state in CuO.

G. Tight-binding parametrizations

Since the earliest papers on cuprates after the discovery of high-temperature superconductivity, tight-binding models of their band structure have played a central role in the theoretical ideas. Due to the near-closed-shell character of both the Cu d states and the O p states, a tight-binding model seems particularly appropriate. Such models are compact and can be used to give insight into difficult problems that are otherwise intractable, a number of which will be discussed below in Sec. XI.

1. Approximate parametrizations

The simplest approach to the application of tight-binding Hamiltonians is simply to take atomic term values for the on-site energies and use predetermined energy overlaps (Harrison, 1980) for the hopping terms, or to use the analogous procedure in the extended Hückel method. This approach gives some idea of the position and shape of the valence bands. Harrison (1988) has shown the shape of layer and chain bands that result in the Y123 system from assuming only nearest-neighbor Cu-O coupling. Richert and Allen (1987) have used this approach to investigate the band structures of the La214 system and the effects of O and La vacancies. Gupta and Gupta (1988) used a cluster tight-binding method to calculate local densities of states. Whangbo *et al.* (1987a, 1987b, 1987c) applied the related extended Hückel method to a study of the La214 and Y123 systems.

Although this *ad hoc* approach provides a qualitative picture of the bands, it often misses specific characteristics that are crucial, and as a result it is not suitable for quantitative studies. For example, the straightforward application of the Hückel approach leads to an entirely unoccupied chain-derived Cu d band in $YBa_2Cu_3O_7$ (Whangbo *et al.*, 1987b), and the *ad hoc* approach leads to sharp Cu d peaks in the unoccupied DOS of $YBa_2Cu_3O_7$ (Richert and Allen, 1988a) and to completely unoccupied Tl-O conduction bands in the Tl2212 compound (Richert and Allen, 1988b). All of these are potentially important features which are at odds with the results of self-consistent calculations. Nevertheless, simple approximate tight-binding representations may be useful for many purposes. Julien, Mayou, and Cyrot-Lackmann (1988) have used such Hamiltonians to demonstrate general features to be expected of the electronic structure of copper oxides.

Since the use of tight-binding methods in models of the cuprates is widespread, it is important to recall the foundations of the tight-binding method and the source of the discrepancies. No doubt some of the discrepancies mentioned above are due to the neglect of crystal-field (Madelung) contributions to the on-site terms, which are not easy to estimate *a priori*. Another important factor,

which is not widely recognized, is that *in practice* the tight-binding parameters are not independent of each other. This is particularly true for the *orthogonal* tight-binding models, which are simplest and therefore are by far the most widely used. When applying a tight-binding model, one thinks in terms of atomiclike basis functions; these functions of course are never specified. Atomic functions are not orthogonal, suggesting that a *nonorthogonal* tight-binding method may be useful for making the common picture more realistic.

For the orthogonal tight-binding method, however, the basis functions are Löwdin-orthogonalized atomic orbitals. Such an orbital centered at the origin contains admixtures of orbitals on nearest neighbors, and for moderate-to-strong hybridization it may contain large numbers of orbitals on second-, third-, ... neighbor shells. Although the combination of orbitals is almost never specified, both the "on-site" energies and the energy ("hopping") integrals are appropriate to Löwdin functions other than atomic orbitals. Clearly such parameters can be quite different from the corresponding parameters appropriate to atomic orbitals. Papaconstantopoulos (1986) has emphasized that a high-quality fit to a self-consistent band structure is the property of a *set of parameters;* if the choice of parameters is changed (corresponding implicitly to a change in the Löwdin orbitals used to represent the bands), the values of all the parameters will change, often significantly.

2. Quantitative parametrizations

Quantitative tight-binding fits to self-consistent band structures have been carried out by Weber (1987), Papaconstantopoulos, DeWeert, and Pickett (1988), Papaconstantopoulos, Pickett, and DeWeert (1988), and Weber and Mattheiss (1988). Weber applied the nonorthogonal tight-binding approach (Mattheiss and Weber, 1982), which was very successful in the $A15$-structure conventional superconductors. In a fit to La_2CuO_4 that included the Cu d, O p, and La d states, Weber retained nonzero wave-function overlap (denoted by $[pd\sigma]$, for example) between the Cu and each of the oxygen sites, expecting that other overlaps should be small. These parameters were quite significant: $[pd\sigma]=0.090$, 0.055 and $[pd\pi]=-0.036$, -0.022 for the overlaps of O_{xy} and O_z, respectively, with Cu. Detailed characteristics of Weber's fit have not been published, but were provided to the present author to allow the description provided below.

Since the site symmetry of all atoms, especially O_{xy}, is low, it is possible that crystal-field splittings are important. Weber indeed found that the σ-bonding p orbital of the O_{xy} atom [$p(x)$ for the atom lying on the x axis] was split below the $p(y)$, $p(z)$ orbitals by almost 0.75 eV. The crystal-field splittings of the Cu d orbitals were found to be only 0.2 eV or less. The on-site energies of the two O sites differered by 0.9 eV (with O_{xy} lowest), with their average being almost identical to the Cu d site energy. This lineup of site energies serves to maximize the hybridization of p and d states and is a striking feature distinguishing copper oxides from other transition-metal oxides. Weber's nonorthogonal tight-binding fit was used to calculate the phonon spectrum and the strength of the electron-phonon interaction; the results are discussed in Sec. X.

Papaconstantopoulos, DeWeert, and Pickett (1988) (PDP) carried out an orthogonal tight-binding fit to the LAPW bands of La_2CuO_4 and Ba_2CuO_4 (Pickett, Krakauer, Papaconstantopoulos, and Boyer, 1987) using La (Ba) d states, O p states, and Cu s, p, and d states. As an example of the quality of fit that it is possible to obtain, their bands for La_2CuO_4 are compared in Fig. 39 with the self-consistent LAPW bands that they used in the fit. The fit is very accurate near the Fermi level, with an rms deviation of 0.08 eV for the 17th band. The

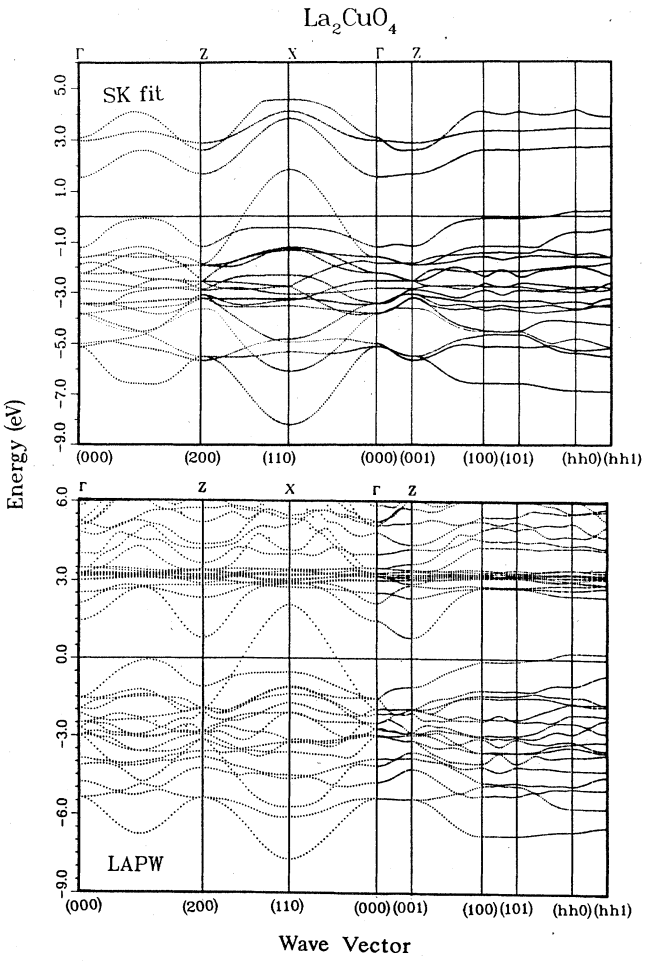

FIG. 39. Comparison of the band structure of La_2CuO_4 resulting from (top) a tight-binding (Slater-Koster) fit to the (bottom) *ab initio* LAPW bands. Only the valence bands (below about +1.5 eV) have been fit carefully. From Papaconstantopoulos, Pickett, and DeWeert (1988).

differences for the lower bands are somewhat larger, but the bands clearly are good representations throughout the valence-band region.

Like Weber, PDP also allowed crystal-field splittings of the Cu d and O p states (although the implementation was different), but found that the derived splittings led to only a very small improvement in the rms fit. The O site energies differed by 0.8 eV, with O_{xy} lowest. Since this result is very similar to Weber's nonorthogonal tight-binding result, one is probably safe in drawing physical inferences from it. PDP simplified the crystal-field splitting on the Cu site to "e_g" and "t_{2g}" parameters (a separation not dictated by symmetry), which led to a splitting of 1.3 eV with the e_g site energy highest. This order of orbitals is consistent with that expected of the Cu ion with (rough) octahedral symmetry, as discussed in Sec. III.B.

The proper representation of crystal-field splittings in tight-binding parametrizations, and their sources, may be an important problem in the copper oxides. One source of splitting is hybridization with near neighbors, and the tight-binding method of Mattheiss and Weber (1982) takes only this contribution into account. The method employed by PDP was simply to allow splittings consistent with the site symmetry regardless of the source of the crystal field. This approach allows the other contribution, from charged ions beyond the range of direct wave-function overlap, to be included. McMahan *et al.* (1988) have also considered this question in their tight-binding representation of the La_2CuO_4 bands. They conclude that, since their LMTO calculation uses atomic spheres that are nearly charge neutral, the Madelung contribution is small compared to that due to wave-function overlap.

An independent estimate of the Madelung contribution to the site energies and crystal-field splittings is obtained by comparing the fits of PDP to La_2CuO_4 and Ba_2CuO_4. Since the Ba compound was calculated and fit solely to provide a basis for doing tight-binding alloy calculations (described in Sec. VI), identical lattice constants and structural parameters were used, and this also simplifies the comparison. The difference between the materials then is the replacement of La^{3+} with Ba^{2+}, although of course this difference of valence charge is shared self-consistently between the Cu and O atoms.

Replacement of La with Ba gave the following differences. The e_g-t_{2g} splitting of Cu remained constant, and the crystal-field splittings of the O ions were not examined. The important differences occurred in the site energies. The O site energy difference increased from 0.8 to 1.4 eV. Somewhat more surprising is that the average Cu d site energy dropped below that of the lowest (O_{xy}) oxygen p energy. This indicates that Madelung terms are very important in determining site energies. More particularly, it raises the question whether such effects are crucial to superconductivity in the La214 system, which, after all, become superconducting only upon the addition of Ba, Sr, or Ca.

As mentioned above, a good tight-binding fit depends on a *set* of parameters, so there is limited value in comparing individual fitting parameters. However, since there has been considerable discussion of simple Cu d, O p tight-binding parametrizations, it may be useful to compare a few of the more important ones. Mattheiss (1987) suggested a simple orthogonal tight-binding picture with equal Cu and O site energies, for which $pd\sigma = -1.85$ eV would reproduce approximately the most bonding and antibonding bands. Weber's nonorthogonal tight-binding fit resulted in -1.62 and -0.98 eV for planar and axial $pd\sigma$ values, while PDP's orthogonal tight-binding gave -1.41 and -0.69 eV, respectively. Recall that Weber's and PDP's values represent different physical parameters; Weber's may have more physical significance, but the orthogonal tight-binding approach used by PDP is the one almost always applied. $pd\pi$ parameters are not negligible; their magnitudes typically lie in the range of 40–60 % of the $pd\sigma$ values.

Proceeding beyond the emphasis on O-Cu p-d hybridization, McMahan, Martin, and Satpathy (1988) established that O-O p-p overlap is also a large, zero-order influence. By performing model LMTO band calculations with Cu d states removed from the basis set, they found a bandwidth of 6.7 eV arising purely from O p states. In tight-binding language this translates into O-O $pp\sigma$ and $pp\pi$ parameters of 1.0 and -0.3 eV, in their simple tight-binding model, which was intended only to reproduce overall features of the band structure. The accurate orthogonal tight-binding fit of PDP, however, produced values of the order of 0.4 eV or less, while Weber's nonorthogonal fit gave planar $pp\sigma = 0.9$ eV and small values for other parameters.

Going beyond the La214 system, DeWeert, Papaconstantopoulos, and Pickett (1989) (DPP) have obtained a quantitative orthogonal tight-binding fit to the valence-band structure of $YBa_2Cu_3O_7$. Including Y d, Cu d, and O p states, leading to 41 basis functions, they obtained a very good fit near E_F and somewhat below while not requiring the lower valence bands to be reproduced so accurately. In the fit they allowed all Cu and O on-site energies to be independent, consistent with the low site symmetry of this material (site symmetries are given in Sec. II.B). The crystal-field splittings of site energies were 2.4 and 1.4 eV for the Cu1 and Cu2 sites, respectively. For the O1, O2, O3, and O4 sites, the crystal-field splittings resulting from the fit were 0.70, 0.95, 2.3, and 1.8 eV, respectively. The mean on-site energies also showed substantial variations, indicating again that it is necessary to take account of the distinct low site symmetries to obtain accurate tight-binding fits to these materials.

To study the electron-phonon interaction in the Y123 system, Weber and Mattheiss (1988) carried out a nonorthogonal tight-binding fit for this material. They used a 46 orbital model, which includes the Cu s and Ba s states in addition to those used by DPP in their orthogo-

nal tight-binding fit. They noted, consistent with the finding of DPP, that a fit of the same quality as was obtained in the La214 system is much more difficult to obtain for the Y123 compound. Some results of their study are discussed in Sec. X.C.

V. SPECTROSCOPY: ELECTRON, PHOTON, POSITRON

Electronic spectroscopy provides a direct probe of the electronic structure of a solid and thus is directly relevant in assessing the validity of any electronic structure model, especially the band picture. Direct and inverse photoemission, in the simplest picture, probes single-hole and single-electron excitations, respectively, and it is relatively straightforward to compare with the band eigenvalues. It was noted in Sec. IV.A that density-functional theory, the formal basis for band theory as practiced, does *not* guarantee that the bands will represent single-particle excitations—the single-particle Green's function is needed for that. However, when solids are "bandlike," a great deal of experience has shown that the density-functional bands are realistic approximations to single-particle excitations. In these cases the density-functional exchange-correlation potential can be considered as a local, energy-independent approximation to the single-particle self-energy. In this section we provide a brief overview of the picture arising from the spectroscopic data and to what extent it is accounted for by local-density approximation band structures or by other models. Perhaps the most detailed discussion of the spectroscopic data through 1987 and their interpretation have been given by Wendin (1987).

A. Valence photoemission: direct and inverse

In addition to probing the valence–conduction-band region of a solid, photoemission at high energies can be used to probe core levels and the resonant interference between core and valence levels. One of the central themes of electron spectroscopies is to determine when valence states, such as Cu d and O p states in the cuprates, are bandlike or display behavior typical of (or related to) localized orbitals, such as core levels. Valence-band satellites and multiplet structure are examples of localized behavior, and both have been seen in the copper oxides. Such features are not described by the density-functional bands, nor indeed by an independent electron picture.

A promising approach for many transition-metal compound data is a local, correlated cluster picture. For the copper oxides this model involves the site energies E_d and E_p and incorporates Coulomb repulsion energies U_d and U_p, as well as a charge transfer energy U_{pd} and the bandwidth W. Local correlations are treated within an isolated impurity, or "correlated cluster," model in which the Cu and surrounding O (ligand) ions are decoupled from the rest of the solid. The measured peaks are most often interpreted in terms of the Cini-Sawatzky methodology (Cini, 1977, 1978; Sawatzky, 1977). This methodology was developed to describe Auger spectra, where two holes are present on a site and interact strongly. In Cu^{2+}-based ionic insulators, when one hole is present in the ground state, the procedure can be applied to a description of photoemission spectra, since the ejection of an electron (if localized) leaves a second hole on the site. Fujimori *et al.* (1987) were among the first to suggest that such strong correlation models could be necessary to account for the spectroscopic data in the new high-T_c copper oxide systems.

Fuggle *et al.* (1988) have presented the corresponding schematic energy-level diagram for divalent Cu compounds, shown in Fig. 40. The diagram indicates neutral, singly ionized, and doubly ionized excitations, corresponding to one, two, and three holes in the neighborhood of a Cu ion that is hybridized with the surrounding oxygen ions. The model is presumed to provide a zero-order picture for any of the copper oxides, and it is sufficient to consider a CuO molecule to describe its features. The supposition is that the picture is reasonable as long as U_d is larger than W.

For a neutral CuO molecule the states considered are Cu d^9, O p^6 and Cu d^{10}, O p^5, denoted $3d^9$ and $3d^{10}\underline{L}$, respectively, in Fig. 40. More generally, $\underline{L}$ denotes a hole residing primarily on the ligand ions neighboring Cu. The energy difference, defining the Cu-ligand transfer energy, is denoted Δ in this figure. These two basis states mix to form bonding and antibonding states, and since the $3d^{10}\underline{L}$ states in a solid form a band (even if the $3d^9$ state is presumed to be completely localized), the mixed states each possess a bandwidth.

Photoemitting an electron introduces the two-hole basis states $3d^8$, $3d^9\underline{L}$, and $3d^{10}\underline{L}^2$. The separation of the $3d^9\underline{L}$ and $3d^{10}\underline{L}^2$ states will parallel that of the $3d^9$ and $3d^{10}\underline{L}$ states of the neutral cluster, so they will mix and

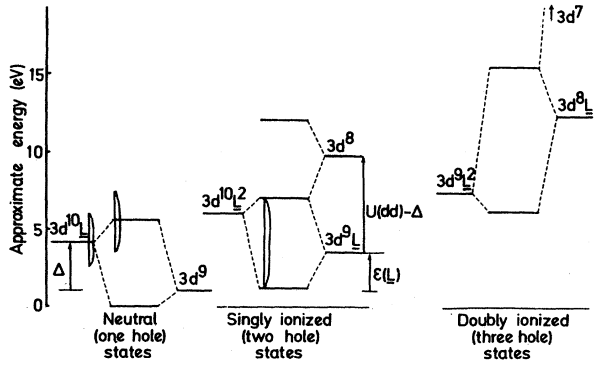

FIG. 40. Schematic energy-level diagram illustrating the states and their relative positions which arise in the correlated cluster model for the interpretation of high-energy spectroscopies in Cu^{2+} systems. See text for description. From Fuggle *et al.* (1988).

band in much the same way. The $3d^8$ state depends on U_d and lies higher. The doubly ionized (three-hole) states are involved in describing the Auger process, in which two holes are created.

Photoemission data for the La214 and Y123 systems and their interpretation have been reviewed recently by Hass (1989). The data up to that time were primarily on ceramic (i.e., polycrystalline) samples. In addition to Hass's extensive list of references, a compendium has been provided by Meyer *et al.* (1988).

First and foremost, it must be kept in mind that direct photoemission spectroscopy (PES), whether in the ultraviolet or x-ray regime, and inverse photoemission, or bremsstrahlung isochromat spectroscopy (BIS), are extremely surface sensitive due to the short escape depths or penetration depths, respectively, of the electrons, which are of the order of 5–20 Å. The difficulty of preparing clean surfaces is widely recognized, as is the likelihood that surface stoichiometry may be different from that of the bulk, due to the high mobility of the oxygen ions and the intrinsic instability of the O^{2-} ion.

The surface problems have been discussed, for example, by Weaver *et al.* (1988). Very recently List *et al.* (1988) have made photoemission measurements on single crystals of $EuBa_2Cu_3O_{7-y}$, which were cleaved at 20 K. Upon warming to 80 K, emission is lost from both the upper and lower portions of the Cu-O hybridization complex, so that the *apparent* valence bandwidth narrows. The Fermi edge is seen clearly at 20 K, but disappears upon reaching room temperature. They conclude that, upon warming from 20 K, oxygen is lost rapidly from the surface region, and superconductivity is also lost near the cleaved surface. Their results suggest that previous photoemission data are not representative of the bulk superconducting material and that it is necessary to prepare surfaces and collect data at low temperature to obtain the photoemission data so important in understanding the electronic structure.

The same caveat applies to inverse photoemission data. In addition, during an inverse photoemission experiment it is possible that the electron beam can alter the surface properties (Wendin, 1987). However, PES and BIS provide potentially the simplest spectroscopies to interpret, since they correspond most closely to the addition of a single hole or electron, respectively, to the solid. As a result there have been extensive applications of these techniques to the copper oxides. Keeping in mind the caveats discussed here concerning the problems of interpretation of the data, we briefly review some of the data that have been obtained.

A combined x-ray-photoemission–BIS overview of the valence–conduction-band region from Meyer *et al.* (1988) is shown in Fig. 41, where a comparison is made with various band DOS calculations (no matrix elements, lifetime broadening, or self-energy shift included), for both $YBa_2Cu_3O_7$ and $La_{1.85}Sr_{0.15}CuO_4$. It can be seen that, on the broad scale of this figure, the band calculations put the spectral density in roughly the appropriate

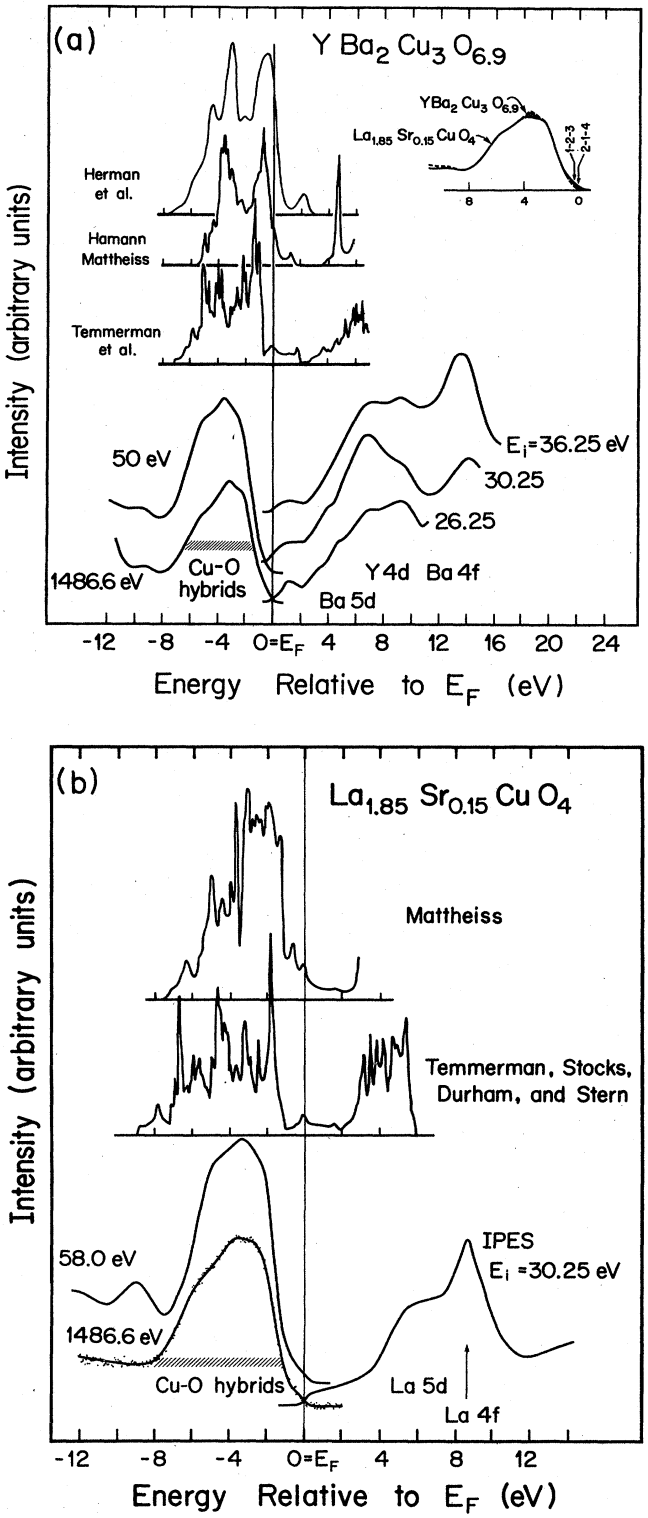

FIG. 41. Collection of direct and inverse photoemission data for the (top) Y123 and (bottom) La214 materials, both oriented with respect to the Fermi level (vertical line). Several band calculations of the spectral density are shown for comparison. From Meyer *et al.* (1988). Inset at the upper right of the top panel illustrates the extreme similarity of the valence-band spectra of the La214 and Y123 materials.

region. The largest discrepancy in this figure is in the conduction region of LSCO, where the experimental spectral density lies higher than is calculated. While much of this discrepancy may be real, it should be kept in mind that most band calculations are less accurate well up into the conduction-band region unless special care is taken, since the calculations are optimized for the valence states.

Another combined PES-BIS comparison which includes the Bi2212 and Tl2223 compounds is shown in Fig. 42. This figure serves to emphasize the similarities of these copper-oxide materials in the valence-band region between the Fermi level and 8-eV binding energy. In each case there is a low-spectral-density region near E_F, but Fermi edges have now been seen in all of these materials (see below), consistent with low but nonzero density of states at E_F.

Angle-integrated PES data have been obtained for both the La214 and Y123 systems at stoichiometry as well as versus concentration x of Sr and concentration y of O vacancies, respectively, and varying photon energies have been used. The concentration x of Sr has negligible effect on the valence-band spectra, while increasing the number of O vacancies in the Y123 system causes all valence-band features to shift to higher binding energy. The data for the La214 system are shown in Fig. 43 together with calculated PES by Redinger, Yu, *et al.* (1987) which include matrix element and lifetime effects. The low-photon-energy data (21.2 and 40.8 eV), which emphasize states arising from O p orbitals, show an edge just below E_F that lies at roughly 1 eV higher binding energy than is calculated. The 1487-eV XPS data, which weight selectively the Cu d states, peak at 2.5 eV higher binding ener-

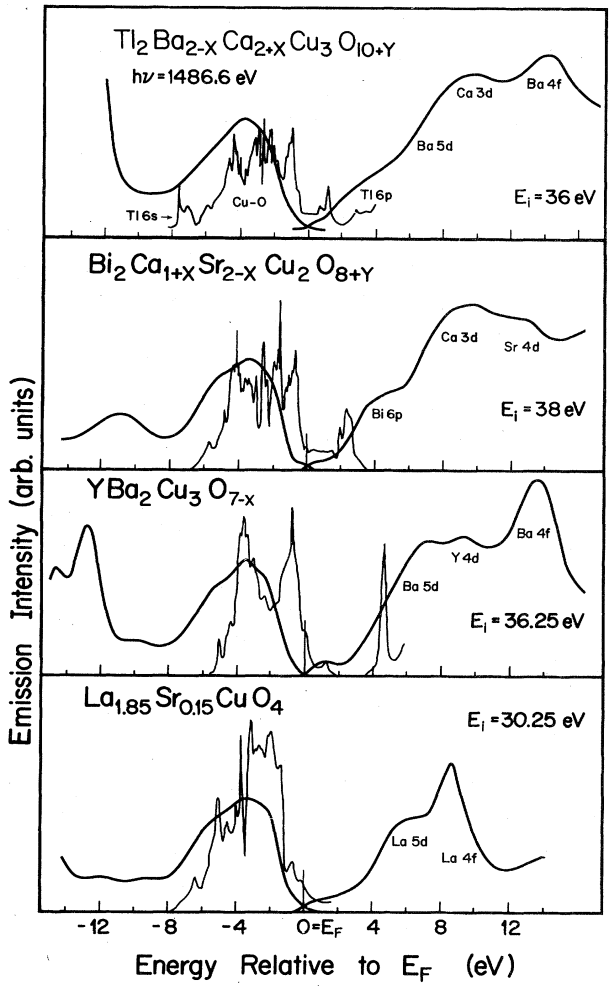

FIG. 42. Combined direct/inverse photoemission data for four copper oxide high-temperature superconductors. The data in the valence-band region within 8 eV of E_F, where Cu d and O p states dominate, are very similar. Differences occur outside of this range due to different semicore and conduction states on the various cations. Courtesy of H. M. Meyer III.

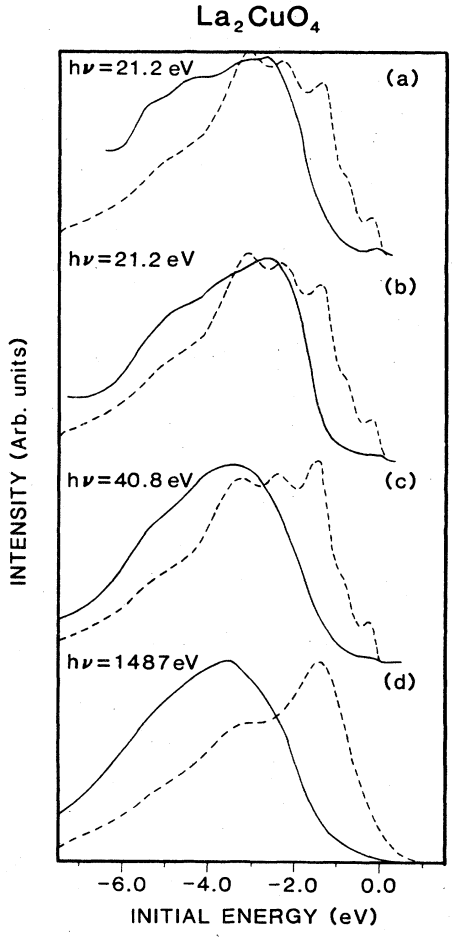

FIG. 43. Ultraviolet and x-ray photoemission data (solid curves) for $La_{2-x}M_xCuO_4$, compared to calculations (dashed curves) that include excitation matrix elements and lifetime broadening but neglect self-energy shifts (which are not known), from Redinger, Yu, *et al.* (1987): (a) $x=0.15$; (b) $x=0.20$; (c) $x=0.20$; (d) $x=0.0$. The calculations underestimate the binding energy of the (mostly Cu d) electrons in this compound.

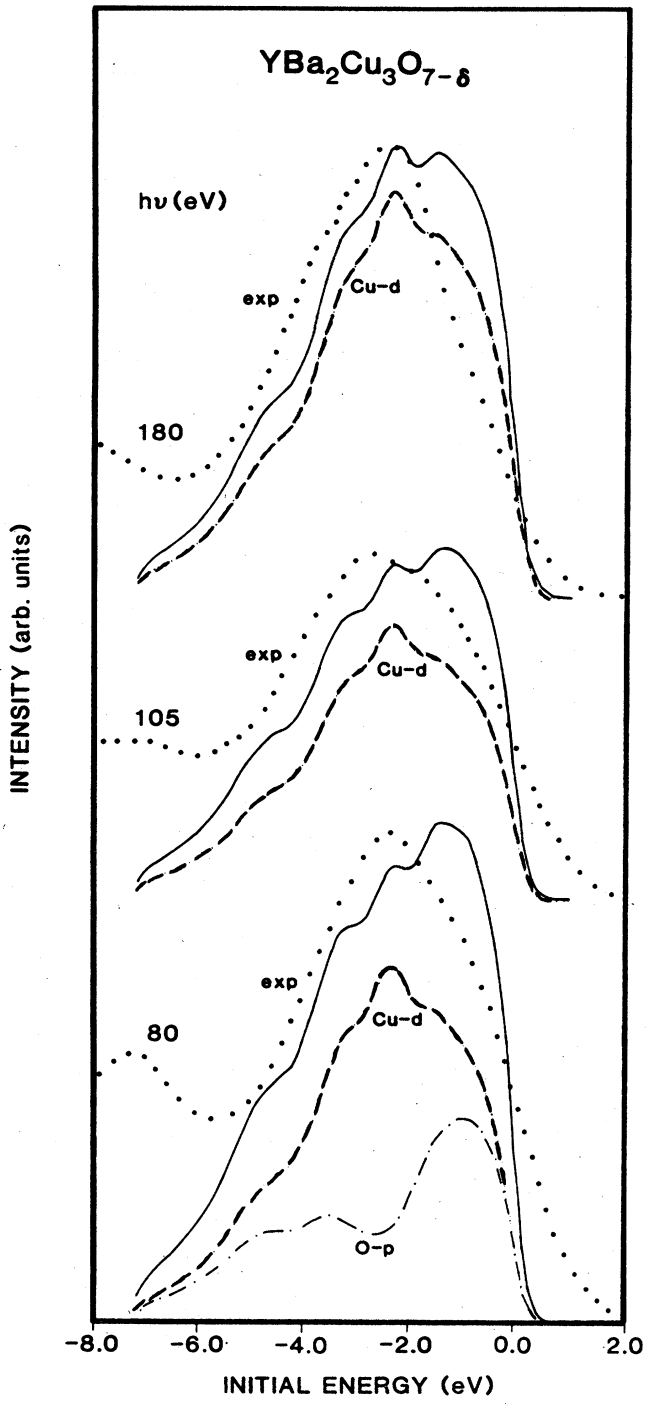

FIG. 44. Ultraviolet photoemission data for $YBa_2Cu_3O_{7-y}$, compared for calculations for $y=0.0$ which include excitation matrix elements and lifetime broadening, from Redinger, Freeman, *et al.* (1987). The different photon energies are labeled. The Cu *d* contribution (dashed line) is separated from the total calculated spectrum (solid line), and the O *p* contribution is shown for the 80-eV case (chain-dashed line). The data (points) peak at 1–2 eV higher binding energy than do the calculated curves; however, the additional broadening seen in the data may account for a portion of the discrepancy. The overall Cu-O bandwidth is in fairly good agreement.

gy than the calculated peak and show less structure. The corresponding comparison for the Y123 system is shown in Fig. 44 and yields similar results, i.e., the Cu *d* spectral density is observed at 1–2 eV higher binding energy than is calculated from the local-density band structure. However, the experimental broadening in the figure is clearly greater than has been accounted for in the calculations, as can be seen from the tail extending 2 eV above E_F.

BIS data on $YBa_2Cu_3O_7$ are shown in Fig. 45 from Redinger, Freeman, *et al.* (1987) and compared with local-density approximation calculations, which again include matrix elements and lifetime effects. Theory and experiment agree rather well on the position and shape of the peak from 0–2 eV above E_F, which is due mostly to O *p* states. Above a minimum at 2.5 eV, both theory and experiment again show a steep rise which in the calculation arises from both O *p* and Y *d* states.

Beyond the valence-band region in both the La214 and Y123 systems, several PES studies have shown peaks at −9-eV and −12 to −13 eV binding energies. Resonant PES studies establish the latter peak to be primarily Cu *d*-like in origin, suggesting the interpretation as a *d* valence-band satellite similar to peaks seen in several other transition-metal systems (CuO, $CuCl_2$, Ni, etc.). Weaver *et al.* (1988) observe that, although it had previously been noted that the intensity of the 9-eV peak diminished with decreasing carbon contamination, their carbon-free samples still exhibit a peak at this energy.

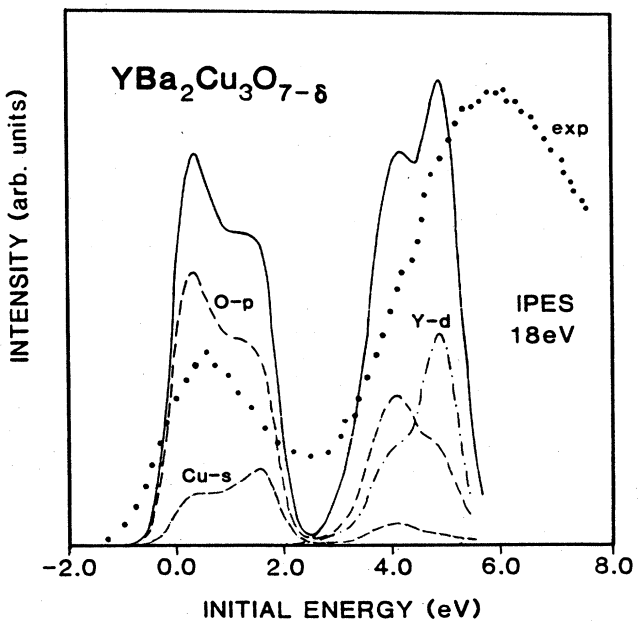

FIG. 45. Calculation of the inverse photoemission spectrum (IPES) of $YBa_2Cu_3O_7$ by Redinger, Yu, *et al.* (1987), compared to the data, shown as dots. The 2-eV-wide peak just above E_F due to Cu-O states is reproduced well in the calculation, and the appearance of Y *d* states at 4-5 eV is also accounted for. The calculations were only carried out to (somewhat below) 6 eV.

They concluded that the peak is intrinsic, that is, not impurity derived, and resonant PES studies indicate it is mainly O $2p$ in origin. Its specific origin remains unclear. Ramaker (1988b) has suggested that it is due to a bound state of two holes on nearest-neighbor oxygen ions. Such an occurrence may be more likely in an insulating surface layer than in the metallic bulk material.

Several recent findings may be revealing. Yeh *et al.* (1989) have studied 200-Å thin films of Bi-Sr-Ca-Cu oxide films with x-ray PES. Oxygen treatment can be used to convert the films from an amorphous insulating phase to an ordered, metallic $T_c = 80$ K phase. Regardless of the treatment, the Cu $2p$ spectra of all films display satellite structure characteristic of Cu^{2+} behavior. They interpret this result to indicate that the same electronic parameters (site energies, hopping integrals) are appropriate throughout the phase diagram. It could also reflect a surface layer which is relatively unchanging compared to the bulk.

Fermi edges, which could not be detected in early studies of La214 and Y123 ceramic materials, have now been seen in several of the superconducting copper oxides. Hillbrecht *et al.* (1989) see reproducible Fermi edges in $Bi_2CaSr_2Cu_2O_{8+\delta}$ which they ascribe to states in the Bi-O layers, and even resolve a peak at 0.17-eV binding energy. No change in the spectrum was seen below T_c, giving no indication of a superconducting gap. Directly opposed this this latter result is that of Imer *et al.* (1989), who also see the Fermi edge in $Bi_2Sr_2CaCu_2O_8$ single crystals but find clear evidence of a gap $\Delta = 30 \pm 5$ meV opening well below T_c ($2\Delta/k_B T_c \approx 8$). The discrepancy between these two measurements remains to be resolved.

A few angle-resolved studies have been reported. Takahashi *et al.* (1988) detected two bands in $Bi_2CaSr_2Cu_2O_8$ which lie at 0.2 and 0.5 eV binding energy at the surface zone center $\bar{\Gamma}$. Both disperse upward, with the upper band passing through E_F midway between $\bar{\Gamma}$ and $\bar{X} = (\frac{1}{2}, 0)(2\pi/a)$. Claessen *et al* (1989), performing angle-resolved BIS studies, identify nondispersive states at 2.9 and ~ 5 eV above E_F. Midway between $\bar{\Gamma}$ and $\bar{X}$, the density of states increases, indicating a band crossing E_F, consistent with the results of Takahashi *et al.*

In crystalline $YBa_2Cu_3O_7$, Stoffel *et al.* (1988) have reported a dispersive band near E_F which could be consistent with energy band calculations. It will be interesting to follow the data as sample and surface quality improve and comparison between theory and experiment is carried out in more detail.

The clear differences between the PES data and the local-density-derived spectra have been discussed widely. The uncertainty of the quality and stoichiometry of the surfaces clouds the comparison and has led to increased emphasis on less surface-sensitive spectroscopies, which are discussed below. The clearest discrepancy lies in the 12-eV satellite, which, although it has not been eliminated as a surface feature, is widely accepted as an intrinsic bulk feature. As noted in Sec. IV.A, such a feature is missing from the local-density band spectrum, indicating large self-energy corrections. This satellite is discussed further in Sec. XI.A.

B. Core-level spectroscopy

Core-level spectroscopies were first applied to the copper oxides to investigate the amounts of Cu^{1+}, Cu^{2+}, and Cu^{3+} configurations in the ground state and their possible variation with doping. The consensus, discussed by Hass (1989), is that Cu^{2+} is dominant and that there is very little evidence of Cu^{3+}.

Taking La_2CuO_4 for illustration, the Cu $2p_{3/2}$ core-level absorption spectra (Nücker *et al.*, 1987) show a main peak around 931 eV, of width 2–3 eV, and a secondary peak centered at 942 eV with 4–5-eV width. These peaks, which are shown for CuO as well as for the La214 material in Fig. 46, are ascribed to $\underline{2p}\,3d^{10}\underline{L}$ and $\underline{2p}\,3d^9$ final states, respectively ($\underline{2p}$ denotes a Cu $2p_{3/2}$ core hole). This interpretation is consistent with the absence of the 942-eV peak in Cu_2O as shown in Fig. 46, since Cu_2O is expected to have no d hole in the ground state.

The width of the main line results primarily from the ligand hole $\underline{L}$ dispersion, related to the O p valence bandwidth, while the width of the satellite at 942 eV arises mostly from multiplet effects. In the metallic regime one may find additional features due to the unoccupied states

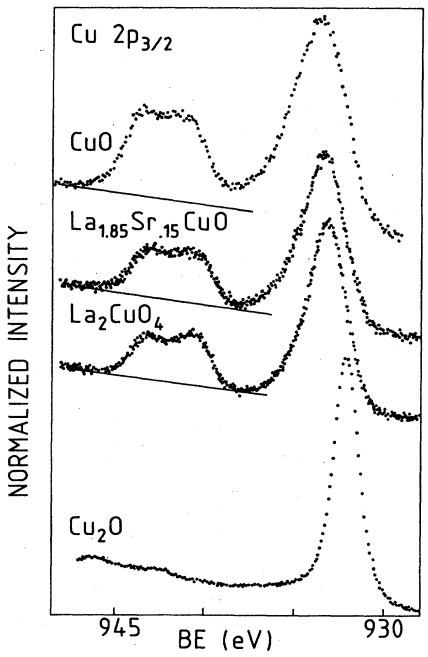

FIG. 46. The main (932 eV) and secondary (940–945 eV) peaks in the Cu $2p_{3/2}$ core-level absorption spectra of $La_{2-x}Sr_xCuO_4$ ($x = 0.0$ and 0.15), CuO, and Cu_2O (BE = binding energy). The secondary peaks are very similar in CuO and in the La214 systems; only their intensities with respect to the main peak differ. The width of the secondary peak is due mainly to multiplet effects. From Fink *et al.* (1989).

(holes) just above E_F. In the standard correlated cluster language, the final state is denoted $\underline{2p}3d^{10}\underline{L}^2$ and is expected to occur on the high-binding-energy side of the main peak. The Y123 system is similar in these respects to the La214 system (Ramaker *et al.*, 1987). A more extensive discussion has been given by Ramaker (1988a).

Bianconi, DeSantis, *et al.* (1988) have made a high-resolution, polarized study of the structure and symmetry of the unoccupied hole states in $YBa_2Cu_3O_{7-y}$. By varying y they identify an extra spectral density from 932 to 933.5 eV for $y=0.0$–0.15, which is absent for $y>0.3$. They assign the new peak to transitions from $3d^9\underline{L}^*$ to the $\underline{2p}3d^{10}\underline{L}^*$ final state, where $\underline{L}^*$ denotes the hole in the ligand orbitals (present in the ground state). More generally, the results can be viewed as reflecting the existence and bandwidth of the lowest unoccupied valence states. The bandwidth of 1.5–2 eV is similar to the unoccupied Cu-O valence bandwidth in the local-density band structures of this material.

Interpretation of the polarization studies (polarization vector ε varied relative to the Cu-O layers) is complicated by the existence of two distinct sites Cu1 and Cu2, whose site energies, and thus core energies, may differ, and with respect to which the hole states may have quite different symmetries. The hole-induced peak (i.e., the one that disappears for $y>0.3$) is more intense for x rays polarized *along the c axis* than for x rays polarized in the Cu-O plane. This indicates that the $d(z^2)$ orbitals are most strongly present in the hole band, or alternatively, they are most strongly hybridized with the O holes in the band. Biaconi, De Santis, *et al.* (1988) suggest that the holes must therefore have strong O4 character, since the O4 atom is the only O atom with $p(z)$ orbitals that couple to $d(z^2)$ Cu orbitals, and it does so for both Cu1 and Cu2 sites.

Park, Oguchi, *et al.* (1988) point out that the local-density band structures of the Y123 compounds provide a natural interpretation of the extra peak seen by Bianconi, De Santis, *et al.* in the oxygen-rich regime. They identify from the partial densities of states mean Cu and O site energies for each inequivalent site; the Cu1 energy E_d lies below the Cu2 d energy by about 0.2 eV and is almost degenerate with the O2 and O3 p energies, while the O1 and O4 p energies lie 1 eV higher. The main line is associated with unoccupied $pd\sigma$ states in the Cu-O layer, for which the O2 and O3 energies are very close to the Cu2 energy. Since the O1 and O4 energies are higher than the nearby Cu1 energy, the hole states will have a reduced amplitude on the Cu1 site and therefore a reduced intensity of the extra peak. The oxygen content dependence reflects the number of holes on the O1 and O4 atoms, and the polarization dependence would be at least qualitatively correct. They also argue that this interpretation depends primarily on the relative site energies rather than the precise position of the local-density bands, and would not be affected greatly by additional correlations.

Oxygen 1s core-level spectroscopy should be helpful in clarifying the nature of the hole states, but there is not yet any consensus on what the intrinsic bulk spectrum is like. The data are sample dependent and sensitive to surface preparation, and interpretation is also complicated by the existence of more inequivalent O sites with varying site core-level energies. References can be obtained from the review of Hass (1989).

The corresponding data for $Bi_2Sr_2CaCu_2O_y$ ($T_c=85$ K samples, presumably with y near 8) have been reported by Bianconi, Castrucci, *et al.* (1988). The position and width of the hole band is similar to that in the Y123 system described above. The polarization dependence reveals, however, that the position of the main peak differs by 0.4 eV for the different polarizations. Since there is only one Cu site in this compound (neglecting complications related to the superstructure in this material), these data would seem to reflect a crystal-field splitting of the core level (an initial-state effect) or some splitting of the final states. Since the hole band appears in both polarizations, Bianconi, Castrucci, *et al.* suggest that the unoccupied states involve both the Cu $d(z^2)$ and Cu $d(x^2\text{-}y^2)$ character in this material.

C. Electron-energy-loss spectroscopy

Fink *et al.* (1989) have provided an overview of the electron-energy-loss spectra (EELS) measured by the Karlsruhe group on the various copper oxides. In high-energy EELS, absorption edges occur at the onset of transitions from a core level to unoccupied states above the Fermi level. For small momentum transfer, the matrix elements lead to dipole transition rules, so at the O 1s edge the absorption should involve unoccupied states with local 2p character near the O atom. Thus EELS measurements provide the potential for obtaining site-selective information on the different O sites. Similarly, transitions from the Cu 2p level should reflect the Cu 3d character of the unoccupied states.

The Karlsruhe group has carried out extensive studies in the region of the O 1s edge around 528 eV. Electron-energy-loss spectra for the $La_{2-x}Sr_xCuO_4$ and $YBa_2Cu_3O_{7-y}$ systems are shown in Figs. 47 and 48. For the antiferromagnetic insulators La_2CuO_4 and $YBa_2Cu_3O_6$, there is no intensity at E_F, consistent with an insulating gap. A steep rise around 3 eV above E_F is interpreted as arising from cation d (and La 4f) unoccupied states. When either of these compounds is doped, by alloying with divalent cations or increasing O content, respectively, considerable spectral weight appears at E_F, indicating that the unoccupied states have strong O 2p character. The weight near E_F increases with increased doping, as shown in Fig. 48.

A standard picture for interpreting the spectra of the copper oxides regards them as doped insulators, with a gap of the Hubbard, or more likely the charge-transfer, type. The holes due to doping then should occupy states below this gap (the "lower Hubbard band"), but presum-

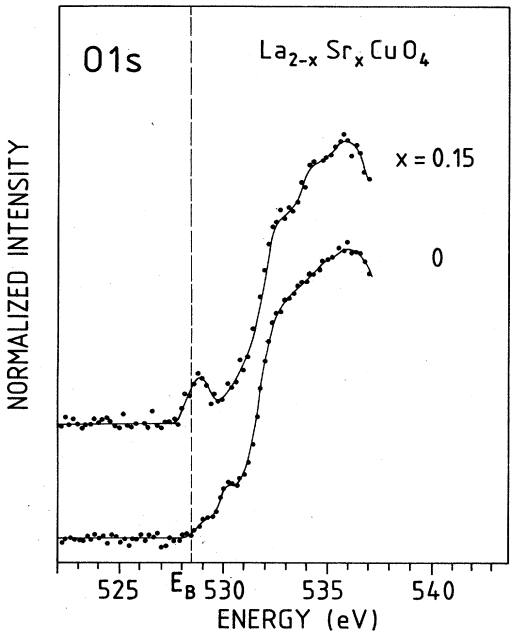

FIG. 47. Electron energy-loss spectrum at the O 1s edge of $La_{2-x}Sr_xCuO_4$, showing the change from vanishing density of O 2p-related states at E_F for $x=0.0$, to a 1–2-eV-wide peak of unoccupied states above E_F for $x=0.15$. From Fink *et al.* (1989).

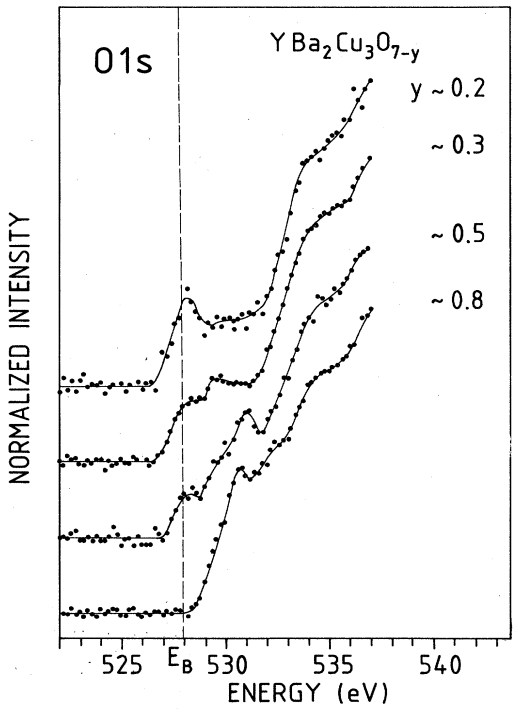

FIG. 48. Electron energy-loss spectrum at the O 1s edge of the system $YBa_2Cu_3O_{7-y}$, showing the increase in O 2p-derived states at E_F as the oxygen concentration increases toward seven, and as T_c increases from zero to 90 K. Note the absence of any Hubbard or charge transfer gap above E_F in the metallic regime. From Fink *et al.* (1989).

ably the gap should remain above this pocket of holes. In Fig. 47 such a gap for the La214 system, if present at all, is seen to be very narrow (no more than about 1 eV). For the Y123 system, shown in Fig. 48, it is clear that there is no gap above the "doped hole states" just above E_F. This lack of gap suggests that the doping levels, at least in the Y123 system, are too large for the compound to be regarded as a doped insulator.

Analogously to the core-level spectroscopy carried out by Bianconi *et al.*, polarization studies by the Karlsruhe group have probed the local symmetry of the unoccupied states by alternatively orienting the momentum transfer parallel and perpendicular to the c axis. These polarizations extract states with local O $p(z)$ and $p(x,y)$ symmetry, respectively. For $YBa_2Cu_3O_7$, shown in Fig. 49, both symmetries are seen, with the O $p(z)$ character having a slightly lower threshold. The differing thresholds could result from slightly different O 1s binding energies at the different sites, or from different energies of the final states. Since it is not possible (at least yet) to discern between these possibilities, so far the existence of distinct O sites is harmful rather than helpful to interpreting the data. Fink *et al.* (1989) have considered models to account for these data as well as those on the insulator $YBa_2Cu_3O_6$. They conclude that the data strongly favor unoccupied (hole) states which have no out-of-plane O

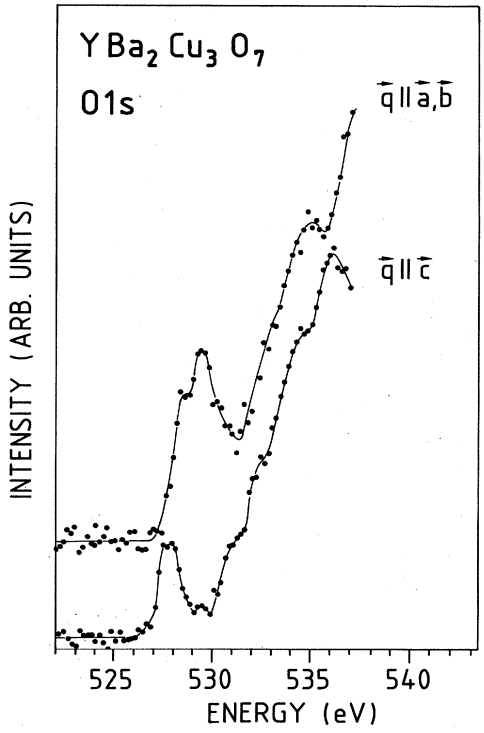

FIG. 49. Electron energy-loss spectrum at the O 1s edge of $YBa_2Cu_3O_7$, showing the strong polarization dependence of the O 2p-related states just above the Fermi level. The strong polarization difference extends up to 5 eV above E_F. From Fink *et al.* (1989).

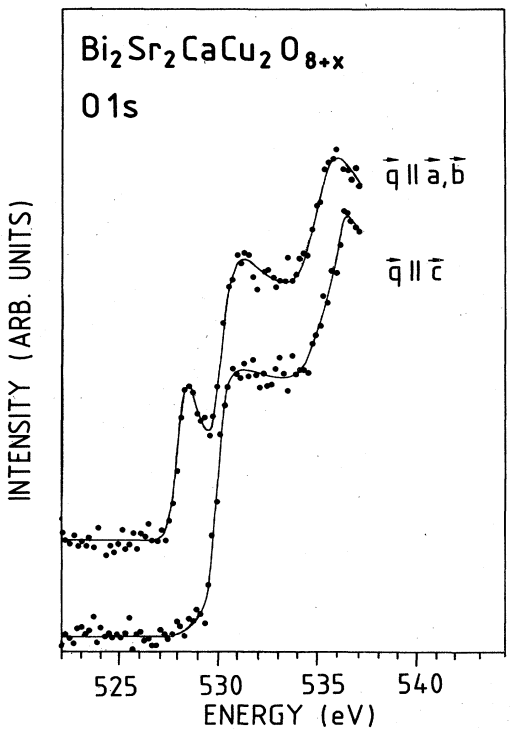

FIG. 50. Electron energy-loss spectrum at the O 1*s* edge of the Bi2212 crystal, indicating the strong polarization dependence of the edge, from Fink *et al.* (1989). These authors conclude that the data eliminate any possibility of O-related holes near E_F that have out-of-plane $p(z)$ polarization.

$p\pi$ character, but may have either $p\sigma$ or in-plane $p\pi$ character.

Fink *et al.* (1989) have also carried out polarization studies on single crystals of $Bi_2Sr_2CaCu_2O_8$. The data are presented in Fig. 50, and show very clearly *no* O $p(z)$ *character* at and just above E_F, but a strong peak with O $p(x,y)$ character. In this case the implication is clear: the hole states have no out-of-plane O $p\pi$ character, but have strong O $p\sigma$ and/or in-plane $p\pi$ character. Fink *et al.* conclude that these data rule out all models of high-T_c superconductivity based on out-of-plane p holes. Himpsel *et al.* (1988) also have reported O 1*s* absorption edge measurements on $Bi_2Sr_2CaCu_2O_8$ which lead them to concur in this conclusion. The analysis of Himpsel *et al.* indicates that the O 2*p* holes have at most 5% $p(z)$ character.

D. Positron annihilation: ACAR

The measurement of the Fermi surfaces of the high-T_c superconductors is crucial for testing any electronic structure model and indeed the Fermi liquid picture itself. Determination of the Fermi-surface areas and masses by the usual methods, such as de Hass–van Alphen or Shubnikov–de Haas oscillations, is rendered almost impossible by at least two complications. First is the high value of T_c itself. The measurements must be carried out in the normal state, above T_c, and the oscillations decrease and vanish quickly with increasing temperature. Second, these methods require clean samples, and it is not obvious that clean enough samples can be fabricated.

One method for the detection of Fermi surfaces that avoids both of these problems is positron annihilation: two-dimensional angular correlation of annihilation radiation (2D ACAR). This method relies on measuring the momentum of the two photons emitted by the annihilation of the positron with an electron in the crystal. This momentum reflects the momentum density of the positron-electron system before annihilation, which contains discontinuities at the Fermi surface. A drawback is that 2D ACAR is not a high-resolution determination of the Fermi surface, but it is extremely useful because it can be used when all other methods fail.

Theoretical knowledge needed to interpret the ACAR data reliably involves the electronic momentum distribution and the positron wave function. The latter has been calculated for crystalline La_2CuO_4 by Jean *et al.* (1988) and for $YBa_2Cu_3O_7$ by von Stetten *et al.* (1988). In the former case the wave function pervades the unit cell, but does sample the Cu-O layers more strongly than other regions in the cell. Thus in this system ACAR should be favorable for sampling a Fermi surface arising from metallic electrons on the Cu-O layers.

For $YBa_2Cu_3O_7$, the situation is more complex. von Stetton *et al.* find that the positron wave function is heavily concentrated near the chains, with the highest density lying parallel to the chains and midway between them. There is very little positron density between the two Cu-O layers, and as a result the wave function samples the layers more weakly than the chains. This information is useful in interpreting the experimental data, which are discussed below. In addition, there have been a number of studies of the positron lifetime (not reviewed here), which show anomalies both at T_c and at other particular temperatures. Knowing that the positron wave function samples the chains more strongly than it does the layers (at least at stoichiometry) puts important constraints on the models suggested for the lifetimes.

Two-dimensional ACAR studies have been carried out by the Tsukuba group for La_2CuO_{4-y} (Tanagawa *et al.*, 1988) and for $YBa_2Cu_3O_{7-y}$ by the Geneva (Hoffman *et al.*, 1988; Peter, Hoffman, and Manuel, 1988) and the Argonne (Bansil *et al.*, 1988; Smedskjaer *et al.*, 1988) groups. Tanagawa *et al.* concluded that the La214 Fermi surface is two dimensional, with a slender electron pillar along Γ-Z and two kinds of hole pillars at the zone boundary, one at the corner and one at the edge. Questions related to the stoichiometry of their sample were not answered in this report, nor did they say whether the crystal displayed a temperature-dependent resistivity characteristic of a metal (indicating non-stoichiometric material) or of a nonmetal (suggesting stoichiometry).

Peter *et al.* and Hoffman *et al.* measured momen-

tum-dependent spectra for $YBa_2Cu_3O_7$ that are typical of other metals with Fermi surfaces. Extracting the Fermi surface involves removing a large, isotropic component of the signal. After doing so, they found they were able to interpret their spectra in terms of the LAPW Fermi surface. The data appear to indicate a large, rounded square, centered at Γ and enclosing holes, similar to the two Cu-O layer sheets in the calculation. A small cylinder centered at Γ and a pair of flattened sheets perpendicular to the chains is also consistent with the ACAR data. The calculated Fermi surface in Fig. 30 does show the pair of flattened sheets, but the cylinder is centered at the zone corner S rather than at Γ. This interpretation of the data is not unassailable, and indeed it is not clear, due to the real space distribution of the positron density, whether the layer-derived Fermi surfaces should be so heavily sampled by the positron.

The data of Smedskjaer *et al.* appear to be consistent with those of the Geneva group. More recently, Bansil *et al.* (1988) have carried through calculations of the actual momentum density $N_{2\gamma}(\underline{p})$ that is measured in the experiment. By broadening the calculated data with the experimental resolution function and comparing the derivative $dN_{2\gamma}(\underline{p})/d\underline{p}$ (to enhance structure), Bansil *et al.* have shown clearly that the structure ($\underline{p}$ dependence) in the data is of just the size and general character to reflect a Fermi surface. The comparison is shown in Fig. 51. Moreover, many (but certainly not all) of the positions where structure occurs in the data agree well with the calculated positions, and the chain-related pieces

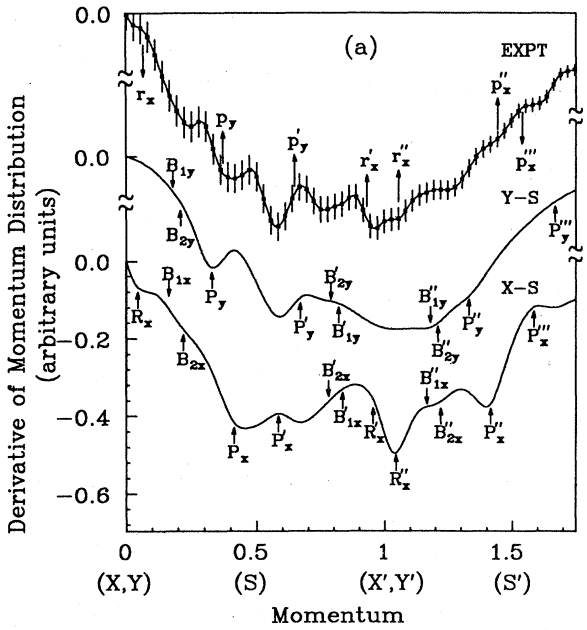

FIG. 51. The momentum distribution spectral function $dN_{2\gamma}(\mathbf{p})/d\mathbf{p}$ (top) in the Cu-O plane, from 2D ACAR experiments, from Bansil *et al.* (1988). The middle and bottom curves are results of local-density calculations along the chain direction and perpendicular to the chain direction.

seem to be more evident, consistent with the calculated positron wave function of von Stetton *et al.* (1988). Similar calculations with a more precise band-structure method, as well as higher-resolution data (especially better statistics) on better crystals, could go farther in establishing the degree of (dis)agreement between band theory and the data, but the present situation strongly points to the existence of a Fermi surface that may be in qualitative agreement with band calculations.

VI. EFFECTS OF DISORDER: ALLOYING AND VACANCIES

In the high-temperature superconducting oxides the effects of disorder have attracted much attention. In the La214 class the reason for the interest is obvious: these materials become superconducting only upon alloying on the La site and/or creation of oxygen vacancies. The result is often described in terms of "doping" of the reference insulator; however, the "doping" level is very high (compared to doped semiconductors, for instance), and the need for a more detailed picture of the resulting disorder is great. In the Y123 system, disorder is not an integral feature of the high-temperature superconductivity, since stoichiometric $YBa_2Cu_3O_7$ is the best superconductor. In this system the interest in disorder is more as a probe of the important interactions, particularly the pairing mechanism, but also as in indicator of the most appropriate viewpoint for describing the electronic structure. The effects of disorder in the Bi- and Tl-based cuprates are less well studied so far, but the sensitivity to preparation conditions suggests that these materials will also display properties that are strongly dependent on alloying and on oxygen vacancies.

A. Oxygen vacancies

The characteristics of O diffusion and the effects of O vacancies are central to the preparation of ceramic samples of the cuprates. The simplest theoretical problem in this arena is the isolated vacancy, for which several possibilities present themselves. Since the oxygens are conventionally pictured as O^{2-} ions, but they leave the crystal as neutral entities, two electrons will be left behind. One possibility is that both electrons remain in the region as deep states in the gap, which in practice might mean that they distribute themselves over not only the vacant site but the neighboring ions as well. At the other extreme is the possibility that the electrons go into itinerant states, a possibility that is most relevant at finite doping levels where the materials are metallic. In this rigid band picture, each oxygen vacancy contributes electrons to the conduction bands.

Burdett *et al.* (1987) carried out Hückel cluster calculations on charged clusters [such as $(Cu_6O_{13})^{14-}$], with and without an internal O vacancy, to model O vacancies in the La214 and Y123 systems. A number of behav-

iors were found to occur, related to the change in band shape and the shift in molecular-orbital energies upon the removal of an O atom. For example, Burdett *et al.* concluded that when every other O1 (chain) atom is removed (corresponding to order $YBa_2Cu_3O_{6.5}$) each Cu1 atom is left in a T-shaped environment that allows two unoccupied $d(z^2\text{-}y^2)$ orbitals to drop in energy. With only two electrons to fill the orbitals, the Fermi level *drops* in energy rather than increasing as a rigid-band picture would predict. This nonrigid behavior is directly related to the self-consistent response of the neighboring Cu orbitals to the presence of the vacancy.

Several studies of ordered O vacancies have been carried out, many indicating the presence of flat bands near E_F as a result. Kasowski, Hsu, and Herman (1987a, 1987b) constructed a supercell by doubling the La_2CuO_4 cell in both in-layer directions, and then removed one O_{xy} atom. Self-consistent calculation of this ordered $La_2CuO_{3.75}$ system found the appearance of a very flat (0.1-eV-wide) vacancy-related band at E_F. Atomic relaxation was not considered in this calculation nor in any of those discussed below, but relaxation is not expected to cause large changes. At the time of this work experimental evidence suggested that O vacancies were *necessary* for formation of the ordered antiferromagnetic state. Since the stoichiometric material does not have flat bands near E_F, Kasowski *et al.* suggested that the antiferromagnetic state is driven by the flat band, suggesting local character, at E_F. Since this time, it has been accepted that stoichiometric La_2CuO_4 is itself antiferromagnetic; hence this interpretation loses its *raison d'être.* In addition, only a few percent O vacancies is necessary to destroy antiferromagnetic ordering. These calculations do, however, indicate that vacancies carry large significant spectral weight at E_F, though no local density of states was given to indicate the magnitude of such an effect or to indicate the amount of spectral weight elsewhere in the valence–conduction-band region.

Sterne and Wang (1988a) made a more direct evaluation of the effect of ordered vacancies on antiferromagnetic order. In conjunction with their local spin-density calculations of stoichiometric La_2CuO_4 discussed in Sec. VIII.C, they carried out parallel local spin-density studies of two versions of ordered $La_2CuO_{3.75}$. In addition to studying a supercell like that of Kasowski, Hsu, and Herman (1987b), they considered another configuration that had inequivalent Cu-O layers, one layer that was stoichiometric and another with O vacancies. In neither case was an ordered antiferromagnetic state found to be stable, and in fact the tendency toward magnetism seemed to be decreased by the vacancies. Sterne and Wang also did not find in their calculations the flat band emphasized by Kasowski *et al.*

Due the strong dependence of T_c and other material properties in the Y123 system on the O vacancy concentration, there have also been studies of O vacancies in this material. Kasowski (1987) studied an ordered $YBa_2Cu_3O_{6.5}$ system by doubling the unit cell along the chain direction and removing every other O1 chain atom. This represents a strong disruption of the quasi-one-dimensional chain states, because it breaks the chain and leaves more or less isolated $(O4)_2$-Cu1-O1-Cu1-$(O4)_2$ units. It is not surprising, therefore, that these units are found to lead to rather flat bands, and some bands are found to lie at or just above E_F. Kasowski suggested that these units could be highly polarizable.

Zaanen, Jepsen, *et al.* (1988) and Zaanen, Paxton, *et al.* (1988) studied a different model of $YBa_2Cu_3O_{6.5}$, in which the unit cell was doubled perpendicular to the Cu-O chain and the O1 atoms removed from every other chain. They obtained a dispersive band crossing E_F which could be modeled in terms of tight-binding Cu1 $d(z^2\text{-}y^2)$, O1 $p(y)$ and O4 $p(z)$ orbitals as

$$E(\mathbf{k})=(\Delta/2)+\{(\Delta/2)^2+2t^2[\alpha^2+1-\cos(\mathbf{k}\cdot\mathbf{b})]\}^{1/2}\ , \tag{6.1}$$

where $\Delta=E_p-E_d$, t and αt are the $(pd\sigma)$ Cu1-O1 and Cu1-O4 hopping integrals, respectively, and $\mathbf{b}$ is the direct lattice vector along the chain direction. O1-O4 interactions are neglected. Zaanen *et al.* then used this tight-binding picture to model vacancies on a chain simply by removing O1 atoms without readjusting any site energies or hopping integrals.

In this nearest-neighbor treatment, removal of chain oxygens breaks the chain into isolated fragments of finite length, each having a number of discrete electronic states proportional to the length. The lowest energy level of each fragment is the same, and the levels are given by $E(\mathbf{k})$ with discrete, evenly-spaced values of $\mathbf{k}$. An additional O vacancy acts as a hole dopant for long chain fragments (low vacancy concentration), but fragments with lengths less than a critical value no longer lead to doping behavior, because the number of states removed from below E_F equals the number of electrons removed. This model provides a framework for understanding the plateaus of T_c versus vacancy concentration that have been determined by several groups (Cava *et al.*, 1987; Tokumoto *et al.*, 1987; Tranquada *et al.*, 1988).

Papaconstantopoulos, Pickett, and DeWeert (1988) (PPD) have used the coherent-potential approximation to study the effects of random O vacancies in La_2CuO_{4-y}. Their tight-binding coherent-potential calculations were based on the tight-binding parametrization (Papaconstantopoulos, DeWeert, and Pickett, 1988) described in Sec. IV.G. In the coherent-potential approximation, one calculates the disorder configuration average of the Green's function of the one-electron problem, by assuming the disorder is random. In the calculations of PPD, a concentration y of oxygen vacancies in La_2CuO_{4-y} was modeled by having each of the four O sites (both O_{xy} and O_z) replaced with a "vacancy" with probability $y/4$. The vacancy was represented by a large positive site energy, and, as usual in the tight-binding coherent-potential approximation, off-diagonal disorder was neglected by keeping the hopping parameters at their stoichiometric

values.

In carrying out the coherent-potential calculations, PPD replaced the oxygen/vacancy site energy by an energy-dependent non-Hermitian self-energy $\Sigma(E)$, which was determined by the condition of zero average scattering. Calculations for $y=0.04$, 0.08, 0.40, and 2.00 served to illustrate the behavior, although certainly the last value is unphysically large. The central result was that the rigid-band picture does *not* hold for O vacancies.

The resultant behavior is pictured in the density-of-states curves of Fig. 52. Comparison with the stoichiometric DOS (not shown) reveals that for small levels of deoxygentation ($y=0.04$) there is indeed no drastic change in the DOS near E_F, as in the rigid-band picture. However, PPD found that, for small y, E_F initially remains nearly constant, and for large values such as $y=0.40$, E_F moves to lower energies, opposite to the prediction of the simple rigid-band model. For $y=0.40$, E_F drops into the (slightly broadened) van Hove singularity, and $N(E_F)$ is nearly doubled. This result is significant for any mechanism of superconductivity that pairs carriers at the Fermi level, since the number of such pairs is proportional to $N(E_F)$. Figure 52 indicates that, although for y values up to 0.40 the shape of the DOS curve changes little, this coherent-potential picture does lead to severe changes in the DOS at (unphysically) large levels of disorder.

The picture that emerges, then, is that the removal of an O atom creates a very large local perturbation, and that the electrons compensate by adjusting their propagation through the lattice to accommodate the vacancies. Although as noted above the *shape* of the DOS is changed little by small levels of O vacancies, the occupied spectral weight is altered in a manner that invalidates the rigid-band picture. PPD found that most of the disorder broadening, represented by $-\mathrm{Im}\Sigma(E)$, is confined to the large DOS region below 1 eV below E_F. The coherent-potential average-scatterer site energy, given by $\mathrm{Re}\Sigma(E)$, is remarkably close to that of the host O atom itself, suggesting that the electrons consistently *avoid* the vacant sites. Therefore in the coherent-potential approximation the removal of y oxygen atoms does not result in the removal of $6y$ valence states, but effectively many fewer.

To summarize, three different methods have modeled oxygen vacancies and obtained nonrigid behavior. In the Hückel-based cluster calculations of Burdett *et al.* (1987) nonrigid behavior arose because of the readjustment of orbitals on neighboring atoms in response to the vacancy. These calculations neglected solid-state effects that were included in the other two calculations, but included the self-consistent electronic responses which were neglected by the two bulk calculations. Zaanen, Paxton, *et al.* (1988) obtained nonrigid behavior due to the vacancy dependence of the energy position of discrete chain fragment states in $YBa_2Cu_3O_{7-d}$. PPD found nonrigid behavior to be a consequence of the propagation of electrons through a lattice containing vacancies. None of these studies considered effects due to lattice relaxation, which can be expected to accompany the removal of a nearly double negative ion. Evidently the question of the effect of O vacancies is a complex one, which has not been answered completely.

B. Cation alloying

The question of cation alloying is a crucial one in the La214 system, because it is only upon alloying La with a divalent cation, Ca, Sr, or Ba, that one alters the material from an antiferromagnetic insulator to a 40-K supercon-

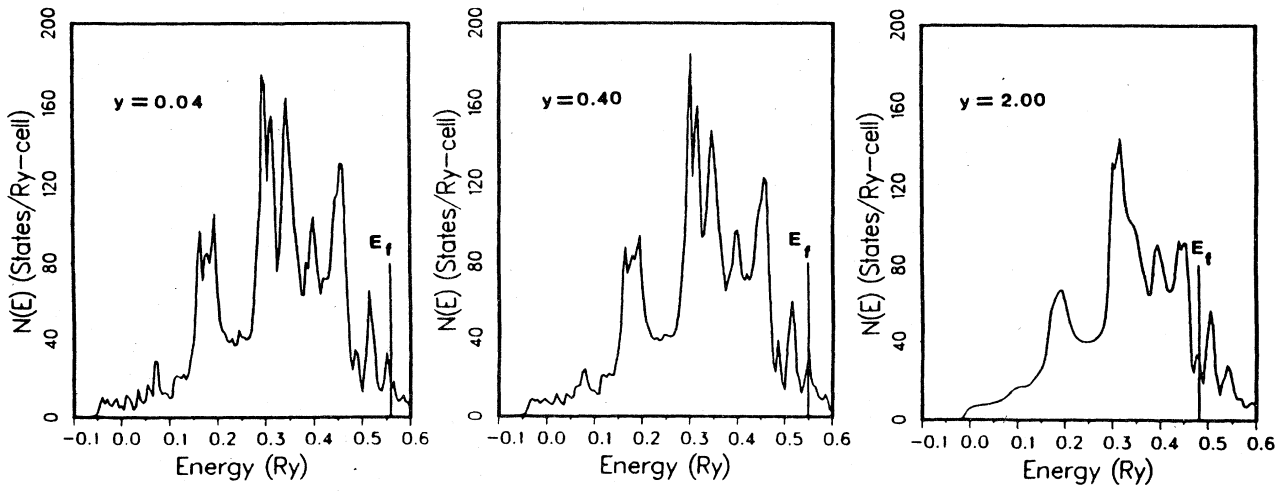

FIG. 52. Density of states for varying O vacancy concentration in La_2CuO_{4-y}, for $y=0.04$, 0.40, and 2.0. These are results from the tight-binding coherent potential approximation calculation described in the text. From Papaconstantopoulos, Pickett, and DeWeert (1988).

ductor. This generally is considered as a generalized "doping" of the material with holes; however, it should be kept in mind that the doping level is quite high. A detailed understanding of cation alloying cannot be achieved without a clear understanding of the antiferromagnetic insulating state itself, about which there is still considerable controversy (see Sec. VIII). However, band-structure calculations can provide important information on differences that arise in the electronic structure due to replacement of La by a divalent cation.

The first such study was that of Pickett, Krakauer, Papaconstantopoulos, and Boyer (1987), in which (paramagnetic) LAPW calculations for $LaBaCuO_4$ were compared with those for La_2CuO_4. All aspects of the atomic structure were the same; one atom of La was replaced with Ba. The valence-band total and partial DOS of the two materials are compared in Fig. 53. In each case the bands are essentially Cu-O bands; nevertheless, there are substantial differences in the DOS. An obvious change is the lowering of E_F upon addition of Ba, because of one less electron per cell. A less obvious change is the rearrangement in the local DOS on both the Cu and the O atoms; overall the valence-band behavior is not at all rigid-band-like. The Cu spectral weight shifts to lower energy, with the prominent peak 2 eV below E_F decreasing markedly in height and a corresponding increase in weight between 3 and 5 eV below E_F; this shift involves primarily "t_{2g}" states. The O_{xy} atoms have their spectral weight shifted upward, but the change is more moderate than on the Cu.

The change in spectral weight on the O_z atoms is most interesting. In $LaBaCuO_4$ the two O_z atoms are inequivalent, being nearly coplanar with either La or Ba atoms. Because of the unit difference in ionic charge between La and Ba, the $O_{z,Ba}$ atoms experience a less attractive electrostatic potential than do the $O_{z,La}$ atoms, and this accounts for the former's local DOS being nearer E_F (less strongly bound) than is the latter. As a result, the $O_{z,Ba}$ atom has a larger DOS at E_F. Both O_z atoms are no longer closed-shell O^{2-} ions as in La_2CuO_4, but have some unoccupied p character and thereby contribute to the metallic behavior. Although the 50% Ba concentration is unphysical, it may be expected that the ionic charge difference between La^{3+} and Ba^{2+} (or Sr^{2+}) may lead to similar effects on nearby O_z atoms in dilute alloys, i.e., the holes may assume some O_z character.

Despite the substantial differences just described, rigid-band-like behavior *does* appear to be followed reasonably well near E_F, where only the $d(x^2\text{-}y^2)$ and $p\sigma$ band contributes to $N(E)$. From Fig. 53 it is evident that there is similar structure near E_F (La_2CuO_4), with the prominent feature of the van Hove singularity occurring around $x=0.15$ remaining upon substitution of Ba for La. The peak height and peak position (versus concentration x) is similar in the two calculations, indicating that a rigid-band picture should be a reasonable first approximation for $x<0.2$.

Schwarz (1987) has used the augmented spherical-wave method (similar in most respects to the LMTO method) to study a smaller concentration of ordered Ba substitution, corresponding to the doubled cell $La_3BaCu_2O_8$. Clearly this will allow a somewhat better picture of the effects of small concentrations of Ba, although at a concentration $x=0.5$ it is still well above the region $x=0.15$ of highest T_c. With Schwarz's choice of cell there are three inequivalent La atoms, six inequivalent O atoms, and two inequivalent Cu atoms; inspecting the differences between them gives a good idea of the local changes due to a Ba atom. For example, the O $2s$ core levels (at roughly -15 eV) are 3–4 eV higher for the O_2 atoms near the Ba ion than those nearest the La ion. The shift in the peak of the valence-band spectral weight is almost as great and somewhat more marked than found by Pickett, Krakauer, Papaconstantopoulos, and Boyer. Considering that the O^{2-} ion is very polarizable and even rather unstable, this raises the possibility that rigid-band doping is not all that is happening in the La214 system. Perhaps the O_z ions are involved in either or both the insulator/metal transition and the superconductivity.

The two Cu atoms that have become inequivalent by the addition of Ba also show differences in detail in their density of states, especially at and just above E_F. The Cu spheres (2.6 a.u. radius) contain charges differing by 0.12 electrons, and Schwarz suggests that once the symmetry is broken by Ba substitution, lattice vibrations could alter the charge on the Cu atoms. Such a phonon/valence fluctuation interaction might be related to electron pairing, although it is unclear that such an argument, which relies on local symmetry-breaking, would apply to the Y123 and Bi- and Tl-based systems.

Stocks *et al.* (1988) have considered this question as well, except that Sr rather than Ba was investigated. Generally the results for $La_3SrCu_2O_8$ were very similar to Schwarz's results. In particular, the charge difference be-

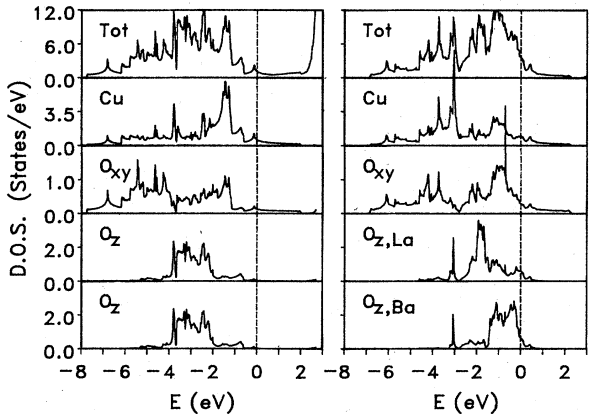

FIG. 53. Comparison of the density of states (DOS) of La_2CuO_4 and $LaBaCuO_4$, showing the effect on the Cu and O spectral densities of replacing a trivalent La ion with a divalent Ba ion. Note particularly the shift of the Cu DOS downward and the shift of the O_z DOS upward by the introduction of Ba. From Pickett, Krakauer, Papaconstantopoulos, and Boyer (1987).

tween inequivalent Cu atoms was the same, and in addition Stocks *et al.* noted changes in atomic charge ("charge transfers") compared to La_2CuO_4 of 0.05 to 0.06 for La, -0.02 to -0.16, for O, and -0.04 to -0.15 for the Cu atoms. The net charge difference lay inside their Sr sphere, which they found to be not as near to 2+ as La is to 3+. The difference in Sr vs La charge seems to be accommodated locally but spread out over both Cu and O atoms, rather than inducing a Cu^{3+} ion, which, as noted in Sec. III.C, requires a large energy.

Stocks *et al.* presented band-structure plots showing that, for these ordered alloy materials, in which alternating Cu-O layers are inequivalent, the corresponding Cu-O $pd\sigma$ antibonding bands crossing E_F are clearly split, by about 0.3 eV. This raises the possibility that the carriers are significantly more perturbed than would follow from the rigid-band picture.

Each of these studies has considered ordered cation substitutions. One study, by Papaconstantopoulos, Pickett, and DeWeert (1988), has employed the tight-binding coherent-potential approximation to study random alloying on the cation site. Using tight-binding fits to Ba_2CuO_4 as well as La_2CuO_4, PPD simulated the alloy by a coherent-potential medium described by a system with La, Ba site energies distributed randomly on the La site; they treated the overlap parameters in a virtual-crystal approximation. Changes in local geometry and local on-site energies due to replacement of La by Ba were neglected. They found that this treatment indeed produced rigid-band behavior near the Fermi level, just as many people have suggested. In particular, the Fermi level fell at the van Hove peak in the density of states at $x=0.14$.

VII. TRANSPORT CALCULATIONS

A. Background: models

The calculation of transport properties in the normal state and comparison of the results with experiment is a stringent test of any theory of the electronic structure of the copper oxide materials. In the standard superconductors such as Nb or Nb_3Sn the normal state is a Fermi liquid for which the quasiparticle energies and wave functions are described exceptionally well by local-density band calculations. The transport properties of several transition metals calculated within Bloch-Boltzmann theory have been found to be in excellent agreement with experiment, even with respect to the temperature dependence (Allen *et al.*, 1986). This is true even in Pd, which, although a nonsuperconductor, like the cuprates shows evidence of magnetic correlations and must have a Coulomb correlation U_d of the order of the d bandwidth of 5 eV. A comprehensive discussion of the alternative models for transport is beyond the scope of this article. However, it is necessary for an understanding of the implications of the band-theory-based results discussed below to have some impression of the alternate approaches being discussed.

In Sec. VIII the band-insulator-versus-Mott-insulator picture of the insulating phases is discussed. In the metallic regime, which is all that will be considered here, a similar general question arises: is the normal state in a Fermi-liquid-like regime, or is it more properly described from an alternative viewpoint based on the strong correlation limit? Many of the transport properties look much like ordinary quasiparticle transport for which the scattering mechanism is electron-phonon scattering, which suggests normal Fermi-liquid behavior. Even the linear T dependence of the resistivity ρ is expected (contrary to some suggestions that ρ is "too linear" for quasiparticle scattering), a point that will be clarified below. One aspect of the data that is difficult to account for is the unusually large temperature derivative of ρ. This value continues to decrease, however, as better samples are made.

Alternative approaches to the local-density-approximation-based Bloch-Boltzmann theory rest either on the strong anisotropy, and resulting quasi-two-dimensional character of the transport, or on the dominance of correlation effects. Emphasizing the two dimensionality, Lee and Read (1987) argued that electron-electron Coulomb scattering can be altered significantly if E_F is at a logarithmic van Hove singularity in $N(E)$. This argument has two clear weaknesses. One is that the band structure, and perhaps the experimental data, does not support the degree of two dimensionality required by this picture.

The second problem is that, although band theory predicts E_F to fall in such a van Hove singularity for $x=0.15$ in the $La_{2-x}M_xCuO_4$ system, there is no general expectation nor support from band theory that E_F will fall in such a singularity for all the materials that show linear T dependencies. Indeed, the linear T behavior persists with varying metal atom and oxygen content with simply a changing magnitude (until the insulating regime is approached), just as if the band structure at E_F were being altered in a continuous and systematic way. Such material variations would be expected to move E_F into and out of van Hove peaks or to wash them out, indicating that the Lee-Read mechanism could not apply generally. Xing, Liu, and Ting (1988) have suggested that conductivity perpendicular to the Cu-O layers should be interpreted in terms of phonon-assisted electron hopping, which they find can account for both the sign and the temperature dependence of single-crystal transport data.

Another picture that has been suggested is the resonating-valence-bond picture of Anderson (1987) and collaborators, whose elementary excitations apparently consist of charged bosons without spin (holons) and spin-$\frac{1}{2}$ excitations without charge (spinons). One point of view is that the scattering of the holons, which carry the current, by the spinons would lead to a linear T dependence of ρ, while another viewpoint leads to a $T^{3/2}$ dependence. This theory is still in a developmental stage.

B. Bloch-Boltzmann theory

The purpose of this section is to evaluate the successes and weaknesses of the band-theory-based Bloch-Boltzmann theory of transport when applied to the copper-oxide materials in the metallic regime. This theory is based on the picture that the elementary excitations are itinerant quasiparticles with well-defined wave vector and unit charge. The resulting transport equations are valid when the scattering processes are independent, i.e., when the distance between successive scatterings, the scattering length l, is much larger than an interatomic spacing. The particular treatment supposes, for the sake of testing the band picture, that the quasiparticle energies are given by the local-density bands, and that the scattering is due to interactions with phonons (and of course static impurities, when present).

The theory has been discussed by Allen, Pickett, and Krakauer (APK) (1987a, 1988b). To derive the expressions for the conductivity σ, the Hall tensor R^H, and the thermopower S, one considers the system in the presence of an external electric field $\mathbf{E}$, magnetic field $\mathbf{H}$, and thermal gradient. The current is given by

$$j_\alpha=\sigma_{\alpha\beta}E_\beta+\sigma_{\alpha\beta\gamma}E_\beta H_\gamma+\nu_{\alpha\beta}\nabla_\beta T+\cdots \tag{7.1}$$

with sums over repeated indices understood. The resulting expressions for the coefficients, assuming electron-phonon scattering and $N(E_F)\hbar\omega_D \ll 1$, are

$$\sigma_{\alpha\beta}=e^2\tau(n/m)_{\alpha\beta}\equiv\frac{e^2\tau}{\Omega_0}\sum_{\mathbf{k}} v_\alpha(\mathbf{k})v_\beta(\mathbf{k})[-\partial f/\partial E(\mathbf{k})] , \tag{7.2}$$

$$\sigma_{\alpha\beta\gamma}=-\frac{e^3\tau^2}{\hbar\Omega_0}\sum_{\mathbf{k}} v_\alpha(\mathbf{k})\{[\mathbf{v}(\mathbf{k})\times\nabla(\mathbf{k})]_\gamma v_\beta(\mathbf{k})\}\times[-\partial f/\partial E(\mathbf{k})] , \tag{7.3}$$

$$\nu_{\alpha\beta}=\frac{e\tau}{\Omega_0 T}\sum_{\mathbf{k}} v_\alpha(\mathbf{k})v_\beta(\mathbf{k})[E(\mathbf{k})-\mu][-\partial f/\partial E(\mathbf{k})] . \tag{7.4}$$

In a variational approach the scattering time τ can be regarded as a parameter to be chosen to maximize the current for a given scattering operator. In the first approximation (constant τ) several results do not depend on the scattering. The anisotropy results exclusively from the anisotropy of the $E(\mathbf{k})$ and its derivatives at E_F.

The expressions for the standard transport coefficients are

$$R^H_{xyz}=\sigma_{xyz}/\sigma_{xx}\sigma_{yy} , \tag{7.5}$$

$$S_{xy}=-\sum_\gamma(\sigma^{-1})_{x\gamma}\nu_{\gamma y} . \tag{7.6}$$

For the tetragonal and orthorhombic systems being considered here, σ and ν are diagonal tensors with two (tetragonal) or three (orthorhombic) independent elements. The third-rank tensor $\sigma_{\alpha\beta\gamma}$ vanishes unless all three indices are distinct, and it satisfies the Onsager relations $\sigma_{yxz}=-\sigma_{xyz}$, etc. This leaves three independent coefficients R^H_{xyz}, R^H_{yzx}, R^H_{zxy} in orthorhombic symmetry, and two in tetragonal symmetry (x and y being equivalent).

In the constant τ approximation, the Hall coefficient is independent of the scattering and depends only on the bands $E(\mathbf{k})$ near E_F. However, involving as it does the *second derivative* as well as the first derivative of $E(\mathbf{k})$, it can be a very sensitive probe of the bands. For a single isotropic parabolic band $E(\mathbf{k})=(\hbar\mathbf{k})^2/2m^*$, R^H is given very simply in terms of E_F and $N(E_F)$, but is usually written, and interpreted, in terms of the "density" of carriers:

$$R^H=1/ne , \tag{7.7}$$

with the sign of the carriers being given by the sign of R^H. Besides being applicable only to a single parabolic band, this formula is somewhat deceptive in that it appears to reflect contributions from each of $n\Omega$ nondegenerate carriers per volume Ω. Actually this expression is derived for a degenerate Fermi-liquid-like system, and a more instructive expression is

$$R^H=-3/[2eE_F N(E_F)] , \tag{7.8}$$

where the sign comes naturally from the sign of E_F, which is positive for electrons and negative for holes. Of course, E_F and $N(E_F)$ cannot both be determined from this single relation, from which the effective mass cancels for simple parabolic bands. The more general expression (7.5) holds for any number of bands and for arbitrary band filling, and the sign of the Hall tensor simply reflects the shape, and particularly the curvature, of the Fermi surface. It is quite possible for R^H to have different signs for different directions of the field, a result that would be nonsensical within the simple expression (7.7) and, as will be seen below, one that actually occurs in the calculations for high-T_c copper oxides.

Before proceeding with specific calculations, let us address the general behavior mentioned above, that of a linear T dependence of ρ. APK (1988a, 1988b) have asked what behavior is to be expected from phonon scattering in these materials. The formula for τ is

$$\hbar/\tau_{ep}=4\pi k_B T\int_0^{\omega_{\max}}\frac{d\omega}{\omega}\alpha^2_{tr}F(\omega)\frac{\hbar\omega/2k_BT}{\sinh(\hbar\omega/2k_BT)} , \tag{7.9}$$

where $\alpha^2_{tr}F$ is the electron-phonon spectral function which enters the resistivity and $\omega_{\max}$ is the maximum phonon frequency. While $\alpha^2_{tr}F$ is not known for any of the cuprates, inelastic neutron scattering has been used to measure $G(\omega)$, which is $F(\omega)$ weighted by neutron-phonon matrix elements rather than by the electron-phonon matrix elements in $\alpha^2_{tr}F$. These spectral functions often are rather similar, and this should be particularly so in these cuprate systems where the electron-

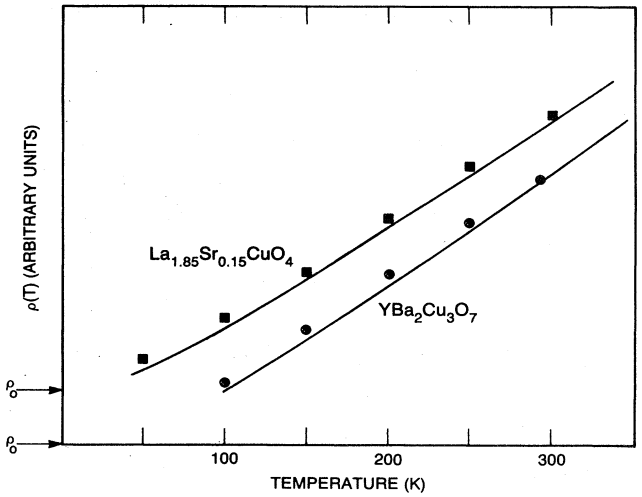

FIG. 54. Calculated shape of the resistivity vs temperature expected for Fermi-surface carriers scattering from phonons in the La214 and Y123 systems. Actual data are shown as the symbols. Note that the residual resistivity and the slope have been adjusted (see text); this illustrates that phonon scattering is predicted by Bloch-Boltzmann theory to be just as linear, to as low a temperature, as is seen in the data. From Allen, Pickett, and Krakauer (1988b).

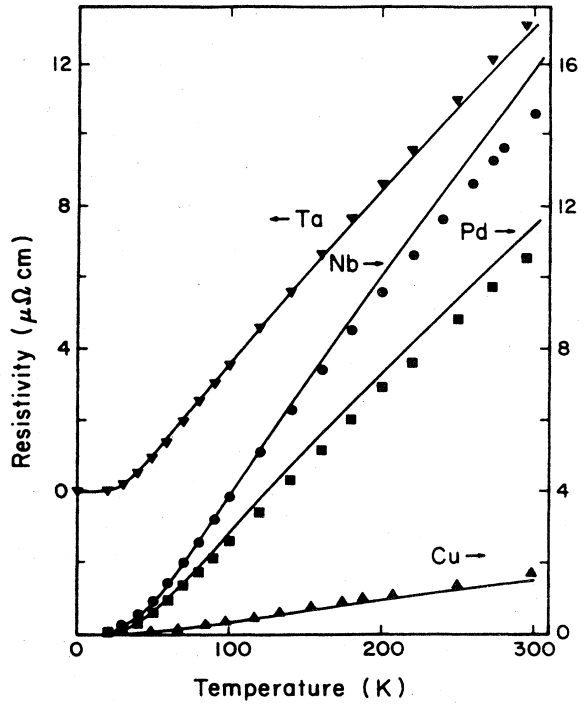

FIG. 55. Resistivity vs temperature for several elemental transition metals, illustrating that linear behavior to low temperature is common in transition-metal systems. Note also that the linear parts of the curves may extrapolate to *negative* values at $T=0$. Symbols represent experimental data, while the curves are from local-density-based Bloch-Boltzmann theory. Values for Ta are displaced by four units for clarity. From Allen *et al.* (1986).

phonon interaction is expected to be dominated by the Cu and O atoms, because the neutron cross section is also largest for these atoms.

Using the data from Renker *et al.* (1987) and Rhyne *et al.* (1987), one can calculate the temperature dependence of ρ as shown in Fig. 54 for both the La214 and Y123 systems. The variation with T is seen to be essentially linear above T_c, just as in the data. Note that only the shape of the curve is being compared in Fig. 54, not the magnitude. This figure makes it very clear that not only is the resistivity *not* too linear for the electron-phonon interaction, but exactly this kind of linear behavior is *predicted* by Bloch-Boltzmann theory with phonon scattering. In fact this kind of "linear" behavior, which is at odds with textbook examples assuming Debye spectra, is seen in many transition-metal systems.

Data for several transition metals, as well as the results of local-density-based calculations (Allen *et al.*, 1986), are shown for comparison in Fig. 55. Not only are they "linear" well below the Debye temperature, they sometimes extrapolate to negative values at $T=0$, contrary to textbook examples. This behavior is the result of strongly non-Debye phonon spectra, a phenomenon especially pronounced in the cuprates. The spectrum for Y123, presented in Fig. 56, shows that there are strong lattice vibrations extending all the way from 10 up to 80 meV (120–1000 K in temperature units). The result is an ex-

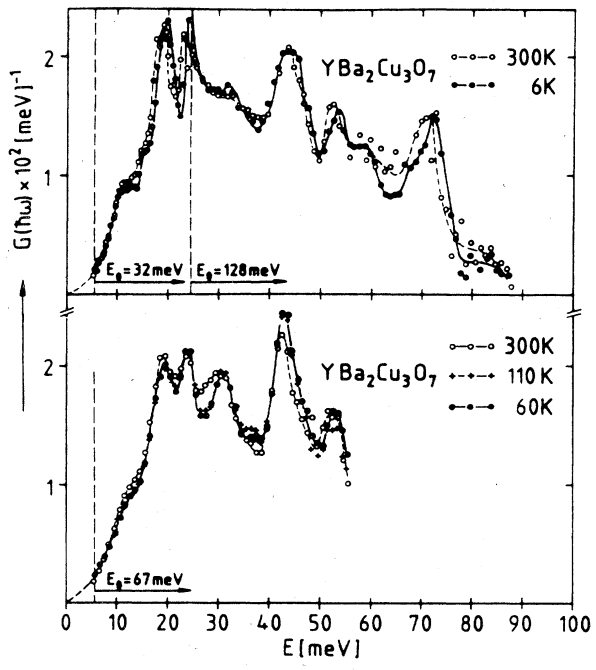

FIG. 56. Measured phonon density of states of $YBa_2Cu_3O_7$, from inelastic neutron scattering measurements of Renker *et al.* (1987). Note that this spectrum is nothing like a Debye spectrum that is often assumed in "pedagogical" examples. Note also the rather small temperature dependence of the data.

tremely structureless $\rho(T)$ curve because the integral in Eq. (7.9) is so weakly dependent on temperature.

C. Calculations using band quasiparticles

1. Hall coefficient and thermopower

The earliest transport experiments were made on ceramic (polycrystalline) samples. Due to the wide variation in stoichiometry and to the unknown effect of anisotropy, these data are very difficult to interpret. For these reasons it is appropriate to compare the calculations only with single-crystal data.

The first crystal data were reported by Suzuki and Murakami (1987) on an LSCO sample with $x=0.06$, $T_c=20$ K; these authors reported a value of 0.92×10^{-9} m^3/C for the Hall coefficient (at 300 K) for a field along the c axis. The corresponding calculations of APK (1987a, 1987b) for both independent components of the Hall tensor in the La214 system are shown in Fig. 57 as a function of concentration x within the rigid-band model. The agreement with the measured value, within a factor of 2.5, was encouraging for the band model, particularly since the first objective was to discern the viability of local-density-approximation-based Bloch-Boltzmann theory. This calculation is also only the lowest-order result.

The measured value is positive, indicating "holelike"

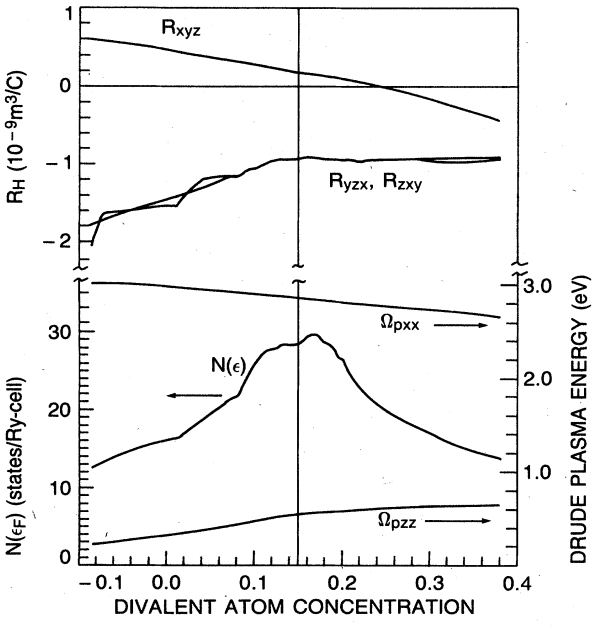

FIG. 57. Quantities related to transport properties of the La214 system, from local density band calculations. Top: The two independent components of the Hall tensor of tetragonal $La_{2-x}M_xCuO_4$, calculated in the rigid-band picture as a function of divalent atom concentration. Bottom: The van Hove singularity in the density of states broadened by small three-dimensional dispersion, and the doping dependence of the Drude plasma energy, as a function of M atom concentration. From Allen, Pickett, and Krakauer (1987a).

transport. The positive sign has been observed in most ceramic samples and has led to a number of models based on a single holelike band. The magnitude, 0.92×10^{-9} m^3/C, corresponds to a Hall number, or "hole density," from Eq. (7.7) of 0.006 holes/formula unit, which would correspond to a low-density semimetal. More recent data (Suzuki, 1989) on oriented crystalline films however, indicate a Hall coefficient that is an order of magnitude smaller, i.e., the Hall number $n=0.06$ is approximately equal to the Sr content x in this range.

Two features of the calculations of APK were unexpected. First, for field directions in the a-b plane, R^H is predicted to be negative, i.e., electronlike, with similar (factor of 2–3 larger) magnitude. Apparently there are still no data for comparison, due to the difficulty of growing crystalline samples in the metallic regime and the shifting emphasis on higher-T_c materials. The second feature is the unexpected prediction that R^H_{xyz} should decrease in magnitude and change sign at $x=0.24$ as the Sr or Ba concentration is increased. Behavior with such a trend has been reported by Ong *et al.* (1987) and by Suzuki (1989) on oriented films of LSCO, although R^H never crossed zero. For x up to 0.1, R^H follows Eq. (7.7) reasonably well, with $n=x$ (within a factor of 2). For larger values of x, however, Suzuki finds that R^H decreases much faster than that simple relation would predict, and for $x=0.36$ the discrepancy is a factor of 100. On the other hand, Suzuki did not find an actual change of sign as predicted by APK. The data of Suzuki and Ong *et al.* are not in agreement beyond $x=0.15$; in fact, the data of Ong *et al.* strongly suggest that a change of sign would occur just above $x=0.20$, in agreement with the band calculations of APK, but their samples ended at this concentration.

The change of sign arises naturally in the band picture for a single, nearly half-filled band such as occurs in La_2CuO_4. For E_F near band bottom, the simple expression (7.7) applies and describes a large, electronlike value of R^H. Near band top, R^H is also large but holelike. In between, R^H varies continuously and passes through zero at band center. Similarly, the inverse band mass defined by the second derivative of $E(\mathbf{k})$ (which is not the most common band mass) vanishes at the center of the band as well.

One component of the Hall tensor in a high-T_c Y123 compound was measured by Tozer *et al.* (1987). However, since their crystal was highly twinned (as are nearly all Y123 crystals), their measurement, which was for the field direction in the plane, corresponds to some average of R^H_{yzx} and R^H_{zxy}. Surprisingly, they found an *electronlike* value of -0.8×10^{-9} m^3/C. This value is in striking agreement with the prediction of APK (1988b), who calculated values of -0.4×10^{-9} m^3/C and -1.1×10^{-9} m^3/C for the field perpendicular to the Cu-O chains and along the chains, respectively. For the field in the third direction, that is, along the c axis, they measured a "holelike" value of 0.2×10^{-9} m^3/C, also in agreement with the band prediction of APK. The calculated values

versus E_F, as in a rigid picture, are shown in Fig. 58, where the data of Tozer *et al.* are shown as dots. In contrast to the La214 system, three is no predicted change of sign near E_F which could be reachable by reasonable amounts of doping.

These results—the strong variation of R^H with doping in the La214 system and the differing signs for different field orientations in the Y123 system—offer strong evidence in favor of the Fermi-liquid picture of the ground state in the superconducting oxides. It is certainly the simplest way to understand these results on a qualitative and semiquantitative level. This interpretation is not complete, however. The behavior of R^H_{xyz} for La214 was found to have a complicated T dependence (Suzuki, 1989). The calculations of APK are only the lowest-order results, which are independent of the scattering and are T independent. In higher-order approximations the details of the scattering likely will lead to T dependence which cannot be foreseen.

APK (1987b, 1988a, 1988b) also calculated the thermopower tensor for both La214 and Y123 systems. The calculation of S requires the energy dependence of the scattering time (for vanishing energy dependence, S vanishes), and they used three separate models to identify the sensitivity. In each case they found a negative value for transport in the *a-b* plane; for perpendicular transport the sign depended on the model of the energy dependence. Crystal data for the Y123 system have been presented by Yu, Naughton, *et al.* (1988), who find S in the *a-b* plane of $YBa_2Cu_3O_7$ to be -2.5 μV/K, and by Crommie *et al.* (1988), who report it to be almost an order of magnitude larger and of opposite sign. It is impossible to draw any conclusions at present regarding the validity of the band picture from the thermopower.

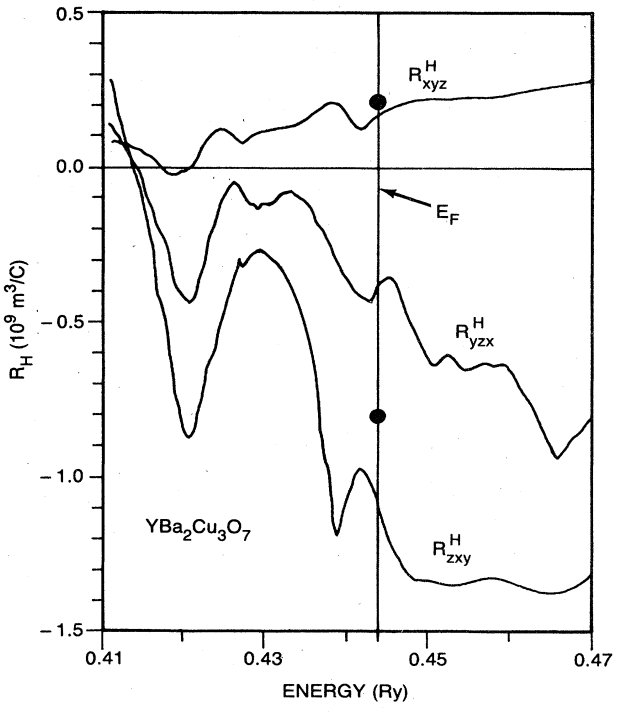

FIG. 58. The three elements of the Hall tensor for $YBa_2Cu_3O_7$, calculated by Allen, Pickett, and Krakauer (1988b) as a function of energy near E_F. Solid points indicate data of Tozer *et al.* (1987) on a twinned crystal; the negative data point should correspond to some average of the two calculated negative values at E_F.

2. Resistivity

Here, as above, we consider only the metallic regime, where there is the best hope of obtaining a viable picture of the transport properties soon, leaving the nonmetallic phases for the future. This regime is also of the most current interest, since it is this phase that is superconducting.

For the in-plane component of the resistivity, the experimental data are clear: $\rho(T)$ is linear in T from T_c, as discussed above, to the point where oxygen begins leaving the material. For the perpendicular component, however, the data are not unanimous. In highly anisotropic crystals the inversion of the measured *I-V* characteristics to obtain the resistivity tensor is nontrivial. However, the use of effective isotropic medium models (Montgomery, 1971) is accepted, and many workers report perpendicular resistivities (in the metallic, high-T_c samples) which change very little with T or increase somewhat at the lower temperatures. These measurements are complicated in the La214 system by the difficulty of preparing bulk crystals for $x > 0.05$, while in the higher-T_c materials the region above T_c may be representative of a changeover between high-T and low-T behavior.

Other behavior has also been reported. While Ossipyan *et al.* (1988) report Y123 crystals for which ρ_c becomes nearly constant as the highest T_c is obtained, Iye *et al.* (1988) report *metallic* (linear in T) resistivity for some of their highest-quality single crystals, with the magnitude being 20–50 times larger than the in-plane values. This observation of metallic behavior along the *c* axis has been supported by infrared spectroscopy by Bozivic *et al.* (1988), who find metallic behavior in the *c*-axis reflectivity for their single crystals and highly oriented crystalline films. Bozivic *et al.* suggest that *c*-axis conduction may be extremely sensitive to planar stacking faults, microcracks, and oxygen inhomogeneities, and that only the best samples are metallic along the *c* axis. At this stage the character of the *c*-axis conductivity must be considered an unsettled question.

The linearity, i.e., the *shape,* of the resistivity was discussed above. The *magnitude* has been the object of discussion as well. Allen, Pickett, and Krakauer (1987a, 1988b) used the following expressions (appropriate for isotropic scattering time τ) to calculate the band quasiparticle prediction based on electron-phonon scattering, to estimate the magnitude of $\rho(T)$, and to compare its derivative with experiment:

$$\rho_{xx}^{ep}=4\pi/(\Omega_{pxx}\tau_{ep})\ , \tag{7.10}$$

$$\hbar/\tau_{ep}=(2\pi\lambda_{tr}k_BT)(1-\hbar^2\langle\omega^2\rangle_{tr}/12k_B^2T^2+\cdots)\ , \tag{7.11}$$

$$\Omega_{pxx}^2=(4\pi e^2/\Omega_0)\sum_{\mathbf{k}}v_{\mathbf{k}x}^2\delta(E_{\mathbf{k}}-E_F)\ , \tag{7.12}$$

$$\lambda_{tr}\langle\omega^2\rangle_{tr}=2\int(d\Omega/\Omega)\alpha_{tr}^2F(\Omega)\Omega^2\ . \tag{7.13}$$

In these equations, in which y and z can be substituted for x, α_{tr}^2F is the spectral function for phonon-limited quasiparticle transport. The important band parameter is the Drude plasma energy tensor $\hbar\Omega_p$, which is the product of the $N(E_F)$ and the mean-square Fermi velocity. Because $N(E_F)$ is large where v_F is small (and vice versa), Ω_p is usually not sensitive to calculational details, whereas the Hall and thermopower tensors are.

Calculated values of Ω_p are listed in Table I, with corresponding values of $N(E_F)$ and the Fermi velocity. In principle Ω_p can be determined by experiment, from the infrared conductivity, from the superconducting coherence length, or from measurements of the London penetration depth, although the infrared conductivity may be affected by interband contributions and may contain many-body renormalizations. APK have examined the experimental literature and found that the values derived from infrared conductivity and coherence length are often within 25% of the band values. The values from penetration depth measurements should be more reliable, however, and they trend to be a factor of 2–3 smaller than the band values. For example, from direct measurements of the penetration depth on twinned crystals, Krusin-Elbaum *et al.* (1989) obtain $\hbar\Omega_{p,ab}=1.4$ eV, compared with the band values $\hbar\Omega_{p,xx}=2.9$ eV, $\hbar\Omega_{p,yy}=4.4$ eV.

The Drude plasma energy is also important because, from Eq. (7.10), it is directly related to the magnitude of the resistivity, and particularly its temperature derivative. Gurvitch and Fiory (1987a, 1987b, 1988) noted that the in-plane resistivity in both the La214 and Y123 systems not only is linear up to high temperature, but also assumes very large values, which are difficult to understand easily. Whereas previous strong electron-phonon coupled metals show saturation of the resistivity to a value of 250–300 $\mu\Omega$ cm, in the cuprates measured resistivities have been much larger. Gurvitch and Fiory used the relation for the mean free path $l=v_F\tau$ and Eqs. (7.10) and (7.11) to argue that the measured resistivities imply that λ (which as usual they equated with λ_{tr}) must be very small, at most 0.1 in the La214 system and 0.3 in Y123. Otherwise the mean free path due to phonon scattering would be smaller than the smallest possible scattering length, the Cu-O separation.

TABLE I. Calculated Fermi-surface parameters (density of states, Fermi velocity, and the Drude plasma energy tensor) for the La214 and Y123 high-temperature superconducting oxides. From Allen, Pickett, and Krakauer (1988b).

	$La_{1.85}Sr_{0.15}CuO_4$	$YBa_2Cu_3O_7$	Unit
$N(E_F)$	28.4	76.0	states/Ry cell (both spins)
$\langle v_x^2\rangle^{1/2}$	2.2	1.8	10^7 cm/s
$\langle v_y^2\rangle^{1/2}$	2.2	2.8	10^7 cm/s
$\langle v_z^2\rangle^{1/2}$	0.41	0.7	10^7 cm/s
$\hbar\Omega_{pxx}$	2.9	2.9	eV
$\hbar\Omega_{pyy}$	2.9	4.4	eV
$\hbar\Omega_{pzz}$	0.55	1.1	eV

APK also noted a related discrepancy, in a different way. They used estimates of λ (again equated to λ_{tr}) from the rigid muffin-tin model to calculate the value of the resistivity. Comparing with the best data available at the time, they found that the calculated values of ρ(295 K), or equivalently $d\rho/dT$, were smaller than experimental values by a factor of 5 and 10–12 for La214 and Y123, respectively. This discrepancy is in spite of the fact that the value of λ they used for La214 is much larger than the derived "upper limit" surmised by Gurvitch and Fiory. They suggested four possible resolutions: (1) λ should be larger, in accordance with the preliminary studies of the electron-phonon interaction reviewed in Sec. X.B, (2) the Drude plasma energy should be smaller than the band values, (3) another scattering mechanism is dominant, or (4) the measured resistivity is not representative of the intrinsic value.

At least in the Y123 system it has turned out that at least suggestion (4) was correct. Recent samples reported by Stormer *et al.* (1988) show resistivities at 100 K almost a factor of 4 smaller than were being assumed by APK and by Gurvitch and Fiory. The slopes, however, may only be up to 50% less, although the resistivity curves are still linear. These seemingly contradictory items arise because the linear resistivity curves sometimes extrapolate to rather large negative values at zero temperature (as large as -40 to -50 $\mu\Omega$ cm). Their values are still quite sample dependent, and perhaps none of the measured values represents the intrinsic resistivity.

The consequence is that the calculated resistivity slope based on the rigid muffin-tin model are somewhat closer to the current "best" data, and the arguments of Gurvitch and Fiory are weakened slightly, but still apply. At least until the data from different groups become consistent, the questions raised here will remain unanswered.

VIII. MOTT OR BAND INSULATORS: ANTIFERROMAGNETISM

A. Transition-metal monoxides: preliminaries

The transition-metal monoxides MnO, FeO, CoO, and NiO comprise the most heavily studied subset of the class of materials known as Mott insulators. In periodic solids there is a strong tendency for the valence electrons to become itinerant because it is favorable for an electron to lower its kinetic energy by hopping from atom to atom;

localization costs kinetic energy due to the increased spatial variation of the wave function. Itinerant states are described well by the band picture, and they give rise to metallic behavior, except in special cases when (1) there are an even number of electrons/unit cell and in addition (2) a band gap occurs just above the uppermost occupied band. These "special cases" of course occur rather commonly in simple compounds, and there are abundant examples for both metals and nonmetals, i.e., semiconductors, where the band picture clearly provides the proper picture of the electronic states.

Since hopping of electrons between atoms will be opposed by the Coulomb repulsion between electrons, Mott (1964) proposed that when this repulsion becomes strong enough a metal-to-insulator transition will occur. The cost in potential energy arising from hopping will outweigh the gain in kinetic energy, and the electronic states are best described as localized rather than itinerant. A considerable amount of study of the transition-metal oxides in general and the monoxides in particular led to the widely accepted picture of these materials as canonical Mott insulators.

A simple argument against the band picture in the transition-metal monoxides (TMMO's) arises when we consider, for example, CoO. This compound has the rocksalt structure, with one Co ($Z=27$) and one O ($Z=8$) atom in the primitive cell. Therefore there are an odd number of electrons in the unit cell, and the band picture must predict it to be metallic. It is observed to be an insulator; does this prove that the band picture is invalid? This observation alone does not, because there is the complicating aspect of the magnetic state: CoO is observed to be antiferromagnetic. The reduced symmetry of the antiferromagnetic phase necessarily requires a doubling of the unit cell, leading to an even number of electrons, and as a result there is no reason *a priori* why the band picture must fail to give an insulating state.

The interrelation of strong intra-atomic correlation and antiferromagnetic behavior is pervasive, although much of the early theoretical work tried to ignore this connection. Mott's picture suggests that in the strongly correlated limit the materials should be insulating regardless of the magnetic structure. However, once states are localized by the strong interactions, the magnetic interactions and the tendency to integral occupation of such states strongly favors the antiferromagnetic state. Such considerations as this led Brandow (1977, 1988) to give a working definition of a Mott insulator as a material that shows local-moment behavior and is insulating, regardless of its magnetic structure. The TMMO's are observed to remain insulating above the Néel temperature T_N (typically a few hundred degrees) and therefore seem to fit this picture naturally. However, short-range correlations probably exist above T_N, which could introduce the concept of a *local antiferromagnetic electronic structure* that might again account for the insulating behavior.

Early on there was an alternative picture of these materials, namely, the antiferromagnetic band picture of Slater (1951). Calculations by Wilson (1968, 1970) for MnO clearly showed insulating behavior, due simply to the fact that the exchange splitting is much larger than the d bandwidth (see the discussion below). Wilson also obtained a gap for NiO, but in this case it was because the crystal-field splitting between the e_g and t_{2g} band complexes was larger than their bandwidths. Due to the somewhat *ad hoc* nature of his exchange potential, these results were tentative. Mattheiss (1972) carried out a systematic study of the $3d$ transition-metal monoxides, neglecting spin polarization, and analyzed the bandwidths and crystal-field splittings with the aid of tight-binding parametrizations. His conclusions concerning the likelihood of obtaining band insulating behavior in these materials were pessimistic and tended to reinforce the Mott insulator viewpoint.

Recently, however, the picture of the TMMO's as the canonical Mott insulators has been called into question again by more sophisticated band-structure studies. The crucial developments in band theory were twofold. First, the standard utilization of self-consistency to generate the one-electron potentials removed the arbitrariness in constructing potentials that was standard procedure in earlier times. Second, the local *spin*-density approximation, again applied in a self-consistent way, has become standard in providing the band picture of magnetism, due to its many convincing successes in the description of transition-metal magnetism. (The local spin-density approximation also has clear shortcomings, as will be discussed below.)

In a series of papers, Terakura, Williams, Oguchi, and Kübler (TWOK) (Terakura, Oguchi, *et al.*, 1984; Terakura, Williams, *et al.*, 1984) have presented in some detail a picture of the 3D transition-metal monoxides as band insulators. It is necessary to be more specific about the electronic structure to follow the argument. The electronic structure generally is viewed within an ionic picture: the O p states lie below the transition-metal d states and are completely occupied, so the O ion is doubly charged negatively, leaving the transition metal as a $2+$ ion. The transition-metal d states therefore are only partially filled. Up to this point there is no basic disagreement between the Mott insulator and band picture viewpoints.

For MnO the picture obtained by TWOK is qualitatively like that of Wilson, being the result of the exchange splitting between majority and minority states being somewhat larger than the d bandwidth $W\sim 3$ eV. However, while the *ad hoc* exchange potential of Wilson had the exchange splitting much larger than W, leading to a gap of 2.7 eV, this inequality is marginal in the work of TWOK, who find a band gap of 0.4 eV. (For various reasons TWOK argue that this value should not be compared directly with the measured optical gap. On a more fundamental level, the spin-density functional formalism does not guarantee a realistic gap, as discussed briefly in Sec. IV.A.) In fact, TWOK find that the observed [111]

magnetic modulation, in which alternating planes of transition-metal atoms have up and down spins, is central in producing the nonmetallic band structure. Only within this magnetic structure is it possible for σ bonding of the e_g states across the nearest-neighbor oxygen ions, which is the strongest bonding interaction, to couple only exchange-split d states. As a result this interaction serves to increase the exchange splitting rather than to enhance the e_g bandwidth.

For FeO, CoO, and NiO the exchange splitting progressively decreases, from ~ 3 eV for MnO to 1.3 eV for NiO, and as a result the moment also decreases. For NiO the band situation is even more intricate than for MnO, because in addition to the σ bonding contribution to exchange, which is as important as in MnO, the [111] spin alignment causes the e_g and t_{2g} subband widths to be determined by π bonding rather than σ bonding. As a result a 0.3-eV band gap arises. In the interest of rounding out this short discussion of the band insulator picture of the transition-metal monoxides, it must be noted that TWOK do not actually obtain gaps for FeO and CoO. However, from the measured moments in these systems it is apparent that there is an orbital contribution to the moment, so it is hardly surprising (or damning) that a spin-only theory fails to describe these two compounds.

A detailed theory of the spectra of most transition-metal oxides no doubt lies somewhere between the extremes of the Mott insulator picture and an LSD treatment. Recently a picture has been developed by Zaanen and co-workers (Zaanen, Sawatzky, and Allen, 1985, 1986; Zaanen and Sawatzky, 1987) in which $d_i^n d_j^n \rightarrow d_i^{n-1} d_j^{n+1}$ transitions (where i,j denote neighboring transition-metal sites) become less dominant because a $d^n p^m \rightarrow d^{n+1} p^{m-1}$ transition involving oxygen holes is energetically favored. Such oxides are referred to as "charge transfer" insulators, which they find to include several TMMO's and perhaps the insulating copper oxides. Further review of this picture would take the present discussion well beyond the intended purpose, which is simply to introduce the issue involved in a possible band insulator picture of copper oxides. Concepts which are central to the charge-transfer picture are discussed in Sec. XI.

For further discussion on the relative merits of the band insulator picture of the TMMO's the original papers should be consulted. The purpose of introducing it here is to emphasize several features that these calculations illustrate. First, it is clear that local spin-density theory is a well-developed approach and at least offers the possibility of describing *some* basic properties of so-called Mott insulators. After all, the exact density functional theory must reproduce an antiferromagnetic insulating ground state. Second, it is necessary to carry out accurate, well-converged computations without unphysical constraints to be certain of the predictions of the theory. This concern will be even more relevant for materials that are more complex structurally, such as the cuprates of interest here. Third, it has become clear that the results can be strongly dependent on the magnetic structure of the material. This feature bears some connection to the discussion of Brandow describing how the *spatial extent* of the localized Wannier functions, which in his view would be most appropriate for describing these magnetic insulators, should be strongly dependent on the magnetic structure of the neighboring atoms. Finally, it must be recognized by the band theorists that obtaining an insulating magnetic ground state is necessary for obtaining any realistic description, but even doing so does not guarantee that the important interactions are being described correctly.

B. Experimental studies of magnetism

The spectroscopy of the magnetic behavior in the La214 and Y123 systems is a subject both too broad to cover in a subsection of this review and not entirely relevant to the electronic structure studies that are to be surveyed here, which are confined to the existence and character of the magnetic structure in the ground state. Nevertheless, several experimental facts must be considered to put the calculational results in proper context, so we try briefly to collect these facts here. More detailed discussions of the experimental data are given by, for example, Aeppli, Harshman, *et al.* (1988), Birgeneau, Gabbe, *et al.* (1988), Endoh *et al.* (1988), Lynn and Li (1988), Tranquada (1988), and Birgeneau and Shirane (1989).

1. La214 system

Changes in the magnetic structure of solids often can be monitored by measuring the magnetic susceptibility. The observation that no appreciable change in the susceptibility occurred at the La_2CuO_4 tetragonal-to-orthorhombic transition around 500 K suggested no magnetic participation in this transformation, as well as very little change in the electronic structure. A peak in the measured susceptibility, typically in the range 150–250 K, suggested magnetic ordering at this temperature. This supposition was first verified by powder-neutron-diffraction studies by Vaknin *et al.* (1987). They identified a superlattice reflection, which they attributed to planar antiferromagnetic ordering shown in Fig. 59(a), which appeared only below the temperature where the peak in susceptibility occurred. This was confirmed by single-crystal neutron diffraction by Freltoft *et al.* (1987), who also identified the spin structure. Several other studies have confirmed and extended these results.

The magnetic structure of La_2CuO_4 is shown in Fig. 59(b). Recall that the crystal structure at this temperature is orthorhombic *Abma* with two formula units per primitive cell, and we use the notation a', b', c' of Sec. II, with $c' \gg a', b'$, for the orthorhombic lattice vectors. The two Cu ions in the Cu-O layer have oppositely directed moments, and the direction of the moments is

along the a' axis, which lies at 45° angle (approximately) to the Cu-O bond. Thus the spin direction points along the direction of corrugation of the Cu-O layer. There is some evidence that (1) the spin on the Cu does not lie strictly in the a'-b' plane but tilts with the CuO_6 octahedra at 5° angle, and (2) there is a small moment on the O_{xy} ion, which lies perpendicular to the Cu moments. We return to these items briefly below when discussing the possible symmetries of the antiferromagnetic state.

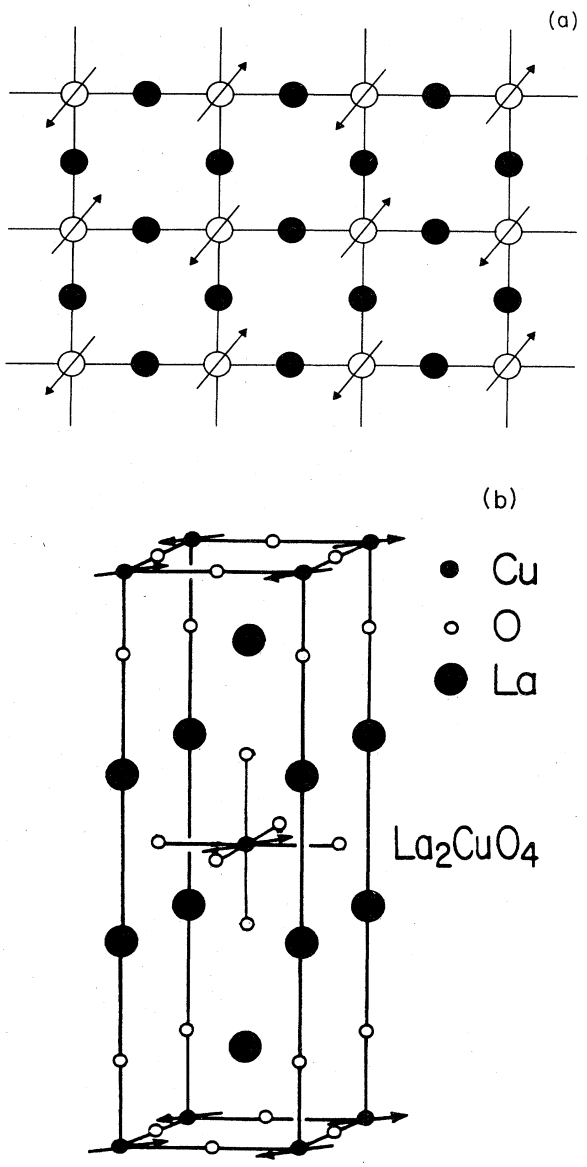

FIG. 59. The magnetic structure of La_2CuO_4 determined by neutron scattering (see text for references). (a) The X-point ordering in the Cu-O plane, with copper and oxygen denoted by open and filled circles, respectively. The moments lie in the plane. (b) A three-dimensional representation of the antiferromagnetic structure. The orthorhombic distortion is neglected in this figure.

Several studies have established that the Néel temperature T_N is extremely sensitive to the oxygen content. The original studies on ceramic materials concluded (Johnston *et al.*, 1987) that stoichiometric La_2CuO_4 is *not* antiferromagnetic, but only becomes so at O deficiencies around $y=0.03$. More recently it seems to have become accepted that the stoichiometric material is antiferromagnetic. This point, which is crucial to a theoretical understanding of the magnetic ordering in this system, seems not to have been settled. Sinha (1988) has suggested that the samples used in the above-mentioned experiments were deficient not only in oxygen but in La as well, since significant La deficiencies have been found in other samples. La substoichiometry could compensate the O vacancies, resulting in material that corresponds crudely to the "half-filled band" limit satisfied by the stoichiometric compound. These questions are difficult to settle absolutely. The oxygen content can be varied systematically in ceramic samples, where the oxygen only has to diffuse a distance of a grain size, and relative oxygen concentrations can be obtained to within 0.01 in favorable cases. However, methods of measuring the absolute oxygen content are accurate to no better than about 0.03, and the absolute La concentrations are also difficult to determine with this accuracy.

Besides being sensitive to oxygen, and probably La, concentration, T_N is also sensitive to divalent metal (Ba, Sr) doping. While the ordering vanishes rapidly with doping, neutron scattering studies have established that in-plane correlations of the moments persist upon doping to the $x=0.06$ level with Sr, and perhaps somewhat beyond. The correlations are such that two-dimensional local antiferromagnetic order is retained over significant coherence lengths. While doping strongly reduces the coherence length, the total magnetic scattering appears to be rather insensitive to doping, at least at moderate doping levels, which has been interpreted as an indication that the size of the Cu moment does not change much.

Values quoted for the magnitude of the ordered moment range from 0.1 to $0.5\mu_B$. Assuming that the $L=2$ orbital moment of the Cu^{2+} ion is quenched by solid-state effects, as seems to be the case in other Cu-based magnetic materials, we would expect the moment to be around $1.1\mu_B$, arising from a $1\mu_B$ spin contribution and a 10% increase due to spin-orbit coupling enhancement of the g factor. The measured moment, which is assumed to be a "reduction" from this value, often has been attributed to spin fluctuations, which are expected to be stronger in 2D than in 3D and could serve to make the ordered component of the moment less than the actual atomic moment. An alternative explanation is that fluctuations are not so important, but that the local moment itself is reduced by hybridization with the O p states. This latter interpretation is supported by the observation of a moment of $0.68\mu_B$ in CuO (Forsyth *et al.*, 1988; Yang, Tranquada, and Shirane, 1988), a 3D solid that should not display pronounced reduction of the moment due to

fluctuations. Another possibility, discussed by O'Keefe and Stone (1962) and earlier workers, is that the reduction in moment and the behavior of the susceptibility can be accounted for by the formation of quasilocal singlet pairs of Cu^{2+} moments, this being a three-dimensional forerunner of the "resonating-valence-bond" picture of Anderson (1987).

Long correlation lengths, of the order of 200 Å, also have been observed above T_N in the undoped material. The implications of this are, first, that the Cu moment is local in nature and is rather robust and, second, that the lack of Curie-Weiss behavior in the susceptibility above T_N is clarified. Curie-Weiss behavior would result from *independent* local moments, but the strong spin coupling results in correlated spins, which must respond collectively to an applied field. The long-range moment correlations above T_N could also be consistent with a picture of a *local* antiferromagnetic band picture in the high-temperature paramagnetic phase.

2. Y123 system

The first search for magnetic scattering in the Y123 system was carried out by Brückel *et al.* (1987) on a ceramic sample with $T_c = 90$ K and O stoichiometry estimated in the range 6.9–7.0. An extensive search found no evidence of any magnetic scattering and placed a very small upper limit on the magnetic scattering possible in this sample.

Tranquada *et al.* (1988) reported powder-neutron-diffraction data on ceramic samples of $YBa_2Cu_3O_{6+x}$ with $x = 0.0$ and 0.15. They identified 3D ordering of Cu spins in the CuO_2 layers with an in-plane wave vector of $(\frac{1}{2},\frac{1}{2},0)$, as pictured in Fig. 59(a). The Cu ions in the two Cu-O layers are ordered antiferromagnetically. The Néel temperature was 400 K for $x = 0.15$ and was greater than 500 K for $x = 0.0$. Referencing the magnetic peak intensities to the Cu^{2+} form factor and assuming that Cu2 but not Cu1 ions are ordered, they obtained an ordered moment of about $0.5\mu_B$ per Cu2.

Magnetic order was measured less directly by inelastic light scattering and by muon spin rotation (μSR) experiments. Lyons, Fleury, Remeika, Cooper, and Negran (1988) reported Raman spectra on a number of twinned crystals with varying oxygen content. For the nonsuperconducting samples with low O content, strong scattering attributed to highly energetic spin excitations (similar to La_2CuO_4) were seen in the range 1000–4000 cm^{-1}, and the intensity of these dropped dramatically in the superconducting samples with large O content. Brewer *et al.* (1988) used μSR studies to establish magnetic order for $0.0 < x < 0.4$ and a Néel temperature that dropped rapidly from around 450 K for $x = 0.0$ to near zero at $x = 0.3$–0.35.

Kadowaki *et al.* (1988) applied neutron scattering to a single crystal of composition $x = 0.35$ and discovered a *second* magnetic transition at 40 K, well below $T_N = 405$ K. This transition is due to ordering of Cu1 spins of small magnitude (of order $0.02\mu_B$). This ordering, however, causes Cu-O layers above and below the Cu1 ion to become ordered ferromagnetically. Coupling across the oxygen-deficient Y layer is such that unit cells along the c direction alternate in spin direction, resulting in a doubling along the c axis. Accounting for this magnetic structure promises to be a demanding task for theorists.

C. Local spin-density calculations

1. La_2CuO_4

The first investigation within the local spin-density approximation into the possibility of accounting for the antiferromagnetic phase of the La214 system was carried out by Leung, Wang, and Harmon (1988). They used an *ab initio* linear combination of atomic orbitals (LCAO) method based on Gaussian orbitals. The charge and spin densities and the potential were also expanded in Gaussian functions, so there were no shape approximations (other than a finite expansion, as in any approach) to these quantities. The von Barth–Hedin form of local spin-density potential, as modified by Moruzzi *et al.*, was used. Their calculations, however, were carried out with La replaced by Sc, because in their LCAO method the decrease in the number of core states resulted in a substantial decrease in computational effort. The Sc d bands were somewhat lower than those found in the La compound, but the Cu-O band complex and Fermi surface were found to be very similar to those reported by Mattheiss (1987) and by Xu *et al.* (1987).

Leung *et al.* did not obtain any antiferromagnetic solution in their study, which was carried out in the observed orthorhombic structure. In an attempt to quantify the antiferromagnetic tendency they applied staggered magnetic fields on the Cu sites to enforce antiferromagnetic moments of up to $0.8\mu_B$. The resulting band structure near E_F along important high-symmetry directions is shown in Fig. 60. The moment makes the two Cu atoms in the cell inequivalent and splits the bands along the M-N-S-L direction, which must be degenerate by symmetry in the paramagnetic state. For an enforced moment of $0.5\mu_B$, which is similar to the maximum reported experimental moment, the splitting in their Sc_2CuO_4 calculation was about 0.15 eV, while the dispersion of these bands is 0.7 eV, so no gap is obtained. They noted however that the dispersion of this band is less in tetragonal La_2CuO_4 (0.43 eV) and is further decreased by 10% by the orthorhombic distortion. Thus it appears that achieving an antiferromagnetic solution may be a delicate problem. A possibility that they did not take into account is that the *local* moment may well be close to the $1\mu_B$ expected for a Cu^{2+} (d^9) ion. The Bragg peak strengths seen in neutron scattering experiments measure the *ordered* moment rather than the actual local moment, and in small moment systems fluctuation effects are

known to reduce the values of the ordered moments.

Leung *et al.* carried out another artificial calculation to further understand the antiferromagnetic tendency in this system. In carrying out the calculation to self-consistency, it is necessary to take an adequate sampling of states over the Brillouin zone. In this system the antiferromagnetic moment splits the band degeneracy at an edge of the zone near the Fermi surface, as shown in Fig. 60, and a careful sampling of this region is essential to establish the existence, or in this case the lack of it, of an antiferromagnetic state. Due to computational considerations, a fully convergent sampling was not attempted. However, in one calculation they (1) overemphasized this region by placing sampling points along the orthorhombic zone boundary, and (2) encouraged an antiferromagnetic solution by occupying the *lower* of the two split bands (those shown in Fig. 60) regardless of the size of the gap between them, which amounts to placing the Fermi level between the split bands. If the splitting were larger than the dispersion of these bands, this occupation would arise naturally.

Within this scheme they obtained an antiferromagnetic solution with a Cu moment of $0.14\mu_B$, as well as a small oppositely directed moment (10% as large) on each of the two O_z ions above and below the Cu ion. However, the mean splitting along *M-N-S-L* was very small, only 0.04 eV. They also found that even the application of a staggered magnetic field could not raise the moment above $0.16\mu_B$. This results because a large fraction of the bands that drive the antiferromagnetism are O_{xy} states, which were forced to have no net moment by the symmetry of their calculation. This strong mixture of Cu and O_{xy} character in the Fermi-level states leads to the prediction that the induced magnetic form factor (i.e., that due to the application of an external field) will have strong contributions from both types of atoms and therefore will not look simply like the Cu *d* form factor (see below).

Due to the use of Sc rather than La and to the fact the convergence of zone sampling was not demonstrated, these results might not be considered conclusive. Several studies have been reported using the LMTO method (see Sec. IV) and the von Barth–Hedin local spin-density exchange-correlation potential. Sterne *et al.* (1988) obtained results for both the high-*T* tetragonal and low-*T* orthorhombic structures which confirmed those of Leung *et al.*, both with respect to the normal self-consistent calculation (showing no moment) and the constrained occu-

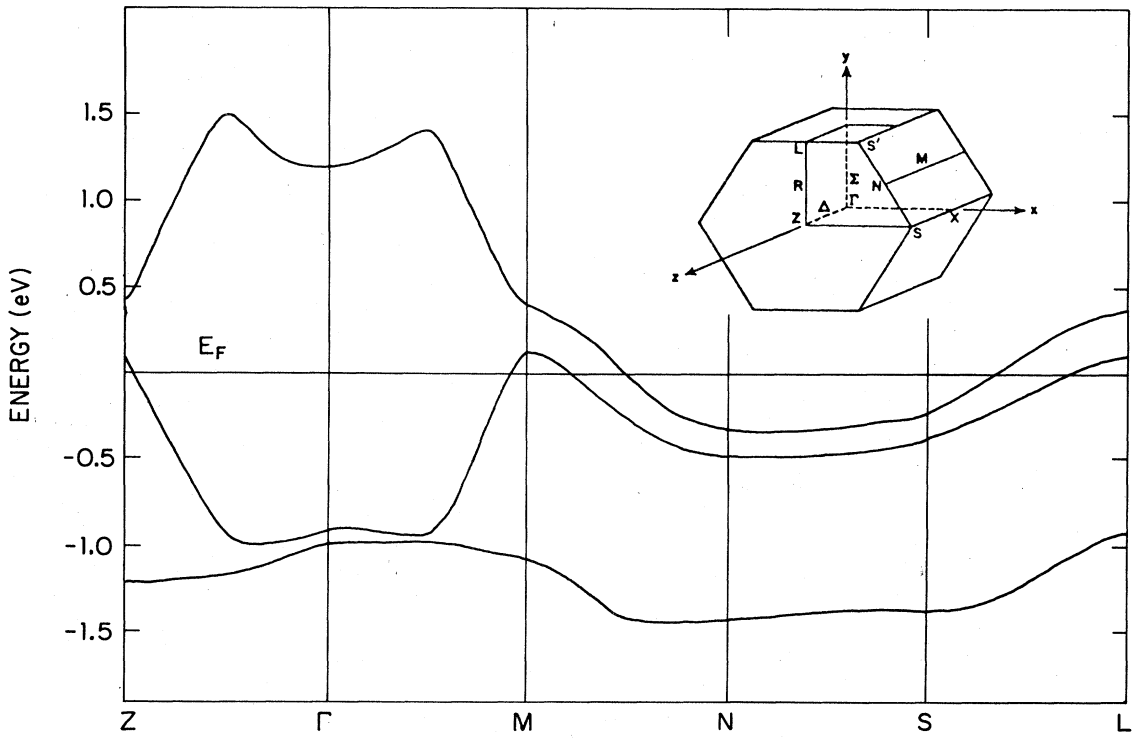

FIG. 60. Band structure near the Fermi level (taken as the energy zero) with an antiferromagnetic moment imposed. The antiferromagnetism lifts the band degeneracy along the *M-N-S-L*, splitting the bands throughout the zone, but no true gap is obtained. From Leung, Wang, and Harmon (1988).

pation model in which the lowest of the split bands is occupied everywhere.

However, using very similar methods, Guo, Temmerman, and Stocks (1988) reported that they did indeed obtain an antiferromagnetic solution with $0.11\mu_B$ per Cu in both the tetragonal and orthorhombic structures, when 80 k points in the irreducible ($\frac{1}{8}$) zone were used for sampling. The energy of the antiferromagnetic structure was only marginally lower than for the paramagnetic state, by 1 mRy. When the number of sampling points was increased systematically, the moment decreased, to a value of $0.05\mu_B$ for 252 k points in the sampling. They concluded that, although converged sampling probably could lead to a vanishing moment, La_2CuO_4 is on the verge of antiferromagnetism within the local spin-density approximation.

Hatsugai and Fujiwara (1988) also carried out LMTO studies with the von Barth–Hedin potential, but did not include the tilting of the Cu-O octahedra. They obtained an antiferromagnetic solution with $0.15\mu_B$/Cu, but did not report the number of points used in the zone sampling. If this number was of the order of 25, their result for the moment would be consistent with that of Guo *et al.* above, as their bands appear to be. They report, however, that the antiferromagnetic state is 50 mRy lower in energy than the paramagnetic state, in considerable disagreement with Guo *et al.*

Kasuya and Takegahara (1988) reported augmented plane-wave calculations of the antiferromagnetic state in La_2CuO_4, although no details of the method and convergence levels were given. They reported obtaining no stable antiferromagnetic state when using the Perdew-Zunger parametrization of the Ceperley-Alder exchange-correlation potential. They studied the effects of an *ad hoc* enhancement of the exchange potential, and found that doubling it led to an antiferromagnetic solution with $0.4\mu_B$ and a gap of the order of 0.1 eV.

Calculations using the self-consistent norm-conserving pseudopotential method have been reported by Shiraishi *et al.* (1988a, 1988b) using the Perdew-Zunger parametrization of the Ceperley-Alder exchange-correlation energies. They report obtaining an antiferromagnetic solution with $0.43\mu_B$/Cu, a relatively wide band gap of 0.6 eV, and an energy that is about 10 mRy lower than the paramagnetic state. Although they do not report details of the calculation, it appears that they applied the local spin-density formalism to the *valence pseudocharge density* rather than to the full density including the cores, which may result in a severe overestimate of the exchange potential in the core region. In local spin-density theory the exchange potential V_{ex} is dependent on the fractional spin polarization $\xi(\mathbf{r})=m(\mathbf{r})/n(\mathbf{r})$, where $m(\mathbf{r})$ is the spin density, and in the small-ξ regime—which is the case in solids—V_{ex} is proportional to ξ. Since nearly all of the polarization occurs in the valence density, it might be reasonable to use the valence pseudocharge densities in the numerator. The use of the pseudocharge density rather than the total density in the denominator will, however, result in artificially large values of ξ where the core density is appreciable but is omitted from the denominator of ξ. Since the d states of Cu are rather compact and overlap the cores considerably, the overestimate of the exchange potential could be substantial, as indeed seems to be the case when we compare it with the all-electron calculations discussed above. Therefore these pseudopotential results should be considered much less indicative of the true situation than the all-electron results.

The LMTO calculations can be criticized both because of the approximations made when solving the local spin-density equations and because there is no absolute consensus on the results. However, due to the general similarity between the LMTO results and those of the LCAO method, there is no clear reason to suspect their implications: La_2CuO_4 is at least near an antiferromagnetic instability in the local spin-density approximation, but there is *no* prediction of a strong local moment. It would be desirable to know the results of a method, such as the LAPW, that makes no shape approximations to the density or potential and also is converged in other respects, especially in the zone sampling.

Pickett and Papaconstantopoulos (1989) have used their accurate tight-binding parametrization of the La_2CuO_4 band structure to investigate the effect of *imposed* (non-self-consistent) antiferromagnetic polarizations on the bands, and the resulting moment. Their study began with the paramagnetic bands, then lowered the spin-up orbitals on one Cu site and raised the spin-up orbitals on the other Cu site before determining the spin-up bands, with analogous treatment of the spin-down bands. If all five Cu d orbitals were spin split, corresponding to a spherically symmetric exchange potential, no gap in the band structure was obtained. Applying the exchange potential only to the $d(x^2\text{-}y^2)$ and $d(z^2)$ orbitals likewise gave no gap, consistent with the fact that nearly all of the Cu character near the Fermi level involves only these two orbitals.

When the exchange potential was applied only to the $d(x^2\text{-}y^2)$ orbital, however, a gap opened easily, and a moment of $0.4\mu_B$ (comparable to the experimental value) was obtained for a spin splitting of 50 mRy=0.7 eV. The corresponding exchange potential in a spin-density functional calculation would have to be highly aspherical, such as would arise from a d^9 Cu ion with one unoccupied $d(x^2\text{-}y^2)$ orbital. This picture is much like that of the local-moment viewpoint and suggests that one shortcoming of the local spin-density approximation is in not producing enough angular variation of the exchange potential, which could produce an orbital dependence to the exchange splitting.

2. $YBa_2Cu_3O_6$

Local spin-density calculations for $YBa_2Cu_3O_6$ have been reported by Szpunar, Smith,and Smith (1988) and by Temmerman, Szotek, and Guo (1988), both of whom

used the LMTO method. Szpunar *et al.* reported obtaining both ferromagnetic and antiferromagnetic solutions with substantial moments, while Temmerman *et al.* reported obtaining a very small (perhaps vanishing in the limit of full convergence) antiferromagnetic moment. Szpunar and Smith (1988) have presented paramagnetic band structures of both $YBa_2Cu_3O_7$ and $YBa_2Cu_3O_6$ that are in serious conflict with the accepted LMTO band structures as reported by several other groups. Flat bands near the bottom of the valence-band region in their calculation may be spurious solutions to the LMTO eigenvalue equations ("ghost bands"), which when included as occupied states in a self-consistent procedure lead to an unphysical one-electron potential, which is reflected in the severely distorted bands in the region of the Fermi level. However, the ferromagnetic and antiferromagnetic bands show no evidence of such anomalies. They are distinct from those of Temmerman *et al.* in showing a band gap of 1–2 eV between the Cu-O valence-band complex and the higher unoccupied bands. This may reflect a difference in basis sets, as discussed below.

In their magnetic calculations Szpunar *et al.* (1988) found that the Cu1 atom always had negligible moment. The ferromagnetic moment was not reported, but the antiferromagnetic state with $0.38\mu_B$ per Cu was stated to be more stable. The antiferromagnetic state was found to be stabilized in their calculations by the opening of a gap at E_F, which was helped by a flattening of bands at the Brillouin zone corner by the exchange potential. The gap in the eigenvalue spectrum was very small, of the order of 0.1 eV.

Temmerman *et al.* (1988) found that their self-consistent solution was very sensitive to the k-point sampling of the zone, a point also noted by Szpunar *et al.* Temmerman *et al.* also pointed out that the results are sensitive to the basis set used in the calculations. Changing the expansion of the wave functions on the O atoms, for example, from $L_{\max}=2$ down to $L_{\max}=1$, changes not only the moment but the amount of charge inside the O sphere (and, by charge neutrality, within other spheres as well). Including up to $L_{\max}=3$ on the Cu and $L_{\max}=2$ on the O led to a smaller moment than when $L_{\max}=1$ was used for the O, and the moment decreased as the k-point sampling increased. Thus while an antiferromagnetic solution was found, the moment was small and uncertain, apparently less than $0.1\mu_B$ per Cu. It will require a more precise calculational method, such as the LAPW method, to determine conclusively the prediction of local spin-density theory for the antiferromagnetic of $YBa_2Cu_3O_6$. It seems likely, however, that local spin-density calculations fail to predict a strong Cu moment in this system, analogously to its shortcomings in the La214 system.

D. What the form factor implies

If local spin-density calculations were successful in obtaining an antiferromagnetic state in these materials, the correctness of such a description could be given a severe test by comparing the calculated magnetic form factor with the experimental measurement. Since the local spin-density approximation fails to produce a viable magnetic state, no such comparison is possible. It is possible to enforce in some way a magnetic moment on the calculation, and Leung, Wang, and Harmon (1988) have done so. Here we review what has been surmised about the magnetic state from the form-factor measurements and present the results of the induced form factor due to the application of a magnetic field.

Form-factor measurements have been reported by Freltoft, Shirane, *et al.* (1988) for a single crystal of La_2CuO_4 with $T_N=185$ K and an ordered moment at low temperature of $0.30\mu_B$. Based on seven measured magnetic reflections, the results roughly follow the Cu^{2+} form factor of Cu, but show deviations beyond the error bars of the experiment. The deviations occur in the 1–3 Å^{-1} range, where Leung *et al.* find a deviation of the calculated form factor due to p-d hybridization ("covalency effect"). However, the measured deviations are not as large as, nor in very good agreement with, the calculated deviations. Freltoft *et al.* interpret the deviation in terms of a small contribution to the moment from the out-of-plane O_z atoms, since the symmetry of the assumed antiferromagnetic state would seem to make the moment on the O_{xy} atom vanish.

Weinert and Fernando (1988) have questioned whether the antiferromagnetic order necessarily requires the moment on the in-plane O_{xy} atom to vanish. Based on symmetry arguments and supported by calculations on a single Cu-O layer, they suggest that lower-symmetry orderings which allow a moment on the O_{xy} atoms are not ruled out by experiment. They claim that to distinguish between the usually assumed high-symmetry state and the lower-symmetry state they suggest, in which a polarized Cu ion would be surrounded by two spin-up and two spin-down O_{xy} ions, would require an inversion of the structure factor at all values of Q.

Cohen, Singh, *et al.* (1989) have investigated the possibility of a lower-symmetry antiferromagnetic state within the local spin-density approximation by carrying out LAPW calculations of La_2CuO_4 in the orthorhombic crystal structure, but with the magnetic symmetry lowered to triclinic, retaining only inversion symmetry. Such calculations allow very general symmetries of magnetic states. Using several different (small) k-point sets, including sets with points on or very near the Fermi surface, they obtained no stable antiferromagnetic solutions. Staggered fields applied to the oxygen atoms resulted in only small moments.

An important check on the correctness of the magnetic response in a band calculation is the field-induced form factor. Since the calculations predict no antiferromagnetic state, there is no good reason to anticipate agreement from such a comparison. Stassis *et al.* (1988) have reported the induced form factor for eight reflections above T_N, which they find can be fit by assuming only the

Cu^{2+} magnetic form factor. This is different from what would result from a paramagnetic band calculation, which would be just the form factor of strongly Cu-O hybridized states at the Fermi level. However, in the light of other data, which indicate that the planes are well ordered two-dimensionally even above T_N, this comparison is invalid. What is being measured is just the field-induced ordering of planes of Cu moments that are already antiferromagnetic, rather than paramagnetic; i.e., the magnetism has not vanished above T_N, rather the correlation length has become finite.

These results, then, are not entirely unambiguous. It seems probable that (1) the moment is very strongly Cu^{2+}-like, but that (2) there are deviations large enough to be seen, and to be concerned with. Whether the deviation from a purely ionic local moment is significant remains to be decided.

IX. LATTICE STATICS AND DYNAMICS: MODELS

A. Parametrized ionic models

The pronounced ionic nature of the copper oxides invites the modeling of their lattice statics and dynamics in terms of long-range Coulomb forces and short-range ion repulsion potentials. Several studies of this nature have been carried out.

Evain *et al.* (1987, 1988) and Whangbo, Evain, *et al.* (1988) have used empirical interatomic potentials to model La_2CuO_4 and $YBa_2Cu_3O_{7-x}$ for $x=0.0$ and 0.5. They take their potentials to be of the form of a sum of ionic (Coulomb), short-range repulsive, and van der Waals potentials whose adjustable parameters are fit to diatomic solid compounds such as CuO, BaO, La_2O_3, and Y_2O_3. A Cu^{2+} configuration was assigned to the copper ion in all studies. For each of these three materials the structural parameters are reproduced rather well: lattice constants are within 1–2 % (often better), and the internal structural parameters are generally very good.

The largest errors in the calculated equilibrium structures occurred in the position of the O4 atom in the Y123 systems, which was off by 0.1–0.2 Å, and in the structure of the tilt-mode distortion in La_2CuO_4, which was only qualitatively correct. Nevertheless, the model predicts the orthorhombic structure of this compound to be more stable than the tetragonal phase, by 0.04 eV/formula unit. Evain *et al.* (1987) concluded, in agreement with the studies discussed in the next subsection, that the structural distortion is not a Peierls instability but rather is driven simply by strong ionic forces. Evain *et al.* (1988) studied the energetics of O vacancies in the Y123 system and suggested that the formation of Cu-O chains in the fully oxygenated phase is driven by an avoidance of (1) right-angle arrangements of oxygen atoms around the Cu1 ion and (2) T-shaped threefold coordinations of Cu1.

Wright *et al.* (1988) also used the same general approach, but found that, for the choice of potentials used by Evain *et al.*, the structures of CuO, Y_2O_3, and $YBa_2Cu_3O_7$ all could not be stabilized. Finding that the Madelung forces on the Ba and Cu2 ions are strongly dependent on the distribution of the balancing (7+) charge among the Cu1 and Cu2 sites, they required a somewhat larger charge on the Cu1 ion (2.4–2.5) than on the Cu2 ion (2.25–2.3) to stabilize the Ba ion at its site. It was also found that the Madelung force on the Cu2 ion was in the same direction as the repulsive and van der Waals forces, necessitating an additional counter force to hold the Cu2 ion in the O2-O3 plane. These characteristics were not sensitive to the chosen ionic charges, as similar results were found if the charges were arbitrarily redistributed to Y^{2+}, Ba^{1+}, Cu^{1+}, and O^{1-}. Another striking result was that the O1 (chain) ion always experienced a small restoring force to displacements in the x direction (perpendicular to the chain), consistent with the observed rapid diffusion of oxygen atoms in this site.

Islam *et al.* (1988) have applied a similar ion-based interatomic potential scheme to model the static and dynamic properties of La_2CuO_4. As in the methods discussed above, the binary oxides were used to derive pair potentials. However, Islam *et al.* found that a satisfactory description of CuO required more than pair potentials, so they introduced a Cu-O bond-bending potential. The predicted equilibrium tetragonal structure was close to the experimental structure, with the largest discrepancy (0.1 Å) occurring in the La-O_{xy} bond length, which is not expected to be a serious problem.

Applying this force model to the dynamics, they found that all calculated frequencies were positive, that is, the tetragonal structure is stable (which is in disagreement with experiment). The model predicts a very soft zone-boundary optic mode for **O** perpendicular to the Cu-O planes. Although the position in the zone and the detailed character of the soft mode is different from the experimentally determined soft mode, the ionic displacements do have some similarities.

B. *Ab initio* ionic model

The purely ionic models discussed above are not related very closely to the detailed electronic structure being reviewed in this paper. However, they are related to a distinct ionic approach, also applied to the cuprates, which is based solely on an assignment of ionic charges and the local-density approximation and is parameter free. This approach is based on the ionic potentials first derived by Gordon and Kim (1972), who assumed simply that the density of a pair of ions is given by overlapping spherical ions, and then calculated the energy of the ion pair within the local-density approximation. The model applied to the cuprates by Cohen and collaborators is the potential induced breathing (PIB) model. It goes beyond the Gordon-Kim prescription by allowing the ions to breathe radially in response to the Madelung potential of the environment. It therefore includes one particular

form of many-atom potential, and one that might be expected to be particularly important for the realistic description of the highly polarizable O ion. This improvement has been found to be necessary in the accurate description of many oxides (Mehl, Hemley, and Boyer, 1986; Cohen, Boyer, and Mehl, 1987).

The PIB model was applied (Cohen, Pickett, Boyer, and Krakauer, 1988a; Cohen, Pickett, Krakauer, and Boyer, 1988; Cohen, Boyer, *et al.*, 1989) to tetragonal and orthorhombic La_2CuO_4 using the formal valences. As a test of the underpinnings of the model, they also carried out a comparison of the underlying charge density derived from overlapping ionic charges with the self-consistent local-density approximation from LAPW calculations (Pickett, Krakauer, Papaconstantopoulos, and Boyer, 1987). A contour plot of the difference between the LAPW crystal density and the overlapping ion PIB density is displayed in Fig. 18. Both the La and the O_z ions are reproduced quite well by the PIB density, indicating that these ions are indeed nearly fully ionic. The Cu and O_{xy} ions, on the other hand, show very significant distortions away from the overlapping ion model. This difference arises from the large d-p hybridization, and the deviations are consistent with unoccupied orbitals of $d(x^2-y^2)$ symmetry on the Cu and $p\sigma$ symmetry on the O_{xy} atoms. These deviations reduce the charge in the bond region compared with overlapping spherical ionic charges.

In the tetragonal phase the static minimum energy structure leads to a c/a ratio of 3.1 rather than the observed value of 3.5, and to a 10% overestimate of the volume (two versions, with different treatment of the kinetic energy, were tried). These discrepancies are due almost entirely to the overestimate of the planar lattice constant, due to the fact that spherical Cu and O ions feel excess repulsion not experienced when the ions are allowed to distort. In spite of the ($\sim$10%) overestimate of the in-plane lattice parameter, this spherical ion model gives roughly half of the axial ratio of 1.28 (Cu-O_z distance relative to the Cu-O_{xy} distance), which is often ascribed to the Jahn-Teller effect (see Sec. III.B). Thus half of the axial ratio is due to the layered crystal structure

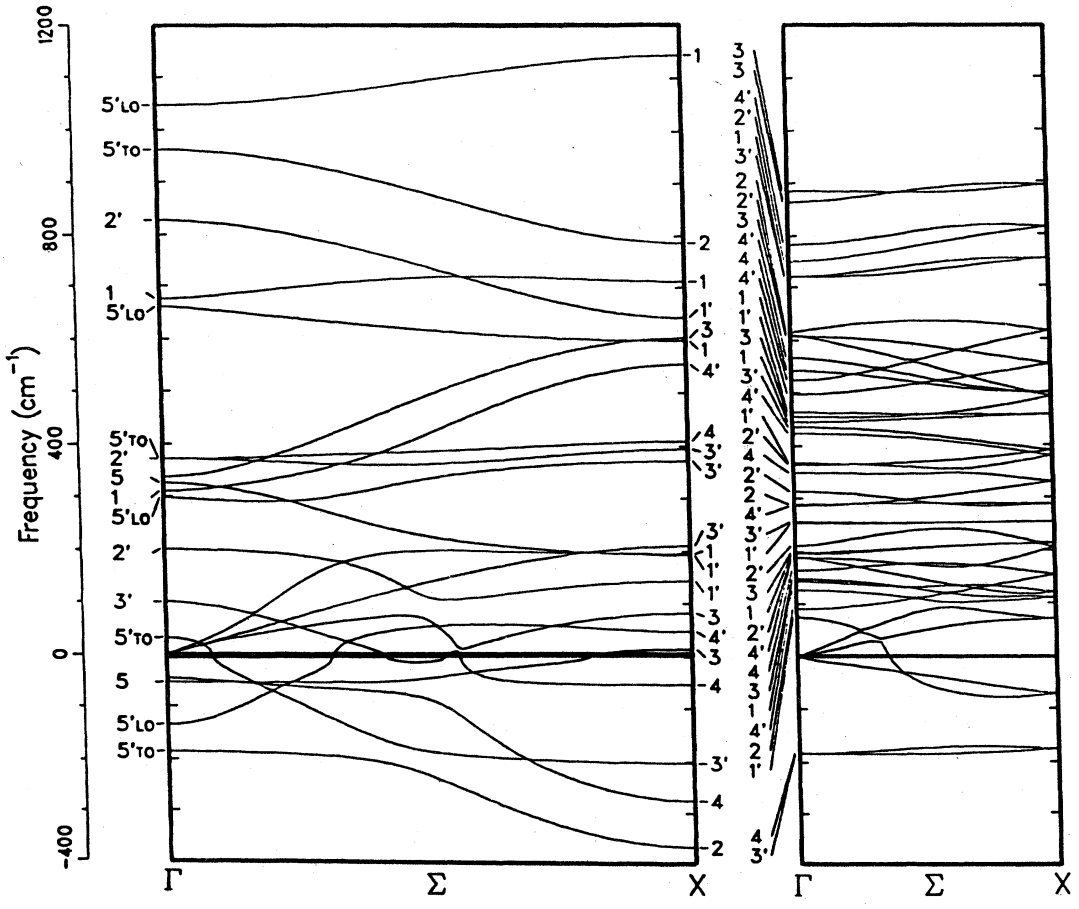

FIG. 61. Calculated phonon dispersion curves for La_2CuO_4, from the potential induced breathing model of Cohen, Pickett, Boyer, and Krakauer (1988): (a) tetragonal phase, shown along $(q,q,0)$; (b) orthorhombic *Abma* phase, shown along the same crystal direction. Negative frequencies indicate unstable vibrations, and the numbers indicate the symmetry labels.

and the strong ionic forces, and the other half arises from taking advantage of the nonspherical Cu-O ions (pseudo-Jahn-Teller effect).

The PIB model correctly predicts that the tetragonal structure is unstable to an orthorhombic distortion which corresponds to the experimentally observed freezing in of the X-point tilt mode (Birgeneau *et al.*, 1987). The qualitative features of the orthorhombic structure are reproduced, but the buckling of the Cu-O layers is greatly overestimated because of the energy gain in allowing the spherical Cu and O_{xy} ions to move away from each other. The PIB model also predicts an even lower symmetry ground state, perhaps monoclinic, which has not been investigated. Experimental evidence of such a lower-symmetry ground state was discussed in Sec. II.A.3.

The lattice dynamics was calculated using the PIB model, for both tetragonal and orthorhombic phases. In addition to allowing the study of stable modes, this model has the advantage that the dispersion curves, which are shown in Fig. 61, immediately highlight unstable atomic motions, which appear as imaginary frequencies (plotted in the figures as negative frequencies). Although the unstable tilt mode and most other unstable modes become stable when the orthorhombic distortion occurs, a mode consisting of sliding O_z and La ions remains unstable. Investigation of the energy surface indicates a "double-well" (actually fourfold, due to the fourfold site symmetries) potential in the tetragonal structure, which is only distorted but not removed in the orthorhombic structure. The expected large-amplitude motion of these ions accounts very well for the large and nearly temperature-independent thermal ellipsoids at these sites seen in structural refinement studies (Sec. II.A).

The PIB model has also been applied to $YBa_2Cu_3O_7$ by Cohen and collaborators (Cohen, Pickett, Boyer, and Krakauer, 1988b; Cohen, Boyer, *et al.*, 1989). Considering that this approach neglects all bonding interactions except ionic forces, the structural parameters are predicted rather well. The cell volume is overestimated by 8%, and c/a is overestimated by 3%. A larger discrepancy occurs for b/a, predicted to be 1.071 versus the experimental value of 1.017. The internal structural parameters are given reasonably well, especially the z positions of the CuO_2 planes. These predictions, and the lattice dynamics discussed next, were obtained *assuming* $Cu^{+2.33}$ and O^{-2} ionic charges.

Cohen *et al.* have presented the harmonic phonon dispersion curves derived from the PIB description. Several modes are found to be harmonically unstable. The most unstable mode occurs at Γ and corresponds to motion of the O1 chain atoms in the $+x$ direction (perpendicular to the Cu1-O1-Cu1 bond) and O4 atoms in the $-x$ direction. The motion of O2 and O3 in opposite directions along z is also unstable. In addition there are zone corner (S) instabilities related to modes which disperse very strongly along the zone boundaries (X-S and Y-S). As in La_2CuO_4, these phonon dispersion predictions are not expected to be accurate, but rather reflect very strong tendencies related to ionic forces.

The PIB model has not been applied to other cuprates in detail. The overlapping ion density it relies on has, however, been compared to the self-consistent density of $YBa_2Cu_3O_7$. An often asked question, and one that has caused controversy in crystal chemistry, is: How does one describe the ionic configuration of a crystal? And, is there a preferred assignment of ionic charges to solids? Krakauer, Pickett, and Cohen (1988) compared the self-consistent crystal density with PIB densities, varying the charges assigned to the ions, and identified which ionic charges led to the lowest rms difference. The difference densities are shown in Fig. 32 and lead to an assignment close to $Cu^{1.62+}$ and $O^{1.69-}$. The assignment of equal charges to the Cu1 and Cu2 ions and to each of the four O sites is suggested by the LAPW calculations, which give very small differences at the inequivalent sites.

Billesbach, Hardy, and Edwardson (1988) have used a version of *ab initio* ionic model to perform constant-pressure molecular dynamics studies of $YBa_2Cu_3O_7$. Their potentials are similar to those of the PIB model, except that they do not allow the ions to breathe; i.e., they are of the Gordon-Kim type. For a variety of choices of the ionic charges of the Cu and O ions, they find that this ionic model leads to an instability of the O1 oxygen, which does not reside on the ideal O1 site of the *Pmmm* space group. Rather the Cu1-O1 chain buckles, with the O1 ion lying in the a-b plane to one side of the ideal site. This behavior is very similar to the PIB instability described above. When the temperature is raised, the crystal breaks apart before the double-well instability can disappear. Modifying the potentials by introducing a phenomenological screening term does not remove the instability. In fact, such displacements of the O1 ion are consistent with the cigar-shaped thermal ellipsoid for this site seen by Beno *et al.* (1987), if the displacements are uncorrelated or not strongly correlated.

X. LATTICE DYNAMICS AND ELECTRON-PHONON COUPLING

A. Experimental evidence: isotope shift of T_c

The interest in investigating pairing mechanisms in the copper oxides has included much discussion of the relevance of the electron-phonon coupling mechanism, which is responsible for superconductivity in conventional superconductors. The strength and character of the electron-phonon interaction is a problem that can be addressed directly, but at considerable computational expense, by electronic structure calculations. Moreover, there have been several experimental indications of strong electron-phonon interactions, the best known being the isotope shift of T_c, which is discussed below.

One indication of electron-phonon interaction strength is the vibrational behavior. Using measurements of the optical properties from the far-infrared to the ultraviolet,

Herr *et al.* (1987) identified infrared-active modes in LSCO at 240 and 495 cm^{-1} that have remarkably large oscillator strength. They suggested that these arise from coupling of optic phonons to the electronic system. A number of studies (Blumenroeder *et al.*, 1987; Bonn *et al.*, 1987; Copic *et al.*, 1987; Chrzanowski *et al.*, 1988; Cooper *et al.*, 1988) have found Raman-active and infrared-active modes whose frequencies and linewidths have strong temperature dependence; one straightforward interpretation is in terms of electron-phonon coupling, although anharmonicity is another possibility. Zeyher and Zwicknagl (1988) have provided a theoretical analysis of the T dependence of Raman- and infrared-active modes in the Y123 system which indicates that this material is in the strong electron-phonon coupling limit. Further, elastic and ultrasonic studies (Bhattacharya *et al.*, 1988a, 1988b; Jericho *et al.*, 1988) show anomalies in their temperature dependence, often closely correlated with T_c, which reflect strong electron-phonon coupling.

The character and strength of the electron-phonon interaction are of central interest, both for understanding the unusual physical properties of the cuprates and for describing the electronic system itself. The electron-phonon interaction has also been widely discussed as a possible pairing mechanism, and as an *impossible* pairing mechanism, for producing values of T_c of 100 K. The isotope shift of T_c, initially expected to be the crucial experiment, has not been as conclusive as was naively expected at first.

The isotope shift is not as simple as is usually assumed: from the definition of isotope exponents α_a for atom a,

$$d\log T_c = -\sum \alpha_a d\log M_a \ , \tag{10.1}$$

the BCS relation for T_c implies that, if the electron-phonon interaction is responsible for pairing, the exponent should be equal to 0.5. In fact, even the early studies (Swihart, 1959, 1962) of the isotope effect pointed out that the isotope shift is a complex property, even for harmonic phonons. It involves not only the change in phonon frequencies but also the readjustment of the amount of retardation of the electron-phonon interaction arising from the change in frequencies; small or even negative values are possible in electron-phonon coupled systems. Several standard superconductors that are established to be electron-phonon coupled have small isotope exponents.

Meservey and Schwartz (1969) have listed isotope shifts for several elemental superconductors. Zr and Ru ($\alpha=0.0$) stand out, while Os ($\alpha=0.2$) and Mo ($\alpha=0.3$) also differ strongly from the "ideal" value of 0.5. Note that these are all very-low-T superconductors. (The value $\alpha=-2.2$ for $\alpha-U$ may still not be understood.)

Katayama-Yoshida *et al.* (1988) have reported the isotope shift replacing ^{16}O by ^{18}O in the Bi-Sr-Ca-Cu-O system and provided references to many of the previous experiments, which will not be reviewed in detail here. Briefly stated, the shifts in T_c due to this O replacement are about 0.4 K (reports range from 0.25–0.6 K) for all of the copper oxides, including the La214 and Y123 systems and the 85- and 110-K phases of the Bi-Sr-Ca-Cu-O materials. The same shift also occurs in the $Ba(Pb,Bi)O_3$ system with $T_c=11$ K, but in the $(Ba,K)BiO_3$ system where $T_c=30$ K, the shift is 1.4 K (Hinks *et al.*, 1988). These shifts translate to isotope exponents for the oxygen of 0.15–0.2 for La214 and roughly 0.03–0.05 for the Y123 and Bi-based materials with T_c above 80 K. Because of the lower T_c for $Ba(Pb,Bi)O_3$, the exponent is about 0.25, while the large change in T_c for the $(Ba,K)BiO_3$ compound gives an exponent of 0.6.

Clearly the electron-phonon interaction is central to the superconducting pairing in the $(Ba,K)BiO_3$, $Ba(Pb,Bi)O_3$, and La214 materials, and it leads to small but measurable shifts in the high-T_c superconductors that are difficult to interpret. Barbee *et al.* (1988) have studied the isotope shift within standard strong-coupling Eliashberg theory and have found that very small isotope shifts seem incompatible with $T_c \sim 100$ K within this theory.

In the following two subsections band-structure-based calculations of the electron-phonon interaction are reviewed. In the final subsection the applications of local-density approximation methods for describing the energetics of copper oxides are reviewed.

B. Rigid muffin-tin and Madelung contributions

In conventional metals and superconductors based on transition metals, the simple rigid muffin-tin model for the scattering of electrons from displaced atoms has provided a quantitatively realistic picture of the electron-phonon interaction (Klein and Pickett, 1982). The rigid muffin-tin approximation is also referred to as the Gaspari-Gyorffy (1973) theory because these authors proposed its use to calculate the McMillan-Hopfield parameter η, which has become a central quantity in the theory of electron-phonon-driven superconductivity. The rigid muffin-tin approximation models the change in the one-electron potential of the crystal, when atom a at $\mathbf{R}$ is displaced, by the rigid displacement of the spherical part of the potential within a muffin-tin (or atomic) sphere surrounding that atom. The rigid muffin-tin approximation involves two main assumptions. First, the dominant scattering is taken as arising from very near the displaced atom; this assumption works best when the displaced atom has wave functions that peak well within the muffin-tin sphere and when the screening length is short. Second, it is assumed that nonspherical contributions to scattering are negligible, as are the changes due to displacement. These assumptions are best satisfied in the cubic elemental transition metals, but also appear to work well in many transition-metal compounds. They are suspect in the copper oxides under consideration here, because there are strong ionic effects that are not encountered in the more standard cases, and these interactions will not be screened nearly as strongly as in

high-density-of-states metals. Moreover, many of the atoms sit at low-symmetry sites, so nonspherical potential scattering may be important. Nevertheless, the first step was to apply this model, and then to characterize its possible shortcomings.

The rigid muffin-tin approximation was first applied to $La_{2-x}Ba_xCuO_4$, for $x=0.0$ (paramagnetic), 0.15, and 1.0, and to the reference compounds $LaCuO_3$ and $BaCuO_3$ by Pickett, Krakauer, Papaconstantopoulos, and Boyer (1987), applying the rigid-band model to the band structure of La_2CuO_4 to obtain $x=0.15$ values. The McMillan-Hopfield parameter η depends on the total DOS, the scattering phase shifts, and the atomic partial DOS's (Klein and Pickett, 1982).

Values of η for each atom were obtained by Pickett, Krakauer, Papaconstantopoulos, and Boyer (1987) for $La_{1.85}Ba_{0.15}CuO_4$ and by Krakauer, Pickett, and Cohen (1988) for $YBa_2Cu_3O_7$. The La, Ba, and Y cations give negligibly small contributions. Contributions from both Cu and O atoms are important, with contributions from the O_z atoms, particularly those near Ba ions, becoming appreciable with increased doping in the La214 system. Not surprisingly, the dominant contributions arise from Cu d–O p scattering. More unexpectedly, the variation with doping in the La214 system is not dominated by the total DOS $N(E_F)$, although it is the single most important factor. In $YBa_2Cu_3O_7$, the O1 atom contributes about as much as all of the other six oxygens together; this difference arises from the distribution of the local density of states between s, p, and d arising from the low-site symmetry, rather than just on its magnitude.

The total electron-phonon interaction strength λ can be expressed as the sum of atomic contributions λ_a, which are given by

$$\lambda_a=\eta_a/(M_a\langle\omega^2\rangle) \tag{10.2}$$

in terms of the atomic mass M_a and an appropriate lattice vibrational energy $\langle\omega^2\rangle$ (Allen, 1980). Since $\langle\omega^2\rangle$ depends on the total phonon spectrum and the electron-phonon coupling, only the combination

$$\lambda\langle\omega^2\rangle=\sum\eta_a/M_a \tag{10.3}$$

gives a representation in terms of purely atomic parameters (the right-hand side). Further progress in evaluating λ requires assumptions about $\langle\omega^2\rangle$.

Pickett, Krakauer, Papaconstantopoulos, and Boyer (1987) suggested the simple picture of dominating CuO modes, due to the strong Cu-O bond-stretching forces noted by Mattheiss (1987) and Weber (1987). Since this force constant is shared by Cu and O vibrations, they assumed $M_{Cu}\Omega_{Cu}^2=M_O\Omega_O^2$ and investigated the dependence of T_c on the oxygen vibration frequency Ω_O. The results for λ and T_c vs Ω_O from the Allen-Dynes (1975) equation are shown in Fig. 62. For $\Omega_O\sim250$ K, they obtained $\lambda=1.5$–2.0 and $T_c>30$ K. This value of Ω_O may be optimistically low, but the clear implication is that, to within factors of the order of 2, the rigid muffin-tin

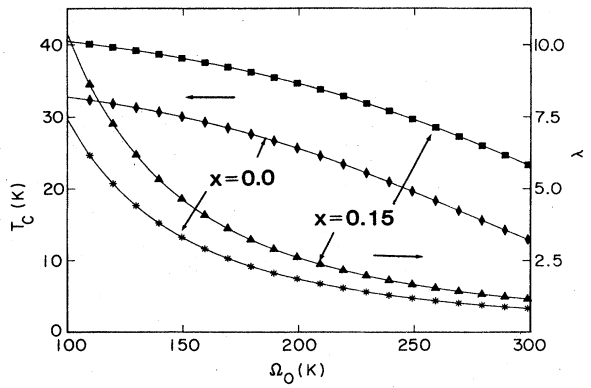

FIG. 62. Calculated values, within the rigid muffin-tin approximation, of the electron-phonon coupling constant λ and transition temperature T_c of $La_{2-x}M_xCuO_4$, for (hypothetical paramagnetic) $x=0.0$, and for $x=0.15$, vs the presumed oxygen vibrational frequency. From Pickett, Krakauer, Papaconstantopoulos, and Boyer (1987).

values can account for T_c of the order of 30–40 K in the La214 system. The rigid muffin-tin calculations, however, give no basis for a higher value of T_c in the Y123 system than in the La214 system; in fact, most ways of carrying out estimates of T_c, such as assuming that the mean frequency is the same, lead to smaller T_c in the Y123 system.

It was observed early on by Pickett, Krakauer, Papaconstantopoulos, Boyer, and Cohen (1987) that unusual, non-muffin-tin contributions to the electron-phonon interaction were occurring in the La214 system. As noted above, there is a very small value of η for the O_z ion within the rigid muffin-tin approximation, and this occurs because there is a very small DOS at the Fermi energy on this ion. However, during studies of the effects of displacing this ion they found that the axial breathing mode involving only the displacement of this ion in the z direction resulted in a shift in charge between the Cu and the in-plane O_{xy} atom. The motion of the O^{2-} ion was causing a Coulomb (Madelung-type) energy shift on the Cu and O_{xy} atoms, which is very poorly screened in LSCO compared to the strong screening in standard strongly coupled metals. Such Coulomb shifts are present in ionic insulators, but charge transfer is not possible in those systems because of their closed-shell nature. In the metallic regime of the La214 system, however, the strong covalence and lack of closed shells allows charge transfer readily. This charge redistribution and its consequences have also been discussed by Cohen, Pickett, Krakauer, and Boyer (1988).

Jarlborg (1987, 1988) has provided the first quantitative estimate of the size of these corrections to the rigid muffin-tin approximation. He noted independently that by carrying out frozen-phonon calculations one can obtain the true electron-phonon matrix element for a particular phonon. Because he used the LMTO method, which retains only the spherical part of the potential, he

concentrated on the change in the spherical potential beyond the rigid muffin-tin value, which in fact is expected to be one of the largest corrections. Whereas the rigid muffin-tin approximation describes scattering between partial waves l, l', with $|\Delta l|=1$ in an expansion around the atom, this change in spherical potential involves a $l'=l$ ($\Delta l=0$) contribution.

For La_2CuO_4 and $LaSrCuO_4$, Jarlborg (1987) studied two frozen phonons: one involving O_{xy} motion parallel to the Cu-O plane (and not specified in detail, but it was *not* the breathing mode), and a second being the axial breathing motion of the O_z atom. He found that, while the in-plane O_{xy} motion led to no significant enhancement, the axial mode led to a tremendous increase, more than doubling his estimate of λ for $LaSrCuO_4$. Presumably axial motions of the La^{3+} ion could have a similar effect.

Jarlborg (1988) also studied the Y123 compound. He found that the O1 and O4 (chain-related) atoms give only a small value of η within the rigid muffin-tin approximation, not because of a very small density of states at E_F but because their density of states is strongly ("purely") p-like and therefore does not allow $|\Delta l|=1$ matrix elements. He considered $\mathbf{Q}=0$ displacements of O1 and O4 atoms in the x, y, and z directions, O2 in the x and z directions, and O3 in the z direction. For the motion of O4 atoms in the z direction, both cases, in which the two O4 atoms move together or against one another, were studied. As in $LaSrCuO_4$, Jarlborg found that contributions from certain O modes, especially O4 displacements in the z direction, could give large enhancement of their contribution to λ from $\Delta l=0$ contributions. He also carried out an analysis that showed that these (self-consistently screened) matrix elements followed the trends one would predict from a simple (unscreened) Madelung shift in potential. However, since only a few of the displacements were enhanced so strongly, it was not possible to estimate the enhancement of λ, which involves an average over all modes of the crystal.

C. Tight-binding theory of lattice dynamics

The most extensive calculations to date of the electron-phonon interaction, which also included evaluations of the phonon spectra, were carried out by Weber (1987) for LSCO and Weber and Mattheiss (1988) for Y123. They employed a nonorthogonal tight-binding fit to the band structures, using a basis set of Cu d, O p, La and Y d, and Ba s states. Once a good fit was achieved, derivatives of the overlap parameters with respect to interatomic separation were obtained, partly from self-consistent calculations with displaced atoms and otherwise from approximate scaling laws. These derivatives gave them the band-structure contribution to the change in energy (and therefore the phonon frequency) as well as the electron-phonon coupling matrix element. Their method of calculations was very successful not only in the elemental transition metals but in the $A15$ superconductors as well (Weber, 1984).

Weber argued that the width of the only band crossing E_F in the La214 system, the Cu-O antibonding $pd\sigma$ band, is determined primarily by the ($pd\sigma$) hopping parameter, making this the focus of emphasis in the calculation of electron-phonon coupling. A separate band calculation with 3% reduced lattice constant was used to derive the value $d\log(pd\sigma)/dR=-1.6$ Å^{-1}. The calculation of the phonon spectrum itself is a rather intricate procedure, requiring information that is not available from the tight-binding parametrization. In previous calculations using this method, the additional information was couched in terms of short-range force constants, which were fit to experimental data for elastic constants and/or selected phonon frequencies. For $La_{2-x}M_xCuO_4$, however, this information was not available, so Weber used a force-constant model for $Ba(Pb,Bi)O_3$ derived from neutron scattering data. It was necessary in addition to estimate some Cu-O and La-O force constants.

Weber treated the doping within the rigid-band model. His calculation of the generalized susceptibility was nearly flat for $x=0.3$, but in reducing x toward zero he found that a strong peak (Kohn anomaly) arose at the X point, a peak nearly three times the zone-center value. The electronic renormalization (in his calculation he included only the band crossing E_F) involves an expression like the susceptibility but containing electron-phonon matrix elements. The matrix elements rarely produce strong $\mathbf{Q}$ dependence but can greatly influence the magnitude of the electronic renormalization in different regions of the Brillouin zone.

For $x=0.0$ Weber's calculation produced a strong Kohn anomaly which made the X-point planar breathing mode unstable. For $x=0.15$ the Kohn anomaly produced a drastic softening of modes near X that are strongly coupled to the Fermi-surface electrons. His calculations of α^2F, the electron-phonon spectral function that enters Eliashberg theory, led to values of λ in the range 2.0–2.5 and values of T_c, calculated from the Eliashberg equations, of 30–35 K. Thus his calculations appear to account very well for the observed values of T_c in terms of strong electron-phonon coupling.

Unfortunately, experimental data soon contradicted the predictions of Weber's calculation. The structural transition was identified (Birgeneau, Chen, *et al.*, 1987) to be *not* due to a soft breathing mode as predicted, but due to a soft tilt mode that was not predicted by Weber's calculation to be soft at all. These glaring discrepancies have been used as evidence that band theory is inapplicable for calculating phonon frequencies in these copper oxides, a position contradicted by more detailed calculations by Cohen, Pickett, and Krakauer (1989) to be described below. It is pertinent therefore to review the assumptions made in the nonorthogonal tight-binding approach to lattice dynamics.

First, it can be argued that Weber's calculation is not applicable for small values of x, since in that regime the

material is an antiferromagnetic insulator, whereas Weber was applying a paramagnetic, metallic band picture. This is certainly true, and there can be no Fermi-surface-driven instability in an insulator. However, more recent Raman and infrared data (on single crystals and oriented films) show little dependence of the lattice dynamics (at $\mathbf{Q}=0$) on the concentration, even in the metallic regime, except for the tilt mode related to the structural transition. Second, Weber's model contains several parameters that are not well pinned down, and it neglects contributions to the force constants that have been suggested by the work of Jarlborg (1987, 1988) and Pickett, Krakauer, Papaconstantopoulos, and Boyer (1987) to be important. Weber's model used only short-range force constants for the "background" contribution, whereas the strongly ionic nature of these materials and the poor screening suggest that longer-range force constants will be necessary. His model also neglected any shift of the site energy of an atom due to its motion or to that of another atom, whereas Jarlborg finds these may be very important. The nonorthogonal tight-binding model, as formulated, works well for high-DOS, strongly screened metals, but it may have distinct shortcomings in low-DOS metals with strong ionic character.

Weber and Mattheiss (1988) have applied the same method to the lattice dynamics and electron-phonon interaction of $YBa_2Cu_3O_7$. In this case the material is metallic and well away from the metal-insulator transition, which occurs near an O concentration of ~ 6.5, so a paramagnetic band structure is appropriate here. They used the same gradients of the overlap parameters as were used in La_2CuO_4, and used short-range force constants that made the calculated phonons close to experimental data. Particular attention was given to the influence of the flat chain-derived band at E_F on the results.

Including only the broad $pd\sigma$ bands (one from each Cu-O layer and one from the chain), Weber and Mattheiss found $\lambda=0.5-1.0$ (the uncertainty is due to computational simplifications), corresponding to $T_c=3-10$ K. The complete calculation, which included the flat $pd\pi$ band as well, resulted in values of λ of 1.3–2.3, corresponding to T_c in the range 20–30 K. Including the flat band caused some transverse phonons near the zone boundaries to soften considerably, particularly phonons involving motions of the Cu1 and O4 atoms along the c axis. This softening arises from Cu1-O4 overlaps which are zero by symmetry before displacement, but have a large gradient with respect to bond-bending interactions. Weber and Mattheiss concluded that the electron-phonon interaction was insufficient to account for values of T_c of 90–100 K. However, their calculation is a clear indication of a very strong electron-phonon interaction in $YBa_2Cu_3O_7$, and the additional terms mentioned above, which they neglected, may increase the coupling strength considerably.

D. Total energy: structural parameters and frozen phonons

The shortcomings of Weber's tight-binding calculations for the lattice dynamics of the La214 system initially seemed to suggest that local-density calculations may not describe even the energetics of the copper oxides correctly. However, careful self-consistent calculations have established that indeed local-density energies are accurate, at least for La_2CuO_4.

Static structural parameters were calculated by Stocks, Temmerman, Szotek, and Sterne (1988) using the LMTO method. Since the approximations made in this method render it inappropriate for calculating the c/a ratio in tetragonal materials, Stocks *et al.* fixed the c/a ratio at the experimental value and calculated the equilibrium volumes for La_2CuO_4 and ordered $LaSrCuO_4$. For La_2CuO_4 the volume is obtained to within better than

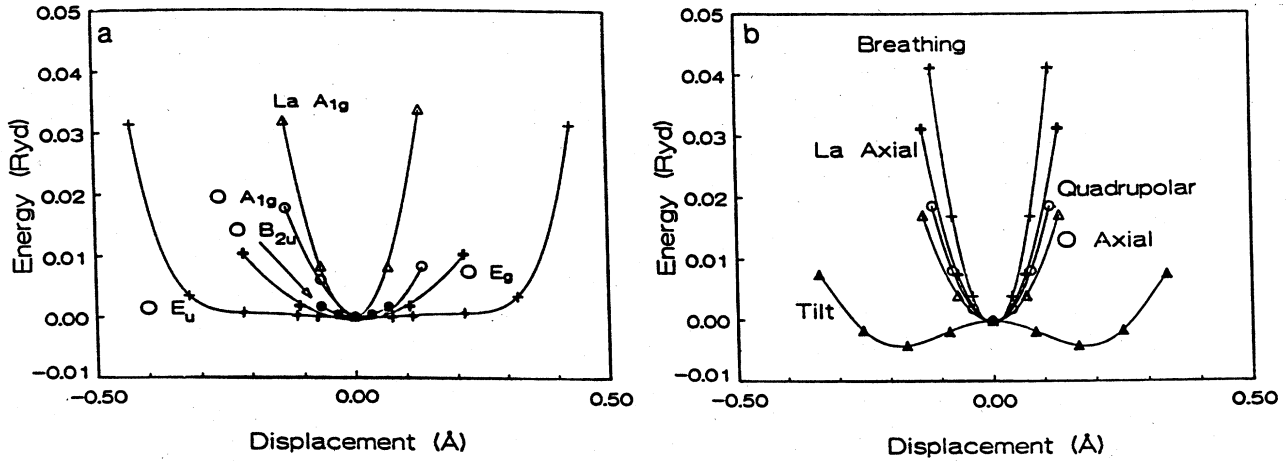

FIG. 63. Examples of total energies for various lattice distortions of La_2CuO_4 vs amplitude of the distortion: (a) zone-center displacements; (b) zone-corner (X) displacements. Except for the zone-center O E_u mode, which is very anharmonic, and the unstable X-point tilt mode (the orthorhombic distortion), the modes are all harmonic. From Cohen, Pickett, and Krakauer (1989).

1% of experiment. This comparison gives fortuitously good agreement, since similar comparisons on much simpler materials typically lead to 3–5 % discrepancies. In addition, it should be noted that the comparison is between a paramagnetic calculation and an antiferromagnetic material; magnetic solutions would be expected to have a slightly larger volume. The trend in volume change with substitution of Sr is also reproduced, but no straightforward quantitative comparison is possible.

In the LMTO method it is possible to decompose the pressure approximately into contributions from each of the constituent atoms. Stocks *et al.* found that such a decomposition leads to positive contributions from both Cu and O atoms, which are balanced only by the negative contribution of La. This attractive La partial pressure arises in the d and f channels of the occupied DOS. Since several analyses have shown that La is nearly completely ionized to La^{3+}, the bonding part of the pressure in this representation may actually be arising from tails of neighboring Cu and O atoms that are reexpanded about the La site. The pressure dependence of the volume was measured and then calculated using identical LMTO methods by Akhtar *et al.* (1988), who found excellent agreement between the theoretical predictions and the measured data.

The only other static structural calculations are by Cohen, Pickett, and Krakauer (CPK) (1989) using the accurate LAPW method. CPK calculated not only the equilibrium volume and the c/a ratio but also the internal structural parameters (z coordinates) of the O_z and La ions. They obtained excellent agreement with experiment. The c/a ratio was calculated within 1% of the experimental value. The calculated volume was 4–5 % less than room-temperature experimental values, but thermal expansion and zero-point motion could increase the volume by 3–5 %. The internal parameters also were excellent, with the O_z position within the scatter of experimental values and the La position within 0.025 Å.

CPK also carried out extensive frozen-phonon calculations for tetragonal La_2CuO_4, using the full-potential LAPW method. For crystal structures as complex as this, the calculations are computationally intensive, and their results for several zone-center and X-point phonon frequencies and eigenvectors represent the most ambitious application to date of the frozen-phonon approach. In such calculations the usual procedure is to freeze-in a phonon eigenmode and to calculate the energy as a function of the phonon amplitude, from which the phonon frequency can be obtained from the quadratic term in the energy. Fu and Freeman (1987) carried out a frozen-phonon optical breathing mode calculation using only a single two-dimensional slab of La_2CuO_4, obtaining an energy surface that was harmonically unstable (negative curvature at zero displacement), but the region of instability was very small. Their mode would be anharmonically stabilized, and they calculated a high frequency ($\sim$110 meV) for the mode.

CPK calculated the energy versus amplitude in full three-dimensional La_2CuO_4 for the following zone-center distortions: O_z axial breathing A_{1g} mode, La axial breathing A_{1g} mode, and the O_z sliding E_g mode, all of which are Raman active; the silent O_{xy} B_{1g} mode; and the infrared-active O_z sliding E_u mode. At the zone center X point they considered all distortions with the symmetry of the O_{xy} planar breathing mode, which is the mode that was incorrectly predicted by Weber (1987) to soften and become unstable. These distortions can be described as the O_{xy} planar breathing motion, the O_z and the La axial breathing distortions, and an O_{xy} "antibreathing" distortion, in which the O_{xy} atoms assume a planar breathing motion with respect to the empty site at $(a/2, a/2, 0)$ in the CuO_2 plane (as opposed to the Cu site). This last distortion has a quadrupolar symmetry with respect to the Cu site. Since the zone-center A_{1g} distortions are coupled, as are all four breathing symmetry distortions at X just described, CPK also calculated the coupling terms. This allowed them to obtain the true eigenfrequencies and eigenvectors for these coupled modes. Since the X-point instability is one of the central features of the structural behavior of La_2CuO_4, CPK also calculated the energy versus the amplitude of the measured orthorhombic distortion.

The calculated energy versus distortion amplitude curves for the zone-center modes are shown in Fig. 63(a). The zone-center distortions are found to be harmonic except for the O E_u distortion, for which the energy is almost constant for O_{xy} excursions out to 0.3 Å, beyond which the curve rises steeply. This behavior is consistent with the observed large thermal ellipsoid of the O_{xy} atom (Sec. II). CPK solved the one-dimensional Schrödinger equations for this oscillator to locate its eigenstates. However, this distortion should be strongly coupled to the corresponding La E_u distortion, which was not calculated, so the results (see below) may not have direct physical significance.

From Fig. 63(b) it can also be seen that the X-point breathing mode symmetry distortions also behave harmonically. Most striking is the finding that the tetragonal-to-orthorhombic (T-O) distortion is predicted correctly, even to the magnitude of the distortion. Only a distortion along the $\langle 110 \rangle$ directions, which must be symmetric, was calculated. Since an identical instability occurs for the $\langle 1, -1, 0 \rangle$ direction, this curve indicates there is a quadruple-well potential for the T-O instability.

The frequencies calculated by CPK, both before and after coupling terms have been taken into account, are compared with the available data on single crystals from Raman scattering and from neutron scattering in Fig. 64. The coupling between the zone-center A_{1g} modes is very small, partly because of the large difference in O and La masses, and the resulting eigenfrequencies are in excellent agreement with the Raman data of Weber, Peters, *et al.* (1988a, 1988b) and Ohana *et al.* (1988). For the X-point modes, the coupling terms are important; in particular, the O_z axial motion is strongly coupled to all of

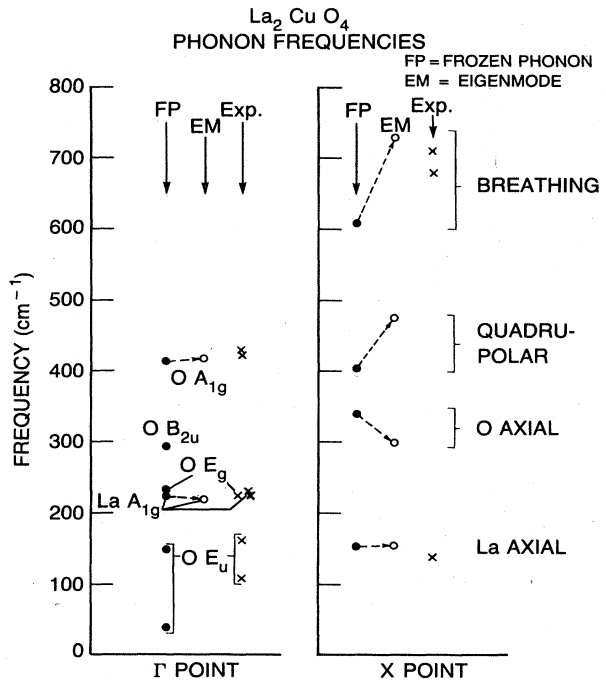

FIG. 64. Comparison of the frequencies of La_2CuO_4 frozen phonons calculated by Cohen, Pickett, and Krakauer (1989) with experimental data of Weber, Peters, *et al.* (1988a, 1988b), Böni *et al.* (1988), and Ohana *et al.* (1988). FP denotes frozen phonon frequencies before coupling of like symmetries is taken into account; EM denotes the eigenmodes that result after including the coupling. The eigenmodes (open circles) should be compared with the data, shown as crosses. Left side, zone-center (Γ) modes; right side, zone-corner (X) modes.

the other motions. Two significant results of this coupling are (1) the mode that is principally the planar breathing motion is driven to *higher frequency,* as opposed to being softened to the point of instability as found by Weber, and (2) the proposed strong coupling of the planar breathing motion to the metallic carriers will be transferred to the lower-frequency O_z axial motion, resulting in an increase in the electron-phonon coupling. As with the zone-center modes, the results are in good agreement with the existing Raman data of Ohana *et al.* (1988) and Weber, Peters, *et al.* (1988a, 1988b) and the neutron scattering data of Böni *et al.* (1988).

In summary, total-energy studies within the local-density approximation establish that this approach correctly predicts for La_2CuO_4 the unit cell volume and bulk modulus, the internal structural parameters, several harmonic phonon frequencies in the tetragonal phase, and the T-O instability. Since the phonon frequencies and the lattice stability depend in detail on the density response function, it seems clear that the local-density approximation is sufficient to give an accurate description of the static density response in La_2CuO_4 and probably in the other cuprates. As discussed in Sec. VIII, the local-density approximation fails to describe the antiferromagnetic state of this material, and it should not be overlooked that these total-energy calculations have been carried out in the (strictly speaking, inappropriate) paramagnetic limit. Apparently the antiferromagnetism is unimportant for describing structural energies in these materials.

XI. BEYOND THE LOCAL SPIN-DENSITY APPROXIMATION: CORRELATIONS

Most of the work described in this article has been based on the spin-density functional formulation of the many-body problem and has relied on the local spin-density approximation to the exchange-correlation interaction between the electrons. Density-functional theory addresses ground-state properties directly; it should reproduce the ground-state charge density, spin density, and associated energy of the system, which gives the crystal structure and lattice dynamics. Often the Kohn-Sham eigenvalues and eigenfunctions give good approximations to the single-particle excitations as well, although they are certainly never exact.

As discussed in Sec. VIII, the local spin-density approximation does not describe the antiferromagnetic ground states of La_2CuO_4 and $YBa_2Cu_3O_6$ properly. The various studies that have been carried out are not in agreement; it may or may not lead to an antiferromagnetic ground state (it appears to be a very close call), but certainly the magnitude of the moment is not reproduced correctly. The resulting band structure shows overlapping bands, whereas the antiferromagnetic state is certainly nonmetallic in its resistive behavior and presumably has a gap of 1 eV or more. This lack of a gap is not damning in itself, since the eigenvalues do not necessarily describe excitation energies. Covalent semiconductors provide a closely scrutinized case in which nothing seems drastically wrong in the energetics, but the local-density band gaps, and perhaps even the true spin-density functional gaps, are smaller by 25–50 % than the experimental values. This difference is now well understood in terms of dynamic correlation corrections that lie beyond spin-density functional theory; they require the Green's-function formulation of single-particle properties. Thus it is possible (but not necessarily correct) to view the metallic band structure in antiferromagnetic band structures as another aspect of the "gap problem." The lack of a band gap does, however, enter into the solution of the spin-density functional equations, where it leads to the occupation of some "wrong" states for obtaining a reasonable antiferromagnetic moment.

The magnetic state itself, however, lies within the realm of the local spin-density formalism, and the local spin-density approximation does not describe it properly. This is by no means a unique occurrence; there are several instances of magnetism in $3d$ transition metals and compounds in lanthanides and actinides which are not described correctly, or even qualitatively, by the local spin-density approximation. Clearly one must proceed "beyond the local-(spin)-density approximation" to un-

derstand the magnetism of the cuprates. We review here briefly approaches that have so far been applied to these materials: (1) extended Hubbard model approaches which may invoke both on-site and intersite Coulomb repulsion energies, (2) quantum-chemical methods of introducing correlation into the wave functions, and (3) the self-interaction correction (SIC) approach, which applies a physically motivated change to the spin-density functional theory. All of these approaches are only in the early stages of study.

A. Constrained local spin-density functional calculations

McMahan, Martin, and Satpathy (MMS) (1988) have suggested an effective Hamiltonian for describing La_2CuO_4, which includes on-site energies E_{Ip}, E_{IIp}, and E_d for the O_{xy} p, O_z p, and Cu d ions, on-site repulsion energies U_p and U_d felt by an extra hole in those states, and a repulsion U_{pd} felt by a hole in an O p state due to an extra hole on a Cu d state (and vice versa). They include hopping integrals V^{pp} and V^{pd}; as discussed in Sec. IV.G, MMS found it essential to include O-O hopping. Such an extended Hubbard model with three distinct sites is probably the most general form of model Hamiltonian that has been considered to date.

Before discussing any of the results, it is necessary to clarify the assumptions underlying such a model Hamiltonian. First, such models are almost always treated as if the basis functions (Cu d, O p) are orthogonal. Thus the basis functions must really be Wannier functions (of d symmetry about the Cu, p symmetry about the O), and as discussed and illustrated in Sec. IV.G, the parameters are distinctly different from those for a nonorthogonal atomic basis set. For model studies this distinction is ignored, and the basis is thought of as atomic orbitals. Moreover, the methods used to estimate the appropriate values of the parameters in such Hamiltonians also attempt to identify atomiclike parameters. Because the hybridization is large in the cuprates, this identification is difficult and rather ill defined (even if the Wannier/atomic function distinction is ignored). Sakai *et al.* (1984), Monnier, Degiorgi, and Koelling (1986), and Gunnarsson, Andersen, *et al.* (1988) have suggested systematic approaches for identifying these parameters. Recently MMS and Hybertsen, Schlüter, and Christensen (HSC) (1989) have described in detail related, but not identical, methods for obtaining the model Hamiltonian parameters in La_2CuO_4.

A second important item is that the parameters of such model Hamiltonians depend on the assumed "vacuum" state. A frequent choice is to use the closed-shell configurations, Cu^{1+} and O^{2-}. Schlüter, Hybertsen, and Christensen (1988) indicate that for the free atom $U_d(Cu^{1+})$ and $U_d(Cu^{2+})$ differ by 4 eV. Another natural choice might correspond to the formal valences, Cu^{2+} and O^{2-}, and the appropriate parameters could be different for this case.

Third, all the parameters are assumed implicitly to be renormalized ("screened") by any electrons not included in the Hamiltonian. The relevant screening of course can depend on the vacuum configuration. Gunnarsson and Jepsen (1988) have found, in the context of transition-metal compounds, that the hopping matrix elements themselves can display large configuration dependence. In their method of determining it, V^2 for Mn, Ce, and U atoms would differ by factors of 2–8, depending on the atomic configuration used in the calculations. The large variation arises because the extent of the localized orbital (d or f in these examples) depends strongly on number of localized electrons on the atom.

Finally, it should be kept in mind that the parameters identified in a given study in practice depend on the method of calculation. (Identifying parameters from experimental data, which we will not discuss here, involves its own set of ambiguities.) Workers using LMTO, LAPW, or LCAO methods (for example) will use quantities that are easy to manipulate and to interpret within their own calculations, and, as in the tight-binding parametrization of the energy bands themselves, only a *set of parameters* is truly meaningful. Now we proceed with a survey of the progress that has been made in identifying these parameters and in assessing their effect.

McMahan, Martin, and Satpathy (MMS) (1988) founded their parametrization on the fact that there is a substantial p bandwidth, 6.7 eV by their LMTO calculation, which arises by direct p-p overlap. This result was ascertained by eliminating the Cu d basis functions from the LMTO basis, and thereby eliminating p-d hybridization. From this band structure they derived the values $pp\sigma = 1.0$ eV and $pp\pi = -0.3$ eV. For O-Cu parameters they obtained $pd\sigma = -1.85$ eV, $pd\pi = 0.75$ eV.

To calculate the Coulomb correlation parameters, their approach is to isolate the relevant orbital so that it is completely unhybridized with any other orbital. If that can be done, its occupation number n is a good quantum number, and n can be calculated using density-functional theory for the energy $E(n)$ and the expansion

$$E(n) = E_0 + \varepsilon_0 n + \tfrac{1}{2} U n(n-1) + O(n^3) , \qquad (11.1)$$

or the eigenvalues ε can be used with the definition

$$\varepsilon(n) = dE/dn = \varepsilon_0 + U(n - \tfrac{1}{2}) + O(n^2) . \qquad (11.2)$$

MMS have applied this procedure to isolated atoms, obtaining agreement with experiment to within 1 eV. Both MMS and Hybertsen, Schluter, and Christensen (1989) have provided comprehensive discussions of the considerations involved in determining such parameters.

Carrying out this prescription for the solid is not trivial, particularly since the appropriate Cu d or O p Wannier functions have never been defined uniquely. For La_2CuO_4 this is less of a problem for the Cu d state than for the O p states, simply because the Cu d state is more localized when hybridization with O p states is turned off, than are the O p states under the same decoupling (because of the p-p hopping discussed above). MMS proceeded, however, to use a constrained density functional

approach (described in more detail below) in a variety of supercells to obtain the U parameters: $U_d = 8.5$ eV, $U_p = 4.1-7.5$ eV, $U_{pd} \geq 0.6$ eV. They suggest that such a value of U_{pd} is negligible, and that a reasonable first approximation is to neglect U_p as well, since it is equal to or smaller than the intrinsic p bandwidth. If these approximations are made, the model reduces to the Anderson lattice model, which has been applied widely to mixed-valence and heavy-fermion systems, where the Cu d state takes the place of the more commonly studied localized f state.

MMS considered the excitations of this model within the impurity Anderson model, in which all of the Cu d "impurity" states are treated as independent. This may not be a reasonable approximation for low-energy excitations, similarly to the case in the heavy-fermion metals. For higher-energy excitations, and perhaps for general characteristics of the insulating ground state, the impurity treatment may be a reasonable approximation. One of their primary results is that, due to the $d(x^2\text{-}y^2)$ hybridization which dominates, the ground state is found to be magnetic with spin $\frac{1}{2}$ and of $d(x^2\text{-}y^2)$ symmetry. Because their treatment is within a local, cluster model, they do not predict specific long-range ordering, but their approach is consistent with the usual picture of antiferromagnetic superexchange.

The hybridization induces a discrete level in the photoemission spectrum above the filled O p bands. This level, which is the first ionization level, is a singlet of two holes, which are strongly correlated, in the sense that they have only small probability of both being on the Cu atom. Eskes and Sawatsky (1988), using a related model, arrive at similar conclusions. MMS conclude that U_p is not in itself strong enough to change qualitatively the itinerant nature of the oxygen bands, but that it does enhance correlation effects in the first ionization state.

The Coulomb repulsion parameters U have been calculated by several groups using methods that differ in some aspects. Hybertsen, Schlüter, and Christensen (1989) have also used the constrained local-density approach introduced by Dederichs *et al.* (1984), but in a way that differs somewhat from the procedure of MMS. Like MMS, they used the LMTO method and supercells, and calculated the energy of a neutral system as a function of the (say) Cu d charge. (In practice, a wide variety of charges on both Cu and O ions were studied to map out the corresponding energy surface.) Unlike MMS, they kept the d orbital fully hybridized with other atomic orbitals, whereas MMS effectively decoupled the Cu d orbital. As a result, the U parameters have a somewhat different meaning, and MMS argue that the procedure of Schlüter *et al.* produces consistently larger parameters.

By comparing one, two, and four formula unit supercells, HSC found the resulting values to show a strong dependence on supercell size. They identified $U_d = 10.5$ eV and, with less certainty, $U_p = 4$ eV and $U_{pd} = 1.2$ eV. They allowed also for a U_{pp} intersite repulsion but found it to be negligible. The value of U_d indeed is somewhat larger than that found by MMS, but, in agreement with MMS, they conclude that La_2CuO_4 is in the regime where both banding and correlation effects are important.

Using very similar computational programs but utilizing the transition state technique, Zaanen, Jepsen, *et al.* (1988) obtained $U_d = 8$ eV. Mila (1988) has obtained an extended Hubbard Hamiltonian with $U_d = 10$ eV and other parameters typical of those mentioned above, except that his energy separation $E_p - E_d = 4$ eV is rather larger than that obtained by other groups.

Estimates of these parameters have also been made from cluster calculations. As discussed in Sec. III.D, cluster local-density calculations provide a different perspective from that of solid-state studies: they cannot represent many aspects of the periodic solid accurately, but as a result of their local approach they may provide insight into characteristics of states like the Cu d state, which shows indications of localized behavior. Studies of $(CuO_4)^{6-}$ clusters by Sarma and Sreedhar (1988) led to the estimate $U_d = 5.3$ eV. Chen, Callaway, and Misra (1988), from $Ba_4Cu_2O_7$ clusters representing the Y123 system, found $U_d = 5.5$ eV and $U_p = 4.8$ eV.

Variations of the extended Hubbard model discussed here have been used to describe the Cu-derived valence-band satellite seen in the cuprates. For CuO, Ghijsen *et al.* (1988) use the correlated cluster model and experimental data to determine $U_d = 9.3$ eV and describe this compound as a charge transfer insulator. The valence-band satellite is described as a predominantly d^8 configuration of Cu.

Shen *et al.* (1987) have used a correlated cluster picture and a variety of experimental data to derive parameters for $La_{2-x}Sr_xCuO_4$ ($x = 0.0$ and 0.2), for $YBa_2Cu_3O_7$, and for CuO. The Cu valence-band satellite lies at very similar energy (about 12.5 eV) in all these materials. Neglecting direct O-O hopping, Shen *et al.* derive values of U_d of 6–7 eV for all materials, and their interpretation of the satellite is again in terms of strong d^8 character with some $d^9\underline{L}$ and possibly $d^{10}\underline{L}^2$. They find that the intensity of the satellite compared to the main valence-band emission is strongly dependent on the charge transfer energy and the Cu-O hopping parameter.

Chang, Cohen, and Penn (1988) also regard the satellite as primarily a d^8 state. Rather than using a correlated cluster picture, however, they evaluate a hole self-energy. They begin with a Hubbard Hamiltonian with a band term describing Cu-O bands in the absence of correlation, and correlation energies U_d and U_p. Using a t-matrix approximation for the hole self-energy, they describe the satellite as a two-hole bound state at the Cu site, which requires a value of $U_d = 5$ eV, somewhat smaller than most values given above. Using their self-energy to calculate the spectral density, they not only find the satellite, as expected, but also find that the self-energy considerably reduces the spectral density within 2 eV of E_F, bringing it into much better agreement with the photoemission data.

The objective of identifying the parameters in model Hamiltonians such as those described above is to account for the observed spectra, as well as to ascertain the likelihood of various pairing models. Examples of such studies are those of Emery (1987) and Stechel and Jennison (1988). The copper oxides appear to present an intermediate regime involving both strong hybridization and strong correlation, which is difficult to treat. Discussion of the attempts to solve such models is beyond the scope of this article.

Before leaving this subject, we should mention one more model. Weber (1988a) has developed a model explicitly treating Cu d-d excitations. These are valence-conserving excitations, which may be low-lying; Weber suggests that they are of the order of 1–2 eV. In the ground state the Cu^{2+} d^9 hole is taken to be in the $d(x^2\text{-}y^2)$ orbital, consistent with the Jahn-Teller distortion in the La214 system. The d-d excitation involves the excitation of this hole into a different Cu orbital, probably the $d(z^2)$ orbital. A doped hole lying primarily on the O ions could interact with these excitations, greatly affecting the hole dispersion relation as well as providing a polarization mechanism by which to pair carriers. This picture may require a somewhat different range of parameters than that obtained by most workers discussed above.

B. Correlated quantum-chemical calculations

Guo, Langlois, and Goddard (GLC) (1988) have applied their generalized valence-bond (GVB) approach to small clusters of Cu and O to model the electronic structure of the La214 and Y123 systems. In their approach they choose a Cu-O cluster, such as Cu_2O_{11} (Cu-O sheet), Cu_3O_{10} (Cu-O chain), or Cu_3O_{12} (Cu-O "stub"), and surround this cluster with point charges out to 8 Å having the standard formal valence to model the crystal field. The electrons of the Cu-O cluster and cation donors are treated explicitly; for example, one calculation corresponds to the $(Cu_3O_{10})^{14-}$ cluster. The Cu core electrons are treated with a pseudopotential to reduce the computational expense. The approach of Guo *et al.* differs from most cluster calculations in that they do not use the local spin-density approximation, Hartree-Fock, or configuration interaction procedures, but apply the generalized valence-bond method of constructing N-electron wave functions.

The generalized valence-bond wave function enforces from the beginning some correlation effects that are expected to be important. For their Cu_2O_7 cluster, for example, GLG formed the generalized valence-bond singlet wave function

$$\Psi = A\,[\Phi^*(\psi_L^*\psi_R + \psi_R^*\psi_L)(\alpha^*\beta - \beta^*\alpha)]\,, \qquad (11.3)$$

where ψ_R, ψ_L denote $d(x^2\text{-}y^2)$-like orbitals centered primarily on the right and left Cu atoms with spin α and β, Φ contains all other orbitals and spins, and A is the antisymmetrization operator. The corresponding triplet state is given by an analogous expression with + and − signs reversed. Roughly, the generalized valence-bond state corresponds to projecting the unrestricted Hartree-Fock state onto a pure singlet (triplet) and then self-consistently optimizing the orbitals.

In all of their calculations, Guo, Langlois, and Goddard find that the Cu ion is in the d^9 configuration, with the singly occupied d orbital being the one which points at the four nearest O atoms [i.e., the $d(x^2\text{-}y^2)$ orbital in the La214 system], in agreement with the standard Jahn-Teller distortion picture. (However, the net charge on the Cu, by their definition, is +0.2 to +0.4, not +2.0.) In contrast to the local spin-density or Hartree-Fock methods, in which one obtains a half-filled band, the generalized valence-bond description may be pictured as having each orbital in the band half-occupied. (Of course, only the cluster analog occurs in a cluster calculation.)

Guo *et al.* find that, due to a large on-site Coulomb repulsion energy, conduction does not take place through the hopping of an electron among the Cu d orbitals. Rather, when the cluster is "doped" with a hole, the one hole state is primarily an O $p\pi$ orbital (not $p\sigma$), and it is spin coupled both to the unoccupied Cu d orbital and to neighboring O $p\pi$ hole orbitals. Due to boundary effects arising from the confinement of electrons to a small cluster, the spin couplings in a small cluster may, however, not be representative of couplings in a periodic solid.

The doping in this study was modeled not only by changing the number of electrons on the cluster, but also by altering the (La, Sr) point charge in a virtual-crystal manner to $+(3-x/2)$. For a concentration $x=0.3$ Guo *et al.* find that the hole favors residing on the apex O_z oxygen rather than the O_{xy} atom favored in the stoichiometric material. These observations reinforce the calculations discussed in Sec. VI that indicate alloying Sr or Ba for La in the La214 system involves more than simply a rigid-band doping of the Cu-O layers. On the other hand, the measurements of Fink *et al.* (1989), discussed in Sec. V, appear to rule out holes with this symmetry in $Bi_2Sr_2CaCu_2O_8$.

The generalized valence-bond calculations were carried out only on small clusters. It is easy to imagine that, due to the lack of freedom to hop to all the sites available in the crystal and due to the neglect of screening appropriate to a crystalline environment, such calculations may overestimate the magnitude of correlations of a localized nature. To better simulate the effects of correlation in the crystal, Guo, Langlois, and Goddard used their N-electron generalized valence-bond cluster wave functions for O_{xy}-centered holes as basis functions for a calculation of the one-hole band in a crystal. The calculation is formally analogous to a linear combination of atomic orbitals (LCAO) band calculation, with the main difference being that the Hamiltonian matrix elements result from the correlated localized generalized valence-bond wave functions rather than from localized one-electron orbitals.

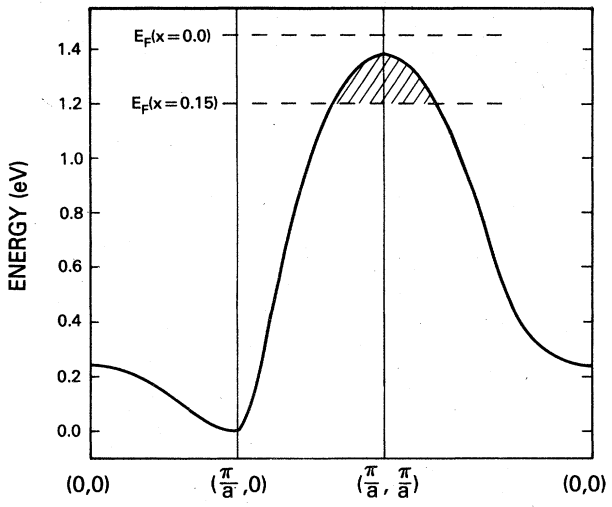

FIG. 65. Band dispersion for holes in a Cu-O layer, shown in the two-dimensional Brillouin zone, which resulted from the generalized valence-bond calculation of Guo, Langlois, and Goddard (1988). Fermi energies E_F are shown for the insulating phase ($x=0.0$) and for the metallic regime ($x=0.15$). The figure was drawn by the author from a contour plot presented by Guo *et al.*

The resulting crystal valence-bond band structure for a single O_{xy} $p\pi$ hole in a Cu-O layer representing the La214 system is pictured in Fig. 65. The electron band maximum (minimum hole energy, most stable state) occurs at the two-dimensional zone corner $(\pi/a,\pi/a)$, with the other extremum occurring not at the zone center but at the zone edges $(\pi/a,0)$ and $(0,\pi/a)$. The total bandwidth is 1.4 eV. At stoichiometry the band is empty of holes and is insulating, apparently independently of the occurrence of long-range (or local) antiferromagnetic order. The Fermi energy for $x=0.15$ is also shown in this figure, assuming all the holes go into this O_{xy} $p\pi$ band. The corresponding Fermi surface that is predicted is a single small circular cylinder centered at the zone corner; it is quite different from that occurring in local-density calculations.

C. Self-interaction corrected local spin-density functional theory

In the local spin-density approximation, an electron in a localized state has an unphysical interaction with itself, which is mostly of the direct Coulomb type but also includes a self-exchange-correlation contribution. The simplest example of the consequences of this spurious self-interaction occurs for the hydrogen atom, whose binding energy is underestimated by about 10% as a result. In crystals the use of Bloch functions, which places $1/N$ of the density of each state on each of the N atoms, leads to formally vanishing self-interaction. However, there are clear examples in which a local description is a more appropriate one, such as deep core states, $4f$ states in rare earths, and apparently the $3d$ states in some transition-metal compounds.

In the self-interaction-corrected local spin-density (SIC-LSD) approximation, the energy functional is given by

$$E_{\rm SIC}[n,\{n_{is}\}] = E_{\rm LSD}[n] - \frac{e^2}{2}\sum_{is}\int\int n_{is}(\mathbf{r})n_{is}(\mathbf{r}')/|\mathbf{r}-\mathbf{r}'| - \sum_{is}\int \varepsilon_{\rm xc}[n_{is}(\mathbf{r})]n_{is}(\mathbf{r})d\mathbf{r} \quad (11.4)$$

where $n_{is}(\mathbf{r})$ is the orbital density of orbital i with spin s, $\varepsilon_{\rm xc}$ is given in Eq. (4.7), and $E_{\rm LSD}$ is the usual local spin density functional. Due to the orbital dependence of this functional, the SIC-Kohn-Sham equations lead to different one-electron potentials for each orbital, and a consequence is that orbitals are no longer orthogonal. In addition, specification of the orbitals (which are Wannier-type) is a difficult problem both conceptually and numerically. For these reasons self-consistent SIC-LSD calculations have been carried out for only a few nonmetals; see, for example, Pederson and Klein (1988).

Svane and Gunnarsson (1988b) have, however, applied a simplified form of SIC theory to a model representing a CuO_2 layer such as occurs in the cuprate superconductors. Rather than attempting to deal with the full Coulomb interaction between electrons, they considered a Hubbard model with only a Cu $d(x^2\text{-}y^2)$ orbital and the O $p\sigma$ orbitals, Cu-O hopping (only), and Coulomb repulsion on both Cu and O. They applied the lattice version of the SIC-LSD theory studied earlier (Svane and Gunnarsson, 1988a). With this model and their method of solution, they found that localized solutions are much more strongly favored by the SIC-LDA than by the local-density approximation alone.

For a variety of parameter values thought to be in the range to represent a CuO_2 layer, they find that both the magnetic moment for the antiferromagnetic state and the gap in the eigenvalue spectrum are increased considerably by the SIC. The moment they obtain is, in fact, about twice the measured value (of about $0.4\mu_B$), and the gap of 2.0–2.5 eV is in the range that has been suggested by experimental data. These results are very encouraging that the SIC-LSD approach is an appropriate method to use in describing the antiferromagnetic state in the copper oxides, but firm conclusions must await a full, *ab initio* implementation of the theory.

XII. SUMMARY

It is far too early to draw any firm conclusions about the best way to picture, and to begin to describe, the electronic structure of the copper-oxide high-temperature superconductors. In fact, it may well be appropriate to describe the magnetic insulating state from one point of view and the metallic regime from another viewpoint. The metal-insulator regime will in any case be a long

time in being unraveled.

Within the metallic regime, a number of the properties seem to be described rather well by the local-density version of density-functional theory. Probably the most quantitative example is that of the calculations of the static structural properties, the lattice instability, and the phonon frequencies of La_2CuO_4, described in Sec. X. To a great extent the electrical transport properties in the metallic regime look typical of quasiparticles, and the calculations described in Sec. VII appear encouraging in this respect, although many questions remain. Even many of the diverse spectral data discussed in Sec. V can be interpreted in terms of the band-structure density of states and corresponding characters of the states.

On the negative side, there are spectral features, particularly the valence-band satellite, indicating that self-energy effects are strong in certain regions of the spectrum. Even for the ground state of the antiferromagnetic insulators, it is clear that there are crucial correlations that are missing from the local-density treatment. How one should try to describe quantitatively the gaps in these materials is also still an open question; the local-density approach does not predict them to be either antiferromagnetic (except perhaps weakly so) or insulators. To what extent these correlations and self-energy effects are important for the very-low-energy carriers, and for the 0.1–5-eV excitations which are widely speculated to be active in these materials, is a monumental task to be addressed in the future, hopefully the near future.

ACKNOWLEDGMENTS

I have benefited from conversations with colleagues and acquaintances too numerous to mention. I have profited from especially close interaction and discussions with many co-workers in the theory group at the Naval Research Laboratory and nearby: P. B. Allen, L. L. Boyer, R. E. Cohen, M. J. DeWeert, B. M. Klein, H. Krakauer, D. A. Papaconstantopoulos, J. W. Serene, and D. J. Singh. I have also benefited from the close interaction and sharing of exciting developments with experimental colleagues, especially D. U. Gubser, M. Osofsky, L. E. Toth, and S. A. Wolf. This article would not have been written without the encouragement of D. A. Papaconstantopoulos. My involvement in the study of high-temperature superconductivity has been facilitated by the support of the Office of Naval Research for the Complex Systems Theory Branch at the Naval Research Laboratory. To a person like myself who was nurtured in the faint hope of increasing T_c by 2° or 3°, the vivid memories of the past two years will never fade. The unraveling during the next few years of the mysteries of high-temperature superconductivity promises to be no less exciting.

REFERENCES

Aeppli, G., and D. J. Buttrey, 1988, Phys. Rev. Lett. **61**, 203.
Aeppli, G., D. R. Harshman, D. Buttrey, E. Ansaldo, G. P. Espinosa, A. S. Cooper, J. P. Remeika, T. Freltoft, T. M. Riseman, D. R. Noakes, B. Ellman, T. F. Rosenbaum, and D. Ll. Williams, 1988, Physica C **153-155**, 1111.
Aharony, A., R. J. Birgeneau, A. Coniglio, M. A. Kastner, and H. E. Stanley, 1988, Phys. Rev. Lett. **60**, 1330.
Akhtar, M. J., C. R. A. Catlow, S. M. Clark, and W. M. Temmerman, 1988, J. Phys. C **21**, L917.
Allen, P. B., 1980, in *Dynamical Properties of Solids,* edited by G. K. Horton and A. A. Maradudin (North-Holland, Amsterdam), p. 137.
Allen, P. B., T. P. Beaulac, F. S. Khan, W. H. Butler, F. J. Pinski, and J. C. Swihart, 1986, Phys. Rev. B **34**, 4331.
Allen, P. B., and R. C. Dynes, 1975, Phys. Rev. B **12**, 905.
Allen, P. B., W. E. Pickett, and H. Krakauer, 1987a, Phys. Rev. B **36**, 3926.
Allen, P. B., W. E. Pickett, and H. Krakauer, 1987b, in *Novel Superconductivity,* edited by S. A. Wolf and V. Z. Kresin (Plenum, New York), p. 489.
Allen, P. B., W. E. Pickett, and H. Krakauer, 1988a, in *High Temperature Superconductors,* MRS Symposium Proceedings No. 99, edited by M. B. Brodsky, R. C. Dynes, K. Kitazawa, and H. L. Tuller (Materials Research Society, Pittsburgh), p. 183.
Allen, P. B., W. E. Pickett, and H. Krakauer, 1988b, Phys. Rev. B **37**, 7482.
Andersen, O. K., 1975, Phys. Rev. B **12**, 3060.
Andersen, O. K., H. L. Skriver, H. Nohl, and B. Johansson, 1979, Pure Appl. Chem. **52**, 93.
Anderson, P. W., 1987, Science **235**, 1196.
Asano, H., T. Ishigaki, and K. Takita, 1987, Jpn. J. Appl. Phys. **26**, L1064.
Aurivillius, B., 1950a, Ark. Kemi **1**, 463.
Aurivillius, B., 1950b, Ark. Kemi **1**, 499.
Aurivillius, B., 1950c, Ark. Kemi **2**, 519.
Axe, J. D., D. E. Cox, K. Mohanty, H. Moudden, A. R. Moodenbaugh, Y. Xu, and T. R. Thurston, 1989, IBM J. Res. Dev. (in press).
Bansil, A., R. Pankaluoto, R. S. Rao, P. E. Mijnarends, W. Dlugosz, R. Prasad, and L. C. Smedskjaer, 1988, Phys. Rev. Lett. **61**, 2480.
Barbee, T. W., III, M. L. Cohen, L. C. Bourne, and A. Zettl, 1988, J. Phys. C **21**, 5977.
Batlogg, B., and R. J. Cava, 1987, Physica B **148**, 173.
Bednorz, J. G., and K. A. Müller, 1986, Z. Phys. B **64**, 189.
Beno, M. A., L. Soderholm, D. W. Capone II, D. G. Hinks, J. D. Jorgensen, J. D. Grace, I. K. Schuller, C. U. Segre, and K. Zhang, 1987, Appl. Phys. Lett. **51**, 57.
Bhattacharya, S., M. J. Higgins, D. C. Johnson, A. J. Jacobson, J. P. Stokes, D. P. Coshorn, and J. T. Lewandowski, 1988, Phys. Rev. Lett. **60**, 1181.
Bhattacharya, S., M. J. Higgins, D. C. Johnson, A. J. Jacobson, J. P. Stokes, J. T. Lewandowski, and D. P. Goshorn, 1988, Phys. Rev. B **37**, 5901.
Bianconi, A., P. Castrucci, M. De Santis, A. Di Cicco, A. M. Flank, P. Lagarde, H. Katayama-Yoshida, A. Marcelli, and Zhao Zhongxian, 1988, in *Towards the Theoretical Understanding of High T_c Superconductors,* Proceedings of the Adriatico Research Conference, 1988, edited by S. Lundqvist, E. Tosatti, M. P. Tosi, and Yu Lu (World Scientific, Singapore), Int. J. Mod. Phys. B **2**, No. 5.
Bianconi, A., M. De Santis, A. Di Cicco, A. M. Flank, A. Fontaine, P. Lagarde, H. Katayama-Yoshida, A. Kotani, and A. Marcelli, 1988, Phys. Rev. B **38**, 7196.
Billesbach, D. P., J. R. Hardy, and P. J. Edwardson, 1989, Phys.

Rev. B **39**, 202.
Birgeneau, R. J., C. Y. Chen, D. R. Gabbe, H. P. Jenssen, M. A. Kastner, C. J. Peters, P. J. Picone, T. Thio, T. R. Thurston, H. L. Tuller, J. D. Axe, B. Böni, and G. Shirane, 1987, Phys. Rev. Lett. **59**, 1329.
Birgeneau, R. J., Y. Endoh, K. Kakurai, Y. Hidaka, T. Murakami, M. A. Kastner, T. R. Thurston, G. Shirane, and K. Yamada, 1989, Phys. Rev. B **39**, 2868.
Birgeneau, R. J., D. R. Gabbe, H. P. Jenssen, M. A. Kastner, P. J. Picone, T. R. Thurston, G. Shirane, Y. Endoh, M. Sato, K. Yamada, Y. Hidaka, M. Oda, Y. Enomoto, M. Suzuki, and T. Murakami, 1988, Phys. Rev. B **38**, 6614.
Birgeneau, R. J., and G. Shirane, 1989, in *Physical Properties of High Temperature Superconductors,* edited by D. M. Ginsberg (World Scientific, Singapore), in press.
Blumenroeder, S., E. Zirngiebl, J. D. Johnson, P. Killough, J. L. Smith, and Z. Fisk, 1987, Phys. Rev. B **35**, 8840.
Böni P., J. D. Axe, G. Shirane, R. J. Birgeneau, D. R. Gabbe, H. P. Jenssen, M. A. Kastner, C. J. Peters, P. J. Picone, and T. R. Thurston, 1988, Phys. Rev. B **38**, 185.
Bonn, D. A., J. E. Greedan, C. V. Stager, T. Timusk, M. G. Doss, S. L. Herr, K. Kamaras, and D. B. Tanner, 1987, Phys. Rev. Lett. **58**, 2249.
Bozivic, I., K. Char, S. J. B. Yoo, A. Kapitulnik, M. R. Beasley, T. H. Geballe, Z. Z. Wang, S. Hagen, N. P. Ong, D. E. Aspnes, and M. K. Kelly, 1988, Phys. Rev. B **38**, 5077.
Brandow, B. H., 1977, Adv. Phys. **26**, 651.
Brandow, B. H., 1988, in *Narrow Band Phenomena,* edited by J. C. Fuggle, G. A. Sawatzky, and J. W. Allen, NATO ASI Series B, Vol. 184 (Plenum, New York).
Brewer, J. H., *et al.*, 1988, Phys. Rev. Lett. **60**, 1073.
Brückel, T., H. Capellmann, W. Just, O. Schaerpf, S. Kemmler-Sack, R. Kiemel, and W. Schaefer, 1987, Europhys. Lett. **4**, 1189.
Burdett, J. K., G. V. Kulkarni, and K. Levin, 1987, Inorg. Chem. **26**, 3650.
Capponi, J. J., C. Chaillout, A. W. Hewat, P. Lejay, M. Marezio, N. Nguyen, B. Raveau, J. L. Soubeyroux, J. L. Thoulence, and R. Tournier, 1987, Europhys. Lett. **3**, 1301.
Cava, R. J., B. Batlogg, C. H. Chen, E. A. Rietman, S. M. Zahurak, and D. J. Werder, 1987, Nature (London) **329**, 423.
Cava, R. J., B. Batlogg, R. M. Fleming, S. A. Sunshine, A. Ramirez, E. A. Rietman, S. M. Zahurak, and R. B. van Dover, 1988, Phys. Rev. B **37**, 5912.
Cava, R. J., *et al.*, 1988, Nature (London) **332**, 814.
Cava, R. J., A. Santoro, D. W. Johnson, Jr., and W. W. Rhodes, 1987, Phys. Rev. B **35**, 6716.
Chang, K. J., M. L. Cohen, and D. R. Penn, 1988, Phys. Rev. B **38**, 8691.
Chen, H., J. Callaway, and P. K. Misra, 1988, Phys. Rev. B **38**, 195.
Chen, I.-W., S. J. Keating, C. Y. Keating, X. Wu, J. Xu, P. E. Reyes-Morel, and T. Y. Tien, 1987, Solid State Commun. **63**, 997.
Chrzanowski, J., S. Gygax, J. C. Irwin, and W. N. Hardy, 1988, Solid State Commun. **65**, 139.
Chu, C. W., J. Bechtold, L. Gao, P. H. Hor, Z. J. Huang, R. L. Meng, Y. Y. Sun, Y. Q. Wang, and Y. Y. Xue, 1988, Phys. Rev. Lett. **60**, 941.
Cini, M., 1977, Solid State Commun. **24**, 681.
Cini, M., 1978, Phys. Rev. B **17**, 2788.
Claessen, R., R. Manzke, H. Carstensen, B. Burandt, T. Busdaps, M. Skibowski, and J. Fink, 1989, "A surface study of the 83 K superconductor $Bi_2Sr_2CaCu_2O_8$ by LEED and angle-resolved inverse photoemission spectroscopy," Kernforschungszentrum Karlsruhe preprint.
Cohen, R. E., L. L. Boyer, and M. J. Mehl, 1987, Phys. Rev. B **35**, 5749.
Cohen, R. E., L. L. Boyer, M. J. Mehl, W. E. Pickett, and H. Krakauer, 1989, in *Perovskite: A Structure of Great Interest to Geophysics and Materials Science,* Geophysical Monograph V.45, edited by A. Navrotsky (Am. Geophys. Union), p. 55.
Cohen, R. E., H. Krakauer, and W. E. Pickett, 1988, unpublished.
Cohen, R. E., W. E. Pickett, L. L. Boyer, and H. Krakauer, 1988a, Phys. Rev. Lett. **60**, 817.
Cohen, R. E., W. E. Pickett, L. L. Boyer, and H. Krakauer, 1988b, *High Temperature Superconductors,* MRS Symposium Proceedings No. 99, edited by M. B. Brodsky, R. C. Dynes, K. Kitazawa, and H. L. Tuller (Materials Research Society, Pittsburgh), p. 825.
Cohen, R. E., W. E. Pickett, H. Krakauer, and L. L. Boyer, 1988, Physica B **150**, 61.
Cohen, R. E., W. E. Pickett, and H. Krakauer, 1989, Phys. Rev. Lett. **62**, 831.
Cohen, R. E., W. E. Pickett, H. Krakauer, D. Singh, D. A. Papaconstantopoulos, and P. B. Allen, 1989, in *Proceedings of the Workshop on the Materials Science of High Temperature Superconductors,* NIST, Gaithersburg, 1988 (World Scientific), in press.
Cohen, R. E., D. Singh, W. E. Pickett, and H. Krakauer, 1989, unpublished.
Collins, R. T., Z. Schlesinger, M. W. Shafer, and T. R. McGuire, 1988, Phys. Rev. B **37**, 5817.
Cooper, S. L., M. V. Klein, B. G. Pazol, J. P. Rice, and D. M. Ginsberg, 1988, Phys. Rev. B **37**, 5920.
Copic, M., D. Mihailovic, M. Zgonik, M. Prester, K. Biljakovic, B. Orel, and N. Brnicevic, 1987, Solid State Commun. **64**, 297.
Crommie, M. F., A. Zettl, T. W. Barbee III, and M. L. Cohen, 1988, Phys. Rev. B **37**, 9734.
David, W. I. F., W. T. A. Harrison, J. M. F. Gunn, O. Moze, A. K. Soper, P. Day, J. D. Jorgensen, D. G. Hinks, M. A. Beno, L. Soderholm, D. W. Capone II, I. K. Schuller, C. U. Segre, K. Zhang, and J. D. Grace, 1987, Nature (London) **327**, 310.
Day, P., M. Rosseinsky, K. Prassides, W. I. F. David, O. Moze, and A. Soper, 1987, J. Phys. C **20**, L429.
Dederichs, P., S. Blügel, R. Zeller, and H. Akai, 1984, Phys. Rev. Lett. **53**, 2512.
Delgado, J. M., R. K. McMullan, G. Diaz de Delgado, B. J. Wünsch, P. J. Picone, H. P. Jenssen, and D. R. Gabbe, 1988, Phys. Rev. B **37**, 9343.
Devreese, J. T., and P. Van Camp, 1984, Eds., *Electronic Structure, Dynamics, and Quantum Structural Properties of Condensed Matter* (Plenum, New York).
DeWeert, M. J., D. A. Papaconstantopoulos, and W. E. Pickett, 1989, Phys. Rev. B **39**, 4235.
Dmowski, W., B. H. Toby, T. Egami, M. A. Subramanian, J. Gopalakrishnan, and A. W. Sleight, 1988, Phys. Rev. Lett. **61**, 2608.
Egami, T., 1987, Solid State Commun. **63**, 1019.
Egami, T., W. Dmowski, J. D. Jorgensen, D. G. Hinks, D. W. Capone II, C. U. Segre, and K. Zhang, 1987, Rev. Solid State Sci. **1**, 101.
Emery, V., 1987, Phys. Rev. Lett. **58**, 2794.
Endoh, Y., K. Yamada, R. J. Birgeneau, D. R. Gabbe, H. P. Jenssen, M. A. Kastner, C. J. Peters, P. J. Picone, T. R. Thurston, J. M. Tranquada, G. Shirane, Y. Hidaka, M. Oda, Y. Enomoto, M. Suzuki, and T. Murakami, 1988, Phys. Rev. B

37, 7443.
Eskes, H., and G. A. Sawatzky, 1988, Phys. Rev. Lett. **61**, 1415.
Eskes, H., L. H. Tjeng, and G. A. Sawatzky, 1989, "A cluster model calculation of the electronic structure of CuO, a model for the high-T_c superconductors," University of Groningen, preprint.
Eumura, Y. J., W. J. Kossler, X. H. Yu, J. R. Kempton, H. E. Schone, D. Opie, C. E. Stronach, D. C. Johnston, M. S. Alvarez, and D. P. Goshorn, 1987, Phys. Rev. Lett. **59**, 1045.
Evain, M., M. H. Whangbo, M. A. Beno, U. Geiser, and J. M. Williams, 1987, J. Am. Chen. Soc. **109**, 7917.
Evain, M., M. H. Whangbo, M. A. Beno, and J. M. Williams, 1988, J. Am. Chem. Soc. **110**, 614.
Fink, J., N. Nücker, H. Romberg, and J. C. Fuggle, 1989, IBM J. Res. Dev. (in press).
FitzGerald, J. D., R. L. Withers, J. G. Thompson, L. R. Wallenberg, J. S. Anderson, and B. G. Hyde, 1988, Phys. Rev. Lett. **60**, 2797.
Fleming, R. M., B. Batlogg, R. J. Cava, and E. A. Rietman, 1987, Phys. Rev. B **35**, 7191.
Fornasini, M. L., G. A. Costa, M. Ferretti, and G. L. Olcese, 1988, Solid State Commun. **65**, 1121.
Forsyth, J. B., P. J. Brown, and B. M. Wanklyn, 1988, J. Phys. C **21**, 2917.
Francois, M., E. Walker, J.-L. Jorda, K. Yvon, and P. Fischer, 1987, Solid State Commun. **63**, 1149.
Francois, M., K. Yvon, P. Fischer, and M. Decroux, 1987, Solid State Commun. **63**, 35.
Freeman, A. J., J. Yu, S. Massidda, and D. D. Koelling, 1987, Physica B **148**, 212.
Freltoft, T., J. E. Fischer, G. Shirane, D. E. Moncton, S. K. Sinha, D. Vaknin, J. P. Remeika, A. S. Cooper, and D. Harshman, 1987, Phys. Rev. B **36**, 826.
Freltoft, T., G. Shirane, S. Mitsuda, J. P. Remeika, and A. S. Cooper, 1988, Phys. Rev. B **37**, 137.
Fu, C. L., and A. J. Freeman, 1987, Phys. Rev. B **35**, 8861.
Fuggle, J. C., 1981, in *Electron Spectroscopy: Theory, Techniques and Applications,* edited by C. R. Brundle and A. D. Baker (Academic, New York), Vol. 4, p. 85.
Fuggle, J. C., P. J. W. Weijs, R. Schoorl, G. A. Sawatzky, J. Fink, N. Nücker, P. J. Durham, and W. M. Temmerman, 1988, Phys. Rev. B **37**, 123.
Fujimori, A., E. Takayama-Muromachi, Y. Uchida, and B. Okai, 1987, Phys. Rev. B **35**, 8814.
Ganguly, P., S. Kollali, C. N. R. Rao, and S. Kern, 1980, Magn. Lett. **1**, 107.
Gao, Y., P. Lee, P. Coppens, M. A. Subramanian, and A. W. Sleight, 1988, Science **241**, 954.
Gaspari, G. D., and B. L. Gyorffy, 1972, Phys. Rev. Lett. **28**, 801.
Geiser, U., M. A. Beno, A. J. Schultz, H. H. Wang, T. J. Allen, M. R. Monaghan, and J. M. Williams, 1987, Phys. Rev. B **35**, 6721.
Ghijsen, J., L. H. Tjeng, J. van Elp. H. Eskes, J. Westerink, G. A. Sawatzky, and M. T. Czyzyk, 1988, Phys. Rev. B **38**, 11322.
Gordon, R. G., and Y. S. Kim, 1972, J. Chem. Phys. **56**, 3122.
Grande, V. B., Hk. Müller-Buschbaum, and M. Schweizer, 1977, Z. Anorg. Allg. Chem. **428**, 120.
Grant, P. M., R. B. Beyers, E. M. Engler, G. Lim, S. S. P. Parkin, M. L. Ramirez, V. Y. Lee, A. Nazzal, J. E. Vazquez, and R. J. Savoy, 1987, Phys. Rev. B **35**, 7242.
Greene, R. L., H. Maletta, T. S. Plaskett, J. G. Bednorz, and K. A. Müller, 1987, Solid State Commun. **63**, 379.
Gunnarsson, O., and O. Jepsen, 1988, Phys. Rev. B **38**, 3568.
Gunnarsson, O., O. K. Andersen, O. Jepsen, and J. Zaanen, 1988, in *Core-Level Spectroscopy in Condensed Systems,* edited by J. Kanamori and A. Kotani, Springer Series in Solid-State Sciences, Vol. 81 (Springer, Berlin), p. 82.
Guo, Y., J.-M. Langlois, and W. A. Goddard, 1988, Science **239**, 896.
Guo, G. Y., and W. M. Temmerman, 1988, J. Phys. C **21**, L803.
Guo, G. Y., W. M. Temmerman, and G. M. Stocks, 1988, J. Phys. C **21**, L103.
Gupta, R. P., and M. Gupta, 1988, Solid State Commun. **67**, 129.
Gurvitch, M., and A. T. Fiory, 1987a, Phys. Rev. Lett. **59**, 1337.
Gurvitch, M., and A. T. Fiory, 1987b, in *Novel Superconductivity,* edited by S. A. Wolf and V. Z. Kresin (Plenum, New York), p. 663.
Gurvitch, M., and A. T. Fiory, 1988, Physica C **153-155**, 1369.
Gutsmiedl, P., G. Wolff, and K. Andres, 1987, Phys. Rev. B **36**, 4043.
Haldar, P., K. Chen, B. Maheswaran, A. Roig-Janicki, N. K. Jaggi, R. S. Markiewicz, and B. C. Giessen, 1988, Science **241**, 1198.
Hamann, D. R., and L. F. Mattheiss, 1988, Phys. Rev. B **38**, 5138.
Harrison, W. A., 1980, *Electronic Structure and the Properties of Solids* (Freeman, New York).
Harrison, W. A., 1988, Phys. Rev. B **38**, 270.
Hass, K., 1989, in *Solid State Physics,* edited by H. Ehrenreich and D. Turnbull (Academic, New York), Vol. 42, in press.
Hatsugai, Y., and T. Fujiwara, 1988, Solid State Commun. **65**, 1271.
Hazen, R. M., L. W. Finger, R. J. Angel, C. T. Prewitt, N. L. Ross, H. K. Mao, C. G. Hadidiacos, P. H. Hor, R. L. Meng, and C. W. Chu, 1987, Phys. Rev. B **35**, 7238.
Hazen, R. M., C. T. Prewitt, R. J. Angel, N. L. Ross, L. W. Finger, C. G. Hadidiacos, D. R. Veblen, P. J. Heaney, P. H. Hor, R. L. Meng, Y. Y. Sun, Y. Q. Wang, Y. Y. Xue, Z. J. Huang, L. Gao, J. Bechtold, and C. W. Chu, 1988, Phys. Rev. Lett. **60**, 1174.
Harshman, D. R., L. F. Schneemeyer, J. V. Waszczak, Y. C. Jean, M. J. Fluss, R. H. Howell, and A. L. Wachs, 1988, Phys. Rev. B **38**, 848.
Herman, F., R. V. Kasowski, and W. Y. Hsu, 1987a, Phys. Rev. B **36**, 6904.
Herman, F., R. V. Kasowski, and W. Y. Hsu, 1987b, in *Novel Superconductivity,* edited by S. A. Wolf and V. Z. Kresin (Plenum, New York), p. 521.
Herman, F., R. V. Kasowski, and W. Y. Hsu, 1988, Phys. Rev. B **38**, 204.
Herr, S. L., K. Kamaras, C. D. Porter, M. G. Dos, D. B. Tanner, D. A. Bonn, J. E. Greedan, C. V. Stager, and T. Timusk, 1987, Phys. Rev. B **36**, 733.
Hillebrecht, F. U., J. Fraxedas, L. Ley, H. J. Trodahl, J. Zaanen, W. Braun, M. Mast, H. Petersen, M. Schaible, L. C. Bourne, P. Pinsukanjana, and A. Zettl, 1989, Phys. Rev. B **39**, 236.
Himpsel, F. J., G. V. Chandrashekhar, A. B. McLean, and M. W. Shafer, 1988, Phys. Rev. B **38**, 11946.
Hinks, D. G., D. R. Richards, B. Dabrowski, D. T. Marx, and A. W. Mitchell, 1988, Nature (London) **335**, 419.
Hoffman, L., A. A. Manuel, M. Peter, E. Walker, and M. A. Damento, 1988, Europhys. Lett. **6**, 61.
Hohenberg, P. and W. Kohn, 1964, Phys. Rev. **136**, B864.
Hulm, J. K., and R. D. Blaugher, 1972, in *Superconductivity in d- and f-Band Metals,* edited by D. H. Douglas (AIP, New

York), p. 1.
Hybertsen, M. S., and L. F. Mattheiss, 1988, Phys. Rev. Lett. **60**, 1661.
Hybertsen, M. S., M. Schlüter, and N. E. Christensen, 1989, "Calculation of Coulomb interaction parameters for La_2CuO_4 using a constrained density functional approach," preprint.
Ihara, H., R. Sugise, M. Hirabayashi, N. Terada, M. Jo, K. Hayashi, A. Negishi, M. Tokumoto, Y. Kimura, and T. Shimomura, 1988, Nature (London) **334**, 510.
Imer, J.-M., F. Patthey, B. Dardel, W.-D. Schneider, Y. Baer, Y. Petroff, and A. Zettl, 1989, Phys. Rev. Lett. **62**, 336.
Islam, M. S., M. Leslie, S. M. Tomlinson and C. R. A. Catlow, 1988, J. Phys. C **21**, L109.
Iye, Y., T. Tamegai, T. Sakakibara, T. Goto, N. Miura, H. Takeya, and H. Takei, 1988, Physica C **153-155**, 26.
Izumi, F., H. Asano, T. Ishigaki, A. Ono, and F. P. Okamura, 1987, Jpn. J. Appl. Phys. **26**, L611.
Izumi, F., H. Asano, T. Ishigaki, E. Takayama-Muromachi, Y. Matsui, and Y. Uchida, 1987, Jpn. J. Appl. Phys. **26**, L1153.
Izumi, F., H. Asano, T. Ishigaki, E. Takayama-Muromachi, Y. Uchida, and N. Watanabe, 1987a, Jpn. J. Appl. Phys. **26**, L1193.
Izumi, F., H. Asano, T. Ishigaki, E. Takayama-Muromachi, Y. Uchida, and N. Watanabe, 1987b, Jpn. J. Appl. Phys. **26**, L1214.
Izumi, F., H. Asano, T. Ishigaki, E. Takayama-Muromachi, Y. Uchida, N. Watanabe, and T. Nishikawa, 1987, Jpn. J. Appl. Phys. **26**, L649.
Jahn, H. A., and E. Teller, 1937, Proc. R. Soc. London, Ser. A **161**, 220.
Jarlborg, T., 1987, Helv. Phys. Acta **61**, 421.
Jarlborg, T., 1988, Solid State Commun. **67**, 297.
Jean, Y. C., J. Kyle, H. Nakanishi, P. E. A. Turchi, R. H. Howell, A. L. Wachs, M. J. Fluss, R. L. Meng, H. P. Hor, J. Z. Huang, and C. W. Chu, 1988, Phys. Rev. Lett. **60**, 1069.
Jericho, M. H., A. M. Simpson, J. M. Tarascon, L. H. Greene, R. McKinnon, and G. Hall, 1988, Solid State Commun. **65**, 987.
Johnston, D. C., J. P. Stokes, D. P. Goshorn, and J. T. Lewandowski, 1987, Phys. Rev. B **36**, 4007.
Jorgensen, J. D., 1987, Jpn. J. Appl. Phys. **26**, 2017.
Jorgensen, J. D., M. A. Beno, D. G. Hinks, L. Soderholm, K. J. Volin, R. L. Hitterman, J. D. Grace, I. K. Schuller, C. U. Segre, K. Zhang, and M. S. Kleefisch, 1987, Phys. Rev. B **36**, 3608.
Jorgensen, J. D., H.-B. Schüttler, D. G. Hinks, D. W. Capone II, K. Zhang, M. B. Brodsky, and D. J. Scalapino, 1987, Phys. Rev. Lett. **58**, 1024.
Jorgensen, J. D., B. W. Veal, W. K. Kwok, G. W. Crabtree, A. Umezawa, L. J. Nowicki, and A. P. Paulikas, 1987, Phys. Rev. B **36**, 5731.
Julien, J. P., D. Mayou, and F. Cyrot-Lackmann, 1988, Solid State Commun. **67**, 985.
Junod, A., A. Bezinge, T. Graf, J. L. Jorda, J. Muller, L. Antognazza, D. Cattani, J. Cors, M. Decroux, O. Fischer, M. Banovski, P. Genoud, L. Hoffman, A. A. Manuel, M. Peter, E. Walker, M. Francois, and K. Yvon, 1987, Europhys. Lett. **4**, 247.
Kadowaki, H., M. Nishi, Y. Yamada, H. Takeya, H. Takei, S. M. Shapiro, and G. Shirane, 1988, Phys. Rev. B **37**, 7932.
Kajitani, T., K. Oh-ishi, M. Kikuchi, Y. Syono, and M. Hirabayashi, 1987, Jpn. J. Appl. Phys. **26**, L1144.
Kanamori, J., 1960, J. Appl. Phys. (Suppl.) **31**, 14S.
Kasowski, R. V., 1987, Superlatt. Microstr. **3**, 383.
Kasowski, R. V., W. Y. Hsu, and F. Herman, 1987a, Solid State Commun. **63**, 1077.
Kasowski, R. V., W. Y. Hsu, and F. Herman, 1987b, Phys. Rev. B **36**, 7248.
Kasowski, R. V., W. Y. Hsu, and F. Herman, 1988, Phys. Rev. B **38**, 6470.
Kasowski, R. V., M.-H. Tsai, T. N. Rhodin, and D. D. Chambliss, 1986, Phys. Rev. B **34**, 2656.
Kasuya, T., and K. Takegahara, 1988, in *Superconducting Materials,* JJAP Series 1, edited by S. Nakajima and H. Fukuyama (Jpn. J. Appl. Phys., Tokyo), p. 251.
Katano, S., S. Funahashi, T. Hatano, A. Matsushita, K. Nakamura, T. Matsumoto, and K. Ogawa, 1987a, Jpn. J. Appl. Phys. **26**, L1046.
Katano, S., S. Funahashi, T. Hatano, A. Matsushita, K. Nakamura, T. Matsumoto, and K. Ogawa, 1987b, Jpn. J. Appl. Phys. **26**, L1049.
Katayama-Yoshida, H., T. Hirooka, A. Oyamada, Y. Okabe, T. Takahashi, T. Sasaki, A. Ochiai, T. Suzuki, A. J. Mascarenhas, J. I. Pankove, T. F. Ciszek, S. K. Deb, R. B. Goldfarb, and Y. Li, 1988, Physica C **156**, 481.
Khomskii, D. I., and K. I. Kugel, 1973, Solid State Commun. **13**, 763.
Kirk, M. D., J. Nogami, A. A. Baski, D. B. Mitai, A. Kapitulnik, T. H. Geballe, and C. F. Quate, 1988, Science **242**, 1673.
Klein, B. M., and W. E. Pickett, 1982, in *Superconductivity in d- and f-Band Metals,* edited by W. Buckel and W. Weber (Kernforschungszentrum, Karlsruhe), p. 97.
Kohiki, S., T. Hamada, and T. Wada, 1987, Phys. Rev. B **36**, 2290.
Kohn, W., and L. J. Sham, 1965, Phys. Rev. **140**, A1133.
Krakauer, H., and W. E. Pickett, 1987, in *Novel Superconductivity,* edited by S. A. Wolf and V. Z. Kresin (Plenum, New York), p. 501.
Krakauer, H., and W. E. Pickett, 1988, Phys. Rev. Lett. **60**, 1665.
Krakauer, H., W. E. Pickett, and R. E. Cohen, 1988, J. Supercond. **1**, 111.
Krakauer, H., W. E. Pickett, D. A. Papaconstantopoulos, and L. L. Boyer, 1987, Jpn. J. Appl. Phys. **26**, 991.
Krusin-Elbaum, L., R. L. Greene, F. Holtzberg, A. P. Malozemoff, and Y. Yeshurun, 1989, Phys. Rev. Lett. **62**, 217.
Lang, M., F. Steglich, R. Schefzyk, T. Lechner, H. Spille, H. Rietschel, W. Goldacker, and B. Renker, 1987, Europhys. Lett. **4**, 1145.
Lee, P. A., and N. Read, 1987, Phys. Rev. Lett. **58**, 2691.
LePage Y., W. R. McKinnon, J. M. Tarascon, L. H. Greene, G. W. Hull, and D. M. Hwang, 1987, Phys. Rev. B **35**, 7245.
Leung T. C., X. W. Wang, and B. N. Harmon, 1988, Phys. Rev. B **37**, 384.
List, R. S., A. J. Arko, Z. Fisk, S.-W. Cheong, S. D. Conradson, J. D. Thompson, C. B. Pierce, D. E. Peterson, R. J. Bartlett, N. D. Shinn, J. E. Shirber, B. W. Veal, A. P. Paulikas, and J. C. Campuzano, 1988, Phys. Rev. B **38**, 11966.
Longo, J. M., and P. M. Raccah, 1973, J. Solid State Chem. **6**, 526.
Lynn, J. W., and W.-H. Li, 1988, J. Appl. Phys. **64**, 6065.
Lyons, K. B., P. A. Fleury, J. P. Remeika, A. S. Cooper, and T. J. Negran, 1988, Phys. Rev. B **37**, 2353.
Lyons, K. B., P. A. Fleury, L. F. Schneemeyer, and J. V. Waszczak, 1988, Phys. Rev. Lett. **60**, 732.
Maeda, H., Y. Tanaka, M. Fukutomi, and T. Asano, 1988, Jpn. J. Appl. Phys. Lett. **4**, L209.
Marksteiner, P., S. Massidda, J. Yu, A. J. Freeman, and J. Red-

inger, 1988, Phys. Rev. B **38**, 5098.
Marsh, P., R. M. Fleming, M. L. Mandich, A. M. DeSantolo, J. Kwo, M. Hong, and L. J. Martinez-Miranda, 1988, Nature (London) **334**, 141.
Massidda, S., J. Yu, and A. J. Freeman, 1988a, Physica C **152**, 251.
Massidda, S., J. Yu, and A. J. Freeman, 1988b, Phys. Rev. B **38**, 11352.
Massidda, S., J. Yu, A. J. Freeman, and D. D. Koelling, 1987, Physica C **122**, 198.
Mattheiss, L. F., 1972, Phys. Rev. B **5**, 290 (Part I), 306 (Part II).
Mattheiss, L. F., 1987, Phys. Rev. Lett. **58**, 1028.
Mattheiss, L. F., E. M. Gyorgy, and D. W. Johnson, Jr., 1988, Phys. Rev. B **37**, 3745.
Mattheiss, L. F., and D. R. Hamann, 1982, Phys. Rev. B **26**, 2686.
Mattheiss, L. F., and D. R. Hamann, 1983, Phys. Rev. B **28**, 4227.
Mattheiss, L. F., and D. R. Hamann, 1988a, Phys. Rev. B **38**, 5012.
Mattheiss, L. F., and D. R. Hamann, 1988b, Phys. Rev. Lett. **60**, 2681.
Mattheiss, L. F., and D. R. Hamann, 1988c, Solid State Commun. **63**, 395.
Mattheiss, L. F., and W. Weber, 1982, Phys. Rev. B **25**, 2248.
McIntyre, G. J., A. Renault, and G. Colin, 1987, Phys. Rev. B **37**, 5148.
McMahan, A. K., R. M. Martin, and S. Satpathy, 1988, Phys. Rev. B **38**, 6650.
Mehl, M. J., R. J. Hemley, and L. L. Boyer, 1986, Phys. Rev. B **33**, 8685.
Melamud, M., L. H. Bennett, and R. E. Watson, 1988, Phys. Rev. B **38**, 4624.
Meservey, R., and B. B. Schwartz, 1969, in *Superconductivity,* edited by R. D. Parks (Dekker, New York), Chap. 3.
Meyer, H. M., III, D. M. Hill, T. J. Wagener, Y. Gao, J. H. Weaver, D. W. Capone II, and K. C. Goretta, 1988, Phys. Rev. B **38**, 6500.
Miceli, P. F., J. M. Tarascon, L. H. Greene, P. Barboux, F. J. Rotella, and J. D. Jorgensen, 1988, Phys. Rev. B **37**, 5932.
Michel, C., M. Hervieu, M. M. Borel, A. Grandin, F. Deslandes, J. Provost, and B. Raveau, 1987, Z. Phys. B **68**, 421.
Michel, C., J. Provost, F. Deslandes, B. Raveau, J. Beille, R. Cabanel, P. Lejay, A. Sulpice, J. L. Tholence, R. Tournier, B. Chevallier, G. Demazeau, and J. Etourneau, 1987, Z. Phys. B **68**, 417.
Mila, F., 1988, Phys. Rev. B **38**, 11358.
Mitsuda S., G. Shirane, S. K. Sinha, D. C. Johnston, M. S. Alvarez, D. Vaknin, and D. E. Moncton, 1987, Phys. Rev. B **36**, 822.
Mizuki, J., Y. Kubo, T. Manako, Y. Shimakawa, H. Igarashi, J. M. Tranquada, Y. Fujii, L. Rebelsky, and G. Shirane, 1988, Physica C **156**, 781.
Monnier, R., L. Degiorgi, and D. D. Koelling, 1986, Phys. Rev. Lett. **56**, 2744.
Montgomery, H. C., 1971, J. Appl. Phys. **42**, 2971.
Moore, C. E., 1952, *Atomic Energy Levels,* Natl. Bur. Stand. Circ. No. 467 (U.S. GPO, Washington, D.C.), Vol. I, p. 45; Vol. II, p. 111.
Moss, S. C., K. Forster, J. D. Axe, H. You, D. Hohlwein, D. E. Cox, P. H. Hor, R. L. Meng, and C. W. Chu, 1987, Phys. Rev. B **35**, 7195.
Mott, N. F., 1964, *Metal-Insulator Transitions* (Taylor and Francis, London).
Nakai, I., S. Sueno, F. P. Okamura, and A. Ono, 1987, Jpn. J. Appl. Phys. **26**, L788.
Nishihara, Y., M. Tokumoto, K. Murata, and H. Unoki, 1987, Jpn. J. Appl. Phys. **26**, L1416.
Nücker, N., J. Fink, B. Renker, E. Ewert, C. Politis, P. J. W. Weijs, and J. C. Fuggle, 1987, Z. Phys. B **67**, 9.
Oguchi, T., K. Terakura, and A. R. Williams, 1983, Phys. Rev. B **28**, 6443.
Ohana, I., M. S. Dresselhaus, Y. C. Liu, P. J. Picone, D. R. Gabbe, H. P. Jenssen, and G. Dresselhaus, 1988, Phys. Rev. B **38**, 2293.
O'Keefe, M., and F. S. Stone, 1962, J. Phys. Chem. Solids **23**, 261.
Ong, N. P., Z. Z. Wang, J. Clayhold, J. M. Tarascon, L. H. Greene, and W. R. McKinnon, 1987, Phys. Rev. B **35**, 8807.
Ossipyan, Yu. A., V. B. Timofeev, and I. F. Schegolev, 1988, Physica C **133-135**, 1133.
Ourmazd, A., J. A. Rentschler, J. C. H. Spence, M. O'Keefe, R. J. Graham, D. W. Johnson, Jr., and W. W. Rhodes, 1987, Nature (London) **327**, 308.
Papaconstantopoulos, D. A., 1986, *Handbook of the Band Structure of Elemental Solids* (Plenum, New York).
Papaconstantopoulos, D. A., 1988, unpublished.
Papaconstantopoulos, D. A., M. J. DeWeert, and W. E. Pickett, 1988, in *High Temperature Superconductors,* MRS Symposium Proceedings No. 99, edited by M. B. Brodsky, R. C. Dynes, K. Kitazawa, and H. L. Tuller (Materials Research Society, Pittsburgh), p. 447.
Papaconstantopoulos, D. A., W. E. Pickett, and M. J. DeWeert, 1988, Phys. Rev. Lett. **61**, 211.
Park, K. T., T. Oguchi, K. Terakura, A. Yanase, and M. Ikeda, 1988, in *Superconducting Materials,* JJAP Series 1, edited by S. Nakajima and H. Fukuyama (Jpn. J. Appl. Phys., Tokyo), p. 260.
Park, K. T., K. Terakura, T. Oguchi, A. Yanase, and M. Ikeda, 1988, J. Phys. Soc. Jpn., **57**, 3445.
Parkin, S. S. P., V. Y. Lee, A. I. Nazzal, R. Savoy, R. Beyers, and S. J. La Placa, 1988, Phys. Rev. Lett. **61**, 750.
Paul, D. McK., G. Balakrishnan, N. R. Bernhoeft, W. I. F. David, and W. T. A. Harrison, 1987, Phys. Rev. Lett. **58**, 1976.
Pederson, M. R., and B. M. Klein, 1988, Phys. Rev. B **37**, 10319.
Peter, M., L. Hoffman, and A. A. Manuel, 1988, Physica C **153-155**, 1724.
Pickett, W. E., H. Krakauer, and P. B. Allen, 1988, Phys. Rev. B **38**, 2721.
Pickett, W. E., H. Krakauer, D. A. Papaconstantopoulos, and L. L. Boyer, 1987, Phys. Rev. B **35**, 7252.
Pickett, W. E., H. Krakauer, D. A. Papaconstantopoulos, L. L. Boyer, and R. E. Cohen, 1987, in *High Temperature Superconductors,* edited by D. U. Gubser and M. Schlüter (Materials Research Society, Pittsburgh), p. 31.
Pickett, W. E. and D. A. Papaconstantopoulos, 1989, in *Atomic Scale Calculations in Materials Science,* edited by J. Tersoff, D. Vanderbilt, and V. Vitek, MRS Symposium Proceedings No. 141 (Materials Research Society, Pittsburgh), in press.
Qadri, S. B., L. E. Toth, M. Osofsky, S. Lawrence, D. U. Gubser, and S. A. Wolf, 1987, Phys. Rev. B **35**, 7235.
Ramaker, D. E., 1988a, in *Chemistry of High-Temperature Superconductors,* ACS Symposium Series No. 377, edited by D. L. Nelson and T. F. George (Am. Chem. Soc., Washington, D.C.), p. 84.

Ramaker, D. E., 1988b, Phys. Rev. B **38**, 11816.
Ramaker, D. E., N. H. Turner, J. S. Murday, L. E. Toth, M. Osofsky, and F. L. Hutson, 1987, Phys. Rev. B **36**, 5672.
Redinger, J., A. J. Freeman, J. Yu, and S. Massidda, 1987, Phys. Lett. A **124**, 469.
Redinger, J., J. Yu, A. J. Freeman, and P. Weinberger, 1987, Phys. Lett. A **124**, 463.
Reinen, D., 1983, Comments Inorg. Chem. **2**, 227.
Renker, B., F. Gompf, E. Gering, N. Nücker, D. Ewert, W. Reichardt, and H. Rietschel, 1987, Z. Phys. B **67**, 15.
Rhyne, J. J., D. A. Neumann, J. A. Gotaas, F. Beech, L. Toth, S. Lawrence, S. Wolf, M. Osofsky, and D. U. Gubser, 1987, Phys. Rev. B **36**, 2294.
Richert, B. A., and R. E. Allen, 1987, Jpn. J. Appl. Phys. Suppl. **26-3**, 989.
Richert, B. A., and R. E. Allen, 1988a, Phys. Rev. B **37**, 7869.
Richert, B. A., and R. E. Allen, 1988b, "Tight-binding descriptions of high temperature superconductors II. $Tl_2Ba_2CuO_6$," preprint.
Sakai, O., H. Tokahashi, M. Takeshiga, and T. Kasuya, 1984, Solid State Commun. **52**, 997.
Saez Puche, R., M. Norton, and W. S. Glausinger, 1982, Mater. Res. Bull. **17**, 1429.
Santoro, A., S. Miraglia, F. Beech, S. A. Sunshine, D. W. Murphy, L. F. Schneemeyer, and J. V. Waszczak, 1987, Mater. Res. Bull. **22**, 1007.
Sarma, D. D., and K. Sreedhar, 1988, Z. Phys. B **69**, 529.
Sato, S., I. Nakada, T. Kohara and Y. Oda, 1987, Jpn. J. Appl. Phys. **26**, L663.
Satpathy, S., and R. M. Martin, 1987, Phys. Rev. B **36**, 7269.
Sawatzki, G. A., 1977, Phys. Rev. Lett. **39**, 504.
Schlüter, M., M. S. Hybertsen, and N. E. Christensen, 1988, Physica C **153-155**, 1217.
Schneemeyer, L. F., J. V. Waszczak, E. A. Rietman, and R. J. Cava, 1987, Phys. Rev. B **35**, 8421.
Schuller, I. K., D. G. Hinks, M. A. Beno, D. W. Capone II, L. Soderholm, J.-P. Locquet, Y. Bruynseraede, C. U. Segre, and K. Zhang, 1987, Solid State Commun. **63**, 385.
Schwarz, K., 1987, Solid State Commun. **64**, 421.
Shen, Z.-X., J. W. Allen, J. J. Yeh, J.-S. Kang, W. Ellis, W. Spicer, I. Lindau, M. B. Maple, Y. D. Dalichaouch, M. S. Torikachvili, J. Z. Sun, and T. H. Geballe, 1987, Phys. Rev. B **36**, 8414.
Sheng, Z. Z., A. M. Hermann, A. El Ali, C. Almasan, J. Estrada, T. Datta, and R. J. Matson, 1988, Phys. Rev. Lett. **60**, 937.
Shimakawa, Y., Y. Kubo, T. Manako, Y. Nakabayashi, and H. Igarashi, 1988, Physica C **156**, 97.
Shiraishi, K., A. Oshiyama, N. Shima, T. Nakayama, and H. Kamimura, 1988a, Solid State Commun. **66**, 629.
Shiraishi, K., A. Oshiyama, N. Shima, T. Nakayama, and H. Kamimura, 1988b, in *Superconducting Materials,* JJAP Series 1, edited by S. Nakajima and H. Fukuyama (Jpn. J. Appl. Phys., Tokyo, 1988), p. 263.
Shirane, G., Y. Endoh, R. J. Birgeneau, M. A. Kastner, Y. Hidaka, M. Oda, M. Suzuki, and T. Murakami, 1987, Phys. Rev. Lett. **59**, 1613.
Siegrist, T., S. Sunshine, D. W. Murphy, R. J. Cava, and S. M. Zahurak, 1987, Phys. Rev. B **35**, 7137.
Siegrist, T., S. M. Zahurak, D. W. Murphy, and R. S. Roth, 1988, Nature (London) **334**, 231.
Sinha, S. K., 1988, Mater. Res. Soc. Bull. **13**, 24.
Skelton, E. F., W. T. Elam, D. U. Gubser, V. Letourneau, M. S. Osofsky, S. B. Qadri, L. E. Toth, and S. A. Wolf, 1987, Phys. Rev. B **36**, 5713.
Skriver, H., 1984, *The LMTO Method* (Springer, Berlin).
Slater, J. C., 1951, Phys. Rev. **82**, 538.
Sleight, A. W., 1988, Science **242**, 1519.
Sleight, A. W., J. L. Gillson, and P. E. Bierstedt, 1975, Solid State Commun. **17**, 27.
Smedskjaer, L. C., J. Z. Liu, R. Benedek, D. G. Legnini, D. J. Lam, M. D. Stahulak, H. Claus, and A. Bansil, 1988, Physica C **156**, 269.
Stassis, C., B. N. Harmon, T. Freltoft, G. Shirane, S. K. Sinha, K. Yamada, Y. Endoh, Y. Hidaka, and T. Murakami, 1988, Phys. Rev. B **38**, 9291.
Stechel, E. B., and D. R. Jennison, 1988, Phys. Rev. B **38**, 4632.
Sterne, P. A., and C. S. Wang, 1988a, Phys. Rev. B **37**, 7472.
Sterne, P. A., and C. S. Wang, 1988b, J. Phys. C **21**, L949.
Sterne, P. A., C. S. Wang, G. M. Stocks and W. M. Temmerman, 1988, in *High Temperature Superconductors,* MRS Symposium Proceedings No. 99, edited by M. B. Brodsky, R. C. Dynes, K. Kitazawa, and H. L. Tuller (Materials Research Society, Pittsburgh), p. 353.
Stocks, G. M., W. M. Temmerman, Z. Szotek, and P. A. Sterne, 1988, Supercond. Sci. Technol. **1**, 57.
Stormer, H. L., A. F. J. Levi, K. W. Baldwin, M. Anzlowar, and G. S. Boebinger, 1988, Phys. Rev. B **38**, 2472.
Subramanian, M. A., C. C. Torardi, J. C. Calabrese, J. Gopalakrishnan, K. J. Morrissey, T. R. Askew, R. B. Flippen, U. Chowdhry, and A. W. Sleight, 1988, Science **239**, 1015.
Subramanian, M. A., C. C. Torardi, J. Gopalakrishnan, P. L. Gai, J. C. Calabrese, T. R. Asker, R. B. Flippen, and A. W. Sleight, 1988, Science **242**, 249.
Sunshine, S., *et al.*, 1988, Phys. Rev. B **38**, 893.
Stoffel, N. G., Y. Chang, M. K. Kelly, L. Dottl, M. Onellion, P. A. Morris, W. A. Bonner, and G. Margaritondo, 1988, Phys. Rev. B **37**, 7952.
Suzuki, M., 1989, Phys. Rev. B **39**, 2312.
Suzuki, M., and T. Murakami, 1987, Jpn. J. Appl. Phys. **26**, L524.
Svane, A., and O. Gunnarsson, 1988a, Phys. Rev. B **37**, 9919.
Svane, A., and O. Gunnarsson, 1988b, Europhys. Lett. **7**, 171.
Swihart, J. C., 1959, Phys. Rev. **116**, 45.
Swihart, J. C., 1962, IBM J. Res. Dev. **6**, 14.
Swinnea, J. S., and H. Steinfink, 1987, J. Mater. Res. **2**, 424.
Szpunar, B., and V. H. Smith, Jr., 1988a, Phys. Rev. B **37**, 2338.
Szpunar, B., and V. H. Smith, Jr., 1988b, Int. J. Quantum Chem. Symp. **22**, 33.
Szpunar, B., and V. H. Smith, Jr., 1988c, Phys. Rev. B **37**, 7525.
Szpunar, B., V. H. Smith, Jr., and R. W. Smith, 1988, Physica C **152**, 91.
Takagi, H., S.-I. Uchida, K. Kitazawa and S. Tanaka, 1987, Jpn. J. Appl. Phys. **26**, L218.
Takahashi, T., H. Matsuyama, H. Katayama-Yoshida, Y. Okabe, S. Hosoya, K. Seki, H. Fujimoto, M. Sato, and H. Inokuchi, 1988, Nature (London) **334**, 691.
Takegahara, K., H. Harima, and A. Yanese, 1987, Jpn. J. Appl. Phys. **26**, L352.
Tanagawa, S., Y. Mizuhara, Y. Hidaka, M. Oda, M. Suzuki, and T. Murakami, 1988, in *High-Temperature Superconductors,* MRS Symposium Proceedings No. 99, edited by M. B. Brodsky, R. C. Dynes, K. Kitazawa, and H. L. Tuller (Materials Research Society, Pittsburgh), p. 57.
Tarascon, J. M., Y. Le Page, P. Barboux, B. G. Bagley, L. H. Greene, W. R. McKinnon, G. W. Hull, M. Giroud, and D. M. Hwang, 1988, Phys. Rev. B **37**, 9382.
Temmerman, W. M., Z. Szotek, P. J. Durham, G. M. Stocks, and P. A. Sterne, 1987, J. Phys. F **17**, L319.

Temmerman, W. M., Z. Szotek, and G. Y. Guo, 1988, J. Phys. C **21**, L867.
Terakura, K., H. Ishida, K. T. Park, A. Yanase, and N. Hamada, 1987, Jpn. J. Appl. Phys. **26**, L512.
Terakura, K., T. Oguchi, A. R. Williams, and J. Kübler, 1984, Phys. Rev. B **30**, 4734.
Terakura, K., A. R. Williams, T. Oguchi, and J. Kübler, 1984, Phys. Rev. Lett. **52**, 1830.
Tokumoto, M., H. Ihara, T. Matsubara, M. Hirabayashi, N. Terada, H. Oyanagi, K. Murata, and Y. Kimura, 1987, Jpn. J. Appl. Phys. **26**, L1565.
Torardi, C. C., M. A. Subramanian, J. C. Calabrese, J. Gopalakrishnan, E. M. McCarron, K. J. Morrissey, T. R. Askew, R. B. Flippen, U. Chowdhry, and A. W. Sleight, 1988, Phys. Rev. B **38**, 225.
Torardi, C. C., M. A. Subramanian, J. C. Calabrese, J. Gopalakrishnan, K. J. Morrissey, T. R. Askew, R. B. Flippen, U. Chowdhry, and A. W. Sleight, 1988, Science **240**, 631.
Torrance, J. B., Y. Tokura, S. J. LaPlaca, T. C. Huang, R. J. Savoy, and A. I. Nazzal, 1988, Solid State Commun. **66**, 703.
Tozer, S. W., A. W. Kleinsasser, T. Penney, D. Kaiser, and F. Holtzberg, 1987, Phys. Rev. Lett. **59**, 1768.
Tranquada, J. M., 1988, J. Appl. Phys. **64**, 6071.
Tranquada, J. M., D. E. Cox, W. Kunnmann, H. Moudden, G. Shirane, M. Suenaga, P. Zolliker, D. Vaknin, S. K. Sinha, M. S. Alvarez, A. J. Jacobson, and D. C. Johnston, 1988, Phys. Rev. Lett. **60**, 156.
Tsai, M-H., J. D. Dow, and R. V. Kasowski, 1988, Phys. Rev. B **38**, 2176.
Vaknin, D., E. Caignol, P. K. Davies, J. E. Fischer, D. C. Johnston, and D. P. Goshorn, 1989, "Antiferromagnetism in $(Ca_{0.85}Sr_{0.15})CuO_2$, the parent of the cuprate family of superconducting compounds," University of Pennsylvania, preprint.
Vaknin, D., S. K. Sinha, D. E. Moncton, D. C. Johnston, J. M. Newsam, C. R. Safinya, and H. E. King, Jr., 1987, Phys. Rev. Lett. **58**, 2802.
von Stetten, E. C., S. Berko, X. S. Li, R. R. Lee, J. Brynestad, D. Singh, H. Krakauer, W. E. Pickett, and R. E. Cohen, 1988, Phys. Rev. Lett. **60**, 2198.
Weaver, J. H., H. M. Meyer III, T. J. Wagener, D. M. Hill, Y. Gao, D. Peterson, Z. Fisk, and A. J. Arko, 1988, Phys. Rev. B **38**, 4668.
Weber, W., 1984, in *Electronic Structure of Complex Systems*, edited by P. Phariseau and W. Temmerman, NATO Advanced Study Institute, Series B: Physics, Vol. 113, (Plenum, New York), p. 345.
Weber, W., 1987, Phys. Rev. Lett. **58**, 1371.
Weber, W., 1988a, Z. Phys. B **70**, 323.
Weber, W., 1988b, Festkörperprobleme (in press).
Weber, W., and L. F. Mattheiss, 1988, Phys. Rev. B **37**, 599.
Weber, W. H., C. R. Peters, B. M. Wanklyn, Changkang Chen, and B. E. Watts, 1988a, Phys. Rev. B **38**, 917.
Weber, W. H., C. R. Peters, B. M. Wanklyn, Changkang Chen, and B. E. Watts, 1988b, Solid State Commun. **68**, 61.
Weinert, M., and G. W. Fernando, 1989, Phys. Rev. B **39**, 835.
Wendin, G., 1987, J. Phys. (Paris) C **9**, 1157.
Whangbo, M.-H., M. Evain, M. A. Beno, U. Geiser, and J. M. Williams, 1988, Inorg. Chem. **27**, 467.
Whangbo, M.-H., M. Evain, M. A. Beno, and J. M. Williams, 1987a, Inorg. Chem. **26**, 1829.
Whangbo, M.-H., M. Evain, M. A. Beno, and J. M. Williams, 1987b, Inorg. Chem. **26**, 1831.
Whangbo, M.-H., M. Evain, M. A. Beno, and J. M. Williams, 1987c, Inorg. Chem. **26**, 1832.
Williams, A., G. H. Kwei, R. B. Von Dreele, A. C. Larson, I. D. Raistrick, and D. L. Bish, 1988, Phys. Rev. B **37**, 7960.
Wilson, J. A., 1987, J. Phys. C **20**, L911.
Wilson, J. A., 1988, J. Phys. C **21**, 2067.
Wilson, T. M., 1968, Int. J. Quantum Chem. II S, 269.
Wilson, T. M., 1970, Int. J. Quantum Chem. III S, 757.
Wimmer, E., H. Krakauer, M. Weinert, and A. J. Freeman, 1981, Phys. Rev. B **24**, 864.
Wright, N. F., G. S. Painter, W. R. Busing and W. H. Butler, 1988, in *High Temperature Superconductors*, MRS Symposium Proceedings No. 99, edited by M. B. Brodsky, R. C. Dynes, K. Kitazawa, and H. L. Tuller (Materials Research Society, Pittsburgh), p. 539.
Wu, M. K., J. R. Ashburn, C. J. Torng, P. H. Hor, R. L. Meng, L. Gao, Z. J. Huang, Y. Q. Wang, and C. W. Chu, 1987, Phys. Rev. Lett. **58**, 908.
Xing, D. Y., M. Liu, and C. S. Ting, 1988, Phys. Rev. B **38**, 11992.
Xu, J.-H., T. J. Watson-Yang, J. Yu, and A. J. Freeman, 1987, Phys. Lett. A **120**, 489.
Xu, Y., W. Y. Ching, and K. W. Wong, 1988, Phys. Rev. B **37**, 9773.
Yamada, K., E. Kudo, Y. Endoh, Y. Hidaka, M. Oda, M. Suzuki, and T. Murakami, 1987, Solid State Commun. **64**, 753.
Yamaguchi, Y., H. Yamauchi, M. Ohashi, H. Yamamoto, N. Shimoda, M. Kikuchi, and Y. Syono, 1987, Jpn. J. Appl. Phys. **26**, L447.
Yan, Q. W., P. L. Zhang, L. Jin, Z. G. Shen, J. K. Zhao, Y. Ren, Y. N. Wei, T. D. Mao, C. X. Liu, T. S. Ning, K. Sun, and Q. S. Yang, 1987, Phys. Rev. B **36**, 5599.
Yang, B. X., R. F. Kiefl, J. H. Brewer, J. F. Carolan, W. N. Hardy, R. Kadono, J. R. Kempton, S. R. Kreitzman, G. M. Luke, T. M. Riseman, D. L. Williams, Y. J. Uemura, B. Sternlieb, M. A. Subramanian, A. R. Strzelecki, J. Gopalakrishnan, and A. W. Sleight, 1989, Phys. Rev. B **39**, 847.
Yang, B. X., J. M. Tranquada, and G. Shirane, 1988, Phys. Rev. B **38**, 174.
Yeh, J.-J., S. B. DiCenzo, E. H. Hartford, Jr., M. Hong, and R. J. Felder, 1989, Appl. Phys. Lett. **54**, 377.
You, H., R. K. McMullan, J. D. Axe, D. E. Cox, J. Z. Liu, G. W. Crabtree, and D. J. Lam, 1987, Solid State Commun. **64**, 739.
Yu, J., A. J. Freeman, and J.-H. Xu, 1987, Phys. Rev. Lett. **58**, 1035.
Yu, J., S. Massidda, and A. J. Freeman, 1988, Physica C **152**, 273.
Yu, J., S. Massidda, A. J. Freeman, and D. D. Koelling, 1987, Phys. Lett. A **122**, 203.
Yu, R. C., M. J. Naughton, X. Yan, P. M. Chaikin, F. Holtzberg, R. L. Greene, J. Stuart, and P. Davies, 1988, Phys. Rev. B **37**, 7963.
Zaanen, J., O. Jepsen, O. Gunnarsson, A. T. Paxton, and O. K. Anderson, 1988, Physica C **153-155**, 1636.
Zaanen, J., A. T. Paxton, O. Jepsen and O. K. Andersen, 1988, Phys. Rev. Lett. **60**, 2685.
Zaanen, J., and G. A. Sawatzky, 1987, Can. J. Phys. **65**, 1262.
Zaanen, J., G. A. Sawatzky, and J. W. Allen, 1985, Phys. Rev. Lett. **55**, 418.
Zaanen, J., G. A. Sawatzky, and J. W. Allen, 1986, J. Magn. Magn. Mater. **54-57**, 607.
Zeyher, R., and G. Zwicknagl, 1988, Solid State Commun. **66**, 617.